Vol. 56 FEBRUARY, 1952 No. 2

THE JOURNAL OF PHYSICAL CHEMISTRY

(Registered in U. S. Patent Office)

Founded by Wilder D. Bancroft

CONTENTS

R. Dean Anderson and H. Austin Taylor: The Preparation and Some Physical Constants of Cadmium Dimethyl.... 161
J. J. Bikerman: Mechanical Destruction of Young and Old Foam Films..... 164
Donald Zucker, Joseph F. Foster and Glenn H. Miller: Design and Performance of a Photoelectric Circuit for Measurement of Streaming Birefringence and Dichroism..... 166
Joseph F. Foster and Donald Zucker: Length of the Amylose–Iodine Complex as Determined by Streaming Dichroism 170
Joseph F. Foster and Donald Zucker: Streaming Birefringence Behavior of Some Subfractionated Amylose Preparations..... 174
Reino Hakala: The Periodic Law in Mathematical Form..... 178
D. H. Volman and G. J. Doyle: The Retentivity of Charcoals by the Approximate Isotherm Method. The Effect of Moisture on the Retentivity of Methyl Ethyl Ether, Neopentane and Methanol..... 182
Kenneth A. Kobe and William L. Motsch: Solubilities of Calcium and Strontium Nitrates in Monoalkyl Ethers of Ethylene Glycol..... 185
Robert A. Powers and Norman Hackerman: Nickel Plating by Chemical Reduction. I. Effect of the Basis Metal.. 187
Wilson J. Broach, Robert W. Rowden and Edward S. Amis: The Reaction in Acid Solution between Tetrabromophenolsulfonphthalein and Silver Nitrate..... 189
N. J. DeLollis: Note on the Displacement Pressure Method for Measuring the Affinity of Liquids for Solids..... 193
Geo. K. Schweitzer and John M. Lee: Racemization Rate Studies on Tris-(2,2′-dipyridyl)-nickel(II) Chloride..... 195
Izumi Higuti and Michie Shimizu: Studies on the Dielectric Property of Substances in the Sorbed State. IV. Freezing Phenomenon of *o*-Nitrophenol Sorbed on Silica Gel..... 198
David Hart: The Periodicity of Chemical Thermodynamic Functions..... 202
Charles C. Templeton and Lyle K. Daly: The System Nickel(II) Nitrate–Water–*n*-Hexyl Alcohol at 25°..... 215
N. Atchuta Ramaiah: Study of Joshi Effect in H_2O and D_2O Vapor..... 218
M. V. C. Sastri and K. V. Ramanathan: Chemisorption of Hydrogen on Zinc Oxide-Molybdenum Oxide Catalyst. Evidence of Heterogeneity of the Surface..... 220
B. J. Thamer and A. F. Voigt: The Spectrophotometric Determination of Overlapping Dissociation Constants of Dibasic Acids..... 225
J. G. Schnizlein, J. L. Sheard, R. C. Toole and T. D. O'Brien: The Preparation of OF_2 and Determination of its Vapor Pressure..... 233
H. Neal Dunning and E. Roger Washburn: Diffusion Coefficients and Some Related Properties of the Butyl Alcohols in Aqueous Solutions..... 235
Andrew Gemant: Cataphoresis Study in Hydrocarbon Oil by Radioactive and Microscopic Methods..... 238
Sydney O. Thompson, John Turkevich and A. P. Irsa: Study of the Fischer–Tropsch Reaction Using Deuterium Gas. 243
J. West Loveland and Philip J. Elving: Application of the Cathode-Ray Oscilloscope to Polarographic Phenomena. I. Differential Capacity of the Electrical Double Layer..... 250
J. West Loveland and Philip J. Elving: Application of the Cathode-Ray Oscilloscope to Polarographic Phenomena. II. Surface Charge Density of the Electrical Double Layer..... 255
J. T. Kummer and P. H. Emmett: Hydrogen Exchange Reactions over Iron Synthetic Ammonia Catalysts at −195° 258
Harold Tarkow and Alfred J. Stamm: The Reaction of Formic Acid with Carbohydrates. I. The Reaction of Formic Acid with Sugars..... 262
Harold Tarkow and Alfred J. Stamm: The Reaction of Formic Acid with Carbohydrates. II. Polysaccharides: A New Method for Determining Accessibility..... 266
Max Bender and Henry Mouquin: Brownian Movement and Electrical Effects..... 272
John O. Edwards: On the Reaction of Hydrogen Peroxide with Donor Particles..... 279
Lyle R. Dawson and Edward J. Griffith: Cryoscopic Studies of Solutions of Potassium and Ammonium Chlorides, and Acetic, Propionic and Benzoic Acids in Formamide..... 281
H. W. Fox and C. H. Chrisman, Jr.: The Ring Method of Measuring Surface Tension for Liquids of High Density and Low Surface Tension..... 284

Founded by Wilder D. Bancroft

THE JOURNAL OF PHYSICAL CHEMISTRY

(Registered in U. S. Patent Office)

Published monthly (except July, August and September) by the American Chemical Society at 20th and Northampton Sts., Easton, Pa.

Entered as second-class matter at the Post Office at Easton, Pennsylvania.

The *Journal of Physical Chemistry* is devoted to the publication of selected symposia in the broad field of physical chemistry and to other contributed papers.

Manuscripts originating in the British Isles, Europe and Africa should be sent to F. C. Tompkins, The Faraday Society, 6 Gray's Inn Square, London W. C. 1, England.

Manuscripts originating elsewhere should be sent to W. Albert Noyes, Jr., Department of Chemistry, University of Rochester, Rochester 3, N. Y.

Correspondence regarding accepted copy, proofs and reprints should be directed to Assistant Editor, Allen D. Bliss, Department of Chemistry, Simmons College, 300 The Fenway, Boston 15, Mass.

Business Office: American Chemical Society, 1155 Sixteenth St., N. W., Washington 6, D. C.

Advertising Office: American Chemical Society, 332 West 42nd St., New York 18, N. Y.

Articles must be submitted in duplicate, typed and double spaced. They should have at the beginning a brief Abstract, in no case exceeding 300 words. Original drawings should accompany the manuscript. Lettering at the sides of graphs (black on white or blue) may be pencilled in, and will be typeset. Figures and tables should be held to a minimum consistent with adequate presentation of information. Photographs will not be printed on glossy paper except by special arrangement. All footnotes and references to the literature should be numbered consecutively and placed on the manuscript at the proper places. Initials of authors referred to in citations should be given. Nomenclature should conform to that used in *Chemical Abstracts*, mathematical characters marked for italic, Greek letters carefully made or annotated, and subscripts and superscripts clearly shown. Articles should be written as briefly as possible consistent with clarity and should avoid historical background unnecessary for specialists.

Symposium papers should be sent in all cases to Secretaries of Divisions sponsoring the symposium, who will be responsible for their transmittal to the Editor. The Secretary of the Division by agreement with the Editor will specify a time after which symposium papers cannot be accepted. The Editor reserves the right to refuse to publish symposium articles, for valid scientific reasons. Each symposium paper may not exceed four printed pages (about sixteen double spaced typewritten pages) in length except by prior arrangement with the Editor.

Remittances and orders for subscriptions and for single copies, notices of changes of address and new professional connections, and claims for missing numbers should be sent to the American Chemical Society, 1155 Sixteenth St., N. W., Washington 6, D. C. Changes of address for the *Journal of Physical Chemistry* must be received on or before the 30th of the preceding month.

Claims for missing numbers will not be allowed (1) if received more than sixty days from date of issue (because of delivery hazards, no claims can be honored from subscribers in Central Europe, Asia, or Pacific Islands other than Hawaii), (2) if loss was due to failure of notice of change of address to be received before the date specified in the preceding paragraph, or (3) if the reason for the claim is "missing from files."

Annual Subscription: $8.00 to members of the American Chemical Society, $10.00 to non-members. Postage free to countries in the Pan American Union; Canada, $0.40; all other countries, $1.20. Single copies, $1.25; foreign postage, $0.15; Canadian postage, $0.05.

The American Chemical Society and the Editors of the *Journal of Physical Chemistry* assume no responsibility for the statements and opinions advanced by contributors to This Journal.

The American Chemical Society also publishes *Journal of the American Chemical Society, Chemical Abstracts, Industrial and Engineering Chemistry, Chemical and Engineering News* and *Analytical Chemistry*. Rates on request.

* * * *(Continued from first page of cover)* * * *

BOOK REVIEW

Phase Transformations in Solids. Edited by R. Smoluchowski, Chairman, with J. E. Mayer and W. A. Weyl. Review by G. H. Cartledge 288
Books Received 288

THE JOURNAL OF
PHYSICAL CHEMISTRY

(Registered in U. S. Patent Office)

Founded by Wilder D. Bancroft

VOLUME 56 FEBRUARY 15, 1952 NUMBER 2

THE PREPARATION AND SOME PHYSICAL CONSTANTS OF CADMIUM DIMETHYL

BY R. DEAN ANDERSON AND H. AUSTIN TAYLOR

New York University, New York 53, N. Y.

Received July 5, 1950

Pure cadmium dimethyl prepared by a Grignard reaction requires careful fractionation to remove ether which is the chief impurity. Measurement shows the triple point to be −2.4° and 5.5 mm. and the normal boiling point to be 105.7°. The density is found to be $2.479 - 0.001631T$; the coefficient of cubical expansion, 1.0×10^{-3}, and the vapor pressure, $\log p = -3116.7/T - 8.0668 \log T + 31.305$. The heat of vaporization is given by $\Delta H_v = 14{,}300 - 16T$ and the boiling point constant is 4.9°.

In synthesizing cadmium dimethyl for other studies it became apparent that what is at present the accepted technique of preparation could be vastly improved both as to quality of product and safety for the operator.

Gilman[1] by the use of anhydrous cadmium chloride improved the procedure of Krause[2] who obtained cadmium dimethyl by the Grignard reaction of methylmagnesium iodide and cadmium bromide in anhydrous ether. The product has a boiling point of 105.5° at 758 mm., a freezing point of −4.5°, density (17.9°/4°) of 1.9846 and index of refraction using the sodium D lines of 1.5488. Herz[3] reported the boiling point as 105.7°, the density (0°) as 2.500 and the refractive index n_0 as 1.786. Recently Bamford, Levi and Newitt[4] made the alkyl by the Krause synthesis and made vapor pressure measurements by the static method reporting a linear relationship between the logarithm of the pressure in mm. and the reciprocal of the absolute temperature, namely, $\log p = 7.764 - 1850/T$. They also report the boiling point as 105.7° and the freezing point, −4.2°.

Of the dangers inherent in the preparation and use of cadmium dimethyl, repeated mention is made in the literature of its explosive nature when overheated. Gilman reports that it may detonate spontaneously if heated above 90°. Its physiological effects on the user include extreme irritation of the eyes on exposure to the vapor with distortion of vision after a few hours. Light sources appear to be surrounded by bright halos and the effect persists for a day or so.

(1) H. Gilman, *Rec. trav. chim.*, **55** 518 (1936); *J. Am. Chem. Soc.*, **68**, 518 (1946).

(2) E. Krause, *Ber.*, **50**, 1813 (1917).

(3) W. Herz, *Z. anorg. Chem.*, **182**, 173 (1929).

(4) C. H. Bamford, D. L. Levi and D. M. Newitt, *J. Chem. Soc.*, **40**, 468 (1946).

Experimental

Synthesis.—From experience gained with preliminary preparations, the synthesis was carried out in a production unit, shown in Fig. 1, mounted in a hood having shatterproof glass.

Methylmagnesium iodide was first made in the conventional way using 512.0 g. of C.P. methyl iodide and 87.8 g. of magnesium turning. A 2-l. reaction flask was fitted with a 20-inch reflux condenser connected to the atmosphere through a drying train and a nitrogen reservoir. A dropping funnel and heavy duty stirrer were connected to the flask. All equipment had either standard taper or ball and socket type joints. An inlet tube was provided so that nitrogen could be led into the reaction vessel beneath the ether surface during the reaction. A bath of ice-water was used to check the reaction when it became too vigorous. About one liter of anhydrous ether was placed in the flask with the magnesium turnings. The apparatus was flushed out with nitrogen before and after this addition. The methyl iodide was introduced through a dropping funnel, in small portions requiring one hour for the addition. The condenser was maintained at −10° by the use of a 25% prestone-water solution pumped through a freezing unit. After the methyl iodide had been added the reaction mixture was kept at moderate reflux for a half-hour on an oil-bath with heating mantle. Stirring and heating were discontinued and the system allowed to cool in an atmosphere of nitrogen.

The ether solution of the Grignard reagent was siphoned into the production unit in a nitrogen atmosphere through

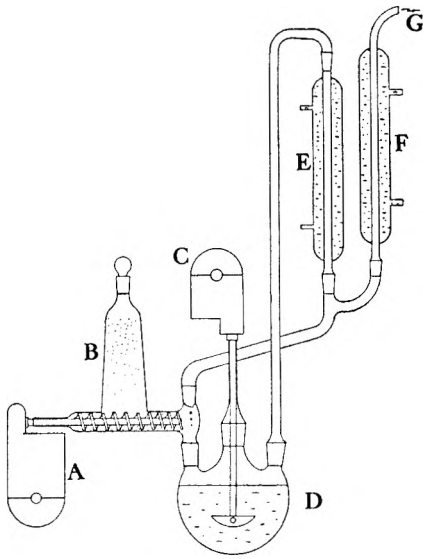

Fig. 1.—Production of cadmium dimethyl.

an assembly replacing the stirrer, C, in Fig. 1. Anhydrous cadmium chloride, 33.10 g. in weight, previously heated at 120° overnight and cooled in a vacuum desiccator was transferred to the hopper B which contained a 7/8 inch wood bit ground to fit into the glass bearing. All bearings and ground joints were lubricated with high vacuum grease. A reduction motor rotating the screw at about 12 r.p.m. was used intermittently as required. All heaters and motors were operated from outside the hood which was not opened until the reaction, once begun, was complete. The condensers E and F maintained at −10° in the manner previously indicated were lagged to prevent water condensation.

With the unit assembled as shown and the stirrer C operating, the whole in a nitrogen atmosphere, reaction was started by adding the cadmium chloride intermittently every five minutes for about five and one-half hours. The heat of reaction was sufficient to maintain a steady reflux of the ether which in turn kept the entrance to the vessel clear of cadmium chloride. The addition completed, artificial heating was supplied for ten hours.

The ether solution of cadmium dimethyl after cooling was siphoned into a 2-l. distilling flask, the residue in the reaction flask being extracted twice with 150-ml. portions of ether and the whole subjected to a preliminary fractionation through a vacuum-jacketted column in a nitrogen atmosphere. The first fraction coming over at 34.7° was ether. As soon as the temperature at the top of the column started to go higher distillation was stopped, the apparatus allowed to cool and a second receiver in the form of a trap set in a bath of Dry Ice in acetone was substituted. Distillation was then continued for several hours under reduced pressure sufficient to maintain the temperature at the top of the column at 70° or less. About 350 ml. of clear liquid was thus collected and transferred to the kettle, R, of the fractionation unit shown in Fig. 2 which carried a thermometer well S, and nitrogen inlet tube, M, attached by a rubber sleeve, N. The capillary, M, was drawn down to a fine bore such that under reduced pressure only two or three minute bubbles entered the liquid per second to ensure smooth boiling. The column, K, comprised three concentric cylinders of Pyrex glass. The inner one was packed with 3/8 inch Pyrex helices and the middle one carried a heating coil mounted on vertical strips of asbestos cord. Thermometers were inserted between these two tubes to record the temperatures at the top and bottom. The outer tube served as insulation.

The take-off head was set into the top of the column. Vapor from the column rose through the vacuum-jacketted section, G, its temperature being noted by a thermometer in the well F, and condensed on the surfaces of D and E. Set for total reflux all the condensate falls through funnel, C, returning to the column through the coil, H, where mild preheating occurs. When set for intermittent takeoff, electromagnet B is activated at regular intervals to tilt funnel C, and divert the reflux into the receiver connected through

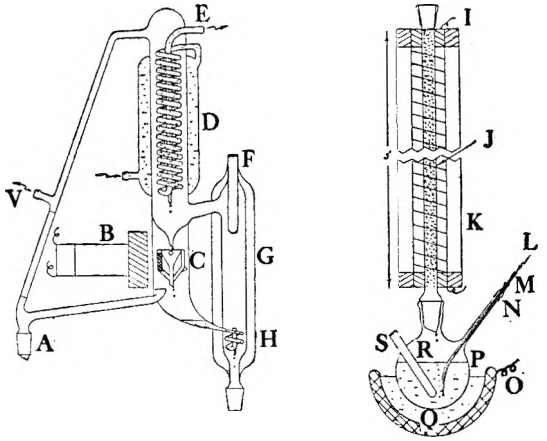

Fig. 2.—Automatic take-off head and fractionating column.

A. An automatic time switch with two-minute cycle or any fraction thereof actuated the magnet.

Fractionation at a 3% take-off ratio was begun at 34.7° and 760 mm. and at the end the pressure had been reduced to 230 mm. to maintain boiling in the kettle at 70°. The contents of the kettle was then transferred by simple distillation into a receiver cooled in liquid nitrogen. In this way about 135 ml. of cadmium dimethyl was collected. A hydrometer check on the density gave a reading in agreement with the reported value. Freezing was observed at −4.7° over a range of about half a degree. Vapor pressure readings were made and finally the liquid boiled at 107.4° and 760 mm. It was apparent that the boiling point was some two degrees higher than the reported value though the freezing point was in agreement with previous findings.

The whole sample was therefore fractionated again through the same apparatus, Fig. 2. Artificial heating of the column was necessary to maintain the column at about a ten-degree gradient. Cooling solution at −10° was used in the reflux head. After a two-hour reflux the automatic take-off head was set to collect one drop out of 750. The first distillate came over at 50° and 230 mm. and when 3 ml. had been collected distillation was proceeding smoothly at 67.2° and 218 mm. An additional milliliter was collected and then the column shut down and the receiver changed. On resuming fractionation, total reflux was maintained for one hour, and the head temperature being 67.2° at 218 mm. take-off at four drops per two-minute cycle was resumed. When no further drifting in temperature and pressure occurred this rate was increased to sixteen drops per cycle or about 2% of the total reflux.

Over a 15-hour period 80 ml. of pure alkyl was collected. The actual distillation time was seven hours, the rest of the time being necessary for shut-downs and regaining equilibrium conditions. At one such shut-down the capillary was changed while the kettle was at 70° and although the rubber sleeve was pinched off as the capillary was withdrawn, some air apparently entered the kettle and the vapor exploded.

Freezing Point Determination.—The freezing point was determined in a flask of about 60-ml. capacity into which 40 ml. of cadmium dimethyl had been distilled. A low range thermometer marked in 0.1° and calibrated, was inserted through a rubber sleeve into the liquid. A side arm on the flask was used for evacuation. An acetone-bath cooled by addition of acetone from an acetone–Dry Ice mixture was used as coolant in a two quart dewar. Investigation showed that a ten-degree temperature gradient was necessary to give a well defined cooling curve. The apparatus was rotated manually while in the bath and temperatures were taken at half-minute intervals. Cooling curves with small undercooling and marked plateaus extending through several minutes showed the corrected freezing point to be −2.4°.

A boiling point determination of the same 40-ml. portion gave a value of 105.7° at 760 mm. Compared with the previous impure sample this showed a fall of 1.7° in boiling point and a rise of 2.3° in the freezing point. A greater change in the freezing point is generally to be expected.

Density Determination.—A Pyrex pyknometer consisting of a tube of volume about 9 ml. carried side arms bent up-

wards at about 75°. They were sections from micro-pipets of 0.2-ml. capacity graduated in 0.01 ml. the graduations being about 1-cm. apart. The open ends carried ground glass covers. A small foot was sealed to each side of the main body so that the pyknometer would stand on a balance pan for weighing. A loading arm ground to replace one of the cover caps was bent downwards such that when its open end was placed beneath a liquid, and vacuum applied to the other arm of the pyknometer, the liquid filled the vessel without leaving any gas trapped.

The pyknometer was calibrated by weighing water sufficient at 20° to fill it to the graduation markings. For cadmium dimethyl the vessel was first flushed with nitrogen, filled as described and capped and weighed. The pyknometer was then placed in a series of different temperature thermostats at each of which volume readings were made. The correction for volume due to the coefficient of expansion of Pyrex was negligible over the fourteen degree range covered.

The density of cadmium dimethyl in g. per ml., corrected for buoyant effect of air was found to be

$$d_{vac.} = 2.479 - 0.001631T$$

over the temperature range 10–24°, using the method of least squares on fifteen volume readings. The volume measurements showed that the coefficient of cubical expansion of the liquid was 1.0×10^{-3}.

Vapor Pressure Determination.—The apparatus used for the vapor pressure measurements is shown in Fig. 3. Below 44° the static method of vapor pressure measurement was used; above 44° the Ramsay–Young method. The apparatus consists of a system of two flasks and three condensers which can be rotated to either of two positions in plane at right angles to the standard taper joint, I. This permits a back and forth distillation of the liquid between the two flasks A and F. The manifold leads to an absolute mercury manometer, M, a nitrogen supply, J, a McLeod gage, K, a trap, L, cooled by liquid nitrogen and thence to a diffusion pump system.

Before loading, the entire apparatus was alternately evacuated (5×10^{-5} mm.) and flushed out with nitrogen to remove oxygen and water vapor. Cadmium dimethyl was distilled through H into flask, A, in a nitrogen atmosphere at 150 mm. Flask, A, was then rotated to the position shown in the diagram and its heating bath put in place, F, the receiver, was cooled in liquid nitrogen. The condensers, D, were water-cooled while E was cooled as before to −10°. Pressure in the system was regulated by control of J and temperature readings of the boiling liquid were made on a calibrated thermometer graduated in 0.1° inserted in paraffin oil in the well, C. Distillation was so smooth that a closed system was used at each pressure and when equilibrium was established simultaneous pressure and temperature readings were made.

For temperatures below 44°, the heating mantle, B, was not used. Instead the product was frozen overnight and evacuated to zero pressure on the manometer. For each pressure reading a constant temperature bath was placed around the cadmium dimethyl and the equilibrium pressure read. For temperatures below room temperature and down to the freezing point a dewar flask containing chilled acetone was used for thermostating.

Thirty-five pressure measurements were made covering the temperature range −2.4° to 106.7°. A plot of log p against $1/T$ does not give a straight line and deviation from linearity is more marked in the low temperature range indicating an increase in heat of vaporization with decreasing temperature. Assuming the heat of vaporization to be a linear

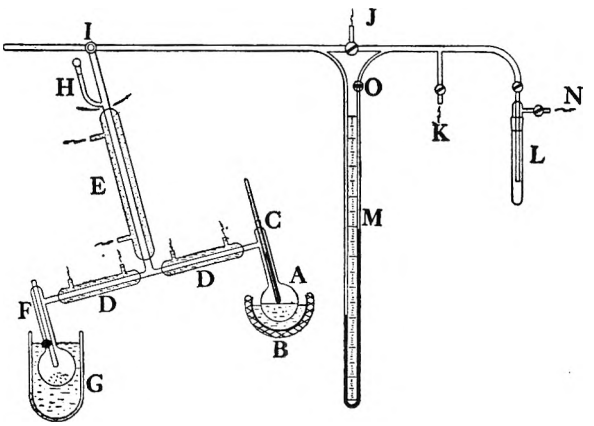

Fig. 3.—Ramsay–Young vapor pressure apparatus.

function of the temperature integration of the Clapeyron–Clausius equation gives a relation of the form: $\log p = A/T + B \log T + C$. Using this equation and the method of least squares on the thirty-five measurements made, the following values, good to six significant figures were found: $A = -3116.74$, $B = -8.06680$, $C = 31.9054$. The log terms in the equation make all these figures in A, B and C important for the evaluation of the pressure at a given temperature. The effect of successively rounding off these values is shown at a few selected points in Table I. It can be seen that five significant figures reproduce the observed values almost as well as six, but that further approximations yield progressively poorer agreement between observed and calculated pressures.

TABLE I

A =	−3116.74		−3116.7		−3117		−3120	
B =	− 8.06680		− 8.0668		− 8.067		− 8.07	
C =	31.9054		31.905		31.91		31.9	
$t°$	$p_{obsd.}$	$p_{calcd.}$	δ	$p_{calcd.}$	δ	$p_{calcd.}$	δ	$p_{calcd.}$	δ
−2.4	5.5	5.9	0.4	5.9	0.4	5.9	0.4	5.0	0.5
45.7	86.0	86.2	0.2	86.1	0.1	87.1	1.1	79.4	6.6
71.5	246.8	247.8	1.8	247.7	1.7	251.2	5.2	251.2	5.2
86.4	418.0	417.5	0.5	416.9	1.1	416.9	1.1	398.1	19.9
98.6	617.0	613.9	3.1	613.8	3.2	616.6	0.4	631.0	14.0
105.7	760.0	756.8	3.2	756.8	3.2	758.6	1.4	794.3	34.3

For the minimum number of figures in the constants A, B and C to maintain agreement with the observed values the following equation is best

$$\log p = 3117.7/T - 8.0668 \log T + 31.905$$

From this equation the heat of vaporization of cadmium dimethyl is found to be $\Delta H_v = 14{,}300 - 16\,T$ with values at the freezing point −2.4° and boiling point 105.7°, 9970 and 8240 cal./mole or 70.0 and 57.8 cal./g., respectively. A molecular boiling point constant of 4.9° then results.

MECHANICAL DESTRUCTION OF YOUNG AND OLD FOAM FILMS[1]

BY J. J. BIKERMAN

Research Laboratories, Merck & Co., Inc., Rahway, N. J.

Received October 24, 1950

Single foam films (1.0–3.5 cm. in diameter) of aqueous disodium α-tocopheryl phosphate, sodium laurate, "acid" sodium laurate and of beer were broken by a stream of mercury droplets. Fresh films (*e.g.*, 5 sec. old) lasted in a mercury shower longer than aged films (*e.g.*, 60 sec. old). Similarly, fresh films of a "benzalkonium chloride" solution endured more punctures by a glass needle than older films. This result is in agreement with Rayleigh's theory of foams. It indicates also that mechanical devices for foam destruction are likely to be less efficacious the fresher the foam. The persistence of untouched single films was shorter for larger films; in several instances it was inversely proportional to the film area; apparently, this cannot be accounted for by the probability theory of rupture.

I. Introduction

The striking insensitivity of foam to mechanical damage is well known.[2] Over 80 years ago Dupré[3] and later Rhumbler[4] dropped solid bodies such as lead granules, cork balls or iron filings through single soap films or columns of soap lather without any damage to the films. On the other hand, mechanical destruction of foam is a recognized industrial process. The disagreement between these two sets of observations might be resolved if the probable cause of the great resilience of foam lamellae is considered.

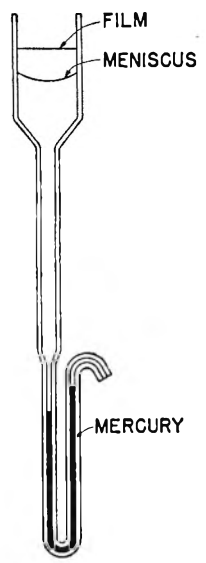

Fig. 1.

It may be deduced from the accepted theory of foam stability[5] that surface films are self-healing because removal of a part of the surface layer exposes the bulk liquid which has a higher surface tension; because of this greater surface tension the exposed patch contracts and again brings the contaminated areas in uninterrupted contact ("Marangoni effect"). This mechanism can be expected to operate as long as there is enough bulk liquid to exhibit the higher surface tension. When the amount of solution between the surface layers in a soap lamella becomes too small, the Marangoni effect should be depressed or even suppressed. Hence, "wet" foams should, and "dry" foams should not, be resilient in respect to mechanical damage.

This conclusion has been tested and confirmed by the experiments described below.

II. Experimental Procedure

The instruments used in the major part of the experiments were modelled after the well-known mercury cleaning device and are exemplified in Fig. 1. The bottom part of the U-tube was filled with mercury, and the rest of the longer branch was then almost filled with the solution to be tested. By slightly immersing a fine pipet into the solution and blowing in air with a rubber bulb, single foam films spanning the tube were produced. Their persistence (life time) t_0 was determined. Then a fine stream of mercury droplets was allowed to fall through the film into the solution (and to join the mercury column under the solution) until the film burst. The excess mercury flowed through the spout into a container and was used for another series of experiments.

The diameters of the tubes along the stretch where the films were produced, were 1.0 and 3.5 cm. in the two instruments employed. The smallest mercury droplets had diameters of either about 0.02 cm., or, in the later experiments, about 0.05 cm., and fell from a height of about 2 cm. The rate of flow of mercury was about 0.5 g./sec. or, in the later experiments, approximately 0.3 g./sec. The temperature of the laboratory varied between 21.2 and 23.2°. To avoid fluctuations due to variations in the temperature, the foaminess of the solutions, and so on, experiments on films of different ages have been performed alternately, *e.g.*, in the order 5 sec., 30 sec., 90 sec., 240 sec., 5 sec., etc.

If the film was t_1 sec. old when first hit by the mercury shower and if this shower continued for t_2 sec. before the film burst, then the lamella was $t_1 + t_2$ sec. old in the moment of rupture. The relation between t_2 on one hand and t_1 or $(t_1 + t_2)$ on the other hand was studied.

Only aqueous solutions were used. They included: (a) 0.43% (w./v.) disodium α-tocopheryl phosphate monohydrate; (b) 3.7% (w./v.) sodium laurate, prepared by mixing an acetone solution of lauric acid (C.P.) with an insufficient volume of 5 *N* NaOH, boiling the acetone off, and adding 5 *N* NaOH until the *p*H, determined with an indicator, reached 8.2 (it became 8.6 after dilution); (c) "acid" sodium laurate solution prepared by short heating 0.05 g. of lauric acid with a solution of 0.659 g. of sodium laurate in aqueous acetone, boiling the acetone off and diluting to 50 cc. with water; this liquid was turbid immediately after preparation, deposited flakes a day or a few days later but could be approximately restored by heating until incipient foam formation; the foaminess of this liquid greatly varied from day to day; (d) 0.32% (w./v.) "benzalkonium chloride" solution, "benzalkonium chloride" being the designation used by U. S. Pharmacopeia (XIV edition) for a mixture of salts $[C_6H_5CH_2N(CH_3)_2R]Cl$, R representing a mixture of the alkyls from C_8H_{17} to $C_{18}H_{37}$; (e) beer.

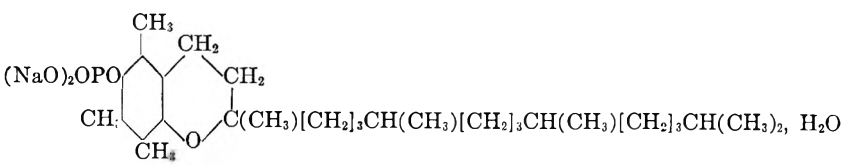

III. Results

Figure 2 shows the decrease of resilience (expressed as time t_2 sec.) when the age at the start of mercury shower (t_1 sec.) or at rupture $(t_1 + t_2)$ increases, for the disodium α-tocopheryl phosphate solution. The 1.0-cm. tube and the bigger mercury droplets were employed. Each t_2 value is the

(1) The main results and conclusions of this paper have been presented at the 118th Meeting of the American Chemical Society, Chicago, Ill., September 7, 1950.

(2) J. J. Bikerman, "Surface Chemistry for Industrial Research," Academic Press Inc., New York, N. Y., 1947, p. 95.

(3) A. Dupré, "Théorie méchanique de la chaleur," Gauthier-Villars, Paris, 1869, p. 352.

(4) L. Rhumbler, *Ergebnisse Physiol.*, **14**, 526 (1914).

(5) Rayleigh, *Proc. Roy. Inst. Gt. Brit.*, **13**, 85 (1890)

mean of 50 determinations. The persistence (t_0) of untouched films was not properly determined but was approximately 7 minutes. *E.g.*, of eight successive untouched films, six did not burst within 300 sec. In another series, three out of six successive films did not burst within 420 sec.

The other results in the 1.0-cm. tube are expressed below as averages of (usually) ten determinations.

Sodium laurate solution, t_0 = 120 to 400 sec.; t_2 = 16 to 20 sec. after t_1 = 5 sec., and t_2 = 3 to 9 sec. after t_1 = 60 sec. Both large and small mercury droplets have been used.

"Acid" sodium laurate solution, t_0 = 200 to 450 sec.; t_2 not measured.

Fresh beer, t_0 = 20 to 60 sec.; t_2 = 2 to 3 sec. after t_1 = 5 sec., and t_2 was less than 1 sec. after t_1 = 20 sec. (small mercury droplets).

Beer, 5 weeks old, t_0 = 90 to 140 sec.; t_2 = 9 sec. after t_1 = 5 sec., and t_2 = 3.5 sec. after t_1 = 30 sec. (bigger mercury droplets).

Beer, 7 weeks old, t_0 = 390 sec.; t_2 not measured.

The results in the 3.5-cm. tube are summarized in Table I. Each figure represents the average of (usually) ten single determinations. Small mercury droplets have been used for the "acid" sodium laurate solution, and bigger droplets for the other solutions.

TABLE I

PERSISTENCE OF UNTOUCHED FILMS (t_0) AND DURATION (t_2) OF t_1 SEC. OLD FILMS IN A MERCURY SHOWER, FILM DIAMETER 3.5 CM.

Solution	t_0, sec.	t_2, sec. t_1 = 5 sec.	t_2, sec. t_1 = 20 sec.
Na_2 α-tocopheryl phosphate	30 to 39	4.5; 5.3	2.1; 2.5
Na laurate	13 to 32	3.7; 6.1	2.4; 2.8
"Acid" Na laurate	35 to 90	13 to 27	5 to 12
Beer, 7 weeks old	18 to 51	Not determined	

As mercury droplets in traversing the films may become coated with the surface-active agent and, therefore, may destroy the films also by reducing the amount of this agent in the foam rather than by purely mechanical means, another procedure was employed to which this objection does not apply. Foam lamellae were produced in a test-tube (diameter, 1.05 cm.) and then destroyed by pricking with a glass fiber the end of which, by heating, was made to a ball 0.056 cm. in diameter. The lamellae were pricked every second. If the number of punctures required for bursting is n, then $n - 1$ seems a justifiable measure of resilience. The "benzalkonium chloride" solution ("d" of Section II) was used for these tests. After t_1 = 5 sec., $n - 1$ was 3.94, and after t_1 = 60 sec. $n - 1$ was 0.08, each figure being the mean of 50 determinations. The rapid decrease of resilience on aging is shown also by this method. The persistence t_0 of the "benzalkonium chloride" films was 128–137 sec. (averages for 10 films).

IV. Discussion

The above results by two methods confirm the expected decrease of the resilience of the film during its aging for films of four very different chemical compositions. In fact, it appears that a foam film bursts "spontaneously" when its resilience reaches a very low value, near zero; then even the slightest damage caused, *e.g.*, by dust particles or air movement is incurable.

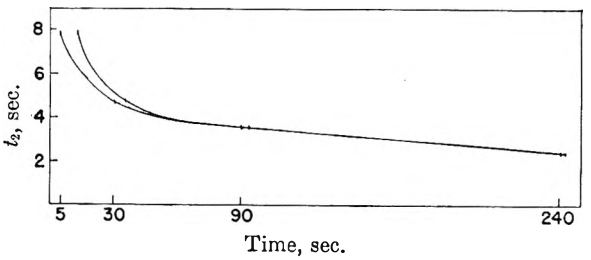

Fig. 2.—Upper curve, age at rupture ($t_1 + t_2$); lower curve, age at start (t_1); both in sec.; ordinate, t_2 sec.

The hypothesis advanced in the Introduction would have been confirmed even better, if the drainage (*i.e.*, the decrease of the water content of the film) were determined for different times t_1, and it could be shown that the decrease of t_2 with increasing t_1 parallels the decrease in the water content. It had been hoped to estimate the volume of liquid in the films from their interference colors. Unfortunately, the films—also of disodium α-tocopheryl phosphate which is chemically the most homogeneous of the substances tested—had no uniform thickness and at any one time exhibited patches of different colors.

The main observation reported in this paper, namely that fresh foams withstand more mechanical damage than do aged foams, should be of importance for the problem of foam destruction. It may be expected that all the mechanical agents—from rotating blades to supersonic waves—would have no effect or only a very limited effect on a fresh foam, and that their efficacy will regularly increase with the foam age.

Comparison of the persistences (t_0) of untouched lamellae in 1.0- and in 3.5-cm. tubes shows what kind of relation exists between t_0 and the diameter of a film. The ratio of t_0 for the two tubes was about 12 for disodium α-tocopheryl phosphate, from 9 to 13 for sodium laurate, 13 for seven-week old beer, and about 5 for "acid" sodium laurate. The film area in the wider tube was about 12 times that in the narrower tube. Thus, it appears that, in some instances at least, t_0 is inversely proportional to the film area.

In analogy to the probability theory of tensile strength, the greater persistence of a smaller film might be thought of as due to the smaller likelihood of a weak spot being present within a smaller area. Following the reasoning applied to adhesive joints[6] and glass threads,[7] the least persistence in a batch of 12 small films should be equal to the average persistence of large films. This conclusion was not supported by the few experiments performed to test it. Apparently, small lamellae differ from large ones not only because they contain less weak spots. Such was also the opinion of Plateau.[8]

(6) J. J. Bikerman, *J. Soc. Chem. Ind.*, **60**, 23 (1941).
(7) J. J. Bikerman and G. H. Fassmore, *Glass Ind.*, **29**, 144 (1948).
(8) J. Plateau, *Acad. roy. Belg., Mém.*, **37** (1869), p. 8 of the memoir.

DESIGN AND PERFORMANCE OF A PHOTOELECTRIC CIRCUIT FOR MEASUREMENT OF STREAMING BIREFRINGENCE AND DICHROISM[1,2]

BY DONALD ZUCKER,[3] JOSEPH F. FOSTER AND GLENN H. MILLER

Iowa Agricultural Experiment Station, Ames, Iowa

Received October 27, 1950

An electronic circuit based on a photomultiplier tube has been designed for the measurement of streaming dichroism and birefringence. This circuit permits the measurement of the positions of both minimum and maximum light absorption in dilute (less than 0.002%) solutions of amylose–iodine complex under conditions where direct visual measurement of the orientation position is impossible. In the case of streaming birefringence the system shows some slight advantages over visual observation under conditions of very low degrees of birefringence.

The lengths of many macromolecules and colloids can be determined by measurements of the angle of orientation in a flowing liquid. The theory of orientation between concentric cylinders and determination of the orientation angle by means of the birefringence of the oriented particles have been considered extensively by many authors.[4]

In the case of the blue amylose–iodine complex, and presumably in the case of many other intensely colored colloids, dichroism is a more convenient property to use than is birefringence.[5] However, while there are a few qualitative reports of the measurement of streaming dichroism in the literature almost no quantitative studies of extinction angle (enabling determination of particle length) have been made on any system. The almost complete extinction found parallel to the optic axis in streaming birefringence is not usually observed in the case of dichroism. Usually the light intensity at the minimum is great enough that minima can be determined only with a low degree of precision if at all. Readings of the position of maximum intensity, which, as will be shown later, are highly desirable, are virtually impossible by direct visual methods.

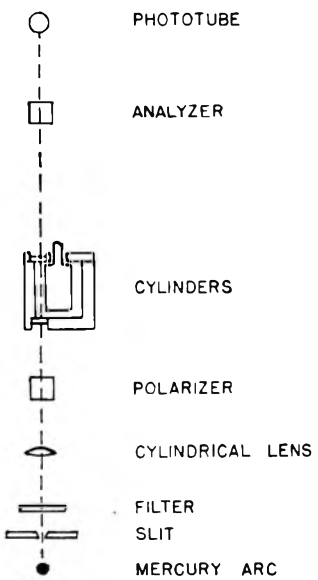

Fig. 1.—Schematic diagram of apparatus for measurement of streaming dichroism.

With photoelectric methods various means are available for opposing most of the signal so that a high sensitivity can be used to measure the small unopposed signal, thus permitting accurate detection of small variations in the light transmitted. However, while the light intensity per unit area may be moderately high, the total flux is very low due to the small cross sectional area of the field, in the authors' apparatus only 0.05 cm.^{2}. This necessitates the use of a multiplier phototube, and even with such a tube the output is often quite small.

It is the purpose of this paper to describe a photoelectric arrangement which has proved very satisfactory for the measurement of streaming dichroism and birefringence, and to demonstrate some of its potentialities.

General Description of Apparatus.—The mechanical and optical parts of the apparatus are outlined in Fig. 1. Light from a mercury arc is collimated by a cylindrical lens and directed through the annular space between the concentric cylinders. The inner of these two cylinders is rotated to produce the desired flow gradient. The light beam then is passed through a polaroid or Nicol prism which can be rotated through any angle, and so to the phototube. This is essentially the birefringence apparatus described by Foster and Lepow[6] except that the polarizer between light source and sample is removed for dichroism measurements.

The photoelectric apparatus consists of various components which will be considered in detail in the following sections. A line operated, regulated high voltage supply provides 600–900 volts for the 931-A phototube used. The output of this tube is amplified with little frequency discrimination, and is then amplified further by an a.c. amplifier tuned to 120 cycles, the frequency of modulation of the mercury arc. The output from the tuned amplifier is rectified, partially opposed when necessary by a stepwise variable voltage obtained from a battery of small dry cells, then is amplified again and measured by a microammeter provided with suitable shunts.

All components are shielded, the shielding being grounded. Coaxial cable is used to make all external connections.

As described, this apparatus was found suitable for our work. In most cases precision has been limited by the nature of the sample and by thermal and reflection effects rather than by the photoelectric apparatus. However, several possible improvements became apparent during construction and use, and will be pointed out in appropriate places.

Light Source.—A General Electric type AH-4 mercury vapor bulb is operated from the 110 volt a.c. line with a suitable transformer. Any line frequency change results in a drop in output of the tuned amplifier. This is usually not serious since the instrument is used mostly for location of minima and maxima, not for measurement of actual light intensity. A power supply with both frequency and voltage regulation would be desirable. In addition to eliminating trouble due to line variations, this would permit operation at a frequency other than a multiple of 60 cycles, reducing pickup of extraneous signals.

High Voltage Supply.—The high voltage supply for the phototube is shown in Fig. 2. Taps are provided at −600, −750 and −900 volts. Switch S_3 and resistance R_1,

(1) Journal paper number J-1852 of the Iowa Agricultural Experiment Station, Ames, Iowa, Project No. 817. Supported in part by a grant from the Corn Industries Research Foundation.

(2) Taken from a thesis submitted by Donald Zucker in partial fulfillment of the requirements for the degree Doctor of Philosophy, Iowa State College, 1950.

(3) Carbide and Carbon Chemical Corp., Oak Ridge, Tenn.

(4) Excellent review articles by J. T. Edsall can be found in *Advances in Colloid Science*, **1**, 269 (1942), and in Cohn and Edsall, "Proteins, Amino Acids and Peptides," Reinhold Publishing Corp., New York, N. Y., 1943, Chapter 21.

(5) R. E. Rundle and R. R. Baldwin, *J. Am. Chem. Soc.*, **65**, 554 (1943).

(6) J. F. Foster and I. H. Lepow, *ibid.*, **70**, 4169 (1948).

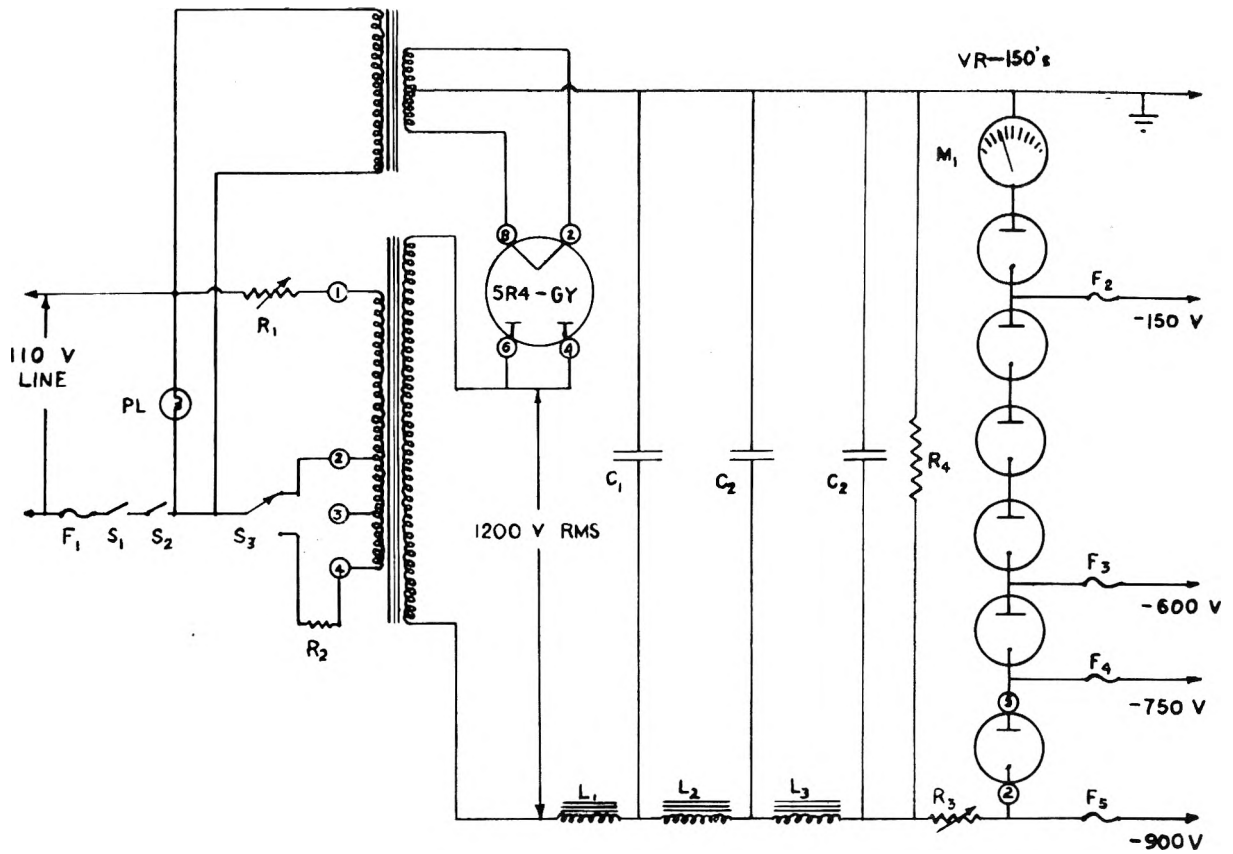

Fig. 2.—High voltage supply: S_1, lid safety switch; S_2, power switch; R_1, 25 ohms, 25 w.; R_2, 10 ohms, 50 w.; R_3, 25,000 ohms, 50 w.; R_4, 1 megohm, 2 w.; C_1, 2 mfd., 2500 v.; C_2, 4 mfd., 1500 v.; C_3, 9 mfd., 1200 v.; L_{1-3}, 16 henries; M_1, 50 ma. meter, approximately 0.035 volt drop at full scale; Pl, pilot light; F_1, 2 ampere fuse; F_2, 5 ma. fuse; F_{3-5}, 1/32 ampere fuses.

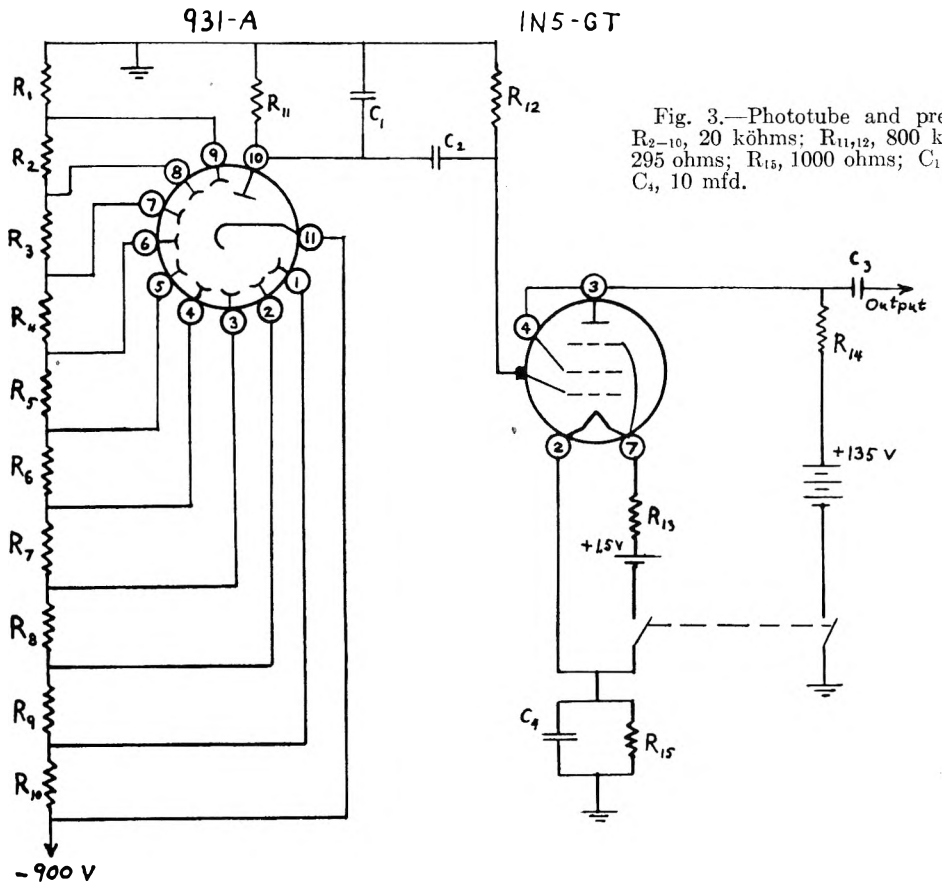

Fig. 3.—Phototube and preamplifier: R_1, 15 köhms; R_{2-10}, 20 köhms; $R_{11,12}$, 800 köhms; R_{13}, 2.6 ohms; R_{14}, 295 ohms; R_{15}, 1000 ohms; C_1, 0.001 mfd.; $C_{2,3}$ 0.01 mfd.; C_4, 10 mfd.

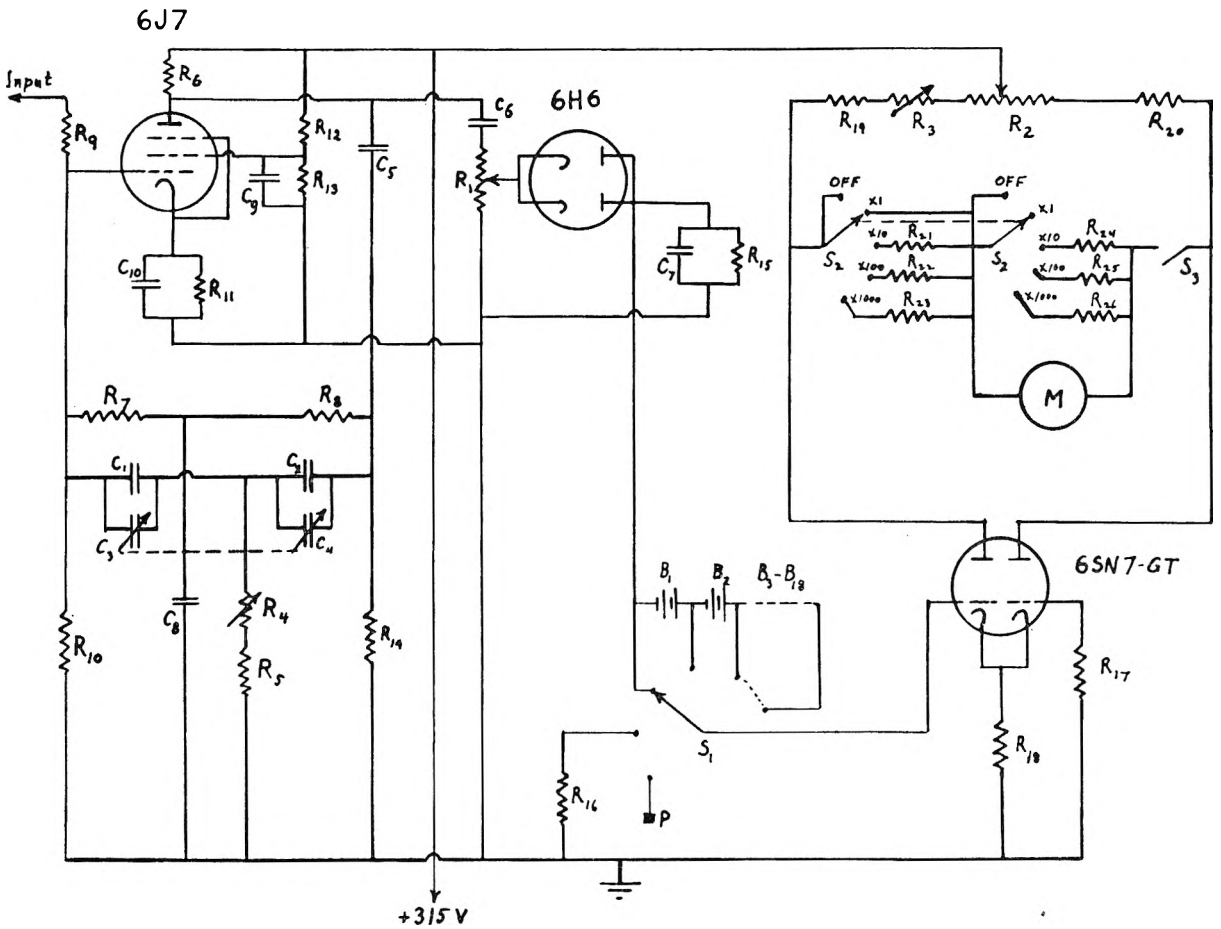

Fig. 4.—Tuned amplifier and output: R_1, 250 köhms; R_2, 10 köhms; R_3, 1000 ohms; R_4, 100 köhms; $R_{5,6}$, 245 köhms, wire; $R_{7,8}$, 490 köhms, wire, ±1%; R_9, 399 köhms, wire; R_{10}, 1 megohm, wire; R_{11}, 2500 ohms, wire; R_{12}, 750 köhms; R_{13}, 1 megohm; R_{14}, 889 köhms; wire; R_{15}, 5.6 megohms; $R_{16,17}$, 300 köhms; R_{18}, 470 ohms; $R_{19,20}$, 7500 ohms; R_{21}, 1588 ohms; R_{22}, 1747 ohms; R_{23}, 1763 ohms; R_{24}, 196 ohms; R_{25}, 18.0 ohms; R_{26}, 1.80 ohms; $C_{1,2}$, 2400 μμf., matched; $C_{3,4}$, 325 μμf., matched; C_{5-7}, 0.01 mfd.; C_8, 7600 μμf.; C_9, 0.05 mfd.; C_{10}, 10 mfd.; M, 50 μa meter; P, external terminal post; B_{1-18}, 3 volt batteries; S_1, grid bias selector; S_2, output factor; S_3, meter cutout.

mounted on the front panel, together with resistance R_3 inside the housing permit adjustment of the V.R. tube current to any desired value. Switch S_2 is a microswitch arranged to open the primary circuit when the lid to the housing is raised.

Phototube and Preamplifier.—The 931-A multiplier phototube, preamplifier and preamplifier batteries are housed together in a fairly air-tight metal box. Sacks of magnesium perchlorate are placed inside as a drying agent, and a drying tube of the same material is attached to a small vent in the case. The on–off switch handle is covered with a thin rubber tube cemented to the case. These precautions keep the air inside dry for the life of the batteries. The circuit for this unit is shown in Fig. 3. Steady signals as from daylight leaks are not transmitted past condenser C_1, and high frequencies are mostly bypassed by C_2. Thus this unit has a slight frequency discrimination. To help produce steadier response, all resistors in this unit are wire. Use of a 1P21 tube instead of the 931-A was considered, but was not found necessary for our purposes.

A piece of exposed and processed film was placed below the phototube, so arranged that it could be placed in or out of the light path by an external control. This film reduces the light transmitted to about 0.12%, and is used to protect the phototube when bright light is encountered.

With the phototube inoperative (high voltage off) a series of small known 60-cycle voltages was applied to its anode, and the output of the preamplifier was measured with an a.c. vacuum tube voltmeter. The voltage gain was found to be about 17, being approximately linear up to an output of at least 9 volts rms which is considerably more than necessary. Testing with an audio oscillator of approximately constant output showed that the gain was essentially the same at 60 and at 120 cycles.

Tuned Amplifier and Output.—The final stages of the apparatus are shown in Fig. 4. The power supply, not shown in the figure, consists of seven Burgess #5308 45-volt batteries in series in a grounded metal box, connected to the amplifier with a shielded cable. A 6.3-volt storage battery provides filament power. A well-regulated, line operated power supply mounted in a separate chassis could perhaps be used, but when such a supply was mounted in the same chassis, considerable difficulty was experienced with unsteady output and pickup of stray 120-cycle signals even though the tuned stage was isolated fairly well from the power supply. This power supply consisted of a 5Y3 used as a full wave rectifier together with a filtering and V.R. tube regulating circuit, and was probably the source of the undesired 120 cycle signal. Battery operation completely eliminated these difficulties. It would be desirable when using battery operation to redesign the output circuit for lower current requirements to lengthen battery life.

The tuned circuit was taken from the circuit of a light scattering apparatus proposed by Zimm[7] without appreciable change except that a two-gang variable condenser is used for tuning. Once the apparatus is tuned, retuning is apparently unnecessary until the power supply battery voltage begins to drop with age and use.

The output from the tuned stage is rectified in a conventional manner, the variable resistor R_1 serving as a gain control. The negative voltage developed by the rectifier circuit is opposed when desired by a positive voltage obtained from dry cells. There are 36 cells giving up to 54 volts in 3-volt steps. As will be shown later the output of the 6J7 is no longer linear with the more extreme signals,

(7) B. H. Zimm, *J. Chem. Phys.*, **16**, 1099 (1948).

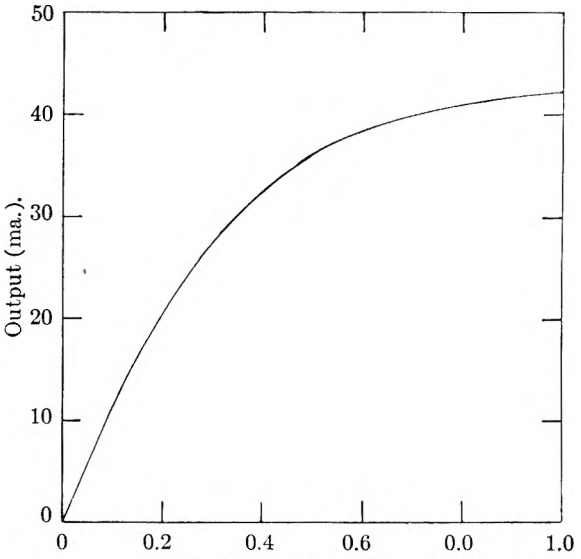

Fig. 5.—Output *versus* light intensity.

but they are nevertheless useful at times. With most of our samples, we have needed 10–40 volts at this point to keep within the limits of the output tube.

Resistors R_2 and R_3 permit meter zero adjustment, and together with the opposing voltages selected by S_1 enable the operator to keep the meter on scale at the highest sensitivity practical (the limit is established by the unsteadiness of the output), even with considerable signal strength. Shunt resistors used with the output meter were selected to give tenfold steps in sensitivity. The two-gang switch used to select the shunt resistance also adds the proper series resistance to maintain the total meter circuit resistance at a constant value to help preserve linearity of this stage.

In the normal operating range the preamplifier was shown to be linear, and the output tube can be kept fairly well in its linear range by selection of the proper grid bias as controlled by S_1. No attempt was made to preserve linearity of the tuned stage, but it is almost certainly the cause of practically all the non-linearity discussed in the next section.

Characteristics.—A known voltage was applied to the input of the tuned amplifier and the output was measured. Since the voltage gain of the preamplifier was already known, and since the phototube current required to produce a given voltage was easily calculated, the current gain of the entire apparatus was readily found. At an equivalent output[8] of 45 milliamperes the gain was about 200,000. From the response data (Fig. 5), we find that the gain in the linear range is about 700,000. With the present apparatus, the usual practical limit of detection of output current change is 10–50 microamperes. Thus phototube current changes of about 10^{-5} to 10^{-4} microampere can be detected, very much less than the dark current value given by the RCA Tube Handbook for this tube.

Apparently phototube random emission is primarily responsible for the instability which limits the useful sensitivity. Admission of a very small amount of light from a flashlight when no other light was present increased the output variations to about 20 μa. from the previous 0.2 μa., showing that random a.c. phototube current is increased with greater signal strength, even though the signal itself is not random.[9] It appears that improvement could be obtained by selection of a tube of lower noise level.

By admitting varying known amounts of light from the mercury arc to the phototube and measuring the equivalent output, the curve of Fig. 5 was obtained. The output is practically linear for the first 10 milliamperes. At 40 ma. sensitivity to change has dropped to about $^1/_4$ the value at low signal strengths.

Applications.—Figure 6 shows the complete curves of output *vs.* analyzer position obtained in the streaming dichroism of a 0.002% tapioca amylose–iodine complex for both senses of rotation at a relatively low rotor speed (450 r.p.m. corresponding to a value of $G\eta/T$ of 5.6). Under such conditions the dichroism is scarcely visible to the eye and the extinction position cannot be measured by direct visual observation. It is obviously possible to measure both the positions of minima and maxima light intensity with a considerable degree of precision with the photomultiplier circuit.

It can be shown geometrically that the extinction position should correspond to one-half the difference in angular position between either adjacent minima or maxima obtained in the two senses of rotation. It will be noted from Fig. 6 that the two values do not check exactly, that is the intensity curves are not symmetrical. This is in general true, especially at low degrees of dichroism. It is presumed that this anomaly is due to errors arising from reflection of

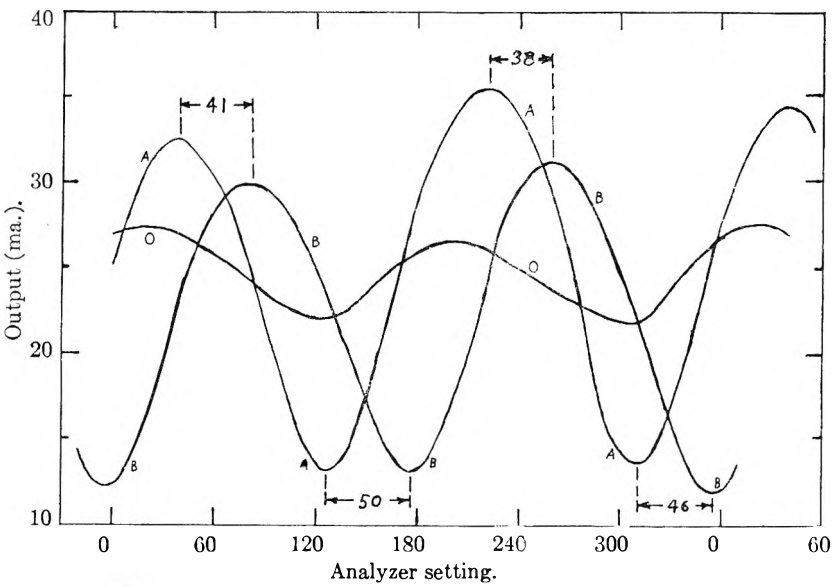

Fig. 6.—Output *versus* analyzer position, streaming dichroism of amylose–iodine complex at 450 r.p.m. and at rest.

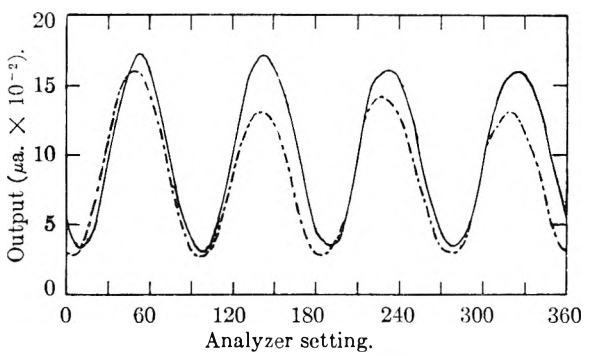

Fig. 7.—Output *versus* analyzer position, streaming birefringence of a denatured ovalbumin solution: ———, A sense; — — —, B sense.

(8) Equivalent output is the actual output given by the output meter plus the product of the grid bias voltage as selected by switch S_1 and the output change produced by a one volt change in this voltage, minus the output with no light to the phototube.

(9) Bennett and Free, *Electronics*, **19**, 116 (1946), state that with this type of tube the noise level is proportional to its d.c. output.

light from the cylinder walls.[10] The practice has been followed of averaging values obtained from maxima and from minima in the hope that this in part corrects for the reflection errors. Comparative studies using polarizer alone, analyzer alone and both polarizer and analyzer in parallel position show no appreciable differences. In practice it is necessary to read only the position of maximum and minimum output without obtaining the complete output curves.

In Fig. 7 are given similar results obtained in the streaming birefringence of a 0.4% solution of acid denatured ovalbumin in 85% glycerol, under conditions where the minima could be measured visually only with some difficulty. Careful comparison of several systems by both methods indicates that at low degrees of birefringence the precision of a given measurement by the electronic method is little if any more precise than a single measurement obtained visually. It is possible, however, to obtain many more data under such conditions electronically without undue eye fatigue so that some advantage is gained. At high degrees of birefringence the visual method is to be preferred.

Again in Fig. 7 one sees that adjacent minima are not exactly 90 degrees apart though alternate minima are 180 degrees apart. This effect is presumed analogous to that mentioned above with regard to the maxima and minima in dichroism. This effect has been regularly observed in birefringence measurements made visually at low degrees of birefringence. It is thought desirable to make measurements at least at two adjacent positions and preferably at all four and to average the results.

(10) NOTE ADDED IN PROOF.—Dr. Martin Goldstein, Department of Chemistry, Harvard, in a private communication has kindly pointed out that he, too, has noted this difficulty and has traced it to birefringence in the mounting glass used in the polarizers. He has been able to reduce the effect by use of strain-free Leitz cover slips.

LENGTH OF THE AMYLOSE–IODINE COMPLEX AS DETERMINED BY STREAMING DICHROISM[1]

BY JOSEPH F. FOSTER AND DONALD ZUCKER[2]

Iowa Agricultural Experiment Station, Ames, Iowa

Received November 16, 1950

The streaming dichroism of amylose–iodine complex has been studied quantitatively in solutions containing only 0.001 to 0.002% amylose. In aqueous solution aggregation is serious. When the complex is prepared in 15% pyridine aggregation is evidently avoided, the length of the resulting complex being shorter than expected on the basis of reported molecular weight data. The systems all appear to be very polydisperse with regard to length; however, the same assumed molecular weight distribution fits data on both orientation angle and degree of dichroism. Results on a series of five subfractionated amylose samples show a positive but surprisingly small correlation between length of the complex and intrinsic viscosity of the parent amylose.

Streaming dichroism in aqueous solutions of the blue amylose–iodine complex has been demonstrated qualitatively by Rundle and Baldwin.[3] The fact that the direction of maximum light absorption was found to be parallel to the direction of orientation was used as substantiating evidence for the helical (molecular) concept of the structure of the complex.[4] Meyer, on the other hand, on the basis of the fact that the intensity of the blue color is proportional to a high power of the amylose concentration, concludes that the complex is micellar.[5]

By making quantitative measurements of the position of preferred absorption as a function of velocity gradient it is possible, in principle, to calculate the length of the orienting unit by application of the orientation theory which has proved so useful in studies of streaming birefringence. The present paper reports results of such studies on the amylose–iodine complex. It appears that in aqueous solution the complex is in general quite highly aggregated, even in solutions containing less than 0.002% amylose. Conditions are found, however, under which strong dichroism can be obtained with apparently little or no aggregation lending further support to the helical hypothesis.

Experimental

Instrument.—The orientation apparatus was the same as has been used previously.[6] The gap width is 0.99 mm., radius of cylinders approximately 3.2 cm. Under conditions approximating true solution of the complex little if any dichroism could be detected visually and under no conditions could the orientation position be measured with any precision by this means. Consequently all measurements were made photoelectrically using a photomultiplier tube and amplifying the circuit as described elsewhere.[7]

Measurement of Orientation Angle.—Measurements were made using an analyzing polaroid without a polarizer. Positions of both maximum and minimum transmitted intensity were determined. Orientation angles were calculated by taking differences between positions of minima (or maxima) obtained in the two senses of rotation. Averages of results obtained from maxima and minima were used in all cases for reasons discussed elsewhere, see ref. 7.[8]

Measurement of Magnitude of Dichroism.—This was measured by introducing both polarizer and analyzer in the crossed position and at 45° to the direction of maximum absorption. The analyzer was then rotated until minimum intensity was attained using the photoelectric circuit. As

(1) Journal Paper Number J-1853 of the Iowa Agricultural Experiment Station, Ames, Iowa. Project 817. Supported in part by a grant from the Corn Industries Research Foundation. Taken from a thesis submitted by Donald Zucker to the Graduate Faculty of Iowa State College in partial fulfillment of the requirements for the Ph.D. degree, July, 1950. Presented before the Colloid Division of the A.C.S. at the Chicago Meeting, Sept., 1950.

(2) Carbide and Carbon Chemical Corp., Oak Ridge, Tenn.

(3) R. E. Rundle and R. R. Baldwin, *J. Am. Chem. Soc.*, **65**, 554 (1943).

(4) R. E. Rundle, J. F. Foster and R. R. Baldwin, *ibid.*, **66** 2116 (1944).

(5) K. H. Meyer, "Natural and Synthetic High Polymers," Interscience Publishers Inc., New York, N. Y., 1942, p. 410.

(6) J. F. Foster and I. H. Lepow, *J. Am. Chem. Soc.*, **70**, 4169 (1948).

(7) D. Zucker, J. F. Foster and G. Miller, THIS JOURNAL, **56**, 166 (1952).

(8) As was pointed out to the author by the referee, the positions of maximum and minimum intensity would be shifted if appreciable birefringence were present and if the principal axes of birefringence and of dichroism did not coincide. It seems safe to conclude that birefringence is negligible in these dilute solutions since concentrations of the order 100 times as great are needed to obtain measurable birefringence in amylose solutions under comparable conditions but without iodine. Moreover it seems probable that optic axes for birefringence and absorption would coincide in this system.

shown by Zocher[9] the difference between the absorption coefficients of the solution in the two directions, $k_1 - k_2$, is related to the angle of rotation of the analyzer δ by the relation

$$k_1 - k_2 = \frac{2 \ln \tan (45 + \delta)}{d}$$

where d is the optical path length.

Preparation of Solutions.—Various solvent systems and conditions were used as will be discussed under Results. It was in all cases necessary to enhance the viscosity of the medium and this was done by adding glycerol. It was found that the concentration of amylose had to be maintained within the limits about 0.001 to 0.003% in the final solution. Below this range the dichroism obtained was too low to measure, above it the transmitted intensity was too low to permit measurements. Best results were obtained in the range 0.0015 to 0.002%. The sample, usually about 1.0 mg., was weighed on a microbalance (or alternatively larger samples weighed and aliquots taken), dissolved in 5.0 ml. of the initial solvent, complexed by adding 0.3 ml. of 0.09 *N* aqueous iodine, in 0.15 *N* KI and finally 50.1 g. of 95% glycerol, previously treated with iodine, added.[10] This yields solution containing approximately 85% glycerol and having a viscosity of 109.9 cp. at 25°. Solutions were then degassed by placing under vacuum (water aspirator) for a few minutes before running into the machine.

Materials Used.—A series of subfractionated amylose samples was kindly provided by Dr. T. J. Schoch. The preparation and some properties of these have been discussed by Lansky, Kooi and Schoch.[11] A sample originally furnished by Dr. Schoch and further purified by Dr. W. Z. Hassid to remove residual amylopectin was furnished through the kindness of Dr. Hassid and is referred to as purified amylose. The sample of amylopectin was prepared in this Laboratory by the usual Pentasol procedure.[12]

Calculations.—Rotary diffusion constants were calculated from extinction angles observed at a given gradient by means of the numerical solutions to the Peterlin and Stuart equation calculated by Scheraga, Edsall and Gadd.[13] Lengths were calculated from the rotary diffusion constants by means of the well-known Perrin equation assuming a prolate ellipsoidal model of axial ratio 50:1.[14]

Results

Potassium Hydroxide Solution as Initial Solvent.—The first studies were carried out by dissolving the samples in 1 *N* KOH and then neutralizing with HCl, either before or after dilution. When there was a delay of even 15 sec. between addition of the iodine and pouring into glycerol evidence of aggregation could be seen in the form of visible clumps. Since it required at least 2 or 3 seconds to mix the solution with the glycerol it seems evident that serious aggregation must have occurred. Aggregation continued, though at a greatly reduced rate, after addition to the glycerol. This was shown by a continued dropping of the orientation angle with time. In 3 or 4 hours the dichroism vanished even though the solution appeared unchanged to the eye. (It is interesting to note that a similarly colored but non-dichroic solution was obtained when the solution was allowed to aggregate 15 seconds prior to being added to the glycerol.)

These solutions yielded calculated lengths in the range 1500 to 2200 Å., the lengths of the various preparations increasing in order of increasing intrinsic viscosity. There was a pronounced dependence of length on velocity gradient indicating polydispersity. The results probably have little significance in view of the probability of aggregation taking place.

Water as Initial Solvent.—It seemed probable that the relatively high salt concentration in the above solutions was at least partially responsible for the aggregation. Solutions were prepared by autoclaving in water and aqueous iodine containing no KI added. The solution of the amylose samples was very incomplete and the blue color faded almost immediately upon adding to glycerol. Addition of KI at this point did not restore the color.

Aqueous Pyridine as Initial Solvent.—Mullen and Pacsu[15] have used aqueous pyridine as a gelatinizing medium for starch. This system has the advantage that the solvent, pyridine, can be removed by boiling without neutralization. The amylose samples did not dissolve fully in 40% (by volume) pyridine at room temperature but dissolved readily when warmed to 80 to 90°. Removal of the pyridine by evaporation with addition of water (to maintain constant volume) yielded solutions which were not visibly aggregated even 2.5 minutes after addition of iodine. Lengths obtained on such solutions were not greatly different from those obtained when 1 *N* KOH was used. By adding the glycerol within a few seconds following addition of iodine fairly good results might be expected by this technique; however, such studies were not pursued since a much better technique was discovered at this point.

It was found that the blue complex could be formed in systems containing pyridine in concentrations up to 15 to 20%. A sample was dissolved in 37% pyridine and diluted with water to give a solution 10% in pyridine. Iodine was added and the solution run into glycerol after 5 seconds. The lengths obtained were far shorter than previously found and there was no evidence for changes taking place during the run. Two more samples were prepared, the elapsed time between addition of iodine and glycerol being 2.5 and 8.0 minutes. The length increased somewhat, the value at an intermediate gradient increasing from about 680 Å. for the sample diluted in 5 sec. to about 850 Å. for the sample which stood 8 minutes. Next 15% pyridine was tried, a series of five samples being allowed to stand various times ranging from a few seconds to 8.5 minutes between addition of iodine and dilution with glycerol. These samples agreed very well, indicating that aggregation had been practically eliminated. Lengths calculated were again very much shorter than those obtained on samples dissolved in KOH.

Results on Purified Amylose.—The most detailed investigation was carried out with the purified amylose sample supplied by Hassid. The

(9) H. Zocher, *Kolloid Z.*, **37**, 336 (1925).

(10) This treatment was effected by adding 0.1 ml. of iodine solution to 50 g. of glycerol and storing overnight. Without this treatment the solutions lost their color within a few hours.

(11) S. Lansky, M. Kooi and T. J. Schoch, *J. Am. Chem. Soc.*, **71**, 4066 (1949).

(12) T. J. Schoch, *Adv. in Carbohydrate Chem.*, **1**, 247 (1945).

(13) H. A. Scheraga, J. T. Edsall and J. O. Gadd, Jr., *J. Chem. Phys.*, **19**, 1101 (1951).

(14) This axial ratio was assumed on the basis that the helices have a diameter of approximately 13 Å. and length in the range 500–1000 Å. The resultant lengths are, however, very insensitive to the assumed value of axial ratio. For example use of an axial ratio of 25 or 100 instead of 50 would affect the calculated lengths by less than 10%.

(15) J. W. Mullen and E. Pacsu, *Ind. Eng. Chem.*, **34**, 1209 (1942).

effects of variation in the technique of preparation of solutions was explored. All of the samples were either dissolved in hot 37% pyridine and diluted to 15%, or dissolved directly in 15% pyridine. Most were heated until dissolved, then cooled quickly and complexed with iodine; several were cooled slowly, and one was cooled quickly, then allowed to stand 11 minutes before complexing. In several cases the iodine was added to the hot solution and then cooled quickly. Excellent agreement was found between results obtained by these different techniques giving confidence that the lengths determined have molecular significance. Typical results in the form of a plot of extinction angle as a function of gradient are shown in Fig. 1. This curve corresponds to lengths of about 1000 Å. at G/T of 2.0 ranging downward to about 600 Å. at 20. The system is evidently far from homogeneous. Also included in this figure is a theoretical curve for an assumed mixture, to be discussed later.

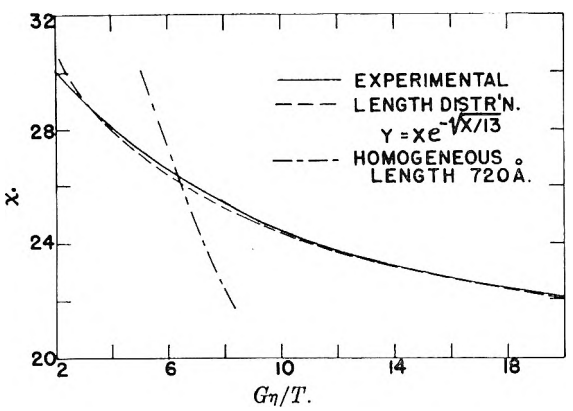

Fig. 1.—Extinction angle as a function of gradient for the iodine complex of the purified amylose of Hassid.

Other Amylose Fractions.—Table I shows calculated length values at two gradients for five of

TABLE I

RELATION BETWEEN LENGTH OF IODINE COMPLEX DETERMINED BY STREAMING DICHROISM AND INTRINSIC VISCOSITY OF AMYLOSE. SUBFRACTIONATED AMYLOSE PREPARATIONS OF SCHOCH

Preparation	ηi	Length (Å.) at $G\eta/T$ = 3.8	Length (Å.) at $G\eta/T$ = 19
C-146 A(11c)	0.80	800	515
C-148/150 A(13b)	1.12	860	560
P-5/6A(8b)	1.37	830	580
P-5/6A(7b)	1.78	900	650
T-7/9A(15b)	2.98	1000	740

the amylose subfractions supplied by Schoch and further results on one of these are given in Fig. 2. All of these runs were carried out in the same manner, that is by dissolving the amylose in hot 15% pyridine, cooling quickly, adding the iodine and pouring immediately into glycerol. It is seen in Table I that there is a qualitative dependence of length on intrinsic viscosity but the dependence is slight, very much less than would be anticipated.

Effect of Amylopectin.—Since it seems unsafe to assume that one ever has amylose completely freed of branched material it was desirable to test the

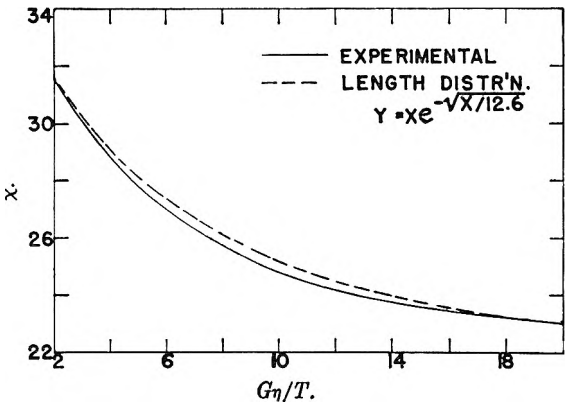

Fig. 2.—Extinction angle of the iodine complex of potato amylose subfraction P-5/6-A(8b) as a function of gradient.

effect of adding amylopectin to the purified amylose. It was found that a mixture containing 95% amylopectin and only 5% amylose (the amylose concentration being similar to that used in the other runs) gave results indistinguishable from those on the amylose alone provided the iodine was added to the cooled solution. When the iodine was added to the hot solution there was poor color development and little dichroism. This tendency was also exhibited by the Schoch amylose samples which had not been exhaustively freed of amylopectin. No reasonable explanation for this behavior has been found.

Magnitude of the Dichroism.—In Fig. 3 are plotted calculated values of "reduced dichroism" (in arbitrary units) plotted as a function of gradient for the sample P-516A (7b). These values were calculated by dividing the observed dichroism at a given gradient by the orientation factor f corresponding to the extinction angle measured at the corresponding gradient. In all cases where the calculations have been made it has been found that the same length distribution function which fits the orientation curves fits also the plots of dichroism *vs.* gradient. The fact that the orientation angles and dichroism results are mutually consistent lends some confidence that the phenomenon being

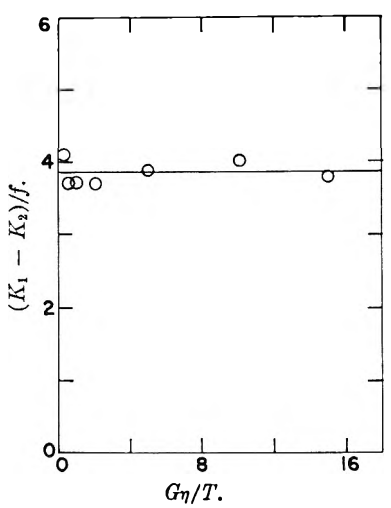

Fig. 3.—Reduced dichroism (arbitrary units) of the iodine complex of potato amylose subfraction P-5/6-A(7b) as a function of gradient.

studied is one of simple orientation, uncomplicated by changes in the shape of the orienting units.

Results on Whole Starch and Amylose Prepared Therefrom.—The fact that amylopectin was without effect on the observed dichroism results made it of interest to study whole starches without fractionation. The possibility of determining the degree of polymerization of the amylose in a starch sample without fractionation is intriguing. A sample of whole potato starch gave lengths ranging from 1070 at a $G\eta/T$ of 3.8 down to 760 at 19. The major amylose fraction which was prepared from this starch in the usual manner by pentasol precipitation gave values only slightly shorter, ranging from 1010 to 720. A second amylose fraction which separated with pentasol on prolonged standing was appreciably shorter as might be expected, the range being 910 to 650.

Discussion

In the crystalline state the amylose–iodine complex is reported to have a periodicity, along the chain, of 7.9 Å., corresponding to one turn of the helix or six glucose units.[16] In other words the length of the complex should be roughly 1.3 Å. per glucose unit if it behaves as a rigid rod. The purified amylose preparation supplied by Hassid is reported by him to have a number average D.P. of 900 as determined osmotically. The observed lengths thus appear at first glance to be fairly reasonable although somewhat low.

However, since the systems appear to be very inhomogeneous and since the lengths determined by streaming dichroism would be very much weighted by the longer molecules it would be expected that the average lengths so determined would be much greater than calculated from the number average D.P. Attempts to fit the results by assuming different polydisperse systems indicate that even the Flory or Kuhn type random distribution functions do not provide sufficient polydispersity. Good fit is obtained (Fig. 1) with the empirically assumed mixture having the distribution

$$y = xe^{-\sqrt{x}/13}$$

where y is the weight of material having a length x (in ångströms).

The number average D.P. calculated from this distribution would be of the order 100, very much less than that reported by Hassid. Considerable improvement in agreement could be made by assuming that the shorter component molecules, which do not contribute appreciably to the dichroism anyway, are removed in fractionation. On the other hand there is no obvious reason why there should be a continuous distribution of this type and it seems more probable there are two or more fractions differing considerably in length, one or all fractions consisting of some type of more or less random mixture.

Several explanations of the short lengths have been considered. One possibility is that there is some high molecular weight material which does not combine with iodine, possibly amylopectin-type material. Again, the major component might be somewhat branched so that while it combines with iodine the resultant complex is shorter than would be calculated on the basis of a linear structure. Hassid has found his sample to have an average of almost exactly one non-reducing terminus per molecule which, if true, clearly eliminates both of these possibilities.

The difficulty of obtaining molecular solutions of amylose might also be invoked. If solution is in all cases incomplete, the osmotic molecular weights would be high, while the present results might be low (if it is assumed that the shorter molecules dissolve more readily).

It is possible that the complex is not completely filled, there being left over free glucose units at each end. The tendency of amylose to saturate itself with iodine[4] militates against this hypothesis. Another closely related possibility is that the complex consists of "hinged" segments. In this case the short lengths would be explained and the fact that only small differences are found between samples differing considerably in intrinsic viscosity would be more readily understandable. On the other hand it might be expected that such a structure would undergo a stretching effect at higher gradients, an effect which is apparently absent as indicated by the good correlation between orientation and magnitude of dichroism. A segment structure would be expected to lead to sharpening of the length distribution and would thus not account for the apparent heterogeneity.

Acknowledgment.—Grateful appreciation is expressed to Drs. T. J. Schoch and W. Z. Hassid for generously donating amylose fractions. Thanks are due Dr. Dexter French for many helpful discussions and for suggesting the segment hypothesis.

(16) R. E. Rundle and D. French, *J. Am. Chem. Soc.*, **65**, 1707 (1943).

STREAMING BIREFRINGENCE BEHAVIOR OF SOME SUBFRACTIONATED AMYLOSE PREPARATIONS[1]

BY JOSEPH F. FOSTER AND DONALD ZUCKER[2]

Department of Chemistry, Iowa State College, Ames, Iowa

Received March 16, 1951

Results of streaming birefringence measurements, over a wide gradient range, are presented for 13 subfractionated amylose preparations covering a range of almost fourfold in intrinsic viscosity. Evidence is presented to indicate that 12 of these, which were prepared by fractional crystallization with octyl alcohol, are contaminated with appreciable amounts of amylopectin. The mean lengths measured at various gradients agree, in general, within 6 to 20% with the lengths of the iodine complexes of the corresponding preparations previously measured by streaming dichroism. It is concluded that the configuration in the solvents used, namely glycerol-containing ethylenediamine and aqueous KOH, is most probably the helical one rather than a random coil. The product of the rotary diffusion constant times the intrinsic viscosity, in the case of the various fractions, is constant within experimental error. The degree of birefringence measured under fixed conditions of concentration, gradient, viscosity and temperature is directly proportional to the intrinsic viscosity of the preparation. The linear increase of birefringence over an extended range of gradient cannot be explained on the basis of the theory developed for rigid molecules and indicates stretching of the molecules to be significant at higher gradients.

Streaming birefringence has been demonstrated in solutions of amylose in ethylenediamine–glycerol solutions by Foster and Lepow.[3] The interpretation of those results was complicated by uncertainty as to the degree of heterogeneity of the preparations. The present contribution presents similar results on thirteen subfractionated amylose preparations of known intrinsic viscosity. Evidence is given to indicate that the amylose molecule in glycerol-containing aqueous KOH or ethylenediamine has substantially the same (helical) configuration as in the iodine complex. The previous indication that the streaming gradient effects some stretching of the amylose molecule is further substantiated.

Experimental

Amylose Fractions.—The amylose fractions used were prepared by Dr. T. J. Schoch of the Corn Products Refining Company by fractional precipitation with octyl alcohol. The method of fractionation and some properties of the fractions have been reported by Schoch and co-workers.[4] The code numbers used in the present paper are those of Schoch so that further details on any given fraction can be obtained from his paper.

It cannot be claimed that these fractions are homogeneous. However, since the fractional precipitation depends on complex formation between the amylose and the alcohol, and since there is good reason to believe that there is an increasing stability of the amylose complexes with increased molecular weight, it seems probable that these fractions are at least comparable in homogeneity to the usual fractionated polymers which are prepared by a non-specific phase separation.

One of Schoch's potato fractions, namely, P-7/9A(17e), was further purified by Dr. W. Z. Hassid of the University of California and shown by him to be free of amylopectin.[5]

Methods.—Weighed samples of amylose were dissolved in ethylenediamine (Eastman Kodak Co., 95–100%). Best results were attained by placing the ethylenediamine in a weighing bottle and the amylose in the lid so that mixing and stoppering of the bottle could be accomplished simultaneously. Agitation could thus be started before excessive clumping had taken place. After solution was substantially complete glycerol was added to a concentration of 70% (by weight), the solution filtered or centrifuged (20,000 *g*) to remove any undissolved lumps, and then placed under vacuum (water aspirator) for 15–30 minutes to remove dissolved gas.

The orientation measurements were made in the same concentric apparatus used previously.[3,6] Measurements were made, with crossed polaroids, of the four minima in each sense of rotation at a given rotational speed, and the extinction angle χ[7] obtained by averaging the results. Measments were made over a wide gradient range, usually five- to tenfold at a given temperature. In addition measurements were made over a broad temperature range, usually at 0.5–2.0°, 25° and 38°. This provided a range in solvent viscosity of about 0.48 to 7.8 poises so that the total range in $G\eta/T$[8] covered was usually about twenty-fold. There was overlap of $G\eta/T$ values at the various temperatures and the results were quite consistent when either χ or Δ (the magnitude of the birefringence in terms of the rotation measured on the Senarmont compensator) were plotted as functions of $G\eta/T$. Other details of measurement were similar to those used previously.[3]

The values of the rotary diffusion constant θ and of the orientation distribution function F corresponding to a given value of χ were determined by means of the tables computed by Scheraga, Edsall and Gadd.[9] Molecular lengths were calculated from values of the rotary diffusion constant by means of the well known Perrin equation assuming a rigid prolate ellipsoidal structure of axial ratio 50:1.[10]

Results and Discussion

Concentration Studies.—The effect of amylose concentration on the orientation angle was determined in the case of two of the amylose fractions. Potato amylose P-5/6A(7b) was studied at concentrations of 3.0, 1.5, 0.8 and 0.2%. There was a progressive decrease in apparent length with decreasing concentration, but the difference between 1.5 and 0.8% solutions was only about 10% over most of the gradient range, and the difference between 0.8 and 0.2% much less. The corn sample C-148/150A(13b) was run at 0.8, 0.4 and 0.2% concentration with practically identical results at all concentrations. Most of the measurements reported were carried out at approximately 1.0% amylose concentration since it was felt that the slight errors in calculated length resulting from interaction would be less than errors which might

(1) Journal paper number J-1918 of the Iowa Agricultural Experiment Station, Ames, Iowa. Project 817. Supported in part by a grant from the Corn Industries Research Foundation. Taken from a thesis submitted by Donald Zucker to the Graduate Faculty in partial fulfillment of the requirements for the Ph.D., July, 1950.

(2) Carbide and Carbon Chemical Corp., Oak Ridge, Tenn.

(3) J. F. Foster and I. H. Lepow, *J. Am. Chem. Soc.*, **70**, 4169 (1948).

(4) S. Lansky, M. Kooi and T. J. Schoch, *ibid.*, **71**, 4066 (1949).

(5) A. L. Potter and W. Z. Hassid, *ibid.*, **73**, 593 (1951).

(6) J. F. Foster and D. Zucker, THIS JOURNAL, **56**, 170 (1952).

(7) The angle between the optic axis and the tangent to the cylinders.

(8) The velocity gradient in sec.$^{-1}$ times viscosity in poises divided by the absolute temperature.

(9) H. A. Scheraga, J. T. Edsall and J. O. Gadd, Jr., *J. Chem. Phys.*, **19**, 1101 (1951).

(10) The calculated length is very insensitive to the assumed value of axial ratio.

TABLE I

EXTINCTION ANGLES AND DERIVED DATA FOR AMYLOSE SUBFRACTIONS AT THREE GRADIENTS

Fraction	Intrinsic viscosity[a]	D.P.$_w$[b]	$G\eta/T = 5$ χ	$\eta\theta/T$	$(\eta\theta/T)\eta_i$	$G\eta/T = 10$ χ	$\eta\theta/T$	$(\eta\theta/T)\eta_i$	$G\eta/T = 20$ χ	$\eta\theta/T$	$(\eta\theta/T)\eta_i$
C-146-A(11c)	0.80	480	26.5	0.98	0.78	26.0	1.9	1.5	25.0	3.4	2.7
C-146-A(1b)	0.94	570	25.2	.86	.81	23.8	1.5	1.4	21.9	2.5	2.3
C-148/150-A(13b)	1.12	680	20.1	.53	.59	20.5	1.11	1.2	20.1	2.1	2.4
P-5/6-A(12d)	1.34	810	21.1	.59	.79	18.7	0.91	1.2	17.5	1.6	2.1
P-5/6-A(12c)	1.37	830	22.5	.68	.93	19.9	1.04	1.4	18.0	1.7	2.3
P-5/6-A(8b)	1.37	830	20.8	.57	.78	18.6	0.89	1.2	17.5	1.6	2.2
C-148/150-A(13a)	1.65	990	19.2	.45	.74	18.1	.85	1.4	17.0	1.5	2.5
P-5/6-A(7b)	1.78	1070	20.9	.58	1.05	18.0	.84	1.5	..	..	..
P-5/6-A(2a)	1.78	1070	17.4	.39	0.69	15.8	.65	1.2	15.5	1.24	2.2
P-5/6-A(4b)	1.86	1120	16.7	.36	.67	15.0	.58	1.1	..	..	..
T-7/9-A(15c)	2.31	1390	13.3	.22	.51	13.3	.45	1.0	13.9	0.99	2.3
T-7/9-A(15b)	2.94	1770	12.3	.19	.56	13.1	.44	1.3	..	..	..

[a] Measured in 1 *N* KOH (ref. 4), units, cc./g. [b] Degree of polymerization calculated from intrinsic viscosity using the relation = 1.66×10^{-3} (D.P.) from Potter and Hassid.[b]

arise due to reflection errors in more dilute solutions.

Effect of Amylopectin.—Most of the samples developed a slight haze during the measurements and the 3.0% solution of the potato amylose mentioned above developed a distinct precipitate. Since similar difficulties had been encountered in attempts to study amylopectin it was thought that the samples might be contaminated by small amounts of this branched polysaccharide.

It was also observed that in most cases the extinction angles were initially low at very low gradients, rose to a maximum and then decreased in the normal fashion with further increase in gradient. This behavior is indicative of the presence of a small amount of a very readily orientable component, again possibly amylopectin.

To check on this possibility runs were made on the specially purified amylose sample of Hassid. This sample did not show appreciable clouding and showed a normal extinction angle curve (Fig. 1) without the initial rise (with the possible exception of the point at lowest gradient). Measurements were also made on this material with increasing proportions of added amylopectin. These solutions showed development of a precipitate and, as shown in Fig. 1, clearly showed the development of the abnormal type of extinction angle curve. It should be pointed out that the percentage of amylopectin given in this figure corresponds to the amount actually added. The actual percentage present is appreciably less due to the loss of the insoluble precipitate since the runs were carried out consecutively on the same amylose sample by centrifuging out the precipitate and adding further amylopectin solution.

It is apparent that the effect of amylopectin is not appreciable at gradients above about twice the value at which the peak occurs in the curve. The lengths reported in this paper correspond to such values and it seems probable that they are little affected by the presence of amylopectin.

Correlation between Rotary Diffusion Constant and Intrinsic Viscosity.—The intrinsic viscosities of the amylose subfractions have been determined by Schoch in 1 *N* aqueous KOH. Table I summarizes data on the extinction angle and the rotary diffusion constant (multiplied by the solvent viscosity in poise and divided by absolute temperature) for each sample as determined at three different gradients.

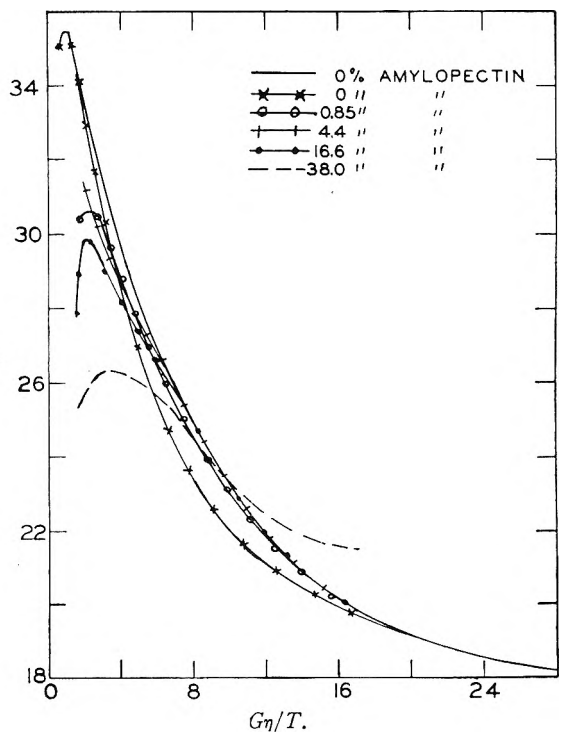

Fig. 1.—Experimental χ *vs.* $G\eta/T$ curves for the purified amylose preparation of Hassid and the effect of addition of varying proportions of amylopectin.

An interesting theory developed recently by Riseman and Kirkwood[11] predicts that the product of the rotary diffusion constant and the intrinsic viscosity should be inversely proportional to the molecular weight of a polymer. This relationship should be the same, except for a numerical factor, whether the molecules are rigid or flexible. This product has been calculated and is shown also in Table I for the various fractions at the three gradients. At the lower two gradients there may be a slight drop in the product with increasing intrinsic viscosity (molecular weight) but the effect is scarcely outside the limits of the experimental error.

(11) J. Riseman and J. G. Kirkwood, *J. Chem. Phys.*, **18**, 512 (1950).

At the highest gradient, however, the product is remarkably constant. This surprising result is not necessarily in conflict with the Riseman–Kirkwood theory, since this theory could be expected to apply only at very low gradients. Due to the extreme weighting by the longer components in streaming birefringence extrapolation of the data to low or zero gradients would appear of doubtful significance. This would be particularly true in the present case where contamination by amylopectin is suspected, but would be true in any case where the samples were even slightly polydisperse. It is thus very difficult to compare experiment and theory in the case of streaming birefringence.

Correlation with Length of Amylose–Iodine Complexes.—The length of the iodine complexes of several of these amylose preparations has been measured by streaming dichroism.[6] Table II summarizes the lengths measured under the two

TABLE II

COMPARISON OF LENGTHS OF AMYLOSE FRACTIONS AS MEASURED BY STREAMING BIREFRINGENCE WITH LENGTHS OF THE IODINE COMPLEXES MEASURED BY STREAMING DICHROISM

	Length (A) at					
	$G\eta/T = 5$		$G\eta/T = 10$		$G\eta/T = 20$	
Fraction	Amylose	I_2 Complex	Amylose	I_2 Complex	Amylose	I_2 Complex
Hassid	780–820	750	720–750	690	660	590
C-146-A(11c)	820	740	660	630	540	500
C-148/150-A(13)b	1000	800	790	660	640	560
P-5/6-A(8b)	980	780	850	670	700	580
P-5/6-A(7b)	970	860	860	740	..	..
T-7/9-A(15b)	1420	950	1070	850	..	..

sets of conditions for six of the fractions at three gradients. The similarity is rather striking. In all cases the lengths of the uncomplexed amylose is slightly longer but in most cases not over 20% and in several cases less than 10%. The agreement is particularly good in the case of the Hassid preparation, a result which is to be expected since the amylopectin contaminant in the other preparations would tend to weight the results, in the case of the uncomplexed amylose, toward longer lengths. The poorest agreement is obtained with the tapioca fraction at low gradient, a result which may very probably be due to amylopectin. Also it should be

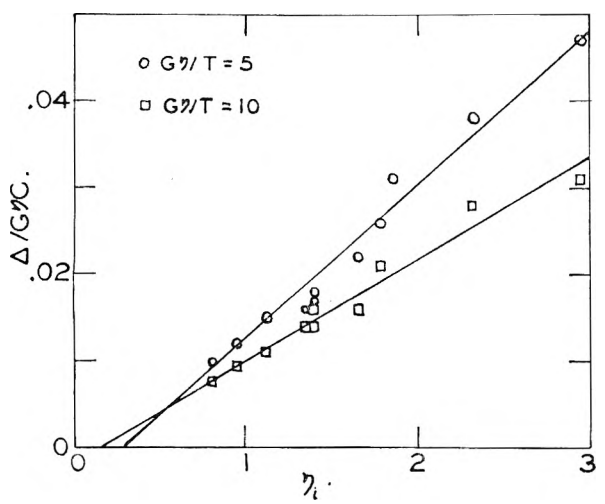

Fig. 2.—Relationship between birefringence and intrinsic viscosity of the fractions.

pointed out that while the present results were obtained at nearly 1.0% concentration the dichroism measurements were made at 0.002% or lower concentration. The difference in length may be accounted for by interaction effects in the present studies.

This somewhat surprising result would indicate amylose in either ethylenediamine–glycerol or aqueous KOH–glycerol (see below) solvents to have essentially the same configuration as in the iodine complex, in other words the helical configuration. It would seem most surprising if the randomly coiled configuration would have so nearly the same length as the helical one. In this connection it is interesting that Dombrow and Beckmann[12] have concluded, on the basis of ultracentrifugal and viscosity studies, that amylose triacetate in methyl acetate also exists in the helical configuration. It appears possible that this may be the normal configuration of this polymer in solution, a fact which would explain the unusually high rigidity indicated by intrinsic viscosity studies.[13]

Correlation between Magnitude of Birefringence and Intrinsic Viscosity.—In Fig. 2 there is plotted, as a function of intrinsic viscosity of the fraction, the value of Δ (measured at two gradients) divided by the corresponding values of G, η and C. The birefringence under a given set of conditions is seen to be a linear function of the intrinsic viscosity. In view of the linear relation, found by Potter and Hassid,[5] betweeen intrinsic viscosities in aqueous KOH and degree of polymerization this implies also a linear relation between birefringence and molecular weight.

In the case of randomly coiled polymers Kuhn and Kuhn[14] have predicted a linear relationship between the "double refraction number" ($\Delta/G\eta C$ in the limit as both G and C approach zero) and the degree of polymerization. (It is not practical in the present case to take the limiting slope at very low gradient due to the influence of the amylopectin contaminant.) In the case of a rigid polymer proportionality to a higher power of molecular weight would be expected, probably the third power.[14] These results thus appear to be at variance with the above conclusion that amylose does not exist in a random configuration.

Gradient Dependence of the Rotary Diffusion Constant and Birefringence.—Table I shows an increase in apparent rotary diffusion constant (corresponding to a decrease in length) with increasing gradient in all cases. This is to be expected in inhomogeneous preparations. Actually the fractions do not appear to be quite as polydisperse by this criterion as by application of streaming dichroism to their iodine complexes.[6] In the case of the Hassid sample application of the Flory type distribution function gave an overcorrection. However, interpretation is complicated by the possibility of molecular stretching, discussed below.

A typical plot of the magnitude of the bire-

(12) B. A. Dombrow and C. O. Beckmann, THIS JOURNAL, **51**, 107 (1947).

(13) J. F. Foster and R. M. Hixon, *J. Am. Chem. Soc.*, **66**, 557 (1944).

(14) W. Kuhn and H. Kuhn, *Helv. chim. acta*, **26**, 1394 (1943); *J. Coll. Sci.*, **3**, 11 (1948).

fringence (in terms of Δ/C, the rotation of the Senarment compensator divided by the concentration C) as a function of velocity gradient is shown in Fig. 3. The nature of the curve is quite different from that expected in the case of simple orientation of rigid molecules as was previously pointed out.[3] The birefringence is theoretically equal to the product of two functions, of which one depends only on the optical properties of the solute molecules and solvent and the other only on the degree of orientation. The latter function, F, can be calculated from the orientation angle.[9] Thus it should be possible to calculate a "reduced birefringence" by dividing the measured birefringence by the value of the orientation function at the corresponding gradient. In the case of amylose it was shown[3] that this calculation yields values which increase almost linearly with gradient, a result which was interpreted as probably due to molecular stretching. It is now apparent that this does not necessarily follow, in a heterogeneous system, due to the fact that the orientation angle and the birefringence are weighted differently by the different components.[15]

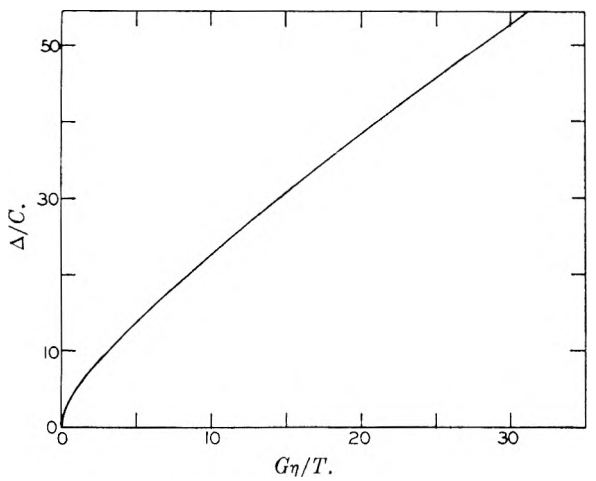

Fig. 3.—Dependence of the magnitude of birefringence on velocity gradient for corn amylose fraction C-146-A(11c).

It is not possible to estimate, with any confidence, the heterogeneity in the amylose samples from the orientation angle results because of the possibility of stretching. To attempt to resolve these two factors, the following approach has been used. Streaming dichroism results on the iodine complexes of some of these amylose samples have been reported.[6] In that case both orientation angle and magnitude of dichroism could be explained adequately on the basis of rigid particles and it seems almost certain that the iodine complex must be fairly rigid. It then becomes of interest to ascertain whether the molecular weight (length) distribution functions which fit those data are also in accord with the flow birefringence results.

In Fig. 4 there is plotted, as a function of gradient, the reduced birefringence, Δ/F, uncorrected for molecular weight distribution, for one amylose preparation. For comparison there is also plotted the curve which would be expected theoretically for rigid molecules having the length distribution which fits the data on the iodine complex of this fraction. The latter curve is normalized to fit the experimental curve at $G\eta/T = 2$. It is apparent that this distribution, which is a broad one,[6] is by no means capable of accounting for the large increase in reduced birefringence with increasing gradient. This result can be best explained on the basis of molecular stretching. Thus if the molecular configuration is indeed the helical one it must be a rather loose helix which is subject to deformation by the gradient.

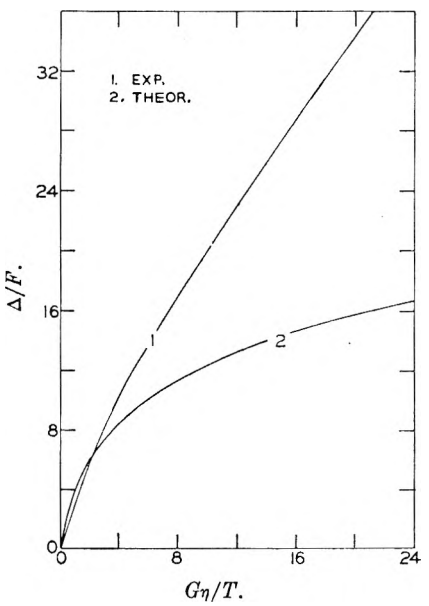

Fig. 4.—Dependence of the reduced birefringence on gradient. For explanation of experimental and theoretical curves see text.

Aqueous Potassium Hydroxide as Initial Solvent.—A few measurements were made by dissolving the amylose in 1.0 N KOH, in place of ethylenediamine, and then diluting with glycerol. Sample P-5/6A(7b) was studied at 0.2% concentration, sample C-148/150-A(13b) at 0.2 and 0.8%. All results were within 10%, in terms of calculated length, of the values obtained in ethylenediamine at similar amylose concentration and at the same value of $G\eta/T$.

Acknowledgments.—The authors are deeply indebted to Drs. T. J. Schoch and W. Z. Hassid who supplied the amylose fractions used in the study.

(15) M. Wales, THIS JOURNAL, **52**, 976 (1948).

THE PERIODIC LAW IN MATHEMATICAL FORM

BY REINO HAKALA

Department of Chemistry, Syracuse University, Syracuse, N. Y.

Received November 3, 1950

Desiderata of the most useful form of periodic table are given. Attention is focused on Janet's table[1] which best meets these requirements. A compact array that describes the order in which the subshells of atoms are filled is given. It most clearly brings out the systematics involved and Janet's table can be derived directly from it. The "general observation that alternate members of a valency group in the periodic table show the greatest chemical resemblance"[2] is provided with a firm mathematical foundation by an analysis of this array. Equations relating the atomic numbers of the alkaline-earth elements and helium (because of its similar electronic configuration) to the principal and orbital quantum numbers of their subshells of highest energy are derived on the basis of an extrapolation of the order in which the subshells of atoms are filled. An equation that describes the author's version of Janet's table is derived. It relates the atomic numbers of the elements to their positions in the table. Various forms of it are given. The periodic law is given mathematical expression. This relates the atomic numbers of the elements to their positions in any periodic table that is based upon the electron configurations of the elements. Fundamentally, then, it relates atomic numbers to electron configurations. (The equation neglects changes in configuration due to the exceptional stability of completed, half-completed, and empty shells. However, these changes occur in only 10% of the known elements and do not always occur when expected, *e.g.*, W has the configuration $6s^25d^4$ instead of $6s5d^5$.) An introduction is given to the determination of general mathematical expressions for both periodic and non-periodic properties of the elements and their compounds. A method is outlined by which expressions may be found that relate several properties to one another independent of electron configurations and positions in periodic tables. A simple way of evaluating the arbitrary constants of functions $\phi(y) = a_0 + a_1 f(x) + \ldots + a_n[f(x)]^n$ is outlined. A known formula of finite differences is generalized to give other formulas which find application in evaluating these arbitrary constants.

The periodic law is without doubt the most important generalization in chemistry. ("The periodic series is a brilliant and adequate means of producing an easily surveyed system of facts which by gradually becoming complete will take the place of an assemblage of the known facts."—Ernst Mach) It is therefore not surprising that so many modifications of the periodic table have been devised, and that so many attempts have been made to obtain a mathematical expression for the periodic law.

Only a few of these tables, however, have found widespread use; and, unfortunately, the many attempts to express the periodic law mathematically were none too successful—mainly because they were based on the old idea that the properties of the elements are periodic functions of their atomic weights.

Since the periodicity in chemical and physical properties arises from a periodicity in the electronic structures of the elements, the mathematical representation of the periodic law must be based on the mathematical analysis of a periodic table founded on the electronic structures of the elements.

Many such tables have been published, in various shapes, both in two dimensions and three. Some preserve the atomic number continuity while others do not. The simplest and most logical of these would be expected to have the simplest shape, to occur in two dimensions only, and to preserve the atomic number continuity. Charles Janet[1] was the first to publish a table that meets these requirements.[3] Slight modifications of it have been published recently by Simmons[4] and by Gibson.[5]

(1) C. Janet, "La Classification Hélicoïdale des Éléments Chimiques," Fascicle No. 4, Beauvais, Imprimerie Départmentale de l'Oise, Nov. 1928.

(2) J. D. Main Smith, "Chemistry and Atomic Structure," Ernest Benn, Ltd., London, 1924, p. 126.

(3) Janet's work was brought to the author's attention last year by Clifton P. Idyll, of Adelphi College, Garden City, Long Island, New York, to whom the author is very grateful.

(4) L. M. Simmons, *J. Chem. Education*, **24**, 588 (1947).

(5) D. T. Gibson, *Chem. and Ind.*, 12 (1948).

The author's version, brought up to date, appears in Table I. This is now to be analyzed.[6]

Two Series of Elements.—When the atomic number sequence of the alkaline-earth family (including helium because it has an electronic structure characteristic of the alkaline-earth elements) is subjected to differencing, the familiar sequence 2, 8, 8, 18, 18, 32 results as the first order difference. Besides indicating the number of elements contained in each period of the table, this sequence, because of its twofold nature, indicates that the atomic number sequence consists of the terms of two separate sequences added alternately together. These separate sequences are 2, 12, 38, 88 and 4, 20, 56.

Differencing these separate sequences should give a clue as to the nature of the function that relates the terms. However, when a table of differences is constructed, it is seen that there are not enough terms present to arrive at a column of constants. Hence additional terms are needed to continue the analysis. These can be obtained by extrapolating the sequence in which the subshells of atoms are filled

				1s
				2s
			2p	3s
			3p	4s
		3d	4p	5s
		4d	5p	6s
	4f	5d	6p	7s
	5f	6d	7p	8s
5g	6f	7d	8p	9s
6g	7f	8d	9p	10s

(This array is read from top to bottom and from left to right, *i.e.*, 1s, 2s, 2p, 3s, 3p, 4s, 3d, ...) The resulting atomic number sequences are 2, 12, 38, 88, 170, and 4, 20, 56, 120, 220 (the *g* shell can hold no more than 18 electrons), and the difference tables are

(6) Part of the author's seminar on "The Periodic Law," Department of Chemistry, Columbia University, Oct. 31, 1946.

Z	ΔZ	Δ²Z	Δ³Z		Z	ΔZ	Δ²Z	Δ³Z
4					2			
	16					10		
20		20			12		16	
	36		8			26		8
56		28		and	38		24	
	64		8			50		8
120		36			88		32	
	100				82			
220					170			

The third order difference is a constant in both cases, which means that the function relating the terms is a polynomial of the third degree

$$Z = a + bx + cx^2 + dx^3$$

and that the values of the argument, x, are equi-spaced. A glance at Table I shows that x can be chosen as equal to $n + l$, whence

$$Z = a + b(n + l) + c(n + l)^2 + d(n + l)^3$$

where Z is the atomic number of the element whose subshell containing the last-added electron[7] has the principal and orbital quantum numbers n and l, and a, b, c and d are constants to be evaluated. The last of these, d, can be found directly by inspection.

Z	$(n + l)$	$(n + l)^2$	$(n + l)^3$
2	1	1	1
12	3	9	27
38	5	25	125

whence the needed equations are

$$2 = a + b + c + 1/6$$
$$12 = a + 3b + 9c + 27/6$$
$$38 = a + 5b + 25c + 125/6$$

The coefficients are found to be

$$a = 1/2,\ b = 5/6,\ c = 1/2, \text{ and } d = 1/6$$

whence, upon simplification

$$Z = [3 + 5(n + l) + 3(n + l)^2 + (n + l)^3]/6$$

for *odd* values of $n + l$.

Similarly, for *even* values of $n + l$

$$Z = [2(n + l) + 3(n + l)^2 + (n + l)^3]/6$$

The above procedure can be repeated for any column of elements in the table, and *two* equations, one for *odd* values of $n + l$, and the other for *even* values, will be found to result in each case.[9] Furthermore, these equations are all polynomials of the third degree.

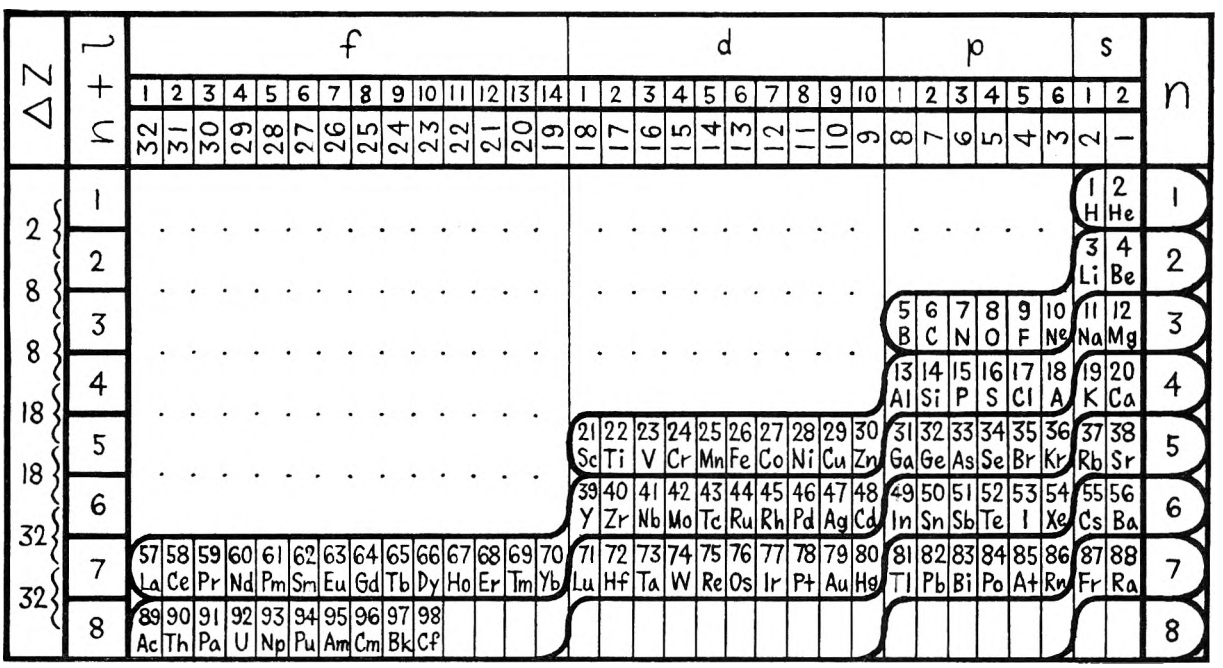

In the general case, where $y = a_0 + a_1x + \cdots + a_nx^n$, for equi-spaced values of the argument

$$a_n = (1/n!)[\Delta^n y/(\Delta x)^n]^8$$

In the two cases above

$$d = (1/3!)(8/2^3) = 1/6$$

To determine the three remaining unknowns, a, b and c, three simultaneous equations are needed. The values necessary in setting up these equations for the sequence 2, 12, 38, 88 are

Equation for the Table.—It is not necessary to work out all of these equations, and then relate them, to find the expression for the periodic law. In Table I, $Z + C - 1$, where Z is the atomic number of any given element and C is the number of the column in which it occurs, is a constant along any one $n + l$ level and is equal to the atomic number of the alkaline-earth element that occurs in that $n + l$ level. Hence substituting $Z + C - 1$ for Z in the above equations for the alkaline-earth elements, and then solving for Z of the given element yields the equations for the entire table

$$Z = [9 - 6C + 5(n + l) + 3(n + l)^2 + (n + l)^3]/6$$

(7) *I.e.*, the subshell of highest energy. Henceforth, for simplicity's sake, it will be called the "last-filled" subshell (although it need not be *closed*).

(8) This expression is readily verified by taking successive derivatives of x^n:

$(d/dx)x^n = nx^{n-1}$; $(d/dx)^2x^n = n(n-1)x^{n-2}$; $(d/dx)^3x^n = n(n-1)(n-2)x^{n-3}$; $\cdots$; $(d/dx)^nx^n = n(n-1)(n-2)\cdots 3\cdot 2\cdot 1 = n!$ And $(d/dx)^nx^{p<n} = 0$.

(9) Main Smith[2]: "It is . . . a general observation that alternate members of a valency group in the periodic table show the greatest chemical resemblance." (Examples are given.)

for *odd* values of $n + l$, and

$$Z = [6 - 6C + 2(n + l) + 3(n + l)^2 + (n + l)^3]/6$$

for *even* values of $n + l$.

Upon multiplying out, collecting terms, and factoring, these become

$$Z = (n + l)(n + l + 1)(n + l + 2)/6 + (n + l + 1)/2 + 1 - C$$

for *odd* values of $n + l$, and

$$Z = (n + l)(n + l + 1)(n + l + 2)/6 + 1 - C$$

for *even* values of $n + l$.

These are the equations for Table I.[10] Since they differ by $(n + l + 1)/2$, they can be combined by the use of a term that has this value for odd values of $n + l$, and equals zero for even values. The resulting single equation that describes Table I is

$$Z = (n + l)(n + l + 1)(n + l + 2)/6 + (n + l + 1)[1 - (-1)^{n+l}]/4 + 1 - C$$

where C and $n + l$ are, respectively, the number of the column and the period in Table I in which the element of atomic number Z occurs (and $0 \leqslant l \leqslant n-1$).

General Equation.—The above equation applies only to Table I. If we can find C in terms of the orbital quantum number, l, of the last-filled subshell (the block of Table I in which the element occurs) and the number of electrons, N, contained in that subshell, we can substitute this relationship for C in the above equation and obtain the completely general form.

C is a measure of the difference in the number of electrons which the atom in question and the alkaline-earth element in the same $n + l$ level possess. The last-filled subshell of any given element will contain a maximum of $2(2l + 1)$ electrons. The subshell corresponding to the next block at its right in Table I (*i.e.*, in reverse spectroscopic order) will contain a maximum of $2[2(l - 1) + 1]$ electrons (where l is still the orbital quantum number of the last-filled subshell of the given element), and the next subshell $2[2(l - 2) + 1]$ electrons, and so on to the end of the $n + l$ level. The sum of these terms is $2(l + 1)$.[2] This expression gives the number of the column with which the block corresponding to l begins; *i.e.*, the column containing the element of lowest Z in that block.

If we subtract $2(2l + 1)$ from $2(l + 1)^2$ and add 1, we obtain the expression $2l^2 + 1$, which gives the number of the terminal column of the block in Table I corresponding to l.

If, instead of subtracting $2(2l + 1)$, we subtract the number of electrons contained in the last-filled subshell and add unity as before, we obtain the number of the column in which the given element occurs

$$C = 2(l + 1)^2 - N + 1$$

When this relationship is substituted for C in the equation for Table I, the general equation results

$$Z = (n + l)(n + l + 1)(n + l + 2)/6 + (n + l + 1) \times [1 - (-1)^{n+l}]/4 - 2(l + 1)^2 + N \quad (\& \; 0 \leqq l \leqq n - 1)$$

This is the periodic law in mathematical form.

Extension to Specific Physical and Chemical Properties.—Since the periodicity in chemical and physical properties is, in the last analysis, due to a periodicity in the electronic structures of the elements, there are without doubt mathematical relationships between the chemical and physical properties of elements and of compounds and the electronic structures of the elements.

The most straightforward way to find these relationships, for both periodic and non-periodic properties, is in a fashion analogous to the above derivation of the periodic law, provided that sufficiently extensive tables of accurate data exist: the first step is to determine empirical (or, sometimes, derived) equations for the property, for each column, in terms of Z or $n + l$; the next step is to compare these equations to find the completely general relationship. In the most favorable case, the equations will vary only by having a different value for a particular constant. Then a relationship must be found between the value of this constant and the corresponding column number. Substitution of this relationship for the constant in one of the equations for the property (for any column, since they differ only in the value of this single constant) then gives the completely general relationship. In less favorable cases, the value of more than one constant will vary. The procedure in these cases is the same as in the case where the value of but one constant varies. If the *form* of the equation varies from one column to the next, then a general form must be devised which includes each of the equations found for the columns as special cases.

It is not always a simple matter to determine the relationship between the dependent and independent variables from the experimental data. Theory sometimes prescribes the form of the equation. Otherwise, the shape of the graph obtained by plotting the experimental data is used as a clue. One should try a semi-logarithmic plot of the data first because this form occurs quite frequently. If the form of the equation is guessed at or is still not known, a difference table of the data or of some function of the data may provide the answer. Worthing and Geffner,[11] list eleven commonly occurring forms and outline the procedure followed in setting up difference tables for them. These authors also discuss other methods of approach and append a list of helpful references. Probably the best single reference on finite differences and other techniques useful in this sort of work is that of Whittaker and Robinson.[12] Milne's book on finite

(10) The reduced cubic equations are

$(n + l + 1)^3 + 2(n + l + 1) = 6(Z + C - 1)$ for *odd* values of $n + l$ and $(n + l + 1)^3 - (n + l + 1) = 6(Z + C - 1)$ for *even* values; and the roots are

$$n + l + 1 = (3(Z + C - 1) + \{[3(Z + C - 1)]^2 + 8/27\}^{1/2})^{1/3} + (3(Z + C - 1) - \{[3(Z + C - 1)]^2 + 8/27\}^{1/2})^{1/3}$$

for *odd* values of $n + l$, and

$$n + l + 1 = (3(Z + C - 1) + \{[3(Z + C - 1)]^2 - 1/27\}^{1/2})^{1/3} + (3(Z + C - 1) - \{[3(Z + C - 1)]^2 - 1/27\}^{1/2})^{1/3}$$

for *even* values. These are shown here because of their beautiful symmetry

(11) A. G. Worthing and J. Geffner, "Treatment of Experimental Data," John Wiley & Sons, Inc., New York, N. Y., 1943, p. 61, Table II.

(12) E. T. Whittaker and G. Robinson, "The Calculus of Observations," Blackie & Sons, Ltd., London, 1944.

differences[13] is also of considerable value, not only for its textual material, but also because of its excellent appendix of reference texts, tables and bibliographies. Once the form of the equation has been found, the arbitrary constants must be evaluated. The method of least squares is the most accurate. All of the mathematics references mentioned above indicate the procedure to be followed. A much simpler method, applicable in many cases, is given below.

If it is desired to relate two properties to one another, then they may be found in terms of Z and C or $n + l$ and C, the two expressions solved for C, and equated. As a result, one of the properties will be expressed as a function of the other property and Z or $n + l$. Most likely, there will be *two* equations: one for *odd* values of $n + l$ (and corresponding values of Z), and the other for *even* values. Equally well, instead of solving the two expressions for C, they may be solved for Z or $n + l$ (in whichever terms they were derived) and equated. In this case, one of the properties will be expressed as a function of the other property and C. Then the relationship between C, l and N, solved for C, may be substituted for C to give one property in terms of the other and l and N.

Two such equations relating one property to another and to Z, $n + l$, or C may be solved for Z, $n + l$, or C (whichever occurs) and equated to give an expression relating four properties to one another *independent* of Z, n, l, C and N. If the two equations relating one property to another and to Z, $n + l$, or C have one of their properties in common, the final expression will relate three properties to one another independent of Z, n, l, C and N. The relationships between various properties may thus be found.

Simple Method of Evaluating the Arbitrary Constants.—The author has worked out a very simple way of finding the values of the arbitrary constants of functions $\phi(y) = a_0 + a_1 f(x) + \ldots + a_n[f(x)]^n$ and equations that can be reduced to this form. It does not provide the most accurate results but is nevertheless quite satisfactory for many purposes.

If the original function, $y = g(x)$, is not itself a polynomial, it must first be transformed into one, $\phi(y) = \phi[g(x)] = a_0 + \ldots + a_n[f(x)]^n$. Then $\phi(y)$ is plotted against $f(x)$ as carefully as possible. Equi-spaced values of $f(x)$ and corresponding values of $\phi(y)$ are then taken from the graph. As many pairs of these values are taken as there are arbitrary constants to evaluate. (Constants to be evaluated: $a_0, a_1, \ldots, a_n$. Pairs of values taken: $f(x)_1$, $\phi(y)_1$; $f(x)_2$, $\phi(y)_2$; $\ldots$; $f(x)_{n+1}$, $\phi(y)_{n+1}$). These pairs of values are used in setting up equations

$$\begin{aligned}
\phi(y)_1 &= a_0 + a_1 f(x)_1 + \ldots + a_n[f(x)_1]^n \\
\phi(y)_2 &= a_0 + a_1 f(x)_2 + \ldots + a_n[f(x)_2]^n \\
&\vdots \qquad\qquad \vdots \qquad\qquad \vdots \\
\phi(y)_{n+1} &= a_0 + a_1 f(x)_{n+1} + \ldots + a_n[f(x)_{n+1}]^n
\end{aligned}$$

which are solved simultaneously to give the values of the arbitrary constants. Only n equations need be set up if the value of $\phi(y)$ for $f(x) = 0$ is known, for then $\phi(y) = a_0$. Pairs of values that are as widely distributed over the graph as possible should be chosen. If only a few pairs are needed, the evaluation of the arbitrary constants should be repeated, possibly several times, using different pairs of values each time, and the results averaged. (This much of the method is not new.)

The equations can be solved simultaneously very simply when they are set up using *equi-spaced* values of $f(x)$. *The functions* $\phi(y)$ and $a_0 + a_1 f(x) + \ldots + a_n[f(x)]^n$ *are subjected to differencing, e.g.*

$$\begin{array}{lll}
\phi(y) & & \\
\phi(y)_1 & \Delta\phi(y) & \\
 & \phi(y)_2 - \phi(y)_1 & \Delta^2\phi(y) \\
\phi(y)_2 & & \phi(y)_3 - 2\phi(y)_2 + \phi(y)_1 \\
 & \phi(y)_3 - \phi(y)_2 & \vdots \qquad\qquad \vdots \qquad\qquad \text{etc.,} \\
\phi(y)_3 & \vdots \qquad\qquad \vdots & \phi(y)_{n+1} - 2\phi(y)_n + \phi(y)_{n-1} \\
\vdots & \phi(y)_{n+1} - \phi(y)_n & \\
\phi(y)_{n+1} & &
\end{array}$$

until a *single* value, the "residue," is reached, *and the residues of the two series of differencing operations equated.* This yields the value of a_n which is then substituted into the first n equations. (These are the simplest ones.) The equations are then simplified and again differenced, giving the value of a_{n-1}. The process is repeated (taking care each time to use *exactly* as many equations as there are unknowns!) until all of the arbitrary constants have been evaluated.

In differencing $a_0 + a_1 (x) + \ldots + a_n[(x)]^n$, all of the coefficients except a_n eventually vanish: as is well known, the nth order difference of a polynomial of degree n is equal to a constant while the nth order difference of a polynomial of degree n is zero. This simplifies the computation considerably: the result of equating the residues of the first two series of differencing operations is

$$\Delta^n\phi(y) = a_n n![\Delta f(x)]^n$$

from which the value of a_n may be directly obtained; the result of equating the next two series of differencing operations is

$$\Delta^{n-1}\{\phi(y) - a_n[f(x)]^n\} = a_{n-1}(n-1)![\Delta f(x)]^{n-1}$$

from which the value of a_{n-1} may be readily obtained; $\ldots$; in general

$$\Delta^{n-p}\{\phi(y) - a_n[f(x)]^n - a_{n-1}[f(x)]^{n-1} - \ldots - a_{n-p+1}[f(x)]^{n-p+1}\} = a_{n-p}(n-p)![\Delta f(x)]^{n-p}$$

The entire process of setting up the equations and solving them simultaneously by differencing is summarized in the following formula (which was derived from the above general formula)

$$\sum_{r=0}^{n-p} \frac{(-1)^r}{(n-p-r)!r!} \left\{ \phi(y)_{n-p-r+1} \sum_{t=n-p+1}^{n} a_t[f(x)_{n-p-r+1}]^t \right\} = a_{n-p}[\Delta f(x)]^{n-p}$$

In using this formula, a_n is found first, then a_{n-1}, etc.

Specific examples of the application of this method to the determination of general mathematical expressions for both periodic and non-periodic properties of the elements and their compounds will be published later together with the results of the least-squares method for comparison.

(13) W. E. Milne, "Numerical Calculus," Princeton University Press, Princeton, N. J., 1949.

THE RETENTIVITY OF CHARCOALS BY THE APPROXIMATE ISOTHERM METHOD. THE EFFECT OF MOISTURE ON THE RETENTIVITY OF METHYL ETHYL ETHER, NEOPENTANE AND METHANOL[1]

BY D. H. VOLMAN AND G. J. DOYLE[2]

Division of Chemistry, College of Agriculture, University of California, Davis, California

Received November 6, 1950

The retentivity of charcoals has been studied using methyl ethyl ether, neopentane and methanol by determining the approximate desorption isotherms of dry and 80% R.H. equilibrated samples in air stream. The presence of moisture on the charcoal has a highly deleterious effect on the retentivity of neopentane, insoluble in water, an appreciable lessening of retentivity for methyl ethyl ether, somewhat soluble in water, and does not impair the retentivity of methanol, completely miscible with water. The approximate isotherm in the presence of water was shown to be derivable from the approximate dry isotherm and the water desorption isotherm.

The term "retentivity" has been variously defined but is generally meant to designate the ability of the adsorbent to hold gas previously adsorbed when the adsorbent is subsequently exposed to an air stream. When an amount of gas insufficient to penetrate an adsorbent is adsorbed, this will distribute itself equally throughout the bed, given enough time, and the partial pressure of gas coming off initially on subsequent exposure to an air stream will be the equilibrium or isotherm value. For large deviations from equilibrium conditions, this may be considerably in error.

Allmand and Manning[3] have shown that it is possible to evaluate retentivity by an approximate isotherm method. A charcoal bed is saturated with vapor at a given partial pressure and then is degassed with adsorbate-free air, the effluent concentration being followed continuously. An approximate isotherm so obtained will be somewhat lower than a true isotherm since the exit end of the bed will contain a greater concentration of adsorbate than the entrance end. However, an isotherm thus obtained may be used to predict the initial exit concentration of adsorbate from a charcoal bed which has previously taken up a known amount of vapor. Such isotherms are then of particular importance in evaluating the performance of gas mask cannister charcoals.

In this study we have used compounds which differ in chemical structure and solubility in water in order to determine the effect of moisture on retentivity. The charcoals used were representative of types in use over the past few years.

Materials and Method

Methyl ethyl ether was prepared by the reaction of sodium ethylate and dimethyl sulfate. The product was finally purified by distillation in a Podbielniak column of 120 theoretical plates. Neopentane was prepared by the reaction of tertiary butyl chloride and methylmagnesium chloride. The methanol was J. T. Baker C.P. absolute.

Six charcoal samples were used; their designation and source follow: A, an air activated coal charcoal from the Pittsburgh Coal and Chemical Company; B, an air activated coconut charcoal from Northwestern University; C, a steam activated wood charcoal from the Carlisle Lumber Co.; D, a zinc chloride activated wood charcoal from the National Carbon Co.; E, an air activated coal charcoal from Northwestern University; F, a whetlerite[4] made by impregnation of charcoal E.

For the approximate isotherm 3-cm. beds of the charcoal were saturated with the gas in an air stream at a concentration of 240 mg./l. at a flow rate of 500 cm. per min. When equilibrium was reached the supply of vapor was cut off, and the bed was allowed to desorb in the air stream. The concentration of gas in the effluent stream was followed continuously. For the experiments under humid conditions, the charcoal was first humidified in position by exposing it to the air stream at 80% R.H. for ten hours previous to the charging process and then carrying out the charging and the desorption in an 80% R.H. stream of air.

The gas flows were established by techniques commonly used for tube testing of charcoal. The analysis of the gases was carried out by means of the hot wire analyzers developed for combustible gas.[5] Three different ranges of sensitivity were available: The first measured the region 0–1 mg./l. with an accuracy of ∓0.004 mg./l.; the second measured the region 0–5 mg./l. with an accuracy of ∓0.02 mg./l.; and the third measured the region 0–50 mg./l. with an accuracy of ∓0.2 mg./l. Results were recorded continuously on General Electric recording millivoltmeters.

Three charcoal tubes could be accommodated at one time. The tubes were water thermostated at 25°. They were 2.75 sq. in. cross section, and a total flow of 1.375 l./min. resulted in a linear velocity of 500 cm./min.

Results and Discussion

Figures 1–6 show the approximate dry and moisture condition approximate isotherms for the three gases used. As a criterion for retentivity one may then take the amount retained for a given effluent concentration in the desorption process.

The dry isotherm for charcoal F, a whetlerite, is not greatly different from that of charcoal E, its base, in the case of both neopentane and methyl ethyl ether. However, the whetlerite retains considerably more methanol than the base at the lower pressures and has some retentivity even at zero pressure. This indicates that some chemical reaction is occurring between the impregnant and methanol. However, when the charcoal is humidified, the impregnant is no longer available for abnormal retentivity of the methanol since it has presumably entered into chemical reaction with water; hence, the isotherm on humidified impregnated charcoal is lower than the base in keeping with the results with methyl ethyl ether and neopentane.

Figure 7 is indicative of the type of result which may be predicted from the approximate isotherm. Three of the charcoals were charged with methyl ethyl ether for 75 minutes at a concentration of 1.0

(1) The experimental work reported here was carried out on a contract between Northwestern University and N.D.R.C. Division 10. This paper is taken from the report of the authors, O.S.R.D. No. 5236, April 23, 1945, unclassified June 15, 1949.

(2) Department of Chemistry, University of Indiana, Bloomington, Indiana.

(3) Allmand and Manning, *J. Soc. Chem. Ind.*, **47**, 369T (1928).

(4) For definition see P. H. Emmett, *Chem. Revs.*, **43**, 69 (1948).

(5) Latimer, Ruben, Norris and Gwinn, O.S.R.D. No. 3048, Dec. 3, 1943.

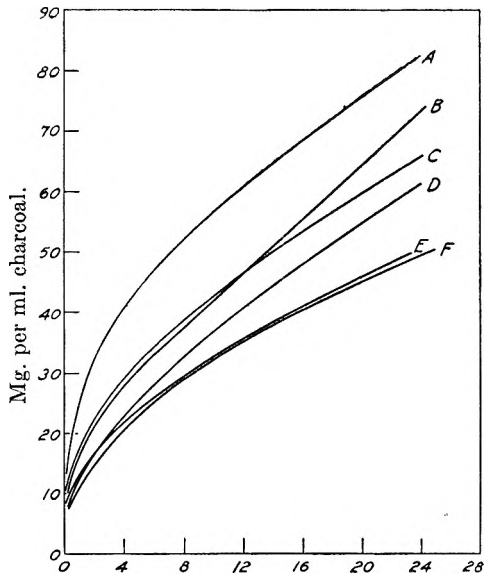

Fig. 1.—Methyl ethyl ether approximate isotherms; dry, 25°.

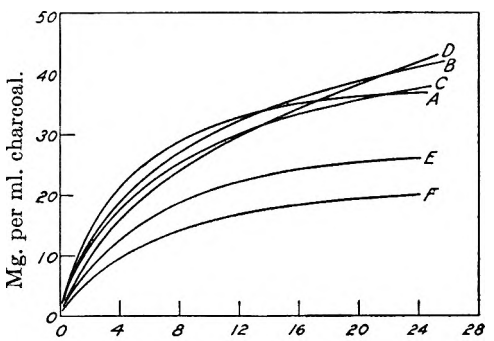

Fig. 2.—Methyl ethyl ether approximate isotherm; 80% R.H., 25°.

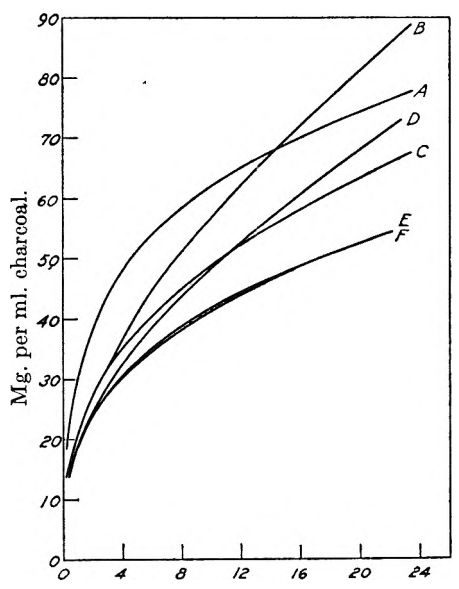

Fig. 3.—Neopentane approximate isotherms; dry, 25°.

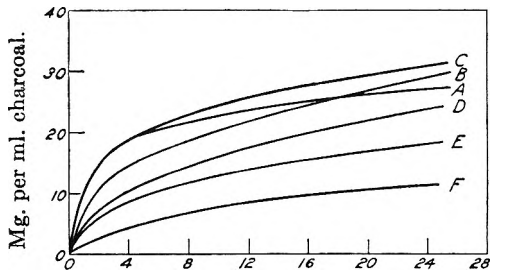

Fig. 4.—Neopentane approximate isotherms; 80% R.H., 25°.

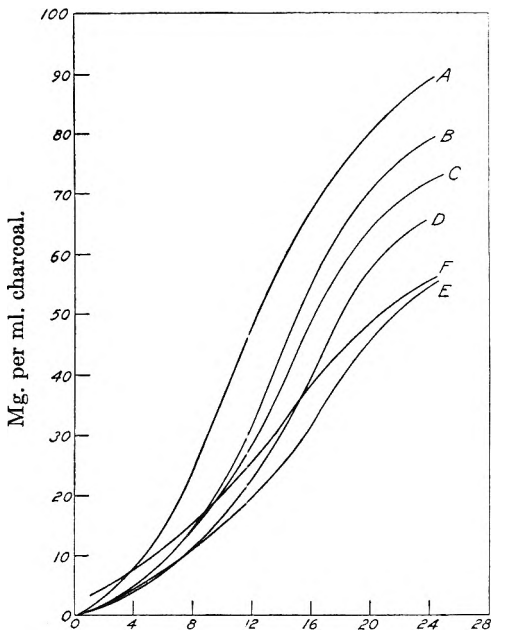

Fig. 5.—Methanol approximate isotherms; dry, 25°.

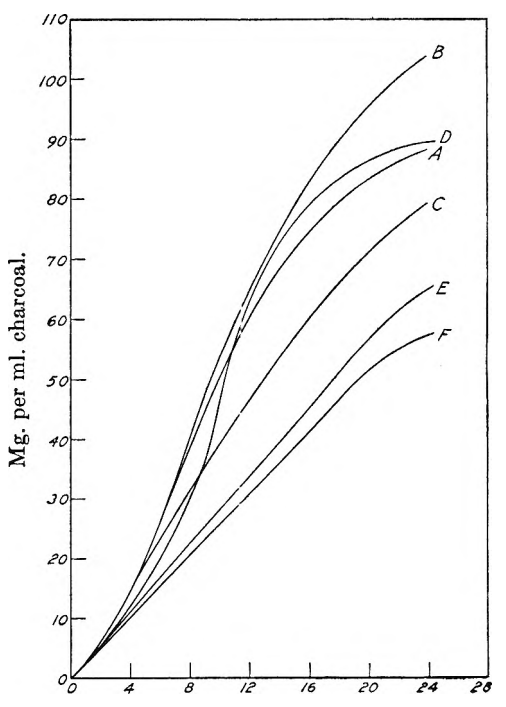

Fig. 6.—Methanol approximate isotherms; 80% R.H., 25°.

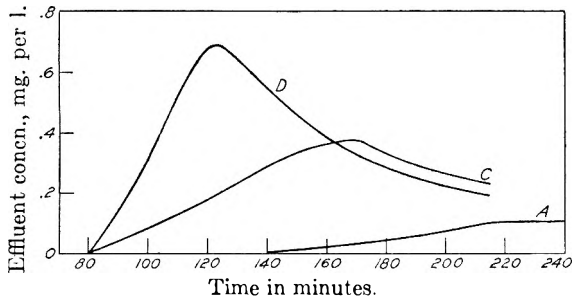

Fig. 7.—Desorption curves; methyl ethyl ether, 25°; 3-cm. beds charged for 75 minutes at 1 mg. per liter.

mg./l. Desorption was initiated at the end of this charging period, and the time axis includes the charging time of 75. If it is assumed that redistribution occurs on the charcoal prior to desorption then, from Fig. 1, the maximum concentration possible in the effluent are 0.16, 0.40 and 0.90, respectively. Since no time was allowed for redistribution it was to be expected that the actual peak concentration would be somewhat lower and would occur after a longer time interval for the charcoals with greater capacities. Thus the maximum concentrations reached were 0.10, 0.36 and 0.69, respectively, after times of 220, 170 and 122 minutes.

The presence of water on the charcoal might be expected to play a dual role as far as retentivity is concerned. First, there is a reduction in retentivity caused by a joint occupation by water and the other adsorbate of space formerly available to the adsorbate alone. Second, there is an increased retentivity due to solubility of the adsorbate in the water on the charcoal. The totality of these two effects would determine the net change exhibited by the 80% R.H. isotherm as compared to the dry isotherm. Thus retentivities of less than the dry case are expected for gases not soluble in water, and retentivities greater than the dry case are possible for gases soluble in water. A comparison of the wet and dry isotherms obtained shows that for neopentane, insoluble in water, there is a larger reduction in retentivity than there is for methyl ethyl ether, somewhat soluble in water. The retentivity of methane, highly soluble in water, is increased under humid conditions, especially at lower pressures.

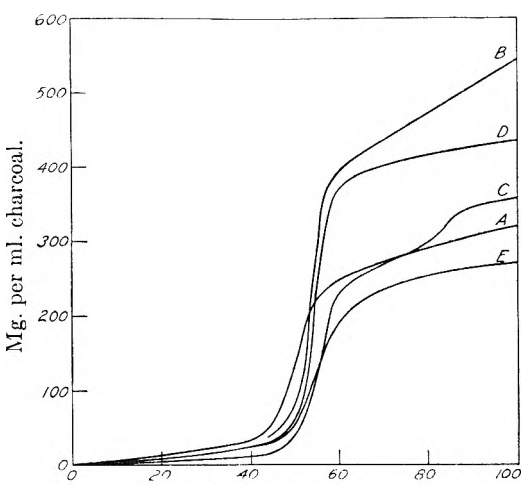

Fig. 8.—Water desorption isotherms, 25°.

TABLE I

CONSTANTS FOR THE EVALUATION OF METHYL ETHYL ETHER ISOTHERMS AT 80% R.H; $k_2 = 0.00253$

Charcoal	N_0 Values for various concentration $C = 24$, $k_3 = 0.250$, mg./ml.	$C = 10$, $k_3 = 0.443$, mg./ml.	$C = 1$, $k_3 = 0.350$, mg./ml.	S_0, mg./ml
A	83	56.5	25.3	288
B	75	42.0	16.7	470
C	67	45.0	17.5	294
D	62	36.8	13.1	414
E	50	32.8	13.3	252

TABLE II

COMPARISON OF CALCULATED AND EXPERIMENTAL 80% R.H. ISOTHERM VALUES FOR METHYL ETHYL ETHER

Charcoal	$C = 24$ Calcd. mg./ml.	$C = 24$ Exptl. mg./ml.	$C = 10$ Calcd. mg./ml.	$C = 10$ Exptl. mg./ml.	$C = 1$ Calcd. mg./ml.	$C = 1$ Exptl. mg./ml.
A	38	37	32	32	9.5	9.0
B	46	42	31	30	7.0	8.0
C	34	38	27	28	7.0	7.0
D	41	42	27	27	5.5	5.5
E	28	26	21	21	5.0	4.5

TABLE III

CONSTANTS FOR THE EVALUATION OF METHANOL ISOTHERMS AT 80% R.H; $k_2 = 0.0072$

Charcoal	N_0 Values for various concentrations $C = 24$, $k_3 = 0.40$, mg./ml.	$C = 10$, $k_3 = 0.78$, mg./ml.	$C = 4$, $k_3 = 1.00$, mg./ml.	S_0, mg./ml.
A	89	37	7.5	288
B	79	22	5.0	470
C	72	21	5.0	294
D	66	17	4.0	414
E	55	15	4.5	252

TABLE IV

COMPARISON OF CALCULATED AND EXPERIMENTAL 80% R.H ISOTHERM VALUES FOR METHANOL

Charcoal	$C = 24$ Calcd. mg./ml.	$C = 24$ Exptl. mg./ml.	$C = 10$ Calcd. mg./ml.	$C = 10$ Exptl. mg./ml.	$C = 4$ Calcd. mg./ml.	$C = 4$ Exptl. mg./ml.
A	86	88	50	50	16	15
B	113	104	51	54	18	15
C	80	79	37	39	14	15
D	98	89	43	46	16	12
E	66	65	30	28	12	11

It is possible to treat the effect of moisture on the isotherm by a quantitative treatment using data of the dry isotherm and the water sorption isotherms.

Assume that the total sorption consists of two parts: (1) Sorption by displacement of water $N_1 = k(S_0 - S_E)$, where k is a coefficient of change from weight of water displaced to weight of adsorbate adsorbed; S_0 is wt. of water on the charcoal in the absence of the adsorbate; S_E is wt. of water on the charcoal in the presence of the adsorbate.

(2) Sorption by solution of the adsorbate in water, $N_2 = k_2CS_E$, where k_2 is a Henry's law constant and C is concentration of adsorbate in the gas phase. Then $N_H = k(S_0 - S_E) + k_2CS_E$, where N_H is the total sorption of the adsorbate on the humidified charcoal.

Now postulate that the amount of water displaced is proportional to the amount of adsorbate sorbed under dry conditions or, $S_0 - S_E = k_1N_0$ where N_0 is the amount of adsorbate held under dry conditions. Then, $N_H = kk_1N_0 + k_2C(S_0 -$

k_1N_0), and, $N_H = (kk_1 - k_1k_2C)\,N_0 + k_2CS_0$. This may be written in the form $N_H = k_3N_0 + k_2CS_0$ at a given concentration, and we further assumed that k_2 is fixed for all concentrations but that k_3 is not.

The constants have been evaluated and a comparison of calculated and experimental values for methyl ethyl ether and methanol has been made, Tables I–IV. The values of S_0 were taken from water desorption isotherms, Fig. 8, and the N_0 values were taken from the dry approximate isotherms.

SOLUBILITIES OF CALCIUM AND STRONTIUM NITRATES IN MONOALKYL ETHERS OF ETHYLENE GLYCOL

BY KENNETH A. KOBE AND WILLIAM L. MOTSCH[1]

Department of Chemistry, University of Texas, Austin, Texas

Received November 20, 1950

The solubilities and phase relationships for calcium nitrate and strontium nitrate in methyl, ethyl and butyl Cellosolves have been determined. Butyl Cellosolve is the most selective of these solvents for the dissolution of calcium nitrate from mixtures containing strontium nitrate.

Strontium nitrate is used extensively in pyrotechnics. In lower grade ores both strontium and calcium carbonates may be present, and it is necessary to remove the calcium nitrate from the strontium nitrate because the former is extremely hygroscopic and specifications require it to be absent. A fractional crystallization procedure has been outlined by Kobe and Stewart[2] who present the 25 and 60° isotherms for the aqueous ternary.

Barber[3] has shown that the monobutyl ether of ethylene glycol will selectively dissolve calcium nitrate from anhydrous mixtures of strontium and calcium nitrates and has based a successful procedure in qualitative analysis on this fact. The authors have used this as a basis for a method of quantitative analysis of strontium and calcium,[4] similar to a method using acetone.[5]

Because of the quantitative separation possible, it was desired to know complete solubility and phase relationships, not only for the butyl ether but also the methyl and ethyl ethers which are also commercially available. Although the monoethyl ether of ethylene glycol is known as "Cellosolve," this word will be used here to designate a monoalkyl ether of ethylene glycol and the individual members will be designated by the name of the alkyl group, as methyl, ethyl or butyl.

Experimental

Reagents.—The calcium and strontium nitrates were analytical grade reagents. The calcium nitrate tetrahydrate was dehydrated at 145° before use.

The Cellosolves were technical grade supplied by the Carbide and Carbon Chemicals Division. Each was distilled under vacuum before use, using a Vigreux column and rejecting the initial 15% and the final 10%. All of the Cellosolves form minimum boiling point azeotropes[6] containing 71 to 78% water, so all traces of water should be removed with the initial 15% rejected.

Procedure.—The warm nitrates from the drying oven were added to Pyrex test-tubes with restricted openings. The tubes were then placed in the oven and held at 140° for 12 hours to remove any traces of moisture that may have been picked up. The tubes were removed from the oven, the desired amount of Cellosolve added and the tube quickly sealed with a gas torch. If a sample was to be used at a temperature where solvated crystals were the stable form, the sample was dissolved completely by heating to a higher temperature, around 100°, and then cooling to form the solvated crystals. Often the ampoule had to be shaken vigorously to cause crystal formation. Calcium nitrate solutions would require several days or not change at all to the stable form unless this initial step was taken. Duplicate samples were rotated on a wheel submerged in the thermostat and one sample was allowed to rotate for a longer period of time. The agitation periods ranged from several days at 30° to about 6 hours at 120°. Temperatures below 30° and above 120° were not used because time to reach equilibrium was too great below 30° and above 120° the nitrate–Cellosolve solution discolored after several hours. Thermostat temperatures were kept within 0.05° of the desired value.

Sampling.—After equilibrium was attained, the sample was allowed to stand until the solution was clear. The top of the ampoule was broken and the liquid sample was removed with a pipet. The pipet tip was covered with a piece of filter paper unless the solution was too viscous, in which case a pipet with an enlarged tip was used. In some cases heated pipets had to be used, but when the system showed an inverted solubility curve a cooled pipet was used. Two samples of the solution were taken from each ampoule and placed in weighing bottles.

Various techniques were used to obtain samples of the solid phases. For samples near room temperature the excess liquid was drawn off and the solid quickly transferred to a weighing bottle. The calcium nitrate disolvate of ethyl Cellosolve dried satisfactorily in a desiccator over anhydrous calcium sulfate. The disolvate of methyl Cellosolve had to be placed on dried cotton to absorb the excess solvent. The deliquescence of the solvated crystals made it difficult to prepare the crystals in pure form.

Analysis.—Water was repeatedly added to the weighed sample in an oven at 100° until no Cellosolve odor remained when it reached dryness. Usually 5 or 6 evaporations were required. Direct evaporation of the Cellosolve invariably left carbonaceous matter. The sample was finally dried at 160° for 12 hours. The loss in weight represented the Cellosolve and the residue was the nitrate in the sample. Use of prepared samples showed this method was accurate to about one part in 750.

The observed crystal type was an aid in determining the solid phase. Calcium nitrate disolvate of methyl Cellosolve has a cubic crystal whereas the monosolvate is hexagonal. Calcium nitrate disolvate of ethyl Cellosolve forms a needle-like crystal.

Discussion

The solubilities of calcium nitrate are given in Table I and those of strontium nitrate in Table II.

(1) Ethyl Corporation, Baton Rouge, La.

(2) K. A. Kobe and P. B. Stewart, *J. Am. Chem. Soc.*, **64**, 1301 (1942).

(3) H. H. Barber, *Ind. Eng. Chem., Anal. Ed.*, **13**, 572 (1941).

(4) K. A. Kobe and W. L. Motsch *Anal. Chem.*, **23**, 1498-9 (1951).

(5) P. B. Stewart and K. A. Kobe, *Ind. Eng. Chem., Anal. Ed.*, **14**, 298 (1942).

(6) Carbide and Carbon Chemicals Corp., "Cellosolve and Carbitol Solvents," New York, N. Y., 1947.

The phase relationships in the calcium nitrate–Cellosolve system are shown in Figs. 1, 2 and 3.

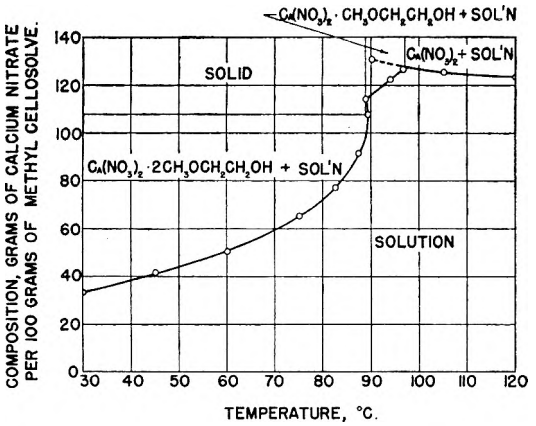

Fig. 1.—Calcium nitrate–methyl Cellosolve.

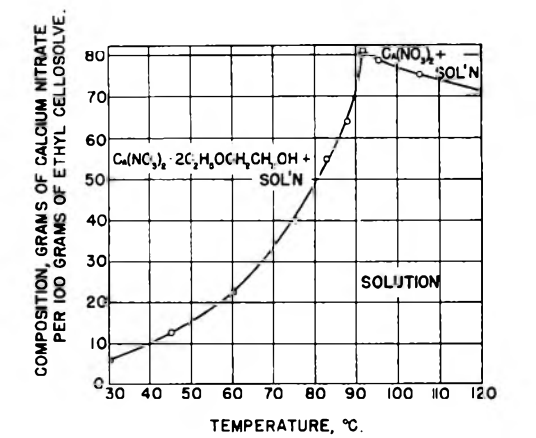

Fig. 2.—Calcium nitrate–ethyl Cellosolve.

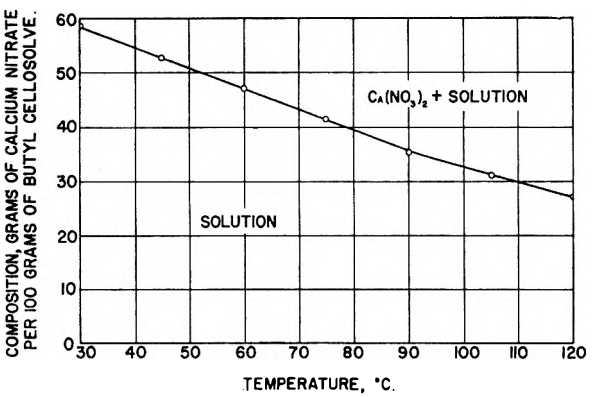

Fig. 3.—Calcium nitrate–butyl Cellosolve.

The system calcium nitrate–methyl Cellosolve is unique in having a transition point of di- to monosolvate at 88.8°, just below the congruent melting point of dissolvate at 89.2°. The monosolvate exists over a short range and the transition to the anhydrous salt would occur at 97.2° and 127.4 g./100 g. Concentrated solutions, above about 100 g./100 g., are extremely viscous and the rate of solution of the salt is low. It is easy to obtain solutions with metastable solid phases, and one such point is indicated on the figure.

TABLE I

SOLUBILITIES OF CALCIUM NITRATE IN CELLOSOLVES

Solubility expressed as grams anhydrous calcium nitrate per 100 grams solvent; T = transition point of disolvate; M = congruent melting point of disolvate; m = metastable.

t, °C.	Methyl g./100 g.	Cello-solve solvate	Ethyl g./100 g.	Cello-solve solvate	Butyl g./100 g.	Cello-solve solvate
30.0	33.2	2	5.9	2	58.4	0
45.0	41.5	2	12.7	2	52.5	0
60.0	50.3	2	22.3	2	46.9	0
75.0	65.2	2	40.1	2	41.5	0
82.5	77.4	2	54.9	2		
87.2	91.8	2				
87.5			64.0	2		
88.8	114.2	2,1 T				
89.2	107.83	2 M				
90.0	130.6	0 m			35.4	0
91.1			80.1	2		
91.2			81.2	2,0 T		
93.8	122.2	1				
95.0			78.6	0		
96.5	126.5	1				
105.0	125.6	0	75.3	0	31.1	0
120.0	123.4	0	71.1	0	27.2	0

TABLE II

SOLUBILITIES OF STRONTIUM NITRATE IN CELLOSOLVES

Solubility expressed as grams anhydrous strontium nitrate per 100 grams solvent. All solid phases are unsolvated.

t, °C.	Methyl cellosolve, g./100 g.	Ethyl cellosolve, g./100 g.	Butyl cellosolve, g./100 g.
30.0	1.66	0.048	0.023
60.0	0.663	.043	.021
90.0	.345	.027	.017
120.0	.187	.021	.015
		% H_2O in solvent	
30.0		0.0	0.023
		1.0	.048
		2.0	.069
		4.0	.195
		8.0	1.21

In ethyl Cellosolve calcium nitrate forms only a disolvate which melts to form the anhydrous salt. No solvate is formed in butyl Cellosolve over the temperature range investigated. The unsolvated salt in all solvents shows a negative temperature coefficient of solubility, or an inverted solubility curve.

The solubility of strontium nitrate is low in all solvents (Table II) and only the unsolvated salt exists. As with calcium nitrate, this form has an inverted solubility curve. A comparison of the two salts shows that butyl Cellosolve is most selective for the extraction of calcium nitrate from the mixed nitrates, and a quantitative method of analysis is based on this.[4] The effect of a small amount of water on the solubility of strontium nitrate in butyl Cellosolve at 30° is likewise shown in Table II where the solvent contains from 1.0 to 8.0% water. The solubility is seen to increase rapidly, so for quantitative separations the solvent must be anhydrous.

NICKEL PLATING BY CHEMICAL REDUCTION. I. EFFECT OF THE BASIS METAL[1]

BY ROBERT A. POWERS AND NORMAN HACKERMAN
Department of Chemistry, University of Texas, Austin, Texas

Received November 20, 1950

It has been shown that surface configuration of the supporting substance is not of major importance in inducing nickel deposition by chemical reduction either through a similarity to the nickel lattice or through catalytic activity due to surface geometry.

Introduction

In attempting to extend to non-metallic surfaces the electrodeless plating method described by Brenner and Riddell,[2] more information on the process occurring at metallic surfaces was desirable. They had found that the reduction of nickel ion by sodium hypophosphite took place only on a limited number of metals, indicating that the metal itself was an integral component, possibly catalytic, or that growth of a nickel lattice required as a basis a similar, perhaps a particular, surface configuration.

If any of these factors were found to be controlling in the deposition process the use of glass or other non-metallic surfaces as such would be eliminated as basis materials for this type of plating. The study reported here was made to establish the importance of this point in the deposition process.

Experimental Methods and Results

The experimental approach was through comparison of electron diffraction patterns of the metal surface prior to plating and of the deposited nickel. The patterns were obtained with an RCA type EMU-1 electron microscope fitted with a diffraction attachment. The acid plating bath, III, described by Brenner and Riddell[2] was used in this work. This bath contained 30 g./l. of nickel chloride, 10 g./l. of sodium citrate and 10 g./l. of sodium hypophosphite. The temperature of the bath during plating was maintained at 95 ± 2°.

Reflection patterns were obtained of SAE 1020 steel blocks, 6 × 6 × 2 mm., after they had been given a 30 second etch in a solution consisting of 1% HNO_3 in absolute ethanol (see Fig. 1). The blocks were then plated as described above for various periods and electron diffraction patterns were again obtained by reflection. It was found that exposure of the steel to the plating solution for as little as 2 minutes obliterated the iron–iron oxide pattern of the steel and replaced it with 2 diffuse rings for which the ratio of the radii was 1.85. The pattern of Fig. 2 for a 2-minute plating time is typical. For plating times of less than about four hours the pattern did not change but those samples which were plated for longer periods gave the typical face centered cubic pattern of nickel. The pattern in Fig. 3 was for a steel block on which nickel had been plated by this procedure for 6 hours.

The initial deposits, continuing through considerable thickness were amorphous since the pair of diffuse rings of radius ratio of 1.85 are ordinarily indicative of such a surface.[3] It is well known, however, that reflection of an electron beam from a surface is dependent on the physical nature of that surface and therefore a deposit that gives a pattern of the type shown in Fig. 2 may yield a more complex pattern of sharp rings on transmission of the electron beam.[4]

Because of this it was decided to study the deposition of thin nickel films by chemical reduction on very thin evaporated metal films. In this way it was possible to strip the films and examine them by electron transmission techniques. Evaporated films of nickel, iron, gold, copper and platinum were prepared by evaporation from a heated tungsten filament and condensation onto glass microscope slides in a chamber evacuated to 5×10^{-5} mm. The metal films were so thin that they imparted only a slight haze to the glass slide.

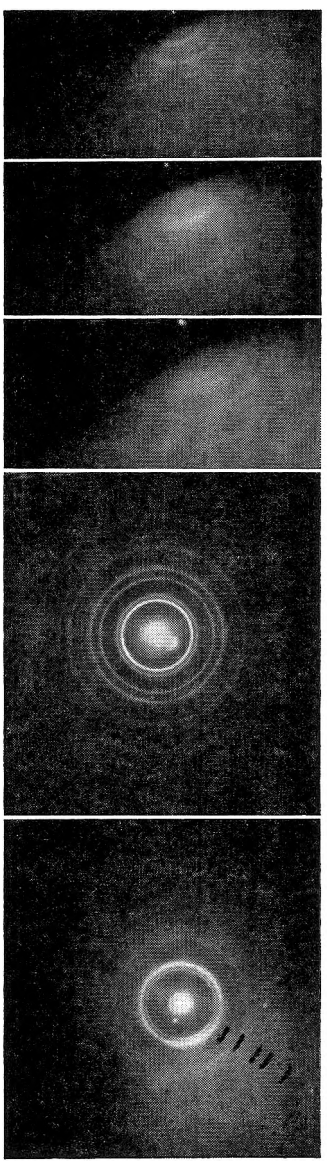

Fig. 1.

Fig. 2.

Fig. 3.

Fig. 4.

Fig. 5.

Nickel deposits were obtained by immersion of the metal-bearing slide in the hot plating solution described above. Plating occurred only on the nickel, iron and gold films in accordance with the earlier observations.[2] Plating was very rapid when it occurred and it was necessary to exercise care in obtaining deposits sufficiently thin to be transparent to

(1) Presented before 5th Southwest Regional Meeting of the American Chemical Society, Oklahoma City, Okla., December, 1949.

(2) A. Brenner and G. R. Riddell, *J. Research Natl. Bur. Standards*, **39**, 385 (1947).

(3) N. K. Adam, "The Physics and Chemistry of Surfaces," Third Edition, Oxford University Press, London, 1941, p. 171.

(4) L. H. Germer, *Phys. Rev.*, **49**, 163 (1936).

the electron beam. Suitable deposits were stripped from the glass slide by soaking in hot water.

These were mounted on 200 mesh stainless steel screens which were inserted into the microscope barrel normal to the direction of the electron beam.

The nickel deposits on both gold and on iron gave diffraction rings typical only of the basis metal. In neither case were there found rings attributable to nickel and there were no indications of preferred orientation. The transmission pattern of a gold film is shown in Fig. 4 and a pattern obtained from nickel deposited on a gold film is shown in Fig. 5. The short arcs indicate where nickel lines would be found if they had been present.

Two other basis metals were included in bulk form. These were chromium and silver and in neither case was there any evidence that deposition had occurred.

TABLE I

Metal	Lattice type	Unit Cell in Å.	Nearest atomic approach in Å.	Nickel deposition
Ni	FCC	3.52	2.48	Yes
Co	FCC	3.55	2.50	Yes
Al	FCC	4.04	2.54	Yes
Fe	BCC	2.86	2.48	Yes
Cr	BCC	2.88	2.50	No
Au	FCC	4.07	2.88	Yes
Ag	FCC	4.08	2.88	No
Pd	FCC	3.88	2.74	Yes
Pt	FCC	3.91	2.76	No
Cu	FCC	3.61	2.54	No

Discussion

The bulk of the experimental evidence given here indicates that initial deposition of nickel follows the lattice structure of the basis metal over a fairly wide range of lattice type and dimensions and eventually assumes a typical nickel structure. The reflection data if taken at face value indicate an amorphous structure on steel. However, these results can be satisfactorily explained as being due to the physical structure of the surface alone. Objection may be made to the fact that in the transmission work the pattern was taken through both the evaporated metal and the deposited nickel. Visual evidence, however, indicated that the thin evaporated films did not separate with the nickel from the glass support. Furthermore, even if it did adhere to the nickel it was so thin in comparison that it would not block out any separate lines due to nickel alone.

An inspection of Table I reveals that chromium and iron have identical lattice type and almost identical dimensions, yet nickel is deposited on iron but not on chromium. The same situation prevails with regard to gold and silver, and to palladium and platinum. This is a definite indication that adsorption of reactants or catalytic effects based upon the geometry of the surface, *i.e.*, the existence of a critical spacing, is not a factor in the deposition process. This point is supported by two additional facts. First, there is the wide divergence in the lattice constants of the six metals Ni, Fe, Au, Al, Pd and Co which do induce plating (for the latter 3, see reference (2)). Second, plating may be induced on metals such as copper by momentary contact with a more electropositive metal such as iron.[2,5] This contact sets up a galvanic cell of which copper is the cathode and which causes nickel to deposit on the copper electrolytically. When the contact is broken nickel will then deposit on the copper by chemical reduction although it would not do so before. Since the contact need be only momentary and no visible nickel deposit need be formed in order to activate the copper, it is reasonable to assume from the diffraction work with gold and iron that the initial nickel deposit has the same lattice structure as the basis copper. Nevertheless it is possible to induce deposition from solution on this structure but not on copper itself.

THE REACTION IN ACID SOLUTION BETWEEN TETRABROMOPHENOLSULFONPHTHALEIN AND SILVER NITRATE

BY WILSON J. BROACH, ROBERT W. ROWDEN AND EDWARD S. AMIS

Contribution from the Department of Chemistry, University of Arkansas, Fayetteville, Arkansas

Received November 27, 1950

The reaction of silver nitrate with tetrabromophenolsulfonphthalein was studied at 25.1° and 30.1°. The reaction mechanism was found to be consecutive first order. The specific velocity constants, the energies of activation, the Arrhenius frequency factors, and the entropies of activation were determined for the removal of the first and second bromine atoms. The specific velocity constant for step 1 was found to be from 8 to 10 times as great as that for step 2. The rates of removals of the third and fourth bromine atoms from the dye molecules were shown to be negligibly slow. The negative entropy values were explained as due either to a rigid activated as compared to a reactant state or to a small transmission coefficient. Transmissions of the reaction mixtures were found to increase with time. This phenomenon was discussed at some length.

The reaction of silver and mercuric nitrates with brominated alkyl and aryl compounds has been studied by various authors.[1]

The kinetics of the reaction between silver nitrate and tetrabromophenolsulfonphthalein, however, have not been studied. It was thought of interest to make a study of the kinetics of this reaction, since it gave promise of being a reaction, the mechanism of which would involve the consecutive removal of bromine atoms from the dye molecule by the silver ion. Since the dye is only slightly soluble in water solution and the silver nitrate could be present in much higher concentrations, it was thought the mechanism might be pseudounimolecular.

Experimental

The brom phenol blue was Eastman Kodak No. 752 tetrabromophenolsulfonphthalein.[1] Other chemicals used were of C.P. grade. The thermostat at 25.1° was constant to ±0.05° and the one at 30.1° was constant to within ±0.01°. Brown bottles were used to prevent possible catalysis of the reaction or decomposition of the precipitated silver bromide by light. Each run was set up by pipetting 200 ml. of 6.97×10^{-4} *M* tetrabromophenolsulfonphthalein, 50 ml. of 0.9974 *M* nitric acid and 50 ml. of 0.08611 *M* silver nitrate into a bottle. The silver nitrate was added last and the time of the beginning of the run was taken as the last drop of silver nitrate entered the reaction bottle. The bottle was stoppered immediately and the mixture shaken and placed in the thermostat. At intervals the bottles were removed from the thermostat, quickly and vigorously shaken and returned to the thermostat. The run was analyzed by filtering through a previously prepared and weighed porcelain crucible containing an asbestos mat. The time of completion of the run was taken when the last of the solution passed through the filter. Timing was not critical since the shortest run, except the first, involved at least 17 hours and the longer runs involved several hundred hours. After filtering the reaction mixture the bottle and crucible were thoroughly washed with distilled water containing approximately 2 ml. of nitric acid per liter of water, then with 95% ethyl alcohol and finally with pure distilled water. If the crucible tended to become clogged with adsorbed dye, alcohol wash was used to desorb the dye. The crucible was brought to constant weight in an oven and the weight of silver bromide determined from the difference in weight of the crucible and the weight of the crucible plus the silver bromide. From the time rate of production of silver bromide the rate of reaction of silver nitrate with tetrabromophenolsulfonphthalein was calculated.

Mechanism.—Burke and Donnan studied the interaction of alcoholic silver nitrate with alkyl halides.[2] They represented the mechanism as being the two simultaneous reactions

$$RI + AgNO_3 + EtOH \longrightarrow AgI + HNO_3 + ROEt \quad (A)$$

$$RI + AgNO_3 \longrightarrow AgI + R\text{-}O\text{-}NO_2 \quad (B)$$

They found that the bimolecular velocity constant was increased by increasing the initial concentration of silver nitrate and to a lesser extent by decreasing the initial concentration of alkyl halide. Baker[3] found that the reaction of *p*-methylbenzyl bromide and *p*-nitrobenzyl bromide followed the mechanism represented by reaction (A) and (B) above (76% in accordance with (A)), but that the reactions were unimolecular throughout. Roberts and Hammett[4] studying the reaction of benzyl chloride and mercuric nitrate in water and dioxane solution concluded that the mechanism was that of the formation of ionic intermediate which they called a carbonium ion, benzyl ion, $C_6H_5CH_2^+$. They found the reaction to be bimolecular with one mole of mercuric ion reacting with two moles of benzyl chloride. The equation for bimolecular reactions was modified by Roberts and Hammett to account for the latter observation. The final products of the reactions were benzyl nitrate and benzyl alcohol, which corresponds to the mechanism in equations (A) and (B) with water substituted for ethyl alcohol in equation (A).

To determine the mechanism of the silver nitrate and tetrabromophenolsulfonphthalein reaction it was thought necessary to test for the presence of nitrate in the organic product, since it is known that ring organic nitrates are readily hydrolyzed in water solution. The absence of organic nitrate was proven by making a specific test for nitrogen. To make this test, the organic product was extracted from the reaction mixture with diethyl ether and the ether was evaporated at room temperature. The dry residue was again extracted with ether and the ether again evaporated at room temperature. The dry residue was taken up in alcoholic Na_2CO_3 solution so that any free nitric acid carried over in the ether extractions would be converted to $NaNO_3$. The alcohol was evaporated and the dry residue was extracted with dry ether and the ether evaporated. The dry residue was again extracted with dry ether and the ether evaporated. This product was used in making the nitrogen test. The nitrogen test was that given by Shriner and Fuson.[5] Repeated tests gave no indication of the presence of nitrate; therefore, from consideration of previous work and from the fact there was no organic nitrate in the products, we believe the over-all mechanism of the reaction is

$$RBr_4 + Ag^+ + 2H_2O \longrightarrow RBr_3(OH) + AgBr + H_3O^+$$

$$RBr_3(OH) + Ag^+ + 2H_2O \longrightarrow RBr_2(OH)_2 + AgBr + H_3O^+ \quad (C)$$

If any organic nitrate is formed it is subsequently hydrolyzed.

In the reactions above, one silver ion reacts with one dye or substituted dye molecule to produce one molecule of AgBr. Since each step requires a collision with a silver ion it would seem reasonable that the step involving the original removal of bromine atom would be much faster than any of

(1) Euler, *Ber.*, **39** 2726 (1906). Chase and Kilpatrick, *J. Am. Chem. Soc.*, **54**, 2284 (1932). Baker, *J. Chem. Soc.*, 987 (1934). Roberts and Hammett, *J. Am. Chem. Soc.*, **59**, 1063 (1937). Panepinto and Kilpatrick, *ibid.*, **59**, 1871 (1937). Amis and La Mer, *ibid.*, **61**, 905 (1939).

(2) Burke and Donnan, *J. Chem. Soc.*, **85**, 555 (1904).

(3) Baker, *ibid.*, II, 987 (1934).

(4) Roberts and Hammett, *J. Am. Chem. Soc.*, **59**, 1063 (1937).

(5) Shriner and Fuson, "The Systematic Identification of Organic Compounds," John Wiley and Sons, Inc., New York, N. Y., 1948, pp. 52–54

the steps. The removal of the second bromine atom would be second in reaction velocity and the removal of third and fourth bromines would be comparatively very slow. These conclusions are reasonable statistically. Therefore, we shall write the over-all reaction for the purpose of calculating experimental results as

$$\underset{(a)}{RBr_4} \dashrightarrow \underset{(x)}{RBr_3(OH)} \dashrightarrow \underset{(y)}{RBr_2(OH)_2} \quad (D)$$

where a, x and y represent the over-all concentrations of original dye and first and second substitution products, respectively. x also represents the silver bromide produced in step 1 and y represents silver bromide from step 2. k_1 is the velocity constant for step 1 and k_2 is the velocity constant for step 2. Mathematically

$$dx/dt = k_1(a - x) \quad (1)$$

$$dy/dt = k_2(x - y) \quad (2)$$

Solution of equation (1) and (2) yields

$$x = a - ae^{-k_1 t} \quad (3)$$

$$y = \frac{ak_2(1 - e^{-k_1 t}) - ak_1(1 - e^{-k_2 t})}{k_2 - k_1} \quad (4)$$

For details see Amis.[6]

Data

In Table I are recorded the data taken at 25.1°.

TABLE I

KINETIC RUNS BETWEEN TETRABROMOPHENOLSULFONPHTHALEIN AND SILVER NITRATE AT 25.1°

$k_1 = 2.95 \times 10^{-2}$; $k_2 = 3.80 \times 10^{-3}$

Run no.	Time, hr.	AgBr, (moles/l.) × 10^3	x, (moles/l.) × 10^3	y, (moles/l.) × 10^3	$(x + y)$, (moles/l.) × 10^3
1	0.17	0.000	0.003	0.000	0.003
2	24.8	.378	.362	.018	.380
3	24.9	.376	.362	.019	.381
4	52.6	.580	.550	.064	.614
5	73.9	.756	.618	.104	.722
6	74.2	.776	.619	.105	.724
7	99.9	.816	.661	.155	.816
8	144.9	.962	.687	.237	.924
9	244.0	1.070	.696	.381	1.077
10	461.0	1.206	.697	.558	1.255

Table II contains data taken at 30.1°.

TABLE II

KINETIC RUNS BETWEEN TETRABROMOPHENOLSULFONPHTHALEIN AND SILVER NITRATE AT 30.1°

$k_1 = 5.30 \times 10^{-2}$; $k_2 = 5.70 \times 10^{-3}$

Run no.	Time, hr.	AgBr, (moles/l.) × 10^3	x, (moles/l.) × 10^3	y, (moles/l.) × 10^3	$x + y$, (moles/l.) × 10^3
1	0.11	0.000	0.000	0.000	0.000
2	17.6	.436	.423	.024	.447
3	17.6	.428	.423	.024	.447
4	23.6	.520	.497	.038	.535
5	23.6	.545	.497	.038	.535
6	51.5	.764	.652	.120	.773
7	95.9	.996	.693	.245	.938
8	148.0	1.098	.697	.361	1.058
9	168.0	1.138	.697	.397	1.094
10	168.0	1.162	.697	.397	1.094
11	244.0	1.192	.697	.503	1.200
12	263.0	1.208	.697	.523	1.220
13	430.0	1.280	.697	.630	1.327
14	527.0	1.330	.697	.658	1.355
15	530.1	1.308	.697	.659	1.356
16	530.8	1.385	.697	.659	1.356

(6) Amis, "Kinetics of Chemical Change in Solution," The Macmillan Company, New York, N. Y., 1949, pp. 14, 15.

In Tables I and II, column 3 contains precipitated AgBr expressed in moles per liter at 25.1° and 30.1°, respectively. Column 4 of Tables I and II contains precipitated silver bromide expressed in moles per liter at 25.1° and 30.1°, respectively, coming from step 1 of reaction (D) and calculated from equation 3. Columns 5 of Tables I and II contain precipitated silver bromide expressed in moles per liter at 25.1° and 30.1°, respectively, coming from step 2 of reaction (D) and calculated by equation (4).

The reaction velocity constants k_1 and k_2 used in calculating x and y were obtained using the following procedure. In early stages of the run it was assumed that step 1 of reaction (D) predominated and therefore the the quantity $(a - x)$ represented the concentration of the dye corresponding to time t. Therefore a plot of precipitated silver bromide against time was made and its slope found at a time sufficiently early so that y was not significant. This slope corresponded to dx/dt in equation (1) and when divided by the corresponding $(a - x)$ gave preliminary values of k_1. The method of obtaining an approximate value of k_2 was to take the slope of the silver bromide–time curve after sufficient time had elapsed so that x was constant. This slope was divided by $(x - y)$ and gave k_2 according to equation (2). $(x - y)$ was obtained in the following way

$$x + y = C \quad (5)$$

where C is total concentration of AgBr precipitated. Then

$$y = C - x \quad (6)$$

and

$$x - y = x - (C - x) = 2x - C \quad (7)$$

Finally k_1 and k_2 were adjusted by trial and error and have the values represented in Tables I and II. From these tables it is observable that k_1 is approximately 8 times k_2 at 25.1° and 10 times k_2 at 30.1°; in the third columns of the tables the actually observed AgBr precipitate is represented. Columns 4 contain values of x, columns 5 calculated values of y, and columns 6 calculated values of $x + y$. All these substances are expressed in moles per liter. The calculated values of $x + y$ should correspond to observed concentration of silver bromide. Observations of columns 3 and 6 in Tables I and II demonstrate that this expectation is fully realized. In Fig. 1 are plotted the concentrations of AgBr $(x + y)$ *versus* times at the two different temperatures. From the figure the agreement of the two is obvious. In Fig. 2 is plotted the concentrations of $a - x$, $x - y$, y and x on curves A, B, C and D, respectively. The curve for $a - x$ *versus* time represents the rate at which original dye is being consumed by step one of the reaction. Curve B represents the rate of change of concentration of the dye intermediate due to a combination of steps 1 and 2 of the reaction. Curve C represents the rate at which final dye product is produced by step 2 of the reaction. This is likewise the rate at which AgBr is produced in this step of the reaction. The curve D represents the over-all rate of production of both intermediate and final dye product. This corresponds to the over-all rate of production of AgBr

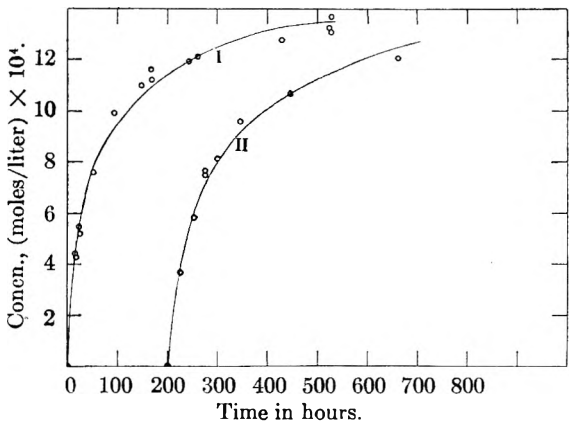

Fig. 1.—Plot of $(x + y)$ and of AgBr *versus* time. The curve represents the calculated values of $(x + y)$ and the circles represent experimental data for AgBr. I, $T = 30.1°$; II, $T = 25.1°$; time in hours at 25.1° = time in hours at 30.1°—200 hours.

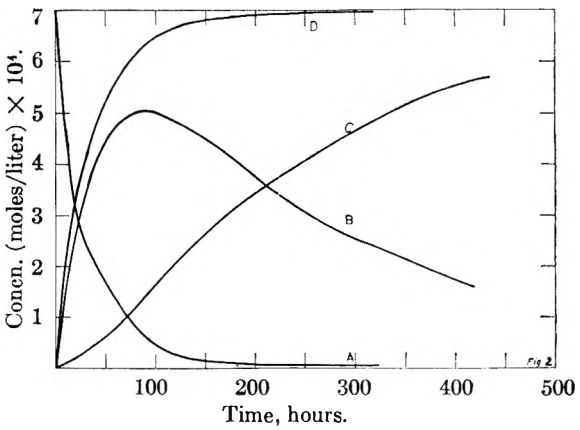

Fig. 2.—Plot of $(a - x)$, $(x - y)$, y and x in moles/liter *versus* time in hours: $k_1 = 2.95 \times 10^{-2}$, $k_2 = 3.80 \times 10^{-3}$, temperature = 25.1°: curve A = $a - x$; curve B = $x - y$; curve C = y; curve D = x.

from step 1. The curves have forms expected for consecutive first order reactions.[7]

The removals of the third and fourth bromine atoms from the dye molecule were negligibly slow compared to removal of the first and second bromine atoms. Even after 1,558 hours at 25.1° only 54% of the bromine had been removed from the dye. Another run stayed at 30.1° for 488 hours and then remained at 70° for 16 hours and only 54% of the bromine had been removed in this run. From these data and when it is taken into consideration from Tables I and II that the specific reaction rate of step 1 is from 8 to 10 times as great as the specific rate of step 2 depending on temperature and when it is also observed that the specific rate of step 1 for a 5° rise in temperature is roughly 1.8 times as great and that the specific rate of step 2 is increased by 1.5 times for the same temperature interval, then it seems entirely justifiable to neglect the rate of removal of the third and fourth bromine atoms over the time and temperature ranges listed in the Tables I and II. Statistically the rates of removal of the third and fourth bromine atoms would be extremely slow, since there would be only half as many bromine atoms available for removal per dye molecule and the chance of a third and fourth collisions of the same dye molecule with a silver ion while the molecule remains sufficiently deformed, correctly orientated, and having necessary energy for reaction is very slight.

The precision of the data is observable from runs 2 and 3 in Table I and runs 2 and 3, 4 and 5, and 9 and 10 of Table II. It is observable that in no case is the precision of duplicate runs less than 5% and in some cases it is less than 1%.

The accuracy of the measurements compared to theory from columns 3 and 6 of Tables I and II is never less than 6.2% and averages 2.8%. The accuracy therefore compares favorably with the precision. These can be considered fair degrees of both precision and accuracy since in the early stages of the run the dye goes over to a colloidal state in these solutions of high electrolyte concentrations as is shown by the Tyndall cone effect. This effect is not dependent on silver nitrate but to the electrolyte concentration as was shown by replacing the silver nitrate by an equal concentration of sodium nitrate. Furthermore the dye is somewhat adsorbed by the precipitated silver bromide and thus a small fraction of the dye is removed from the effective zone of action with silver nitrate even though the solutions are shaken regularly. The fact that the dye does become somewhat colloidal and is to a small extent adsorbed on the silver bromide makes filtration slow and requires careful washing with both water and organic solvent. It is obvious that these effects did not greatly influence the over-all rates, but their influence on precision and accuracy were, no doubt, important.

In Table III are listed the calculated values of the energies of activation, Arrhenius frequency factors and entropies of activation for the specific reaction rates k_1 and k_2. The energies of activation were calculated using the equation

$$\Delta E = 2.303\, R\, \frac{T_2 T_1}{T_2 - T_1} \log \frac{k_{T_2}}{k_{T_1}} \qquad (8)$$

the Arrhenius frequency factors were calculated using equation

$$\log Z = \frac{\Delta(T \log k)}{\Delta T} \qquad (9)$$

and the entropies of activation were obtained from Eyring's equation[8] which is

$$Z = \kappa \frac{k^1 T}{h} e^{\Delta s/R} \qquad (10)$$

In this equation κ is the transmission coefficient taken as unity, k^1 is Boltzmann gas constant, h the Planck constant, Δs the entropy of activation

TABLE III

ENERGIES OF ACTIVATION. ARRHENIUS FREQUENCY FACTORS AND ENTROPIES OF ACTIVATION FOR THE SILVER NITRATE–TETRABROMOPHENOLSULFONPHTHALEIN REACTION FOR THE TEMPERATURE RANGE 25.1° TO 30.1°

Step	Temp. interval, °C.	Energy of activation ΔE, cal.	Arrhenius frequency factor log Z	Entropy of activation Δs, cal./degree
1	25.1–30.1	21,050	13.90	−11.2
2	25.1–30.1	14,570	8.26	−36.6

(7) Daniels, "Chemical Kinetics," Cornell University Press, Ithaca, N. Y., 1938, p. 29.

(8) Ref. 6, p. 151.

and the rest of the symbols have their usual significance.

The negative values of activation entropies observed in Table III may be due to an activated complex which is more rigid than the reactant dye molecule.[9]

However, these low entropies of activation could result from low Arrhenius frequency factors arising from small transmission coefficients. In other words, a κ value less than unity.[9]

It is observed that the values of both ΔE and log Z are much greater for step 1 than for step 2. Thus the Arrhenius frequency factor in step 1 as compared to step 2 more than compensates for the higher energy of activation required by step 1, permitting this step to be the much faster of the two.

Absorption data on the reaction mixture were taken at various times, using a Beckman model DU quartz spectrophotometer. The absorption runs were set up exactly as the kinetic runs and all reactions were at the same concentrations in both types of measurements. At specified times samples were removed from the reaction vessel, centrifuged for 10 minutes, and liquid sample siphoned from above the solid sediment. These were measured against a standard made up freshly each time exactly as the original run was made. In Fig. 3 are plots at various time intervals of the wave length of light in millimicrons *versus* percentage transmission of sample compared to the standard.

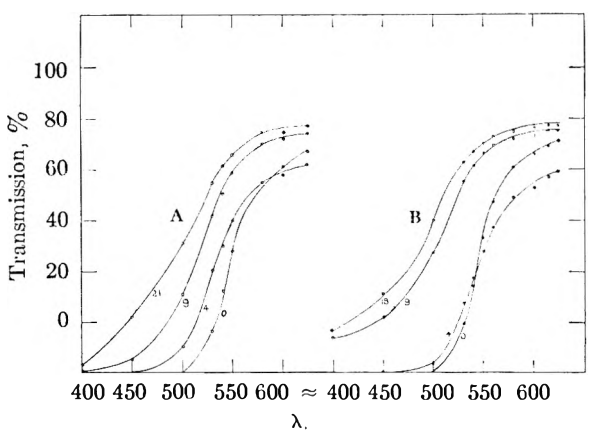

Fig. 3.—Plot of the per cent. transmission *versus* the wave length, λ, in mμ for tetrabromophenolsulfonphthalein in $AgNO_3$ + HNO_3 and in $NaNO_3$ + HNO_3 solutions: A, $AgNO_3$ + HNO_3 solution of dye: 0 days, 4 days, 9 days, 21 days; B, $NaNO_3$ + HNO_3 solution of dye: 0 days, 4 days, 9 days, 18 days.

It is observed for a given wave length the percentage transmission increases with time in both silver nitrate–nitric acid solution of dye and the sodium nitrate–nitric acid solution of dye. This is true except for the very earliest period of time for which the absorption wave has a little different slope than for the other time intervals and actually crosses one of the shorter interval curves in both types of solutions. The increase of transmission with time cannot be attributed to the replacement of bromine atoms in the dye molecules by hydroxyl radicals since the curves are similar for silver nitrate and sodium nitrate solutions although the latter salt causes no substitution of bromine by hydroxyl. The fact that the curves in both salt solutions at the beginning of the runs have different slopes from those of the curves at longer time intervals may be due to the early conversion of the dye to a colloidal state. Some of the increase of transmission with time is no doubt due to the adsorption of the dye by precipitated silver bromide; however, this must be a minor cause, since again sodium nitrate produces no silver bromide. Hence the larger part of the increase must be due to some change with time in the absorptive capacity of the dye molecules for the wave lengths of light studied. This change could be due to a fading reaction of the dye in strong acid solution of salts similar to the acid fading of triphenylmethyl dyes.[10] Whatever the change in the dye molecule, it does not affect the rate with which silver ion replaces bromine in the dye molecule.

As to whether the reaction is heterogeneous can be investigated from the following considerations.

First suppose the reaction to take place only at the surfaces of colloidal silver bromide or assume the reaction to be catalyzed by this salt. These assumptions would be illogical since it would be impossible to see how the reaction would be initiated because originally there is no silver bromide present. Then too the reaction would, in the early stages of the run, speed up with time since the amount of silver bromide would increase. In the case of absorption this would be true until the dye present had all been absorbed on the surface of the bromide and from then on the rate would decrease due to the depletion of the dye.

Actually the rate was found always to depend on the concentration of the dye remaining unreacted, according to our theory, and the observed time rate of production of silver bromide decreased in agreement with these calculations.

Second assume that the reaction took place only on the surface of colloidal dye particles. Then a molecule would have to be absorbed on the colloidal dye surface only long enough for two bromine atoms to be removed, and then give place to, and not at any future time interfere with, the absorption of an unreacted dye molecule. This would seem improbable. Why should an unreacted dye molecule be absorbed and a reacted one be desorbed and not interfere by being reabsorbed? How would such a mechanism give a rate proportional to unreacted dye concentration.

It seems more probable that the dye became colloidal to a certain extent almost immediately and that these colloidal dye particles which by observation remained in suspension were loosely constructed and permeable to silver ion. The extent of the colloidality was included in the rate constants so that the calculated rate based on the concentration of unreacted dye, including the initial concentration of dye, agreed with the observed rate of production of silver bromide.

The reaction is too complex and the theory and observation are in too close agreement for the interpretation to be merely fortuitous.

(9) Glasstone, Laidler and Eyring, "The Theory of Rate Processes," McGraw-Hill Book Co., Inc., New York, N. Y., 1941, p. 297

(10) Biddle and Porter, *J. Am. Chem. Soc.*, **37** 1571 (1915).

NOTE ON THE DISPLACEMENT PRESSURE METHOD FOR MEASURING THE AFFINITY OF LIQUIDS FOR SOLIDS

BY N. J. DELOLLIS

National Bureau of Standards, Washington, D. C.

Received December 11, 1950

An investigation was made of the possibility of using a displacement pressure method of determining the affinity of a liquid for a solid. Considerable difficulty was encountered in trying to get reproducible results and in trying to duplicate previous work in the field. One of the main factors contributing to the difficulties was the length of time necessary before one could assume that a state of equilibrium existed within the cell. The displacement pressures observed for three-phase systems, *i.e.*, water/organic solvent/solid, are of doubtful value because immiscible liquids are partially soluble in each other and such a system becomes self contaminating. Preferential adsorption of the better wetting liquid on the solid phase results, and interferes with the liquid-solid relationship of the poorer wetting liquid. These facts indicate that the displacement pressure cell is unsuitable for the determination of attractive forces between liquids and solids.

In an experimental investigation of the affinity of various liquids for activated carbon and lampblack, an attempt was made to employ a method based on the displacement pressure of a liquid penetrating a porous plug of the compressed solid. Measurements of this type have been reported by Bartell and collaborators[1] and others.[2,3]

Considerable difficulty was experienced in getting significant data and reproducible results were not obtainable. This note is a brief description of the experiments and an analysis of some of the difficulties inherent in the method.

Penetration of a porous mass by a liquid is established by the surface tension, γ, the average pore size, r, the viscosity of the liquid, η, and the angle of contact, θ, formed by the liquid in contact with the solid. Washburn[4] related these quantities to the rate of penetration in the equation

$$\frac{dl}{dt} = \frac{r\,\gamma\cos\theta}{4\,\eta l}$$

where l is the length of liquid in the capillary space in time t. When equilibrium conditions are obtained, the pressure, P, of the advancing liquid is[1]

$$P = \frac{2\,\gamma\cos\theta}{rg}$$

where g is the gravitational constant.

In the method used, static or equilibrium conditions are assumed and the viscosity term for different liquids drops out of consideration. A powdered plug is compressed in a cell. The wetting liquid advances into the plug from one end of the cell and gas pressure opposes this advance from the other end of the cell. The pressure necessary to produce a static equilibrium condition is P. Where two liquids are used, the wetting liquid tends to displace the poorly wetting liquid, and the gas pressure P is the amount of pressure necessary to produce static equilibrium. The wetting ability is taken to be a measure of the affinity or adhesion of the liquid for the solid.

In these experiments two cells were used. The first cell was essentially a duplicate of the one used by Bartell and Whitney.[5] It consisted of a cylinder to hold the plug of carbon powder and a piston with which to exert and maintain pressure on the plug. Bolted yokes over each of these parts held them together. Leather and polyethylene gaskets were used to make the cell airtight. An opening at the wetting-liquid end of the cell led to a glass capillary by which the movement of the liquid in the cell was observed. An opening at the opposite end of the cell led to a mercury manometer and to a tank of compressed nitrogen.

The second cell, developed to eliminate as many joints as possible, consisted of two flanged cylindrical parts. The carbon plug was contained in one part. A heavy spring seated in the second part exerted a constant pressure on the carbon plug when the cell was assembled by bolting at the flanges. A lead gasket was used between the flanges. The method of tamping and compression was similar to that of Bartell and Whitney.[5]

A 200-mesh activated carbon was used for most of the experiments. For some experiments it was heated to 500–600° in an evacuated flask. The carbon was wet with benzene while in a vacuum, then added to the cell as a sludge. For other experiments it was heated to 500–600° in the dry state and the liquid was added only after the powder had been compressed in the assembled cell. A benzene–gas–carbon system was used for most of the experiments. Compression loads on the various carbon plugs ranged from 1000 to 6000 p.s.i. The observed equilibrium pressures averaged about 380 g./cm.^{2}, ranging from 250 g./cm.^{2} to 450 g./cm.^{2} with no noticeable correlation with the compression loads used. Water gave no measurable equilibrium pressure. The water–benzene–carbon system gave an equilibrium pressure of 400 g./cm.^{2}

Since water alone gave a zero displacement pressure and water with benzene gave results comparable to benzene alone, the inference is that benzene has a zero wetting angle with carbon at all times, *i.e.*, in both a gas–benzene–carbon system and in a water–benzene–carbon system. D. D. Eley and D. C. Pepper[3] observed the same properties for a water–glass contact angle in a water–glass–liquid system, *i.e.*, that water had a zero wetting angle with glass in the presence of the second liquid. They also observed that the values

(1) F. E. Bartell and H. J. Osterhof, "The Measurement of Adhesion Tension, Solid Against Liquid," Colloid Symposium Monograph, Vol. V, 1927, pp. 113-134.

(2) S. H. Bell, J. O. Cutter and C. W. Price, "The Bartell Cell Technique," Symposium on Wetting and Detergency, London, 1937, p. 19.

(3) D. D. Eley and D. C. Pepper, *Trans. Faraday Soc.*, **42**, 697 (1946).

(4) E. W. Washburn, *Phys. Rev.*, **17**, 273 (1921).

(5) F. E. Bartell and C. E. Whitney, THIS JOURNAL, **36**, 3115 (1932).

for adhesion tension were not reproducible but varied widely from experiment to experiment.

In one series of experiments the same carbon plug was used without disassembling the cell. This plug was compressed under a 6000 p.s.i. load. Between each experiment the cell assembly containing the plug was vacuum dried for 16 hours at 120°. With this plug, ethylene dichloride gave practically a zero displacement pressure and benzene gave a pressure in the same range as previously observed, despite the high compression load. For ethyl acetate an equilibrium pressure of 400 g./cm.^{2} was observed.

An important factor in all of the displacement pressures observed was the uncertainty in the time required for a state of equilibrium within the cell. Bartell and his co-workers[6] observed the indicator column with the unaided eye or with a magnifying glass. This method would tend to give relatively high displacement pressures since with the unaided eye motion below a certain rate is not noticeable. In this work a 20-power Brinell microscope whose field was graduated in tenth of a millimeter was used to observe a bubble in the indicator columns. The usual bubble speeds observed were 0.1 millimeter per 20 to 30 seconds, but some were less than 0.1 millimeter per 100 seconds. This slow movement, together with the temporary reversals that took place every time the pressure was either lowered slightly from too high a pressure level or raised slightly from too low a pressure level, made any displacement pressure value doubtful. There was always the possibility that any change of direction in the motion of the liquid in the glass capillary would turn out to be only a temporary reversal if sufficient time were allowed to elapse. The pressures observed were all considerably less than those recorded in the literature.[7]

Experimental results of other investigators can be cited to indicate the uncertain nature of the solid surface under the conditions of these experiments. Heats of wetting experiments[8] have shown that as little as 0.01% of water in benzene will be preferentially adsorbed on a polar solid immersed in the benzene. With this amount of water in the benzene the heat of wetting value is more than twice the value obtained for pure benzene. With 0.02% of water in benzene a heat of wetting value is obtained which is practically the same as that for pure water.

A straight-line relationship was observed when the interfacial tensions between water and 17 organic solvents were plotted against the adhesion tensions determined by Bartell and Osterhof[1] for the systems carbon–water–organic solvents.

The results of this investigation indicate that a three-phase system including two immiscible liquids is self-contaminating[9]; when water and benzene come into contact they will dissolve to a small extent in each other and one or the other will be preferentially adsorbed on the solid phase depending on whether it be polar or non-polar. Under these conditions the existence of a reproducible contact angle with valid physical significance is doubtful, since the surface of the solid is modified by the sorbed substance. Any values measured on such a system would, therefore, be relatively independent of the solid phase and would depend, instead, primarily on the interfacial relations between the two liquids.

(6) Private correspondence

(7) F. E. Bartell and C. N. Smith, *Ind. Eng. Chem.*, **21**, 1102 (1929).

(8) W. D. Harkins and R. Dahlstrom, *ibid.*, **22**, 897 (1930).

(9) G. E. Boyd and W. D. Harkins, *J. Am. Chem. Soc.*, **64**, 1190 (1942).

RACEMIZATION RATE STUDIES ON TRIS-(2,2′-DIPYRIDYL)-NICKEL(II) CHLORIDE

BY GEO. K. SCHWEITZER AND JOHN M. LEE

Department of Chemistry, University of Tennessee, Knoxville, Tenn.

Received December 5, 1950

The complex compound tris-(2,2′-dipyridyl)-nickel(II) chloride was prepared. Resolution of this compound was then obtained by fractional crystallization with ammonium *d*-tartrate. The molecular rotation of 4294 degrees at 5893 Å. and 23.5° compares favorably with values reported previously for the hexahydrate. The rates of racemization in water were determined in the temperature range 16.5° to 40.0°. The energy of activation for this racemization was calculated to be 21,900 cal. per mole. Excess dipyridyl has no effect upon the rate of racemization, but excess nickel(II) ions had a slight accelerating influence. These results tend to discount the ionization mechanism theory of racemization. Acid and base produced almost identical accelerating effects. It is probable that this merely means that the active complex is most stable in neutral or very slightly acid solutions. The effects upon the racemization rates by mixed solvents were noted. In the acetone–water, dioxane–water, methanol–water and ethanol–water systems, a non-linear retardation of the rate with varying concentration of the non-aqueous solvent was obtained. Activation energy calculations gave no indication of a change in mechanism.

Relatively few investigators have undertaken racemization rate studies on optically active inorganic coördination compounds in solution. The effect of temperature on a number of racemization rates has been reported. Several studies of the effects of added ions on the rates appear in the literature. Only two authors report any observations on racemizations in mixed solvents. Werner[1] noted that a solution of 7 parts acetone to three parts water had a retarding effect upon the rate of racemization of potassium tris-(oxalato)-chromate-(III). Bushra and Johnson[2] also found that acetone in aqueous solution had a retarding effect upon the racemization of the potassium salts of tris-(oxalato)-chromate(III), tris-(oxalato)-cobaltate(III) and bis-(oxalato)-ethylenediaminechromate(III). They made comparisons of rates only at 0.000, 0.059, 0.098 and 0.144 mole fractions of acetone.

In view of the small amount of work that has been reported, it was proposed to explore some of the factors influencing the rate of racemization of another optically active coördination compound. The complex that was selected was tris-(2,2′-dipyridyl)-nickel(II) chloride because of its ease of resolution, low optical density, high initial rotations in dilute solution, and favorable racemization rate. It was proposed to observe the effects of the following variables upon the racemization rate: excess of common constituents, temperature, hydrogen and hydroxide ions, and mixed solvents.

Preparation and Resolution.—Blau[3] first reported the preparation of tris-(2,2-dipyridyl)-nickel(II) chloride. With some modifications, his method was used by Morgan and Burstall[4] and Jaeger and van Dijk.[5] The procedure adopted in this research was slightly different than any of these methods. The difficultly soluble 2,2′-dipyridyl reacts readily with nickel(II) chloride hexahydrate in the presence of a slight amount of water. To 4.46 g. of 2,2′-dipyridyl and 2.27 g. of nickel(II) hexahydrate, 8 ml. of water was added. A clear, deep red solution resulted when the mixture was warmed. Upon cooling, pink-violet plates crystallized in good yield. The product was filtered with suction and then dried in a vacuum desiccator over concentrated sulfuric acid for 24 hours. The yield of tris-(2,2′-dipyridyl)-nickel(II) chloride was 5.11 g.

As previously reported by Morgan and Burstall[4] and Jaeger and van Dijk[5] ammonium *d*-tartrate was employed as the resolving agent. It was found, however, that more consistent resolutions were obtained by starting with *d*-tartaric acid. Neutralization of 98 g. of *d*-tartaric acid by adding 140 ml. of concentrated ammonium hydroxide gave the proper concentration of ammonium *d*-tartrate when the resulting solution solution was diluted with 80 ml. of water. This solution was warmed to expel excess ammonia until it was just slightly basic as tested with alkacid paper. To the warm solution, 5.1 g. of tris-(2,2′-dipyridyl)-nickel(II) chloride was added. The solution was then mechanically stirred for one hour. After checking the activities of fractions which were removed at various temperatures as the solution was allowed to cool, it was found that the more active fractions had crystallized upon reaching 20°. The excess ammonium *d*-tartrate collected in a separate layer in the bottom of the beaker. With slight agitation, the active tris-(2,2′-dipyridyl)nickel(II) *d*-tartrate could be suspended in the solution, decanted from the ammonium *d*-tartrate, and filtered with suction. The precipitate was taken up in as little cold water as possible and the tris-(2,2′-dipyridyl)-nickel(II) chloride was precipitated immediately with concentrated ammonium chloride solution. Solution and reprecipitation of the salt was carried out again. Very little racemization takes place if these steps are carried out at a temperature near the ice point. The light pink active form was then dried over concentrated sulfuric acid in a vacuum desiccator with constant pumping. After one hour, the very dry product was removed and placed in a tightly sealed screw-lid bottle. Under such conditions, the active complex may be kept for an almost indefinite period. One sample so prepared showed no appreciable loss in rotary power after six weeks.

Apparatus.—The polarimeter used in this investigation was a Joseph and Jan Fric model which is equipped with a vernier to read directly to 0.01°. A circulating pump made by the American Instrument Company was employed to force water from a constant temperature bath through a jacketed 2-dm. polarimeter tube of 11-ml. capacity. The required low temperatures were obtained through the use of cooling coils from a standard refrigerating unit, while a Sargent heating element with a mercury thermostat provided temperature control within 0.1°. A sodium vapor lamp supplied by the G. W. Gates Company provided the polarimeter with a monochromatic light source.

Racemizations in Water.—Solutions of the complex were made with sample weights held close to 50 mg. in 15 ml. This volume gave a slight excess over the amount required for the polarimeter tube, while the weight of complex gave initial rotations of from 3 to 5°, depending upon the temperature and the time elapsed before making the initial reading. In aqueous solution, the complex was found to undergo racemization at an over-all rate indicative of a first order reaction. Sample curves are shown in Fig. 1 to indicate the general quality of the data. All rate calculations were made by the method of least squares. By using sample weights of from 35 to 110 mg. in 15 ml., it was shown that the racemization rate in this concentration range is independent of the concentration of the complex. With the concentrations indicated, checks in rates were obtained to within 0.1 minute.

(1) Werner, *Ber.*, **45**, 3061 (1912).
(2) Bushra and Johnson, *J. Chem. Soc.*, 1937 (1939).
(3) Blau, *Monatsh.*, **19**, 668 (1898).
(4) Morgan and Burstall, *J. Chem. Soc.*, 2213 (1931).
(5) Jaeger and van Dijk, *Z. anorg. allgem. Chem.*, **227**, 304 (1936).

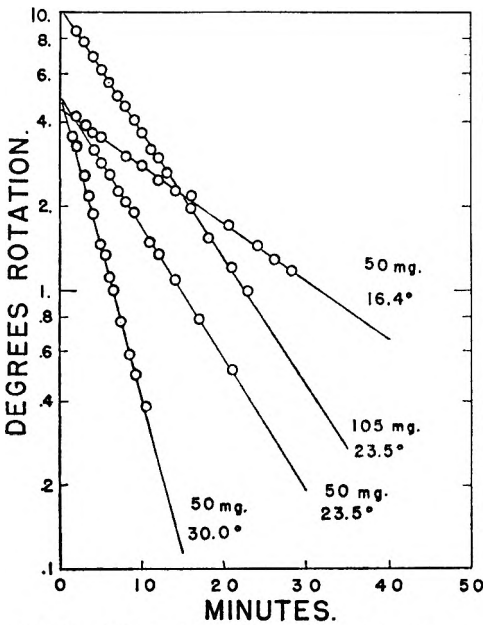

Fig. 1.—Illustrative racemization rate curves.

The influence of temperature upon the reaction rate is shown in Table I. The excellent agreement between the

TABLE I

INFLUENCE OF TEMPERATURE UPON RACEMIZATION RATE

Temp., °C.	Half-life, min.	k, min.$^{-1}$	Investigator
16.5	14.8	0.0468	
17.0	14.2	.0488	(4)
18.0	13.6	.0509	(5)
18.5	12.3	.0563	
20.0	10.0	.0693	(7)
23.5	6.8	.1019	
30.0	2.8	.2472	
40.0	0.9	.7700	

values observed in this work and those reported by other investigators[4,5] can be noted by reference to Fig. 2. The

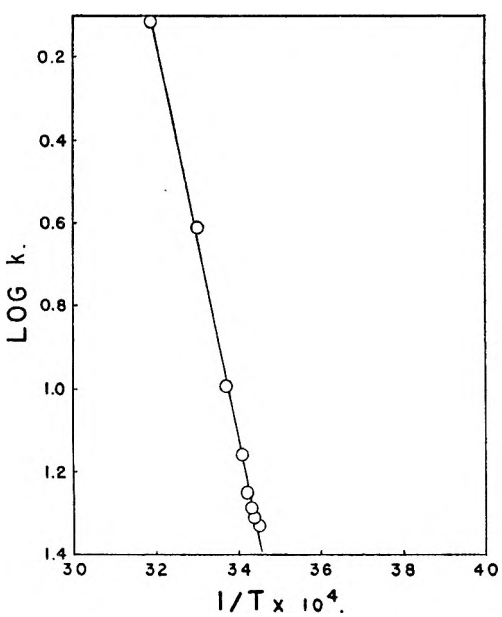

Fig. 2.—Racemization rate constants in water *versus* reciprocal temperature.

slope of the line in Fig. 2 was found to yield for the activation energy in pure water a value of about 21,900 cal. per mole. The procedure used in this investigation for the resolution of the complex compound resulted in rotations similar to those previously reported. Morgan and Burstall[4] found a molecular rotation of 3735° at 5461 Å. and 17°. Jaeger and van Dijk[5] reported a molecular rotation of 4271° at 5893 Å. and 18°. These values compare with a molecular rotation of 4294° at 5893 Å. and 23.5° as obtained in this investigation.

Effects of Acid and Base.—The effects of hydrogen ions and hydroxide ions as supplied by hydrochloric acid and sodium hydroxide are shown in Fig. 3. Contrary to the findings of Ray and Dutt[6] using active tris-(biguanidine)-cobalt(III) chloride, no tremendous accelerating influence was obtained with the hydroxide ion, nor did the hydrogen ion retard the rate. The actual accelerating influence of the hydrogen ion does agree with the findings of Beese and Johnson[7] with potassium tris-(oxalato)-chromate(III). Apparently the effects of acid and base are specific for each complex.

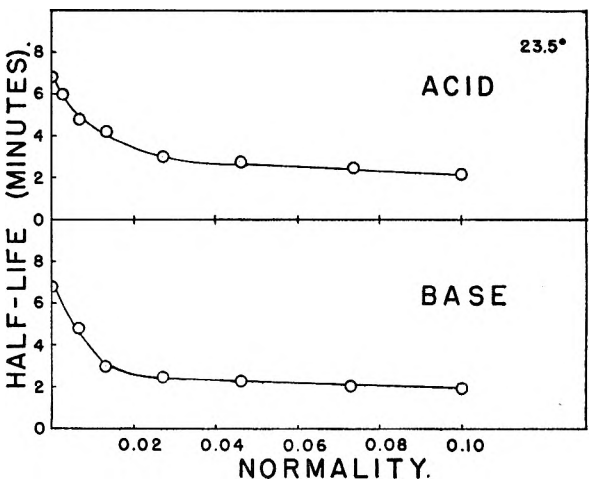

Fig. 3.—The effects of acid and base concentrations upon the racemization half-life.

Effects of Excess Constituents.—In order to test the applicability of the ionization mechanism theory for the racemization of the nickel (II) complex, it was decided to investigate the influences of excess common constituents. Some limitation was imposed by the low solubility of 2,2′-dipyridyl in water. However, the samples containing from 5 to 90 mg. of 2,2′-dipyridyl and 50 mg. of complex in 15 ml. of solution, no significant suppression of the racemization rate was noted. Upon the addition of nickel (II) chloride hexahydrate, a slight increase in the rate was obtained. Tests using samples of from 10 to 70 mg. in 15 ml. of solution showed a decrease in the half-life of 0.8 minute at the maximum sample weight. The relation between half-life and excess nickel(II) ion was linear for points in between the 0 and 70 mg. positions. Assuming that the relation continues to be linear, this indicates that a concentration of 0.08 *M* would be required to reduce the half-life from 6.8 to 3.4 minutes at 23.5°.

Racemization in Mixed Solvents.—In the investigations of mixed solvent effects, all solutions were accurately measured with a buret in the amounts required to give a final volume of 15 ml. The mixed solvents were then equilibrated in the constant temperature bath before addition of the active complex. Sample weights were held as near 50 mg. as possible. Check runs showed no variation greater than 0.5 minute. With all systems studied, a non-linear retardation of the racemization rate as compared to that in pure water was observed.

Two of the systems, acetone–water and dioxane–water, presented a difficulty due to the lack of solubility of the active complex in the non-aqueous solvents. Because of this property, a complete evaluation of the two systems was not obtained. By observing Figs. 4 and 5, it may be seen that

(6) Ray and Dutt, *J. Indian Chem. Soc.*, **20**, 81 (1943).

(7) Beese and Johnson, *Trans. Faraday Soc.*, **31**, 1632 (1935).

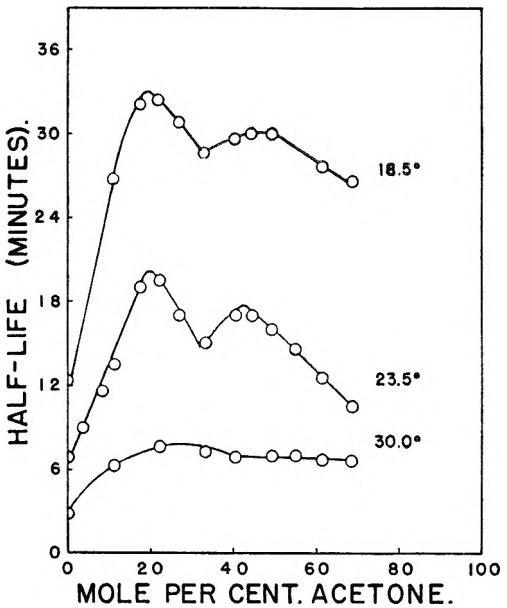

Fig. 4.—Half-lives of racemization in the acetone–water system.

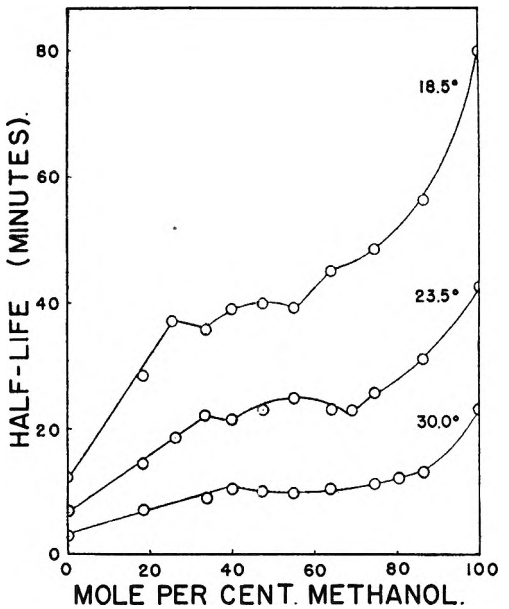

Fig. 6.—Half-lives of racemization in the methanol–water system.

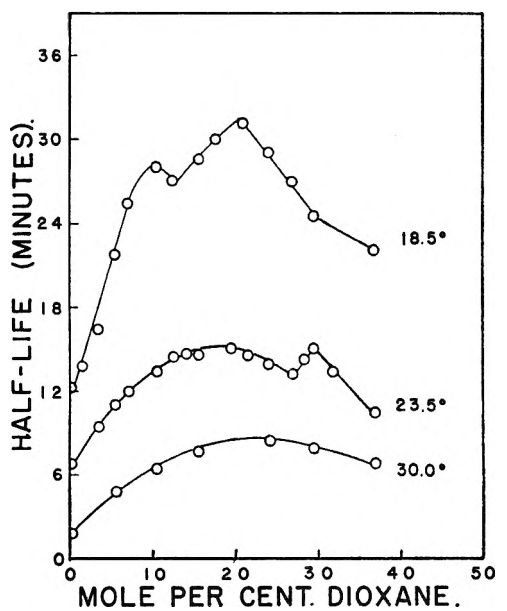

Fig. 5.—Half-lives of racemization in the dioxane–water system.

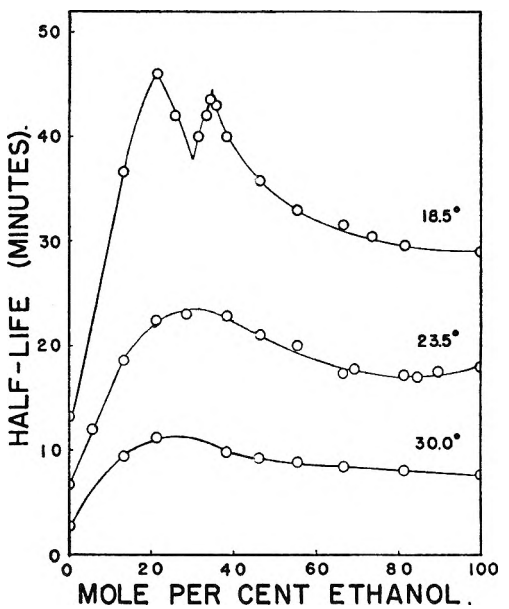

Fig. 7.—Half-lives of racemization in the ethanol–water system.

a two-peaked curve is indicated in both the acetone and the dioxane systems with an increase in peak clarity as the temperature decreases. The dioxane system has a feature of dissimilarity with the acetone system in that it shows a shift in the maxima with decreasing temperature.

The more water-like methanol and ethanol were found to be excellent solvents for the active complex. As might be expected, methanol was the better of the two. The same increasing sharpness of maxima with lowered temperatures is shown in Figs. 6 and 7. It may be seen that in the methanol–water system a regular shift in the peaks occurs. Although the most water-like, methanol retarded the racemization of the active complex to a greater degree than did any of the other solvents.

Calculations of activation energies using the half-lives at the three temperatures and the same concentrations indicate some slight variations from the value obtained in pure water. However, no essential difference was noted for the values calculated between the peaks and the valleys in the curves. All values as calculated fell within the range 22,000 ± 2,000 cal. per mole.

Conclusions

The findings concerning the racemization in water were in complete accord with reported work of previous investigators. The loss in rotation followed a rate coincident with that of first order reactions. Inasmuch as the reported effects of acid and base are somewhat different from those as reported on other complexes, it is probable that the variation may be assigned to the varying degrees of stability of the complexes. The results can probably be related to the ease of decomposition of the complexes in different *p*H ranges.

Such results as were obtained by adding excess common constituents would tend to discredit the theory of racemization by ionization. This is particularly so, since the effect of acceleration pro-

duced by the nickel(II) ion is the opposite of that required to support the theory.

The rather anomalous series of curves obtained in the mixed solvent studies are felt to be related to both the nature of the complex and the mixed solvent. Werner[1] and Bushra and Johnson[2] also found that the addition of acetone to aqueous solutions of several active complexes retarded the racemization rate. Three different tris-(bidentate) type complexes were involved in these investigations. However, in no previous instance was an extensive delineation of the effects of mixed solvent systems carried out.

It has been noted from data available in the literature that with the acetone–water and ethanol–water systems, a plot of viscosity, heat capacity or refractive index as a function of mole per cent. of the non-aqueous solvent gives a curve with the same general outline as was obtained in this investigation. These curves, however, do not show the double peaks which were obtained in the racemization rate studies. Neither does the viscosity, refractive index, or heat capacity of pure water, ethanol or methanol seem to correlate with the experimental values of the half-life.

The solvent system appears to play an important part in the racemization. In just what way is not clear. For instance, even though methanol is very similar to water, it retarded the rate greatly. Just how important the presence of the solvent is in the process of racemization might be illustrated thus. Morgan and Burstall[4] stated that *d*-tris-(2,2′-dipyridyl)-nickel(II) chloride lost half of its rotation in five days, but under more nearly anhydrous conditions afforded in this investigation, the active complex showed no appreciable loss after six weeks.

Acknowledgment.—This paper constitutes contribution number 96 from the University of Tennessee Department of Chemistry. The authors wish to express their thanks to the Research Corporation for the grant which made this work possible.

STUDIES ON THE DIELECTRIC PROPERTY OF SUBSTANCES IN THE SORBED STATE. IV. FREEZING PHENOMENON OF *o*-NITROPHENOL SORBED ON SILICA GEL

BY IZUMI HIGUTI AND MICHIE SHIMIZU

Chemical Institute, Faculty of Science, Tohoku University, Sendai, Japan

Received December 6, 1950

Dielectric polarization of *o*-nitrophenol sorbed on silica gel has been determined in a range of temperature from 10 to 110°. These values, depending on the amount of the sorbate and the temperature showed to make clear discrimination between states of the sorbate, *i.e.*, states of adsorption, capillary liquid and the frozen liquid. Determining the radius of pore in which the sorbate commences to freeze at the given temperature, we have confirmed the theory of the freezing point depression of the dispersed liquid.

Introduction

In the preceding paper,[1] where experimental results of measuring the dielectric polarization of nitrobenzene sorbed on silica gel were described, the freezing phenomenon of the capillary liquid was evidenced and the radii of pores for the commencement of freezing were obtained at a number of temperatures. A theoretical formula, connecting the freezing temperature of the capillary liquid condensed in pores with their radii, was also derived,[2] and found to be in good agreement with the experimental results. In view of few experimental results existing in this field, it may be desired to perform some more experiments for the silica gel and *o*-nitrophenol system, so that the present study has been attempted, using the same experimental method[1] which previously proved to be convenient and pertinent for this purpose.

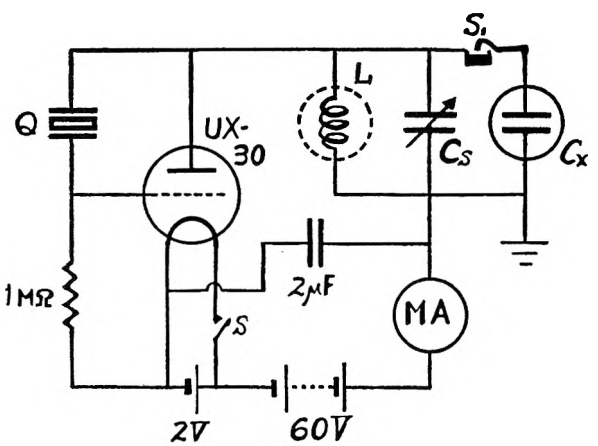

Fig. 1.

Experimental

The electric capacity was measured with a circuit shown schematically in Fig. 1. The whole circuit system was set in a box covered with metal plates in order to avoid the effect of external stray field. When the oscillating circuit is tuned to a fixed frequency of the quartz oscillator of 3 MHz., manipulating externally the standard condenser with a long glass rod outside of box, the indication of milli-ammeter (MA) changes abruptly owing to the decrease of direct current. The difference in scale readings (C_s) on and off switch (S_1) gives the electric capacity (ΔS) of the measuring cell. With this circuit the deflection of MA is sufficiently sensitive to the variation of C_s and its reproducibility is within ± 0.005 of unit scale. The preparation and the procedure of charging the sorbate are the same as in the previous experiment.[3]

(1) I. Higuti, *Sci. Rep. Tohoku Univ.*, Series I, **33**, 174 (1949).

(2) I. Higuti, *ibid.*, **33**, 231 (1949)

(3) I. Higuti, *ibid.*, **33**, 99 (1949).

The melting point of *o*-nitrophenol which was purified by distilling the commercial product four times, was 44.9 ~ 45.0° in accord with the value in the literature, and showed no sign of variation in melting point after heating it to 150° for many hours.

Experimental Results

(A) Density of *o*-Nitrophenol.—Densities of liquid as well as solid *o*-nitrophenol were determined in a wide range of temperatures, in order to apply them in later calculations. The results obtained are given in Table I.

TABLE I

DENSITY OF *o*-NITROPHENOL

Temp., °C.	Density	Temp., °C.	Density	Temp., °C.	Density
Solid		40	1.541	60	1.275
0	1.599	45	1.533	70	1.266
10	1.584	Liquid		80	1.257
20	1.570	45	1.288	100	1.239
30	1.555	50	1.284	110	1.230

(B) Heat Capacity and Heat of Fusion of o-Nitrophenol.—For the same reason mentioned above, heat of fusion and heat capacity of liquid and solid *o*-nitrophenol were determined by means of a conductometric calorimeter. Experimental results on heat capacity are presented in Fig. 2 and the latent heat of fusion was found to be 3.79 kcal/mole, somewhat less than 4.30 kcal./mole in the "I.C.T." On account of volatility of this substance at high temperatures, these values cannot be taken to be accurate enough but will be available in the later section.

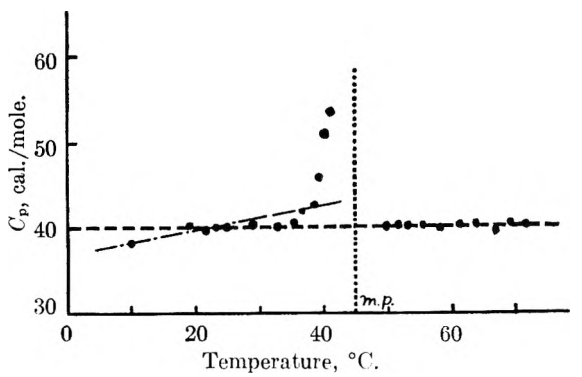

Fig. 2.

(C) The Relation between the Dielectric Polarization (ΔS) and the Temperature at Various Amounts of Sorption. Expt. No. 0 refers to the measurement of ΔS of the cell which contains only the silica gel. Experimental number in the ascending order expresses the measurement at every addition of a definite quantity of the sorbate. The results obtained are represented in Fig. 3. The ordinate (ΔS) denotes the difference in readings on the scale of the standard condenser whose single unit is 21.5 $\mu\mu$F. In Expt. No. 0, ΔS decreases almost linearly with the temperature increase. In experiments from Nos. 1 to 6, the curves seem to exhibit a slight maximum at *ca.* 60°. In Expt. No. 7 the curve shows a steep descent in lower temperature range, and, in addition, values obtained for the first time on increasing or decreasing temperature did not coincide with each other, giving an apparent hysteresis loop, as frequently observed in sorption isotherms. Nevertheless, on repeating measurements twice in sequence, all the values were reversed on the lower curve for descending or ascending temperature. This puzzling phenomenon seems to have some connection with the mechanism of freezing of the capillary liquid, because in this experiment, as described in the later section, some of the sorbate begins to freeze at these temperatures. Experiment No. 8 was generally similar to No. 7, but the observed values were reversed on the same curve, though the equilibrium was reached quite slowly. There appeared a break in the curve of Expt. No. 9 at a temperature lower than the normal melting point, and it shifted gradually to this point in Expt. No. 10 ~ No. 12. In general, it took a still longer time to attain equilibrium at lower temperatures in experiments succeeding No. 9. This seems to be in connection with the super-cooling of the condensed liquid. In this paper, the authors do not attempt to clarify the mechanism of this phase transition. On comparing the main feature of these experiments with those in the case if nitrobenzene reported[1] previously, it may certainly be concluded that, in spite of the lack of data for the dielectric constant of *o*-nitrophenol, the break points at temperatures lower than the normal melting point are due to the freezing of liquid condensed in the capillary pores.

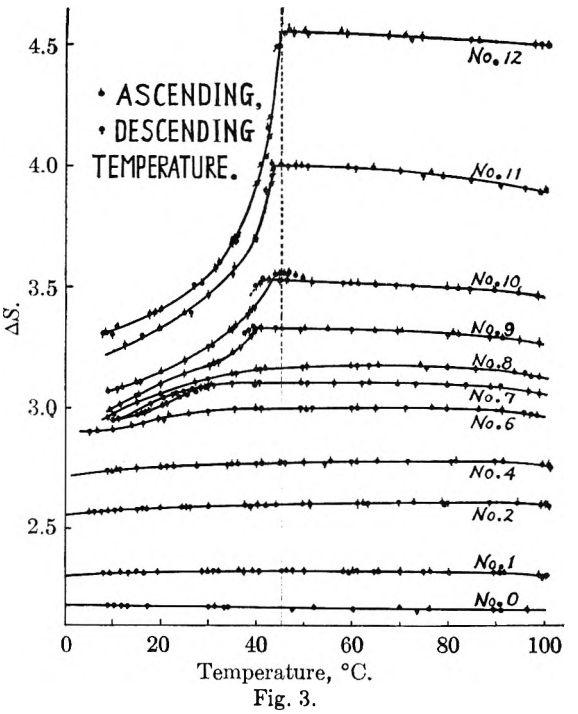

Fig. 3.

(D) The Correlation between the Sorbed Amount (a) and ΔS at Constant Temperature.—By taking a section of the curves in Fig. 3 at constant temperature, we can obtain the $a \sim \Delta S$ relation at any desired temperature. These values are presented in Table II. Increments, $\Delta^2 S$, calculated from values of ΔS in Expt. No. 0 are certainly due to the contribution by the sorbate. The $\Delta^2 S \sim a$ relations exhibited in Fig. 4 are in general linear accompanying some break points, the first of which is in the vicinity of $a = 0.72$ g./g. At this point, lines at 10 and 20° change their directions downwards and those at higher temperatures than 30°, upwards. In general, the angle of intersection becomes smaller as the temperature increases and the break point is no more perceptible at 100°.

In view of the conclusion, established in the case of nitrobenzene, the first portions of straight lines for small amount of sorption might be attributed to the so-called adsorption (see also the next section), and the second portions turning upwards, to the capillary condensation. At temperatures lower than the normal melting point, the second or third portion might be due to the frozen state of the sorbate condensed in capillary pores.

Although not shown in the figure, values of Expt. No. 12, which were obtained with the largest amount of sorbate, deviate upwards at temperatures higher than the normal melting point. This is probably due to either the dielectric polarization of the sorbate condensed in large pores, as ascertained in the preceding paper,[1] or some of the sorbed amount in the free liquid state. The sorbed amount in Expt. No. 12 is slightly less than the saturation value of *o*-nitrophenol, calculated from the benzene isotherm at 0° on the gel of the same lot. If, however, the sorbent might probably suffer shrinking from the repeated heat treatment at above 100° during these experiments, there would be present in the cell some free liquid at higher temperatures and none at lower temperatures. By this reasoning the authors would prefer the latter consideration to the former and it will be referred to in a later section.

TABLE II

CORRELATION OF THE SORBED AMOUNT AND DIELECTRIC POLARIZATION (ΔS)

Expt. no.	Sorbed amount, mg./g.	0°	10°	20°	30°	40°	50°	60°	70°	80°	90°	100°
0	0	2.183	2.181	2.178	2.176	2.173	2.170	2.166	2.163	2.159	2.156	2.152
1	146.2	2.309	2.312	2.314	2.316	2.318	2.320	2.322	2.321	2.320	2.318	2.317
2	396.9	2.556	2.572	2.588	2.599	2.605	2.610	2.612	2.612	2.610	2.606	2.600
3	480.1	2.646	2.659	2.672	2.684	2.693	2.700	2.702	2.701	2.696	2.690	2.682
4	551.2	2.718	2.733	2.748	2.762	2.773	2.780	2.783	2.783	2.782	2.780	2.775
5	624.2	2.787	2.804	2.820	2.835	2.846	2.852	2.854	2.854	2.851	2.847	2.842
6	750.2	...	2.918	2.942	2.977	2.996	3.002	3.005	3.004	2.998	2.988	2.978
7	828.1	...	2.953	3.002	3.077	3.096	3.100	3.100	3.099	3.091	3.078	3.062
8	891.6	...	2.975	3.052	3.122	3.159	3.172	3.172	3.170	3.164	3.154	3.140
9	998.9	...	3.015	3.095	3.178	3.308	3.326	3.321	3.315	3.307	3.296	3.283
10	1165.3	...	3.084	3.150	3.242	3.416	3.510	3.506	3.499	3.491	3.482	3.471
11	1546.5	...	3.236	3.322	3.449	3.706	4.002	3.996	3.981	3.959	3.935	3.909
12	1823.3	...	3.318	3.427	3.567	3.855	4.556	4.548	4.538	4.526	4.510	4.498

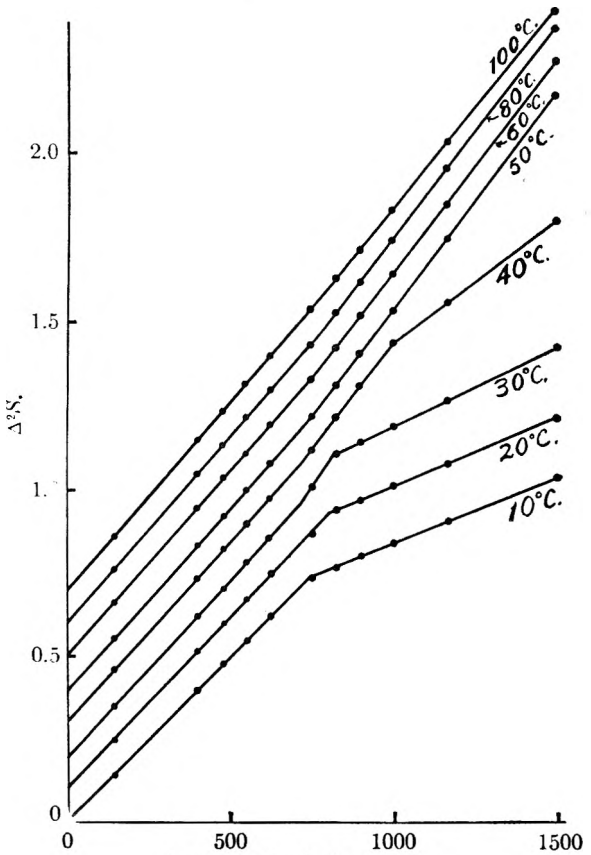

Fig. 4.

Discussion of Results

(1) **The Sorbed Amount and the State of Sorbate.**—If the first portion could be attributed to the so-called adsorption and the second one to the capillary condensation, as mentioned above, the first break point would correspond to the critical limit of the sorbed amount, that is, the sorbate in excess would be in the state of the capillary liquid. The critical amounts of sorption are given in Table III.

TABLE III

THE SORBED AMOUNT AT THE FIRST BREAK POINT

Temp., °C.	30	40	50	60	70	80	90	average
Sorbed amt., g./g.	0.72	.72	.76	.74	.75	.74	.77	.74

By the analogous way, as described in the case of nitrobenzene, the critical point for the commencement of capillary condensation of *o*-nitrophenol can be theoretically calculated on the basis of the isotherm of benzene at 0° on the same silica gel and value 0.448 g./g. of the sorbate was obtained. Great accuracy cannot be expected for these experimental values, owing to the small angle of intersection as shown in Fig. 4. In this case, the discrepancy is pretty large but it might reasonably be interpreted in the following way. Hitherto the author has experimentally found that substances which have a benzene ring in their molecular structures, such as nitrobenzene or *o*-nitrophenol, show a large dielectric polarization in the so-called adsorption state, even comparable to that of the capillary liquid, whereas alcohols, especially at lower temperatures, have distinctly different values according to the state of either adsorption or condensation. These findings will be of importance for investigating the nature of forces, exerting between sorbate molecules and bare surfaces of solid. Further study of this phenomenon is now proceeding in this Laboratory. At any rate, on the basis of this experimental fact, the discrepancy for the first break point found in the present experiment, might be explained, considering that the dielectric polarization of the adsorbate as well as the first capillary liquid, condensed in narrower pores are the same and the first straight lines as shown in Fig. 4 are due to both states of the sorbate. The anomaly found in lines at 10 and 20° in Fig. 4, where lines due to the frozen state start at the first break may be interpreted by the preceding view on the states of the sorbate.

(2) **Dielectric Constants in Various States of Sorption.**—In Table IV there are values of dielectric constants of *o*-nitrophenol, sorbed on silica gel in various states, which have been calculated by the method proposed in the previous paper[3] from the inclinations of lines in Fig. 4. The value for the frozen state becomes large with increasing temperature, whereas that for the second condensed state decreases. In adsorbed state it has a maximum value at an intermediate temperature. These values cannot be compared with those of the ordinary liquid owing to a lack of data in the literature.

(3) **The Sorbed Amount at the Critical Limit for the Commencement of Freezing at Various**

TABLE IV

DIELECTRIC CONSTANT OF o-NITROPHENOL IN VARIOUS STATES OF SORPTION

Temp. °C.	10	20	30	40	50	60	70	80	90	100
Adsorption and 1st condensation	6.09	6.23	6.29	6.39	6.44	6.46	6.47	6.40	6.39	6.49
2nd condensation	..	..	7.96	7.31	7.29	7.18	6.96	6.92	6.73	6.49
Frozen solid	3.41	3.55	4.00	5.24	..	..	..	..	..	..

Temperatures.—If the straight lines with decreased inclination might be due to the frozen state of the sorbate, the break points may be taken as the critical points where the sorbate begins to freeze at each temperature. The sorbed amounts at these points are given in the second line of Table V. As in the preceding paper,[3] radii of capillary pores corresponding to these amounts of sorption

TABLE V

Temperature, °C.	10	20	30	40
Sorbed amount, mg./g.	732	800	830	1000
Corresponding capillary radius, Å.	46.7	64.4	85.2	171
Corr. radius, Å.	67.8	96.1	135	268
σ calcd. 1 erg./cm.	43.8	42.8	33.8	22.5
σ calcd. 2	35.0	35.6	29.0	19.9
σ calcd. 3	50.8	53.2	45.9	31.9
σ lit. 1	43.1	41.8	40.6	39.4
σ lit. 2	45.4	44.1	42.9	41.8
ΔH_T, kcal./mole	3.43	3.56	3.69	3.78

have been calculated by the same method, based on the experimental isotherm of benzene at 0° on the silica gel of the same lot as one used in this experiment. The third line of Table V shows these values. The physical meaning of these values is that o-nitrophenol may be in the liquid state, for example, even at 20° if it will condense in capillary pores whose radii are less than 64.4 Å.

(4) **Comparison of Experimental Results with the Theoretical Formula in Regard to the Freezing Point Depression.**—In a previous paper,[2] a formula of the form

$$\frac{\Delta T}{T_0} = \frac{2\sigma M}{\gamma \rho \Delta H_t} \qquad (1)$$

has been derived thermodynamically for the freezing point depression of capillary liquid condensed in a pore whose radius is r. In the above formula, T_0, M and ΔH_T are the normal melting point, the molecular weight and the heat of fusion of the sorbate; σ and ρ are the surface tension and the density of the liquid, respectively. To the first approximation, the capillary liquid may be considered to have the same properties as the normal liquid. As the surface tension of supercooled liquid is uncertain, instead of calculating ΔT, σ was computed by substituting experimental results for r and ΔT and other data in the literature into the formula, thus obtaining σ calcd. 1 in the fifth row of Table V. σ lit. 1 in the eighth row are the values extrapolated linearly from values at two higher temperatures measured by Hewitt, *et al.*,[4] and σ lit. 2 in the ninth row are calculated by combining the value of parachor at 45.2° given by Bhatnagar, *et al.*,[5] with the density measured in the present experiments. Theoretically calculated values of surface tension may be seen, to the first approximation, to be in agreement with those in the literature, especially at low temperatures. On the other hand, formula (1) is an approximate form which is applicable only in a narrow temperature range of ΔT, as fully described in the previous paper.[2] We can apply it, however, even for large ΔT, if we use the value of ΔH_T at actual melting point instead of that at the normal melting point. Heat of fusion at any desired temperature can be computed by the thermodynamic formula of the form

$$\Delta H_T = \frac{\Delta H_0}{T_0} T - T \int_T^{T_0} \frac{(C_p^L - C_p^S)dT}{T} \qquad (2)$$

ΔH_T values, thus determined on the basis of the calorimetric data, as given in Fig. 2, are presented in the tenth row of Table V. On carrying out the computation with these values of ΔH_T, we obtain σ calcd. 2 in the sixth row. The agreement, however, is in general less favorable. These discrepancies, though of minor significance, might be considered to be due to the shrinkage of the sorbent, as suggested in the preceding section, on account of being heated at higher temperatures above 100° many times for more than one year. For this reason it is more probable to make a correction for the benzene isotherm at 0°, on the basis of which capillary radii have been computed. From the benzene isotherm, reducing the sorbed amount by 10%, we have different values of capillary radii for the critical limit, as given in the fourth row instead of the third row of Table V. σ calcd. 3 in the seventh row, calculated with these values of radii and ΔH_T in the tenth row are remarkably different from those of σ calcd. 1 or σ calcd. 2. The correction made in the calculation is of some arbitrary character. In view of the result brought by this correction, however, the above assumption for the nature of discrepancies may be valid essentially. Hence, with correction less in the first portion and more in the later portion of the isotherm, computed values of surface tension will fit completely to the experimental results. However, without any reasonable basis of carrying out such corrections precisely, it is meaningless to go further on this line. However that may be, we can say that experimental results have given additional evidence that the freezing point depression of the sorbate depends on the radius of capillary pores in which it is condensing and that its magnitude (ΔT) is given by the formula derived thermodynamically in the previous paper.[3]

In conclusion the authors express their cordial thanks to Prof. F. Ishikawa for his helpful advices and encouragement throughout this work and also to Mr. Koichi Kobayashi to whom we are indebted for the heat capacity measurements. It is also noted that the expense of this research has been partially defrayed from a Grant in Aid for Fundamental Scientific Research by the Department of Education.

(4) J. H. Hewitt and T. F. Winmill, *J. Chem. Soc.*, **91**, 441 (1907).

(5) S. S. Bhatnagar and B. Singh, *J. chim. phys.*, **25**, 21 (1928).

THE PERIODICITY OF CHEMICAL THERMODYNAMIC FUNCTIONS

BY DAVID HART

Chemical Research Laboratory, Picatinny Arsenal, Dover, New Jersey

Received December 18, 1950

An extensive study of the periodicity of chemical thermodynamic functions has developed definite relationship between atomic number and equivalent heat of formation, entropy, oxidation-reduction potential, ionization potential and electronegativity for oxides. Halides and sulfides also have been studied.

I. Introduction

Ever since the time of Berthelot[1] attempts have been made to determine whether a more or less general relationship exists between the heats of formation of inorganic compounds and the periodic system. While the results of these attempts showed a definite relationship within each periodic group, it was not until recently, when Trombe[2] considered the heat of formation per gram atom of halogen instead of the molecular heat of formation of the halide, that any general relationship was indicated. An excellent summary of these attempts is given by Süe[3] who, like Trombe, plotted that the heat of formation per gram atom of the electronegative element as a function of the atomic number of the less electronegative element in the compound. However, Süe applied this method to oxides, sulfides and nitrides as well as to halides and obtained a series of saw-tooth curves. He also tried to relate the heats of formation of inorganic compounds to the average ionization potentials, *i.e.*, the energy required to separate all the valence electrons of an element divided by the number of these electrons.

Using the concept of electronegativity, Pauling[4] introduced a certain amount of order into inorganic thermochemistry. The electronegativity, which is directly related to the heat of formation, was plotted as a function of the atomic number.

As a result of a systematic investigation, begun in 1942, of a number of inorganic oxidation–reduction reactions between finely divided solid particles,[5–8] the existence of a more or less general relationship between a number of thermochemical as well as thermodynamic functions and the periodic system was recognized. Some of these functional relationships have not yet appeared in the literature. It is the purpose of this paper, therefore, to show that a careful consideration of these relationships will reveal the existence of considerable amount of order in the field of inorganic thermochemistry.

II. Equivalent Heat of Formation and Atomic Number

If the equivalent heats of formation of the oxides of the elements are plotted as a function of the atomic number, a series of curves is obtained which show a very definite and interesting periodicity. By the equivalent heat of formation of oxides is meant the value obtained by dividing the heat of formation by the number of equivalents of oxygen.

In Fig. 1, only those values were taken for the oxides which correspond to the predicted valence given by the periodic table. Solid lines were drawn between points obtained from the heats of formation values available in the literature. The values were taken from Bichowsky and Rossini,[9] Latimer,[10] Thompson,[11] Kelley,[12,13] and the National Bureau of Standards.[14] By following the pattern indicated, dotted lines were drawn from which the approximate values of the equivalent heats of formation of oxides can be estimated for which there are at present no data in the literature as to their heats of formation. From the estimated equivalent heats of formation taken from the figure, the corresponding heat of formation can be calculated. The curves obtained are a series of approximately parallel straight lines with some deviations for the oxides of the elements at the beginning of a period. Thus, for the first period, all except lithium oxide fall on a straight line. For the second period, sodium oxide does not fall on the straight line and magnesium oxide is also somewhat off. The maxima of these curves occur with lithium oxide for the first period, the divalent element oxides for the second and third periods, and the trivalent element oxides for the other periods.

III. Equivalent Free Energy of Formation of Oxides and Atomic Number

Although the standard heat of formation, $-\Delta H_f^0$, of the oxides at 298.16°K.[15] has been considered a rough measure of the stability, the true measure of this property is considered to be the standard free energy of formation, $-\Delta F_f^0$ at 298.16°K. In a series of publications beginning with 1932, Kelley[12] of the U. S. Bureau of Mines, gives the most probable values of the standard free energies of formation at 25°. In 1942 Thompson[11] published a

(1) Berthelot, "Thermochemie," Vol. I, p. 284.
(2) C. R. Trombe, *Acad. Sci.*, **218**, 457 (1944).
(3) Pierre Süe, *J. Chim. Phys.*, **42**, 45 (1945).
(4) Linus Pauling, *J. Am. Chem. Soc.*, **54**, 3570 (1932).
(5) George C. Hale and D. Hart, U. S. Patent 2,461,544 (1949).
(6) George C. Hale and D. Hart, U. S. Patent 2,467,334 (1949).
(7) George C. Hale and D. Hart, U. S. Patent 2,468,061 (1949).
(8) D. Hart, Unpublished Results and Picatinny Arsenal Technical Reports.
(9) F. R. Bichowsky and F. D. Rossini, "The Thermochemistry of the Chemical Substances," Reinhold Publishing Corp., New York N. Y., 1936.
(10) W. M. Latimer, "The Oxidation States of the Elements," Prentice-Hall, Inc., New York, N. Y., 1938.
(11) M. deKay Thompson, "The Total and Free Energies of Formation of Oxides of Thirty-Two Metals," The Electrochemical Society, Inc., New York, N. Y., 1942.
(12) K. K. Kelley, U. S. Bureau of Mines, Bull., 350 (1932).
(13) K. K. Kelley and C. T. Anderson, U. S. Bureau of Mines, Bull., 384 (1935).
(14) F. D. Rossini, D. D. Wagman, W. H. Evans, L. Levine and I. Jaff, "Selected Values of Chemical Thermodynamic Properties" N. B. S. Circular 500, U. S. Govt. Printing Office, 1951.
(15) G. N. Lewis and M. Randall, "Thermodynamics and the Fre Energy of Chemical Substances," McGraw-Hill Book Co., Inc., New York, N. Y., 1923.

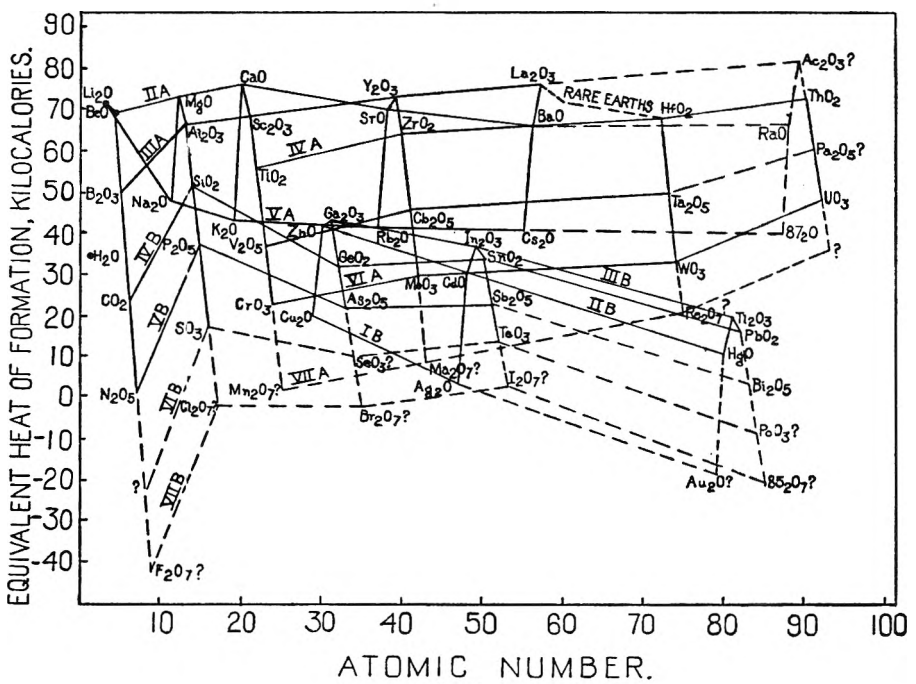

Fig. 1.

comprehensive critical survey of free energy relations for thirty-two metallic oxides. More recently the National Bureau of Standards,[13] with the aid of the U. S. Navy Department, Office of Naval Research, is compiling "Tables of Selected Values of Chemical Thermodynamic Properties." However, many values for the free energy of formation of oxides still are not available. In Fig. 2 the equivalent free energies of formation of the oxides, calculated from available free energies of formation, were plotted as a function of atomic number.

The curves obtained were a series of approximately parallel straight lines, similar to those in Fig. 1 for the equivalent heats of formation. The corresponding decomposition potentials were calculated and an appropriate scale placed on the right-hand side in Fig. 2. Here, too, solid lines were drawn between points obtained from the literature values and dotted lines were drawn to follow out the pattern. In this manner approximate values for equivalent free energies of formation were obtained from which approximate values for the corresponding free energy of formation could be calculated which are not available in the literature.

A tabulation of the values used to obtain Figs. 1 and 2 is given in Table I. Included in this table

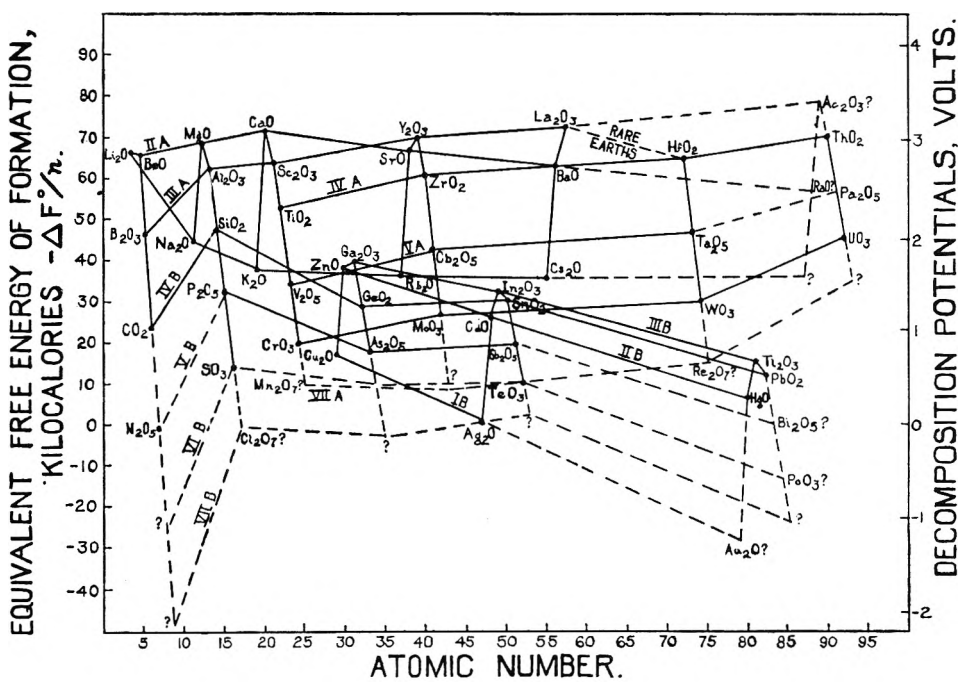

Fig. 2.

TABLE I

CHEMICAL THERMODYNAMIC PROPERTIES OF THE ELEMENTS AND OXIDES

Periodic group	Atomic number	Element	Entropy of elements at 298.16°K. $S°$, cal./deg. mole	Oxide	Entropy of oxide at 298.16°K. $S°$, cal./deg. mole	Entropy of formation of oxide $\Delta S°$, cal./deg.	Standard heat of formation ΔHf^0, kcal./mole	Equivalent heat of formation ΔHf^0, kcal.	Standard free energy of formation ΔFf^0, kcal./mole	Equivalent free energy of formation $\Delta Ff^0/n$, kcal.	Electronegativities of the Elements
	1	H	31.2[a]	H_2O	16.72	− 39.0	− 68.3	−34.2	− 56.7	−28.4	2.1
IA	3	Li	6.7	Li_2O	(5.9)	(− 32)	−142.3	−71.2	−132.8	−66.4	1.0
	11	Na	12.2	Na_2O	17	− 31.9	− 99.45	−49.7	− 89.9[19]	−45.0	0.9
	19	K	15.2	K_2O	(22.9)	(− 32)	− 86.2	−43.1	− 76.7	−38.4	.8
	37	Rb	16.6	Rb_2O	(25.7)	(− 32)	− 82.8	−41.5	− 73.4	−36.7	.8
	55	Cs	19.8	Cs_2O	(32.1)	(− 32)	− 82.1	−41.1	− 72.6	−36.3	.7
	87		(22.5)		(37.5)	(− 32)	(− 81)	(−40.5)	(− 71.5)	(−35.8)	.7
IB	29	Cu	7.96	Cu_2O	24.1	− 16.3	− 39.84	−19.92	− 34.98	−17.49	1.8
	47	Ag	10.21	Ag_2O	29.09	− 15.8	7.31	− 3.66	− 2.59	− 1.3	1.8
	79	Au	11.4	Au_2O	(34.8)	(− 12.5)					2.3
IIA	4	Be	2.28	BeO	3.37	− 23.4	−139	−69.5	−132	−66	1.5
	12	Mg	7.77	MgO	6.55	− 25.6	−146.1	−73.1	−138.5	−69.3	1.2
	20	Ca	9.95	CaO	9.5	− 25.0	−151.7	−75.9	−144.2	−72.1	1.0
	38	Sr	12.5[16]	SrO	13.0	− 24.0	−140.8	−70.4	−133.6	−66.8	1.0
	56	Ba	16.2[16]	BaO	16.8	− 23.9	−133	−66.5	−125.9	−63.0	0.85
	88	Ra	(19.9)	RaO	(19.9)	(− 24.5)					0.8
IIB	30	Zn	9.95	ZnO	10.5	− 24.1	− 83.17	−41.59	− 76.05	−38.0	1.5
	48	Cd	12.3	CdO	13.1	− 23.7	− 60.86	−30.43	− 53.79	−26.9	1.5
	80	Hg	18.5	HgO[g]	17.2	− 26.4	− 21.68	−10.84	− 13.99	− 7.0	1.9
IIIA	5	B	1.7	B_2O_3	(2.4)	(− 74.5)	−339.8	−56.6	−317.6	−52.9	2.0
	13	Al	6.75	Al_2O_3	12.5	− 74.5	−399.0	−66.5	−376.8	−62.8	1.5
	21	Se	8.0[16]	Sc_2O_3	(15)	(− 74.5)	−410	−68.3	−387.8	−64.6	1.3
	39	Y	10.5[16]	Y_2O_3	(20)	(− 74.5)	−440	−73.3	−417.8	−69.6	1.2
	57	La	13.7	La_2O_3	(26.4)	(− 74.5)	−457	−76.2	−434.8	−72.5	1.1
(Rare Earths)											
	89	Ac		Ac_2O_3		(− 74.5)	(−490)	(−82)	(−468)	(−78)	1.0
IIIB	31	Ga	10.2	Ga_2O_3	24	− 69.9	−258	−43	−237	−39.5	1.6
	49	In	12.5	In_2O_3	29	− 73.5	−222.5	−37.1	−200.5	−33.4	1.6
	81	Tl	15.4	Tl_2O_3	(35.4)	(− 74.5)	−120	−30	− 98.1	−16.4	1.9
IVA	22	Ti	7.24	TiO_2	12.01	− 43.2	−225[17]	−56.3	−212.1	−53.0	1.6
	40	Zr	9.18	ZrO_2	12.03	− 46	−258.2	−64.6	−244.4	−61.1	1.6
	72	Hf	13.1	HfO_2	19.6	− 42.5	−271.5	−67.9	−258.8	−64.7	1.3
	90	Th	13.6	ThO_2	19.6	− 43.0	−293	−73.3	−280.2	−70.1	1.1
IVB	6	C	1.36[d]	CO_2	51.06		− 94.05	−23.51	− 94.26	−23.74	2.5
	14	Si	4.47	SiO_2	10.00	− 43.77	−205.4	−51.35	−192.4	−48.1	1.8
	32	Ge	10.14	GeO_2	(13)	(− 46)	−128.3	−32.1	−114.5	−28.6	1.7
	50	Sn	12.3	SnO_2	12.5	− 48.8	−138.8	−34.7	−124.2	−31.05	1.8
	82	Pb	15.51	PbO_2	18.3	− 46.21	− 66.12	−16.53	− 52.34	−13.09	1.8
VA	23	V	7.05	V_2O_5	31.3	−105.3	−373	−37.3	−344	−34.4	1.8
	41	Cb	8.47[16]	Cb_2O_5	(32.5)	(−107)	−463.2	−46.32	−431	−43	1.6
	73	Ta	9.9	Ta_2O_5	34.2	−108.1	−499.9	−49.99	−470.6	−47.06	1.4
	91	Pa		Pa_2O_5							1.4
VB	7	N	45.77[a]	N_2O_5	36.6		− 10	− 1			3.0
	15	P	10.6[e]	P_2O_5	(29.7)	(−114)	−367.0	−36.70	−333	−33.3	2.1
	33	As	8.4	As_2O_5	25.2	−114.1	−218.6	−21.86	−184.6	−18.46	2.0
	51	Sb	10.5	Sb_2O_5	29.9	−113.6	−234.4	−23.4	−200.5	−20.05	2.1
	83	Bi	13.6	Bi_2O_5	(35.7)	(−114)					1.8
VIA	24	Cr	5.68	CrO_3	(17.2)	(−62)	−138.4	−23.1	−120	−20	2.1
	42	Mo	6.83	MoO_3	18.68	− 61.65	−180.33	−30.06	−161.95	−27	2.1
	74	W	8.0	WO_3	19.90	− 61.6	−200.16[18]	−33.36	−182.47	−30.4	2.1
	92	U	11.1	UO_3	(22.6)	(− 62)	−291.6	−48.6	−273	−45.5	
VIB	8	O	49.003[a]								3.5
	16	S	7.62[f]	SO_3	17.7	− 63.4	−105.2	−17.5	− 86.3	−14.5	2.5
	34	Se	10.0	SeO_3	(20.1)	(− 63.4)					2.3
	52	Te	11.88	TeO_3	(22)	(− 63.4)	− 83.6[17]	−13.9	− 64.6	−10.8	2.1
	84	Po									2.0
VIIA	25	Mn	7.61	Mn_2O_7							2.3
	43										
	75	Re	8	Re_2O_7			−297.5	−21.3			
	93										
VIIB	9	F	48.6[a]								4.0
	17	Cl	53.29[a]	Cl_2O_7							3.0
	35	Br	36.4[b]								2.8
	53	I	27.9[c]								2.6
	85										2.4

[a] Value for diatomic gas. [b] Value for diatomic liquid. [c] Value for diatomic solid. [d] Graphite. [e] White; red = 7. [f] Rhombic. [g] Red.

(16) V. Kireev, *Acta Physicochim., U. R. S. S.*, **21**, 55 (1946).

(17) B. Neumann, C. Kroger and H. Kunz, *Z. anorg. allgem. Chem.*, **232**, 335 (1937).

(18) G. Huff, E. Squitieri and P. E. Snyder, *J. Am. Chem. Soc.*, **70**, 3380 (1948).

(19) V. A. Kiren, "Zhurnal fizicheskoi khimie Leningrad," **22**, 847 (1948).

are other chemical thermodynamic functions such as the entropies of the elements and oxides, the entropies of formation for the oxides, ionization potentials and electronegativities. The values in parentheses were estimated from the figures given in this paper.

The following conclusions may be drawn from Table I: (1) Any oxide of an A family has a greater heat of formation and free energy of formation than any oxide of the corresponding B family. (2) In Groups IA, IB, IIA, IIB, IIIB and IVB, the heats of formation of the oxides decrease with increasing atomic number except for the following: (a). The first two oxides of Group IIA, BeO and MgO, have lower heats of formation than the other oxides of this group. (b) In Group IVB the first oxide, CO_2, a gas, has a lower heat of formation than the other oxides, which are solids. (3) In Groups IIIA, IVA, VA, VIA and VIIA, the heats of formation and free energy of formation of the oxides increase with increasing atomic number. (4) In Groups VB, VIB, and VIIB, the heats of formation fluctuate alternately beginning with a relatively low value, then high and then low again. Similar conclusions may be drawn for the equivalent heats of formation and equivalent free energies of formation.

The oxides were then arranged in the order of decreasing equivalent heat of formation as in Table II. This same order is obtained for the equivalent free energies of formation. From this table it appears that the equivalent free energies of formation rather than the free energies themselves are a measure of the relative stabilities of the oxides at ordinary temperatures. Of course, these values do not afford a true measure of the relative stabilities at the much higher temperatures employed in metallurgical practice. To determine these, calculations would have to be made of the free energies of formation at different temperatures, using the standard equation given by K. K. Kelley[20]

$$\Delta F^\circ = \Delta H_0 + aT \log T + bT^2 + cT^{-1} + IT$$

Such calculations have been made by Ellingham[21] for the oxides and sulfides generally used in metallurgy. He plotted the variation with temperature, of the free energy of formation of the oxides and sulfides. He expressed the free energy of formation in kilocalories per gram molecule of oxygen, O_2, for the oxides and per gram molecule of sulfur gas, S_2, for sulfides. Had he used equivalent free energies of formation in each case, the relationships would have been the same, but comparison between the oxides, sulfides and other types of inorganic compounds such as halides, nitrides and others could then be made.

TABLE II

CHEMICAL THERMODYNAMIC PROPERTIES OF THE OXIDES IN THE ORDER OF EQUIVALENT HEATS OF FORMATION AND EQUIVALENT FREE ENERGY OF FORMATION

Oxide	Heat of formation, $-\Delta Hf^\circ$, kcal./mole	Equivalent heat of formation, $-\Delta Hf^\circ/n$, kcal.	Free energy of formation, $-\Delta Ff^\circ$, kcal./mole	Equivalent free energy of formation, $-\Delta Ff^\circ/n$, kcal.
Ac_2O_3	(490)	(82)	(468)	(78)
La_2O_3	457	76.2	434.8	72.5
CaO	151.7	75.9	144.2	72.1
Y_2O_3	440	73.3	417.8	69.6
ThO_2	293	73.3	280.2	70.1
MgO	146.1	73.1	138.5	69.3
Li_2O	142.3	71.2	132.8	66.4
SrO	140.8	70.4	133.6	66.8
BeO	139	69.5	132	66
Sc_2O_3	410	68.3	387.8	64.6
HfO_2	271.5	67.9	258.8	64.7
BaO	133	66.5	125.9	63.0
Al_2O_3	399.0[22]	66.5	376.8	62.8
ZrO_2	258.2	64.6	244.4	61.1
B_2O_3	339.8[23]	56.6	317.6	52.9
TiO_2	225	56.3	212.1	53.0
SiO_2	205.4	51.4	192.4	48.1
Ta_2O_5	499.9	50.0	470.6	47.1
Na_2O	99.5	49.7	89.9	45.0
UO_3	291.6	48.6	272.4	45.4
Cb_2O_5	463.2	46.3	431.2	43.1
Ga_2O_3	258	43	237	39.5
K_2O	86.2	43.1	76.7	38.4
ZnO	83.6	41.6	76.1	38.0
Rb_2O	82.9	41.5	73.4	36.7
Cs_2O	82.1	41.1	72.6	36.3
87	(81)	(40.5)	(71.5)	(35.8)
V_2O_5	373	37.3	344	34.4
In_2O_3	222.5	37.1	200.5	33.4
P_2O_5	367.0	36.7	333	33.3
SnO_2	138.8	34.7	124.2	31.05
H_2O	68.3	34.2	56.7	28.4
WO_3	200.16	33.4	182.5	30.4
GeO_2	128.3	32.1	114.5	28.6
CdO	60.86	30.43	53.79	26.9
MoO_3	180.33	30.1	161.95	27
CO_2	94.05	23.5	94.26	23.56
CrO_3	138.4	23.1	120.0	20.0
Sb_2O_5	234.4	23.4	200.5	20.1
As_2O_5	218.6	21.9	184.6	18.5
ReO_4	297.5	21.3		
Cu_2O	39.84	19.9	35.0	17.5
Tl_2O_3	120	20	98.1	16.4
SO_3	105.2	17.5	86.3	14.4
PbO_2	66.12	16.5	52.34	13.1
HgO	21.68	10.84	13.99	7.0
Ag_2O	7.31	3.7	2.6	1.3
N_2O_5	10	1	....	...

IV. Oxidation-Reduction Potentials and Periodicity

Since the order of the oxides as given in Table II resembled the electromotive series of the metals, the oxidation–reduction potentials of the elements were plotted as functions of atomic number. Most of the values employed were taken from Latimer.[9] A series of curves were obtained which resemble those in Figs. 1 and 2 for the equivalent heats of formation and equivalent free energies of formation of the oxides. It is possible by means of the curves in Figs. 3 and 4 to estimate those oxidation–reduction potentials which are not now available in the literature.

It is interesting to note that the value of the oxidation–reduction potential in alkaline solution

(20) K. K. Kelley, U. S. Bureau of Mines Bull., 406 (1937).

(21) H. J. T. Ellingham, *J. Soc. Chem. Ind.*, **63**, 125 (1946).

(22) P. E. Snyder and H. Sitz, *J. Am. Chem. Soc.*, **67**, 6835 (1945).

(23) W. A. Roth, *Z. Naturforsch.*, **1**, 574 (1946).

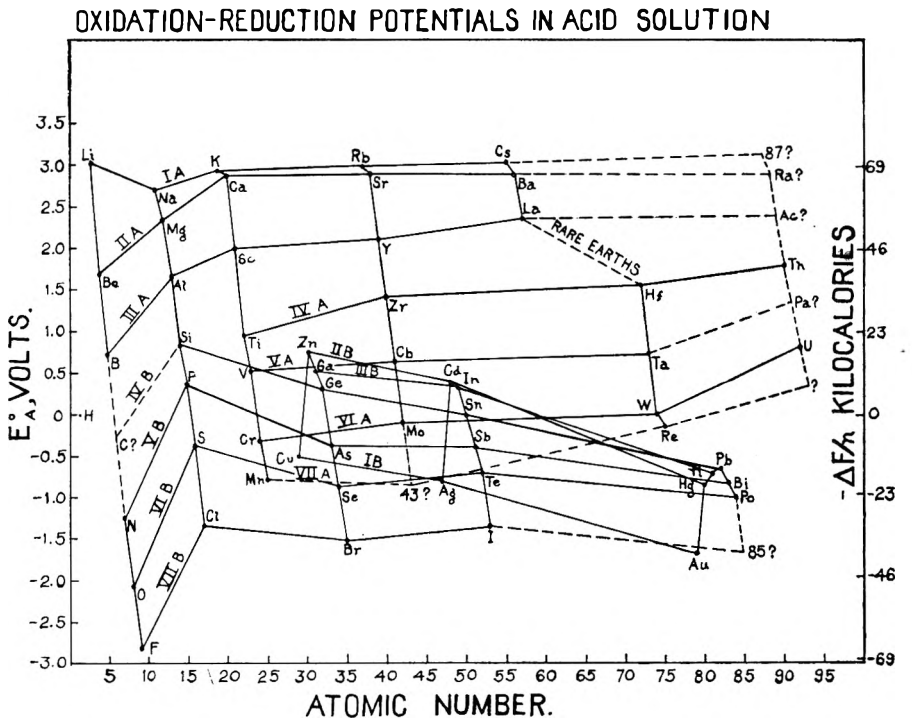

Fig. 3.

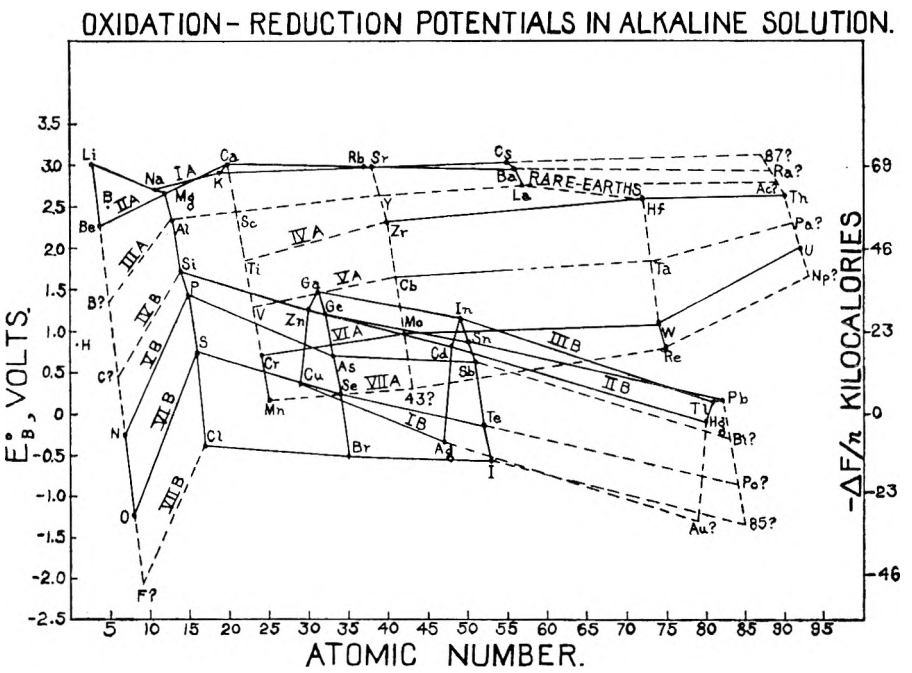

Fig. 4.

for boron as given in Latimer,[10] namely, 2.5 volts, does not fall on the first straight line in Fig. 4, whereas in Figs. 1, 2 and 3, the values for boron do fall on the first straight line. The indications are, therefore, that the value of the 2.5 volts for the oxidation–reduction potential of boron in alkaline solution may be too high. A value of approximately 1.5 volts is indicated from the curve in Fig. 4.

A comparison was made between the decomposition potentials of the oxides as calculated from the equivalent free energies, and the oxidation–reduction potentials in acid and alkaline solution for the corresponding elements. Table III shows this comparison for some of the more common metals. It is interesting to note that the order of decreasing equivalent free energy of formation for the oxides is, with few exceptions, the same as the order of decreasing oxidation–reduction potentials of the metals in alkaline solution. The similarity is not nearly as great between the order of the oxides and the oxidation–reduction potentials of the metals in acid medium. This is to be expected, since the latter involves a change from metal to ion, while the forma-

TABLE III

A COMPARISON OF THE ORDER OF EQUIVALENT FREE ENERGY OF FORMATION OF OXIDES WITH THE ORDER OF OXIDATION-REDUCTION POTENTIAL FOR THE CORRESPONDING METALS

Oxide	Equivalent heat of formation, $-\Delta H/n$, kcal.	Equivalent free energy, $-\Delta F/n$, kcal.	Decomposition potential, volts	Standard oxidation-reduction potentials in alkaline solution, E_B^0, volts	Metal product	Standard oxidation-reduction potentials in acid solution, E_A^0, volts
MgO	73.1	69.3	3.00	2.67	$Mg(OH)_2$	2.375[21]
Al_2O_3	66.5	62.8	2.72	2.35	$H_2AlO_3^-$	1.67
ZrO_2	64.6	61.1	2.66	2.32	H_2ZrO_3	1.43
TiO_2	56.3	53.0	2.30	(1.85)		0.95
SiO_2	51.4	48.1	2.06	1.73	$SiO_3^=$	0.84
MnO	48.3	(44.9)	1.95	1.47	$Mn(OH)_2$	1.05
Cr_2O_3	45.5	(42.1)	1.82	1.3	$Cr(OH)_3$	0.71
ZnO	41.6	38.0	1.66	1.216	$ZnO_2^=$	.76
SnO_2	34.7	31.1	1.34	0.88	$Sn(OH)_6^=$	.01
Fe_2O_3	33.1	(29.7)	1.29	0.56	$Fe(OH)_3$	.036
WO_3	33.4	30.4	1.28	1.1 *ca.*	$WO_4^=$	.01
CdO	30.4	26.9	1.26	0.815	$Cd(OH)_2$	.40
MoO_3	30.1	27	1.14	.97	$MoO_4^=$	− .1
NiO	29.2	(25.8)	1.12	.66	$Ni(OH)_2$	.25
CoO	28.8	(25.4)	1.10	.73	$Co(OH)_2$	.28
Sb_2O_3	27.6	(24.2)	1.05	.66	SbO_2^-	− .212
Bi_2O_3	22.9	(19.5)	0.85	.46	BiOOH	− .32
CuO	19.3	(15.9)	0.69	.224	$Cu(OH)_2$	− .345

tion of oxides involves a change from metal to oxide and the potentials in alkaline solution involve a change from metal to hydrated oxide or hydroxide.

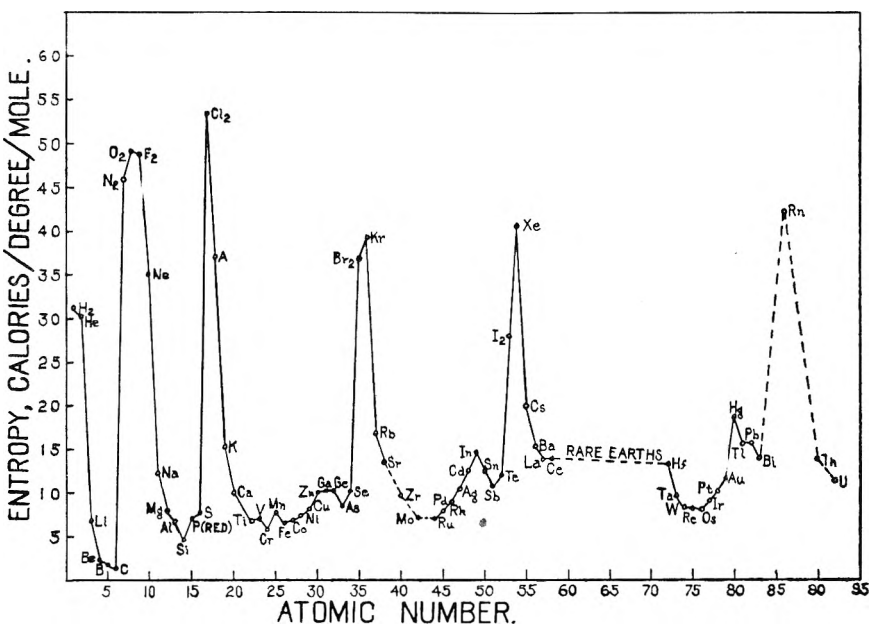

Fig. 5.

V. Entropy and Periodicity

If the entropies of the elements at 298.16°K. are plotted as a function of atomic number, certain periodic regularities are observed, as shown in Fig. 5. For the first period, a maximum occurs at oxygen. For the second period the maximum occurs at chlorine. However, for the other periods, maxima occur at the inert gases: namely, Krypton, Xenon and Radon. From the curves in Fig. 5, approximate entropy values may be estimated for those elements whose entropies are not available in the literature.

Latimer[25] has shown that the entropy of a number of solids may be represented by the sum of the entropies of the atoms in the solid, using the equation

$$S^0 = 3/2\ R \ln \text{at. wt.}_1 + 3/2\ R \ln \text{at. wt.}_2 + \cdots + nS_1$$

The constant S_1 was evaluated by Latimer from the general equation, using the value 19.70 for the entropy of potassium chloride, and found to be equal to −0.94. Although this equation is applicable to a number of halogen salts, it was found not to be

(24) G. E. Coates, *J. Chem. Soc.*, 478 (1945)

(25) W. M. Latimer, *J. Am. Chem. Soc.*, **43**, 818 (1921)

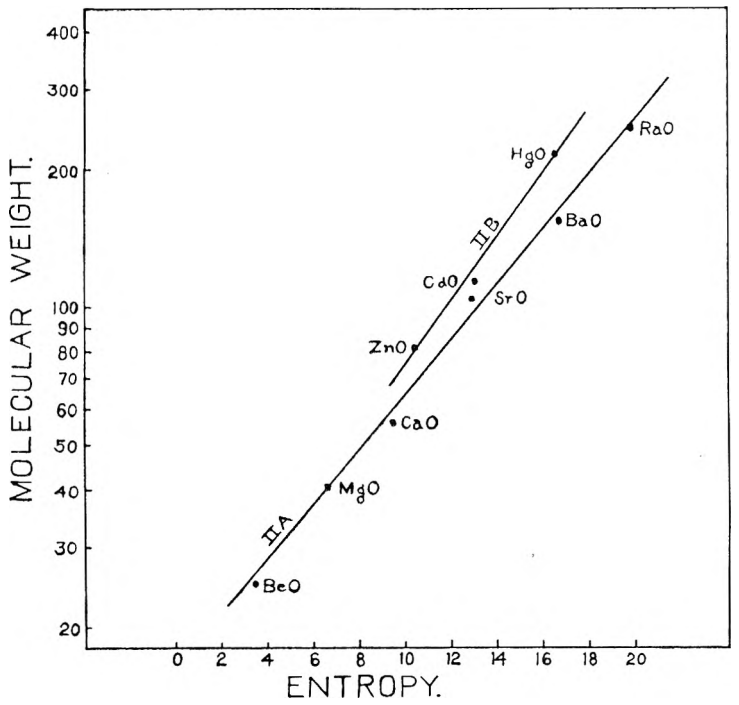

Fig. 6.

applicable to the solid oxides. Wenner[26] indicated that straight lines are obtained when the molar entropies at 25° are plotted against the log of the molecular weight, for each type of inorganic compound, such as the oxides MO, MO_2; the halides MX, MX_2; the sulfides MS and others. However, applying this rule to the solid oxides, the author found that this empirical relationship occurred only with the oxides in the same periodic group. Thus in Fig. 6 the solid oxides of Group IIA fall on one line, while those of Group IIB, which are similar, fall on another line. The same is true for the solid oxides of Groups VA and VB in Fig. 7. It should be noted that for the solid oxides of Groups IVA and IVB in Fig. 8 considerable deviations from the straight-line rule occur. However, by making use of all of these curves, the following entropies were estimated; Au_2O, 34.8; RaO, 19.9; Tl_2O_3, 35.4; GeO_2, 11.8; Cb_2O_5, 32.5; Bi_2O_5, 35.8; CrO_3, 15.2; UO_3, 20.3. Using these estimated values, ΔS^0 for these oxides was calculated. These values have been included in Table I in parentheses.

With the exception of sodium oxide, the entropies of the oxides of Group IA are not known. Therefore, the entropy–log molecular weight plot cannot be made. Similarly, there are insufficient data on the entropies of the oxides of Groups IIIA, VIB and VII to make entropy–log molecular weight plots. However, an examination of the entropies of the formation of the oxides, ΔS^0, in Table I indicates that for each periodic group the entropy of formation of the solid oxides is approximately the same. The entropy of formation for sodium oxide may be calculated as

$$\Delta S^\circ(Na_2O - 2Na - 0.5O_2) = -31.9$$

Assuming that the entropy of formation of the other oxides in Group IA is approximately the same as that for sodium oxide, namely, −32 calories per degree, the entropies of the other oxides in this group at 298.16°K. were calculated from the equation

$$\Delta S^\circ(M_2O - 2M - 0.5\,O_2) = -32$$

The entropy values calculated were as follows: lithium oxide 5.9; potassium oxide 22.9; rubidium oxide 25.7; and cesium oxide 32.1. Using the value of −32 for ΔS^0 and making use of the expression for the second law of thermodynamics[15]

$$\Delta F_T^\circ = \Delta H_T - T\Delta S_T$$

the free energies of formation for these oxides were calculated. Similarly, for Group IIIA only the entropy for aluminum oxide is given in the literature. From this value the entropy of formation may be calculated as −74.5. Assuming the same value for the entropy of formation of the other solid oxides in this group, the entropies for the oxides were calculated to be as follows: boron trioxide 2.4; scandium oxide 15; yttrium oxide 20; and lanthanum oxide 26.4. The free energies of formation for these oxides were calculated from the above expression for the second law of thermodynamics also using the value of −74.5 for ΔS^0.

For Group VIB only the entropy of solid sulfur trioxide is given in the literature.[10] From this value, the entropy of formation is calculated to be −63.4. Assuming the same value for the entropy of formation of the other solid oxides in this group, the entropies of these oxides were calculated to be as follows: SeO_3 20.1 and TeO_3 22.

In the case of Groups VIIA and VIIB, there are insufficient data available to make even these calculations and estimations. However, approximate values for the equivalent free energies and equivalent heats of formation can be obtained from Figs.

(26) R. R. Wenner, "Thermochemical Calculations," McGraw-Hill Book Co., Inc., New York, N. Y., 1941.

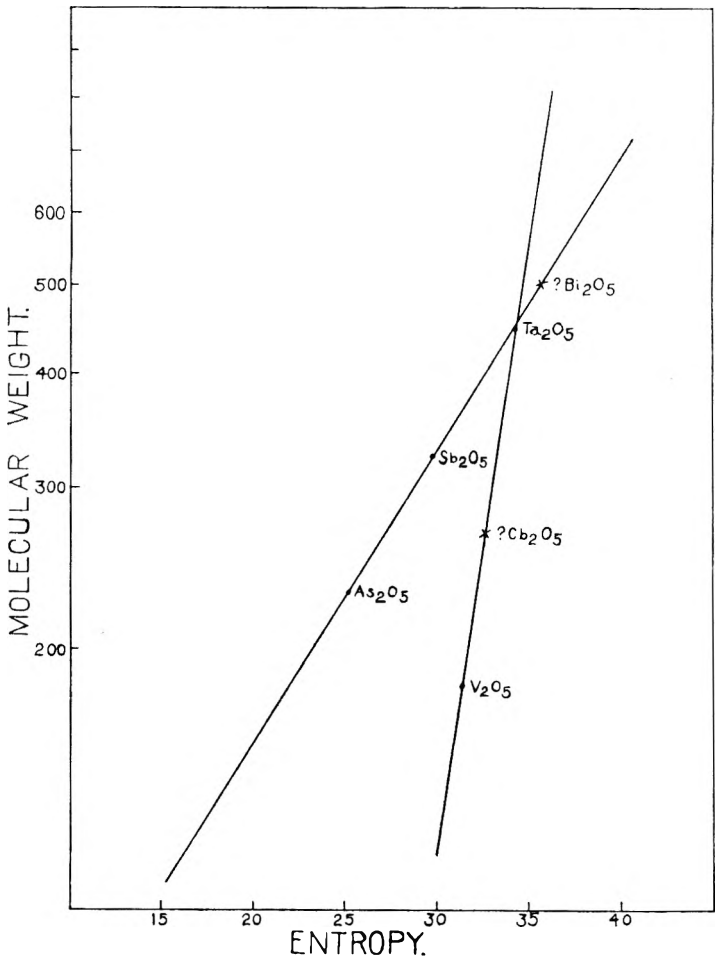

Fig. 7.

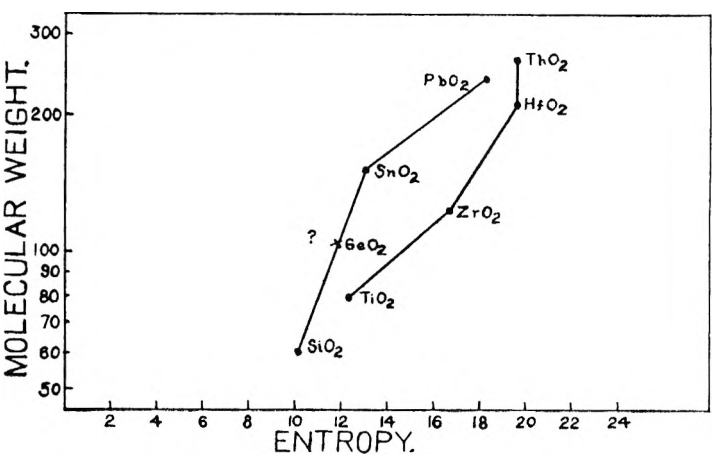

Fig. 8.

1 and 2. From these, the approximate values for the free energies and heat of formation may be calculated.

VI. Ionization Potentials

The energy required to completely remove the most loosely bound electron in its lowest energy level from an atom is known as the first ionization potential of the element. The second ionization potential is the energy necessary to remove the most loosely bound electron in its lowest energy state from the ion that is formed after one electron has already been removed.

Using the values of Herzberg,[27] Tate and Smith,[28] Yakimirskii,[29] the National Bureau of Standards Tables,[14] and Bichowsky and Rossini,[9] the first, second, third and fourth ionization potentials of the

(27) G. Herzberg, "Atomic Spectra and Atomic Structure," Prentice-Hall, Inc., New York, N. Y., 1937.

(28) J. R. Tate and P. T. Smith, *Phys. Review*, **46**, 733 (1934).

(29) K. B. Yakimirskii, *Izvest. Akad. Nauk-SSSR., Otdel. Khim. Nauk.*, 554 (1948).

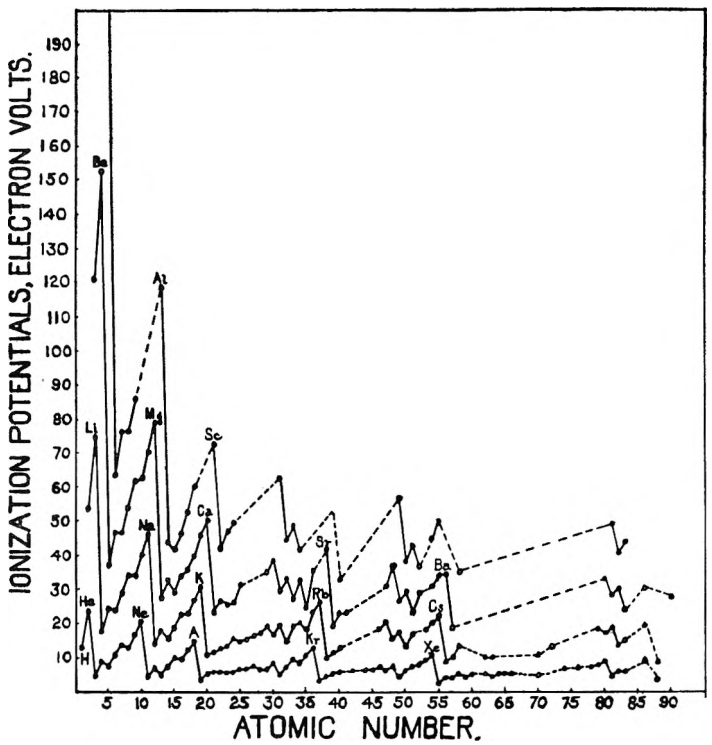

Fig. 9.

elements were plotted against the atomic number. Figure 9 shows the periodic relationship obtained.

In general, for the first ionization potentials, there is an increase from alkali metal to inert gas. Thus maxima occur with the inert gases while minima occur with the alkali metals. However, the energy required for the removal of the first p electron is somewhat lower than that necessary for the removal of the preceding s electron (see boron, aluminum, gallium, indium and thallium in Fig. 9). Also a slightly lower energy is required for the removal of the fourth p electron, than that for the third p electron (see oxygen, sulfur and selenium in Fig. 9). On passing from an inert gas to the next alkali metal, there is a great decrease in the ionization potential. The added s electron is relatively well shielded from the nuclear charge.

The second ionization potential for any element is always larger than the first, the third always larger than the second, and each subsequent ionization potential larger than the preceding one. Of course, this is to be expected, since more energy is required to remove an electron from a positively charged ion than from a neutral atom, and the required energy increases with increased charge in the ion. However, it should be noted that much more energy is necessary to remove an electron from a positive ion of an inert gas structure than from an ion in which the periodic valence has not been satisfied. Thus, after one electron has been removed from sodium, the electron configuration remaining is similar to the inert gas neon, and considerable energy is necessary to remove the next electron. In the case of magnesium, two electrons must be removed before an inert gas electron structure is obtained and these two electrons are relatively easy to remove as compared with the removal of the third electron. Similarly, for aluminum, three electrons must be removed to form an inert gas configuration.

For the second ionization potentials of the elements, maxima are obtained for the alkali metal ions while minima are obtained for the alkaline earth metal ions having one positive charge. Proceeding from the first to the second, from the second to the third and then to subsequent ionization potentials, maxima occur at the ions possessing inert gas electronic configurations while minima occur at the ions resembling the alkali metal electronic structures. Thus there is a shift of one to the right for the maxima and minima in Fig. 9 in passing from the first ionization potential to the second and then to each succeeding ionization potential.

In Fig. 10 the total ionization potentials, *i.e.*, the energy necessary to separate all of the valence electrons, were plotted as a function of the atomic number. A series of approximately parallel lines were obtained which became more nearly parallel with the increasing number of valence electrons. Minima occurred with the alkali metals of Group IA as well as with the metals of Group IB. A similar series was obtained by Süe[3] using the average ionization potentials, *i.e.*, the energy required to remove all of the valence electrons divided by the number of electrons (Fig. 11).

The curves in Figs. 10 and 11 resemble, to some extent, those obtained for the equivalent free energies of formation of the oxides. However, the latter must differ somewhat, as indeed they do, since they take into account the electron affinity of the elements for oxygen and of oxygen for the elements.

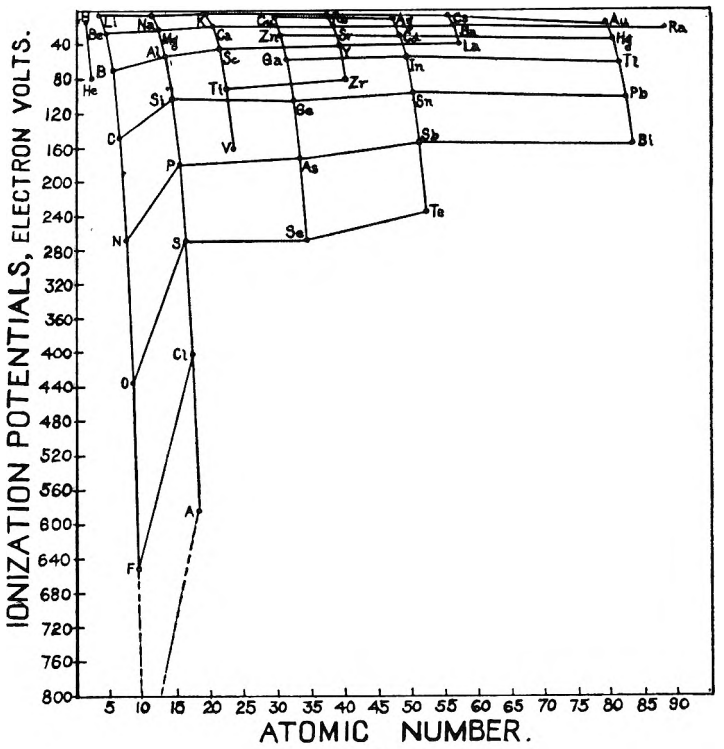

Fig. 10.

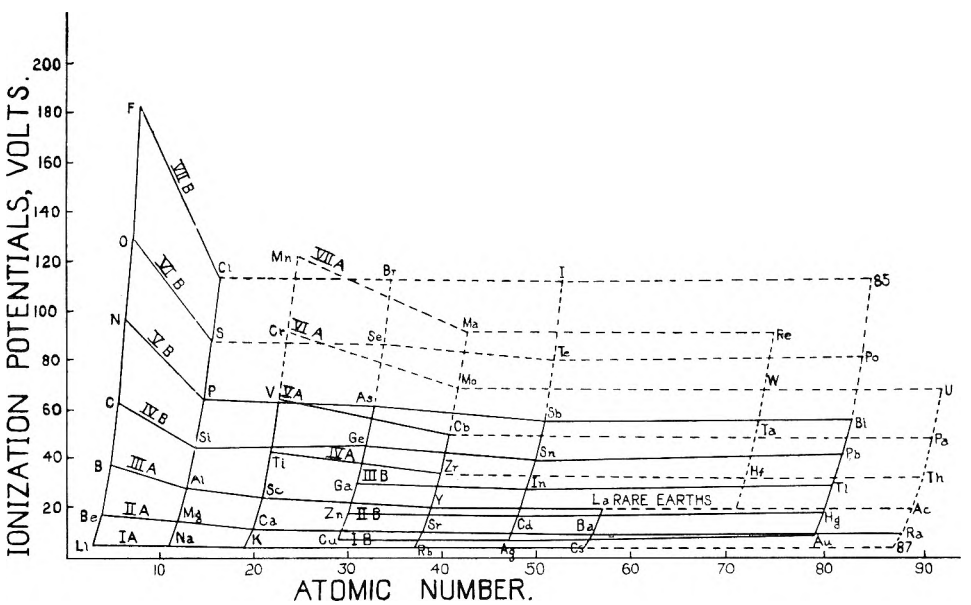

Fig. 11.

VII. Electronegativities

Pauling[30] employed the term electronegativity to express the electronic attraction of a neutral atom in a stable molecule. This idea was developed by quantitative considerations of simple wave mechanics and agrees quite closely with the ionic resonance theory which states that a combination of two dissimilar atoms possess more than pure covalent energy. The following empirical relationship was developed by Pauling

$$(A - B) = 23.6(X_A - X_B)^2 \qquad (1)$$

(30) Linus Pauling, "The Nature of the Chemical Bond," Ithaca, N. Y., 1944.

$(A - B)$ is the extra ionic resonance energy. X_A and X_B are the electronegativities expressed in electron volts. 23.06 is the factor for converting electron volts to calories.

This led to the formulation of the Electronegativity Scale. Since nitrogen and oxygen in their standard states (N_2 and O_2) have a much greater stability than that which corresponds to the single N–N and O–O bonds, Pauling proposed the equation

$$Q = 23.06\ \Sigma\,(X_A - X_B)^2 - 55.1n_N - 24.2n_O \qquad (2)$$

Q is the heat of formation of a gaseous molecule containing single bonds from elements in their

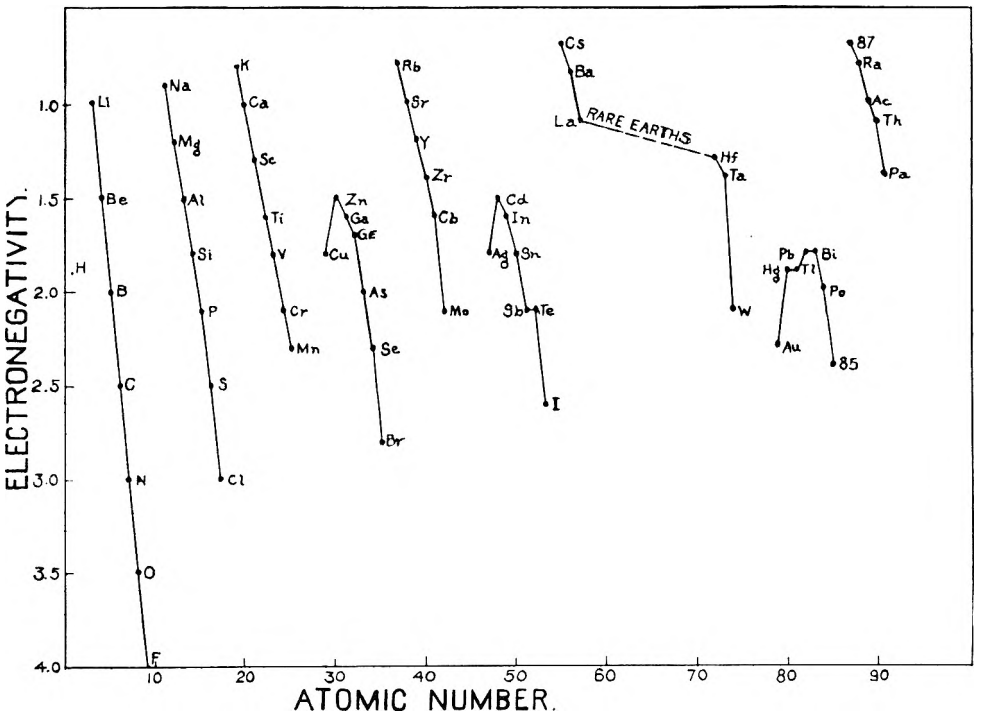

Fig. 12.

standard states. n_N and n_O are the number of nitrogen and oxygen atoms, respectively, in the compound under consideration.

Haissinsky[31] compared Pauling's relation between the electronegativities of the atoms and the heat of formation with the experimental data. He found that the approximate nature of the relation was improved by introducing the heat of sublimation into equation 2 as

$$Q = 23.06\ \Sigma\ (X_A - X_B)^2 - L - 55.1n_N - 24.2n_O \quad (3)$$

L is the heat of sublimation of the compound whose heat of formation in the gaseous state is Q. In most of the cases studied by Pauling, L was relatively small compared with Q, which would make equation 3 the same as 2. Using equation 3 it was possible for Haissinsky to calculate the electronegativities for the entire periodic system, and with the aid of the calculated electronegativities, to interpret the periodicity of certain groups of inorganic compounds. P. Daudel and R. Daudel[32] further improved the agreement between the results of Pauling's theory of electronegativity and the experimental data by the introduction of the concept of "charge effect." Furthermore, this concept of charge effect accounts for the increase in electronegativity with increasing valence of an element.

Using the values of Haissinsky, the electronegativities were plotted as a function of atomic number. In general, a series of approximately parallel lines were obtained and the curves in Fig. 12 resemble those obtained for the equivalent heats of formation and equivalent free energies of formation of the oxides in Figs. 1 and 2, respectively. While the concept of electronegativity does lead to a certain amount of systematization in inorganic thermochemistry, the electronegativity of an element cannot be considered a constant characteristic of the element. It will vary to a greater or less extent depending upon the other element in the molecule of the compound. Similarly, the variations between the curves for the equivalent heats of formation of the oxides and the curves for the equivalent heats of formation of other classes of inorganic compounds may be attributed to the difference in bond strength between the elements and oxygen and the elements and the other electronegative element under comparison such as sulfide, nitride, chloride, etc.

(31) M. Haissinsky, *J. Phys. Radium*, **7**, 7 (1946).
(32) P. Daudel and R. Daudel, *ibid.*, **7**, 12 (1946).

VIII. Halides, Sulfides and Other Inorganic Compounds

The equivalent heats of formation of the chlorides were plotted as a function of the atomic number and are shown in Fig. 13. The curves obtained were a series of approximately parallel lines resembling those obtained for the equivalent heats of formation of the oxides. However, for the chlorides, the deviations from the straight line were much less than those for the oxides. Thus, the maxima of the curves for the chlorides occur with the alkali metals. Comparing the curves of the chlorides with those of the oxides, the minima occur with the same elements, namely, copper, silver, gold, bromine, iodine and element 85. In order to compare the curves of all of the halides, their equivalent heats of formation were plotted as a function of atomic number on one graph (Fig. 14). They form a series of straight lines which are approximately parallel to each other, having the same maxima and minima. As pointed out by Trombe[2] and Süe,[3] each of the halides appears to be separated from the next by a fixed distance, indicating a constant difference between the equivalent heats of

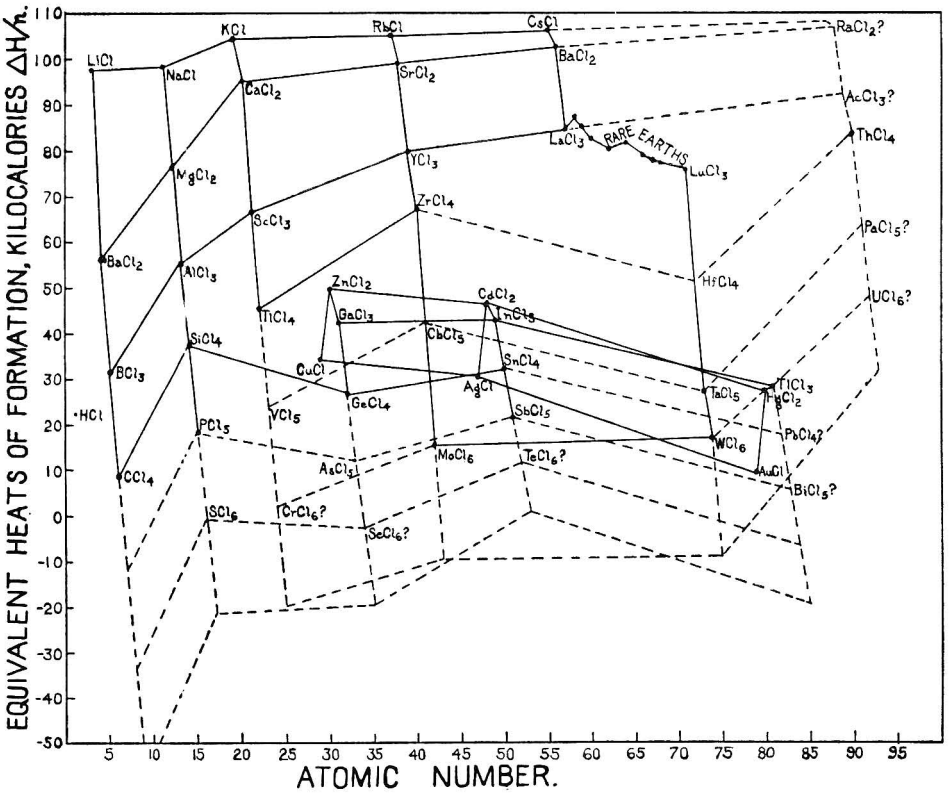

Fig. 13.

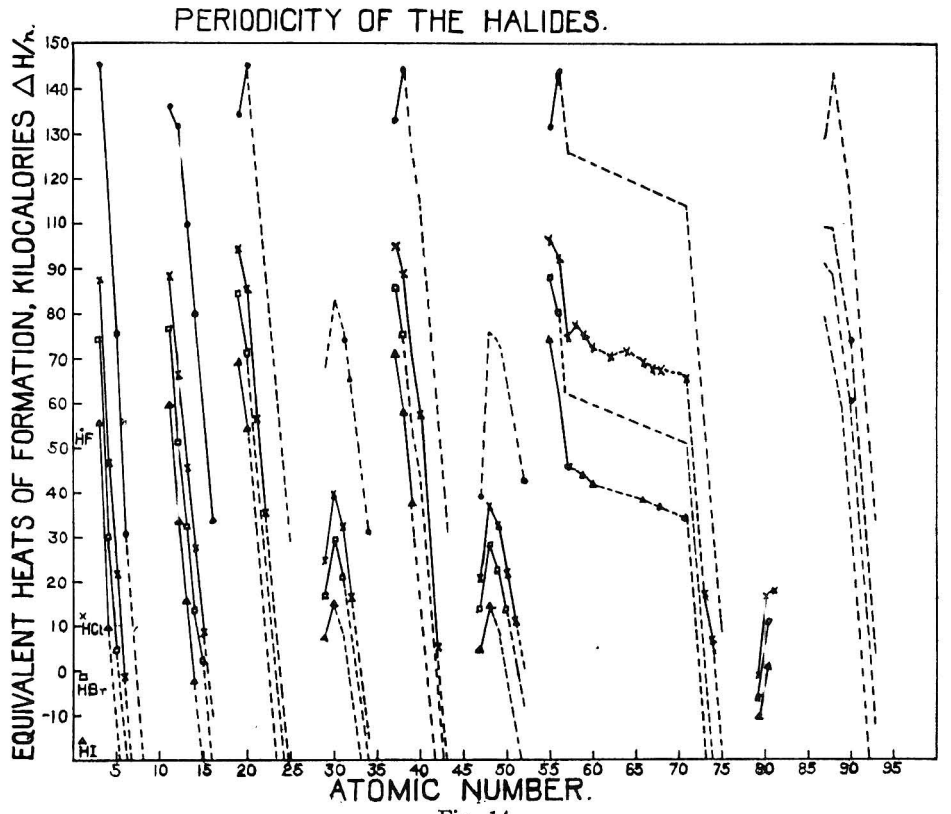

Fig. 14.

formation of the halide for the same element regardless of the atomic number. Therefore, since the average differences between the heats of formation of two halides are approximately constant irrespective of the element, if the heat of formation of one halide is known, it is possible to calculate the heats of formation for the other halides.

By plotting the equivalent heats of formation as

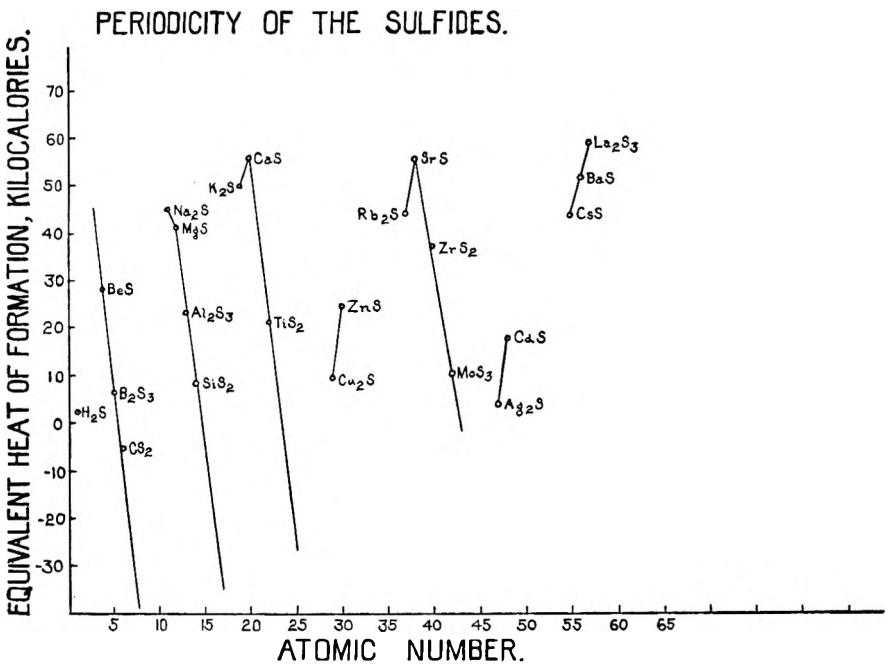

Fig. 15.

a function of atomic number, similar curves may be obtained for other classes of inorganic compounds. Thus, Fig. 15 shows the equivalent heats of formation of the sulfides as a function of atomic number. Only a few values are available in the literature for the standard heats of formation of the sulfides (Table IV). These were taken essentially from the National Bureau of Standards Values,[14] Bichowsky and Rossini[9] and K. K. Kelley.[33] Some estimated values from Fig. 15 also are given in Table IV in parentheses. However, because of the sparsity of the data, not many estimates can be made. The maxima for the first two periods occur with the alkali metals. For the third and fourth periods, the maxima occur with the alkaline earth metals, while for the fifth period the maximum appears to be lanthanum sulfide.

TABLE IV

THERMOCHEMICAL PROPERTIES OF THE SULFIDES

Sulfide	Standard heat of formation ΔHf^0, kcal./mole	Equivalent heat of formation $\Delta Hf^0/n$, kcal.
H_2S	− 4.82	− 2.41
Li_2S		
BeS	− 56.1[3]	− 28
B_2S_3	− 40[8]	− 6.7
CS_2	21.0	5.2
N_2S_3	(270)	(27)
Na_2S	− 89.8	−44.9
MgS	− 82.1	−41.1
Al_2S_3	−140.5	−23.4
SiS_2	− 34.7	− 8.7
P_2S_5	(60)	(6)
K_2S	− 99.5[34]	−49.8
CaS	−113.4	−56.7
Sc_2S_3	(−234)	(−39)
TiS_2	− 84[8]	−21
V_2S_5 ?	(− 50)	(− 5)
CrS_3 ?	(66)	(11)
Cu_2S	− 19.0	− 9.5
ZnS	− 48.5	−24.3
Ga_2S_3		
GeS_2		
As_2S_5		
Rb_2S	− 88	−44
SrS	−113.1[8]	−56.6
Y_2S_3	(−276)	(−46)
ZrS_2	−148[8]	−37
Cb_2S_5	(−220)	(−22)
MoS_3	− 61.2	−10.2
Ag_2S	− 7.60	− 3.80
CdS	− 34.5	−17.3
In_2S_3		
SnS_2		
Sb_2S_5		
Cs_2S	− 87[8]	−43.5
BaS	−111.2	−55.6
La_2S_3	−351.4	−58.6
HfS_2		
Ta_2S_5		
Au_2S		
HgS	− 13.9	− 7
Tl_2S_3		
PbS_2 ?		
Bi_2S_5		

(33) K. K. Kelley, U. S. Bureau of Mines Bull., 434 (1941).

(34) J. D'Ans and E. Lax, "Taschenbuch für Chemiker und Physiker," Springer-Verlag, Berlin, 1943.

THE SYSTEM NICKEL(II) NITRATE–WATER–*n*-HEXYL ALCOHOL AT 25°[1]

BY CHARLES C. TEMPLETON[2] AND LYLE K. DALY

Department of Chemistry, University of Michigan, Ann Arbor, Michigan

Received December 19, 1950

The system nickel(II) nitrate–water–*n*-hexyl alcohol has been investigated at 25° between the limits: $Ni(NO_3)_2 \cdot 6H_2O$, water and *n*-hexyl alcohol. The phenomena involved in the region of two liquid phases are analogous to the corresponding portion of the aluminum nitrate–water–*n*-hexyl alcohol system. The hexahydrate is the solid phase in equilibrium with the saturated two liquid phase system. The differential molar rate at which water is carried into the alcoholic phase by nickel nitrate is about 4.

In continuance of studies[3] of ternary systems of the type salt–water–organic solvent, the system nickel(II) nitrate–water–*n*-hexyl alcohol has been investigated at 25° between the limits: water, *n*-hexyl alcohol and $Ni(NO_3)_2 \cdot 6H_2O$.

Method.—All measurements were made at 25 ± 0.05°. The manipulative details were the same as those described in a previous study of the system aluminum nitrate–water–*n*-hexyl alcohol.[3] Water was determined by use of Karl Fischer reagent. Nickel was determined, by the use of standard procedures, either gravimetrically[4] or colorimetrically[5] with dimethylglyoxime. It has been assumed that no hydrolysis occurred: *i.e.*, that the $Ni(NO_3)_2$ content of any phase is proportional to the Ni content. Admittedly this has not been proved as exhaustively in the present case as in the aluminum nitrate case.[3] To this extent we are reasoning by analogy. By now we have established a fairly characteristic pattern of behavior for the distribution of nitrates between water and oxygen-containing organic solvents, the ease of aluminum nitrate being typical. If there were any appreciable hydrolysis, $Ni(NO_3)_2$ could not be considered as a proper phase rule component.

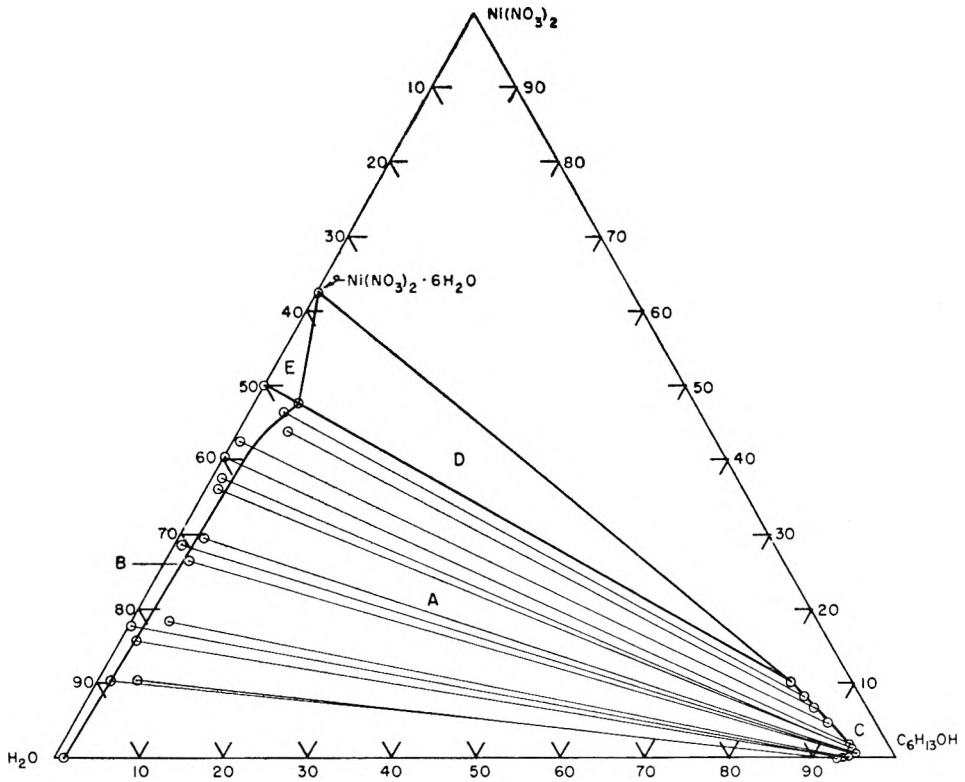

Fig. 1.—The system nickel(II) nitrate–water–*n*-hexyl alcohol at 25° (compositions in weight percentages): regions A, two liquid phases; B, single water-rich liquid phase; C, single alcohol-rich liquid phase; D, $Ni(NO_3)_2 \cdot 6H_2O$ and two liquid phases; E, $Ni(NO_3)_2.6H_2O$ and water-rich liquid phase.

Experimental

Materials.—General Chemical Company Baker and Adamson Reagent grade $Ni(NO_3)_2 \cdot 6H_2O$ was used without further purification. The sum of the *maximum* limit of all impurities was 0.42%.

n-Hexyl alcohol (Eastman Kodak Co. Practical Grade) was distilled twice through a 30-cm. Vigreux column at a reflux ratio of about 6:1, the middle fraction only being retained after each distillation. This product was used for systems to which water was added. For systems in which the water entered only as water of crystallization from the nitrate, the above alcohol was made anhydrous by refluxing and distillation over magnesium metal turnings. A Karl Fischer analysis showed the anhydrous alcohol to contain less than 0.003% water.

Data

In Table I are listed the tie-line data for the distribution of nickel (II) nitrate between water

(1) This work was performed under Project No. 2 of Contract No. AT(11-1)70 with the U. S. Atomic Energy Commission.

(2) Shell Oil Company, 3737 Bellaire Blvd., Houston 5, Texas.

(3) C. C. Templeton, THIS JOURNAL, **54**, 1255 (1950).

(4) N. H. Furman, Editor, "Scott's Standard Methods of Chemical Analysis," D. Van Nostrand Co., Inc., New York, N. Y., 1939.

(5) E. B. Sandell, "Colorimetric Determination of Traces of Metals," Interscience Publishers, Inc., New York, N. Y., 1944.

and *n*-hexyl alcohol. In the cases of incomplete entries, some of the solution samples were ruined before the analysis could be completed; the remaining data are of value in the consideration of the extraction of water into the organic phase.

Various of the data in Table I have been transformed into other units which are more appropriate for certain aspects of the discussion; these additional values are recorded in Table II. The "apparent" mole-fractions are calculated on the assumption that there is no alcohol in the aqueous phase and no water in the alcoholic phase. This is an arbitrary scheme for comparing nitrate extractabilities which was adopted in previous studies.[3,6,7] The molalities for the alcoholic phase are referred to 1000 g. of *n*-hexyl alcohol.

Discussion

In Fig. 1 is presented the ternary phase diagram for this system, plotted on a weight percentage basis. As compared to the study on aluminum nitrate,[3] the most obvious shortcoming is the scatter in the values for the alcohol content of the aqueous phase. As was previously pointed out,[3]

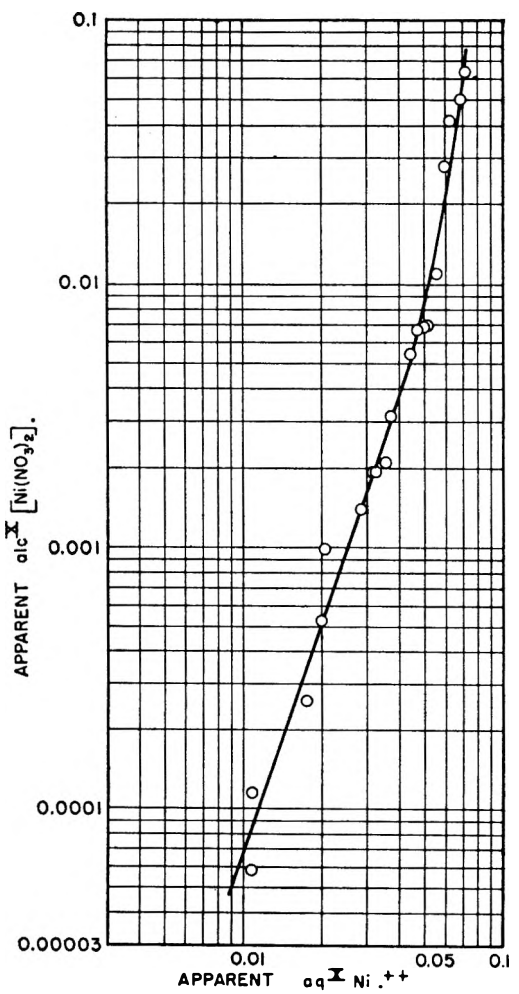

Fig. 2.—Distribution of nickel(II) nitrate between water and *n*-hexyl alcohol at 25°.

(6) B. F. Rothschild, C. C. Templeton and N. F. Hall, THIS JOURNAL, **52**, 1006 (1948).

(7) C. C. Templeton, *J. Am. Chem. Soc.*, **71**, 2187 (1949).

TABLE I

THE SYSTEM NICKEL(II) NITRATE–WATER–*n*-HEXYL ALCOHOL AT 25°

	Weight percentages					
	Aqueous-rich Phase			Alcoholic-rich Phase		
Run	$Ni(NO_3)_2$	H_2O	*n*-Hexyl alcohol	$Ni(NO_3)_2$	H_2O	*n*-Hexyl alcohol
XVI[a]	47.7[c]	46.9	5.4	10.31[c]	7.35	82.34
I	....	..	...	9.35[c]	7.01	83.64
OO	46.5[c]	49.5	4.0	8.21[c]	6.91	84.89
XVII	43.9[c]	50.2	5.9	6.92[c]	6.37	86.71
VII	42.5[b]	56.8	0.7	4.80[b]	5.75	89.45
II	....	..	...	2.45[b]	4.89	92.66
III	40.1[b]	60.1	(−0.2)	1.93[b]	4.75	93.32
V	37.8[b]	61.3	0.9	1.23[b]	4.61	94.16
IV	36.8[b]	64.1	(−0.9)	1.20[b]	4.60	94.20
F	36.2[b]	62.7	1.1	1.19[b]	4.68	94.13
VI	35.7[b]	65.8	(−1.5)	0.96[b]	4.58	94.46
VIII	29.5[b]	67.5	3.0	.55[b]	4.70	94.75
G	28.6[b]	70.8	0.6	.37[b]	4.83	94.80
XII	26.55[c]	70.9	2.6	.344[b]	4.80	94.86
IX	26.4[b]	69.6	4.0	.346[b]	4.80	94.90
H	23.8[b]	..	...	.247[b]	4.73	95.02
XI	18.2[c]	77.3	4.5	.177[b]	5.50	94.33
M	17.8[b]	82.1	0.1	.0926[b]	5.78	94.13
J	15.8[b]	82.3	1.9	.0464[b]	5.76	94.19
K	10.3[b]	88.5	1.2	.0203[b]	6.18	93.80
X	10.18[c]	85.0	4.8	.0104[b]	5.99	93.91

[a] Saturated system. [b] Colorimetric. [c] Gravimetric.

TABLE II

CONCENTRATION DATA CALCULATED FROM DATA OF TABLE I

	Apparent mole fractions		Alcoholic phase molalities	
Run	aq.^{x}Ni^{++}	alc^{x}[$Ni(NO_3)_2$]	$Ni(NO_3)_2$	H_2O
XVI	0.0706	0.0640	0.686	4.96
I	....	....	.612	4.65
OO	.0680	.0499	.530	4.52
XVII	.0624	.0415	.437	4.07
VII	.0596	.0275	.294	3.57
II	....	....	.145	2.92
III	.0550	.0109	.113	2.82
V	.0506	.0069	.0715	2.72
IV	.0488	.0068	.0698	2.71
F	.0478	.0067	.0692	2.76
VI	.0469	.0054	.0556	2.70
VIII	.0366	.0031	.0318	2.72
G	.0352	.0021	.0214	2.82
XII	.0321	.00193	.0198	2.80
IX	.0318	.00194	.0200	2.81
H	.0281	.00140	.0142	2.76
XI	.0205	.00099	.0103	3.24
M	.0200	.00052	.00538	3.40
J	.0175	.000260	.00270	3.40
K	.0109	.000114	.00118	3.66
X	.0108	.000058	.00061	3.54

the Karl Fischer method involves a much larger absolute error for the aqueous phase than for the alcoholic phase. Further, both the gravimetric and colorimetric dimethylglyoxime methods for nickel are more susceptible to error than the simple, well-behaved ignition determination of aluminum. All of these errors are reflected in the values for alcoholic content, since these are taken by difference.

The stable hydrate for the $Ni(NO_3)_2$-H_2O system at 25°, $Ni(NO_3)_2 \cdot 6H_2O$, is also the solid phase for the two liquid phase saturated ternary system. This was verified by analysis of the solid phase for nickel: found, 61.3, 61.8% $Ni(NO_3)_2$. Expected: 62.83% $Ni(NO_3)_2$. Literature values included in the

phase diagram are the solubility of $Ni(NO_3)_2 \cdot 6H_2O$ in water at 25° as 50.0 g. $Ni(NO_3)_2$ per 100 g. saturated solution,[8] and the solubility of *n*-hexyl alcohol in water at 25° as 0.62%.[9]

Anhydrous *n*-hexyl alcohol was mixed with $Ni(NO_3)_2 \cdot 6H_2O$ and agitated for several days. This alcoholic phase was found to contain 10.30% $Ni(NO_3)_2$ and 7.29% H_2O. Within experimental error, this is the same composition as the alcoholic phase of the two liquid phase saturated system. If water entered the alcoholic phase only through the dissolution of $Ni(NO_3)_2 \cdot 6H_2O$, and if this substance continued to be the only equilibrium solid phase, the water content should be (10.30) (6) (18.02)/(182.7) or 6.10%. It appears most probable that this sample consisted of the alcoholic liquid phase, solid $Ni(NO_3)_2 \cdot 6H_2O$, and a new solid phase containing less water than the hexahydrate. This was not pursued further simply because the main interest of this research is in the liquid–liquid range.

In the alcohol corner of Fig. 1, there is obviously a region (C) of a single unsaturated alcoholic phase. The complete boundaries of this region are left undetermined by the present study.

In Fig. 2 is shown the usual plot for the distribution of nickel(II) nitrate between the two phases. The behavior is similar to that of all the other nitrates which have been studied.

In Fig. 3 is plotted the curve for the determination of the amount of water which is carried into the alcoholic phase by nickel(II) nitrate. The slope of the linear portion of the plot is 3.8. Subject to the assumptions underlying this procedure,[3] this suggests that four water molecules are associated with one molecular of $Ni(NO_3)_2$ in the alcohol-extracted complex. The plot is not rigorously linear, since the dotted curved line is probably a truer representation of the data. However, the method based on the straight line is the only means currently available for judging the relative hydrations of these complexes.

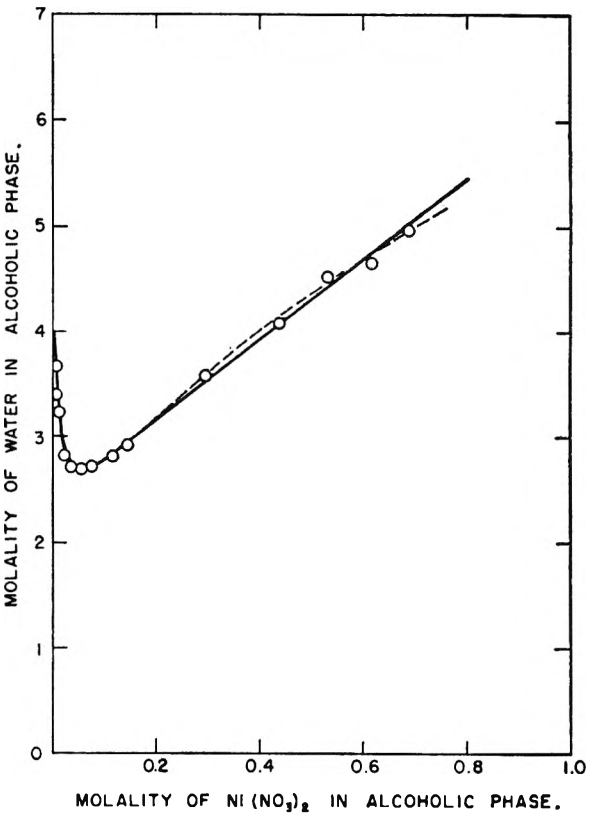

Fig. 3.—Determination of rate at which water is carried into alcoholic phase by nickel(II) nitrate.

(8) A. Sieverts and L. Schreiner, *Z. anorg. Chem.*, **219**, 105 (1934).

(9) J. A. V. Butler, D. W. Thompson and W. H. Maclennan, *J. Chem. Soc.*, 674 (1933).

STUDY OF THE JOSHI EFFECT IN H_2O AND D_2O VAPOR

BY N. ATCHUTA RAMAIAH

Department of Chemistry, Benares Hindu University, Benares, India

Received December 27, 1950

Occurrence of large negative Joshi effect ($-\Delta i$), *viz.*, a photodecrease of the discharge current i and its H.F. pulses in excited water vapor was investigated over a wide range of experimental conditions and attributed on Joshi's theory which contemplates that negative ion formation (i) due to capture by excited particles of photoelectrons (ii) released from an adsorption-like electrode layer (iii) reduces i, to the large electron affinity of OH. Conditions favoring (i), *viz.*, large pressures (up to a limit) and low potentials V, as also those leading to enhanced (ii) *viz.*, large intensities and frequencies of light, augment $-\Delta i$. Formation of (iii) due to aging under discharge increased numerically $-\Delta i$; its time development obeyed a relationship suggested for sorption. $-\Delta i$ was pronounced in vessels coated with KCl which was known to enhance sorption of OH. Rise of temperature by 40° increased $-\Delta i$, as also H.F. part of i in which $-\Delta i$ predominates. Positive effect ($+\Delta i$), a photoincrease of i and H.Fs., was observed at very low and large V which disfavor (i). Temperature inhibited $+\Delta i$. Variation of $+\Delta i$ with other parameters was similar to that of $-\Delta i$. Reversals $+\Delta i \rightleftarrows -\Delta i$ with V, intensity and circuital capacitance suggested the simultaneous occurrence of $+\Delta i$ and $-\Delta i$ as actually revealed by current oscillograms. These studies were extended to D_2O vapor; the results were similar.

Joshi's theory[1] for the phenomenon $\mp\Delta i$,[2] an instantaneous and (under unexceptional conditions[3]) reversible photovariation of the discharge current i due to an exciting potential V (expressed in kilovolts kv., r.m.s.), postulates: Formation of an adsorption-like layer (i) of ions, electrons and excited particles derived from the discharge space; emission from (i) of electrons by external light; current decrease $-\Delta i$, as a space charge effect, due to negative ion formation (ii) by electron capture by excited particles; conditions disfavoring (ii) give $+\Delta i$. It follows from (ii) that the magnitude and range of occurrence of $-\Delta i$ should depend upon the nature, chiefly electron affinity (E, Cal.) of the medium, as illustrated by the observed order,[4] chlorine ($E_{Cl} = 88$[5a])>bromine ($E_{Br} = 84$[5a])> iodine ($E_I = 75$[5a])>oxygen ($E_O = 87$,[6] $E_{O_2} = 62$[5b]), etc. Production of $-\Delta i$ in metallic vapors due to their enhanced E under excitation, was predicted and actually observed by Joshi.[1c] Under discharge, water vapor ($E_{H_2O} = 18$[7]) dissociates into H ($E_H = 16$[5a]) and OH ($E_{OH} = 86$[5b]).[8] The large E_{OH} value suggested the present work.

Water vapor at various pressures p_{H_2O} (3–32 mm.) was excited by transformer discharge in a Siemens-type full- (A), wire-in-cylinder like semi- (B) ozonizers and tubes with external sleeves (C). As in other systems,[2] the Joshi effect, $-\Delta i$, was undetected below the "threshold potential," V_m where i increases rapidly with V, following the onset of discharge. In a typical series (A, p_{H_2O} = 15 mm., 30°), at 0.66 kv., *i.e.*, just above V_m, $\%\Delta i$ ($100\ \Delta i/i_{Dark}$) in the positive and negative halves of i as observed with a diode was, respectively, 33.3 and 19.6% current suppression due to light from a 200-watt (glass) bulb; and 21.3 in total i measured by a thermojunction. Increas in V decreased $-\%\Delta i$, a general Δi characteristic.

At $p_{H_2O}<3$ mm., $-\%\Delta i$ was negligible; progressively, increased from 2.3 at 4.5 mm. to 48.3 at 13.6 mm. and then decreased, *e.g.*, to 23.0 at 31.8 mm. (A, 0.66 kv.). At identical corresponding potentials $(V - V_m)/V_m$ increased p affects $-\%\Delta i$; this suggests that the homogeneous reaction is not unsignificant to Δi. At constant p_{H_2O}, rise of temperature from 300–340° K. increased $-\Delta i$ and $-\%\Delta i$, as also the H.F. part of the current $i_{H.F.}$, which latter has been established by Joshi[9] to be the chief seat of $-\Delta i$.

As in other systems,[2] the Joshi effect increased with light intensity; at large values of the latter $-\Delta i$ showed saturation. At constant intensity the magnitude of $-\Delta i$ was in the order: unfiltered white (7800–3700 Å.) > violet (4064–5166 Å.) > green (5180–5860 Å.) > red (6390–6600 Å.). Absorption by H_2O or OH in violet and green is negligible; as suggested by Joshi[2] Δi is, therefore, not entirely a consequence of selective light absorption in the vapor phase.

The appreciable positive Joshi effect, $+\Delta i$, occurred just near V_m in A and B and at large V in C. Light intensity and frequency affected $+\Delta i$ similarly to $-\Delta i$. Increased temperature inhibited $+\Delta i$. It increased with p_{H_2O} up to a limit, and then decreased. $+\Delta i$ decreased precipitously and inverted to $-\Delta i$ in A and B with but a small rise and in C with a small decrease of V. At the transition potential (in C), suggestively enough, a reversal either way $+\Delta i \rightleftarrows -\Delta i$ occurred by intensity alteration. Using frequency filters, it was found that at a given V, whilst $i_{H.F.}$ showed $-\Delta i$, the total i gave $+\Delta i$. This finding (as also the reversals $+\Delta i \rightleftarrows \Delta i$) follows from Joshi's suggestion[1b] that depending upon the conditions, $+\Delta i$ and $-\Delta i$ coöccur; the detector shows the balance. This was further confirmed by oscillographic studies. Figure 1 is one typical result. Generally, $+\Delta i$ and $-\Delta i$ are characterized by amplitude increase and decrease, respectively, of H.F. pulses constituting $i_{H.F.}$ Coöccurrence of $\pm\Delta i$ is revealed by an increase of some H.F. amplitudes and simultaneously decrease of others (see Fig. 1).

The adsorption-like layer (i) postulated by Joshi elucidates the observed influence of "aging" and electrode-filming on Δi.[1,10b] The former was

(1) S. S. Joshi, *a. Proc. Ind. Sci. Cong., Phys. Sec.*, Abst. 26 (1946); *b. ibid.*, Abst. 27 (1947); *c. Curr. Sci.*, **16**, 19 (1947).

(2) S. S. Joshi, Presidential Address, *Proc. Ind. Sci. Cong., Chem. Sec.* (1943); *Nature*, **151**, 561 (1943).

(3) B. R. Marathe and S. S. Bommannavar, *Nature*, **165**, 890 (1950).

(4) G. S. Deshmukh, *J. Ind. Chem. Soc.*, **24**, 211 (1947).

(5) (a) C. D. West, THIS JOURNAL, **39**, 503 (1935); (b) J. Weiss, *Trans. Faraday Soc.*, **31**, 968 (1934); **36**, 856 (1940).

(6) G. Glockler, *Phys. Rev.*, **45**, 111 (1934).

(7) A. Farkas and L. Farkas, *Trans. Faraday Soc.*, **34**, 111 (1938).

(8) A. A. Frost and O. Oldenberg, *J. Chem. Phys.*, **4** 642 (1936).

(9) S. S. Joshi, *Nature*, **154**, 147 (1944); *Curr. Sci.*, **13**, 253 (1944) *Proc. Ind. Acad. Sci.*, **22**, 389 (1945).

(10) (a) S. R. Mohanty, Ph. D. Thesis, 1949, p. 269; (b) M. V. Ramanamurty, *ibid.*, **25**, 255 (1948).

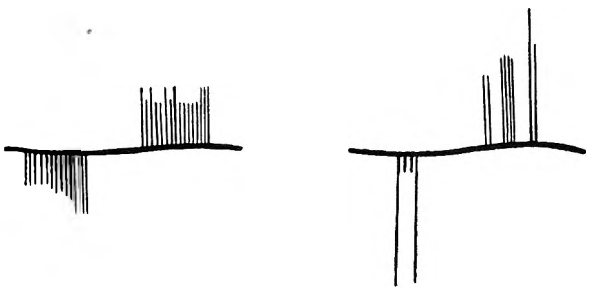

Fig. 1.

studied in freshly prepared vessels. In all of them, initially Δi was undetectable; it developed only after a definite interval and increased progressively to a maximum within, say, 2 hours of aging. The necessary period of aging for the inception of Δi was shortened appreciably under conditions favoring adsorption (*vide infra*). This time development of Δi is attributable to that of adsorption contemplated in (i) of Joshi's theory. The following relation holds *for the initial phase* of sorption on glass S_t at time t of a number of gases[11]: $S_t^m = kt$; m and k are constants. Since according to Joshi, sorption determines *inter alia* the corresponding Δi,[10b] one would expect the influence of aging to follow $\Delta i_t^m = k't$. It is instructive to see in Fig. 2 that as required by this relation, the plots of log Δi, log % Δi *versus* log t are sensibly linear for water vapor studied by the author; and also for chlorine and oxygen from published data[10] for the aging influence on Δi.

(11) D. H. Bangham, *Phil. Mag.*, (7) **5**, 735 (1928); D. H. Bangham and F. P. Burt, *Proc. Roy. Soc.* (*London*), **A105**, 481 (1924); *cf.* also E. Swan and A. R. Urquhart, THIS JOURNAL, **31**, 251 (1927).

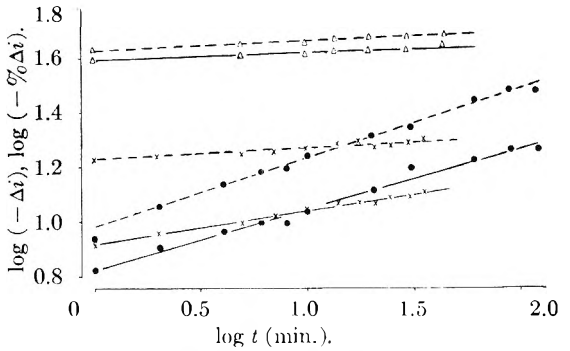

Fig. 2.—Δ—Δ and Δ- -Δ, chlorine; ×—× and ×- -×, H_2O vapor; ●—● and ●--●, oxygen; ——, log $(-\Delta i)$ − log t; – – –, log $(-\%\Delta i)$ − log t.

That the intercept on the y-axis may be a measure of predischarge sorption, is being investigated.

The results of Taylor and Lavin[12] and Frost and Oldenberg[8] show that adsorption of OH on glass is augmented by KCl. Series of observations of Δi were, therefore, made using discharge tubes with and without an electrode-film of KCl. With this film, it was remarkable that not only was the magnitube of Δi about four times larger, but the initial aging period was negligible compared with the 20–30 minutes found with blank vessels.

$\pm\Delta i$ in D_2O vapor resembled closely that in H_2O for all above mentioned parameters.

The author expresses his grateful thanks to Professor S. S. Joshi, for suggesting the problem, and for his kind interest and valuable guidance during the work; and to the Ministry of Education, Government of India, for a fellowship.

(12) H. S. Taylor and G. I. Lavin, *J. Am. Chem. Soc.*, **52**, 1910 (1930).

CHEMISORPTION OF HYDROGEN ON ZINC OXIDE–MOLYBDENUM OXIDE CATALYST. EVIDENCE OF HETEROGENEITY OF THE SURFACE

BY M. V. C. SASTRI AND K. V. RAMANATHAN

General Chemistry Section, Indian Institute of Science, Bangalore 3, India

Received January 3, 1951

The chemisorption of hydrogen by zinc oxide–molybdenum oxide has been studied between 186° and 375°, employing the temperature-variation technique of Taylor and Liang. Temperature variations above 250°, gave rise to desorption and re-adsorption phenomena typical of surface heterogeneity. No such effect was noticed for temperature changes below 250°. The rate of adsorption on the bare surface has been determined at four temperatures between 186° and 350°. Equations have been derived for estimating the point of minimum adsorption following a temperature increase. The value calculated for the minimum adsorption, by applying these equations, agrees closely with that actually observed. The energies of activation of adsorption are calculated for three temperature ranges. The abnormal variations noticed at the higher temperatures are explained on the basis of heterogeneity of the surface. It is pointed out that isothermal determinations of adsorption on bare surfaces, do not give a correct estimate of the active area of the adsorbent. The surface area of the adsorbent has been determined by the application of the B.E.T. and the Harkins–Jura equations to the adsorption isotherm of nitrogen, at the temperature of liquid air.

The technique developed by Taylor and Liang[1] for the study of isobaric changes in adsorption at different temperatures has been of especial help in the elucidation of the heterogeneity of catalyst surfaces for chemisorption, because this technique enables the detection of desorption and readsorption phenomena which escaped observation, when ordinary methods were used. The Taylor–Liang method differs from the older technique in two important respects. In it, the evacuation of the adsorbent between two adsorption measurements, at different temperatures is deliberately omitted and the pressure is kept constant at a selected value in measuring adsorption at the two temperatures. The new method is advantageous inasmuch as an isobar is obtained directly and any unsuspected changes in adsorption, throwing light on the heterogeneous nature of the catalyst surface, are readily observed. This method has been applied in the present work to the study of the adsorption of hydrogen on a zinc oxide–molybdenum oxide catalyst.

This catalyst has been previously investigated in the orthodox manner by Taylor and Ogden[2] and also by Taylor and Strother.[3] They found that in separate regions of temperature, both the van der Waals and the activated types of adsorption of hydrogen occurred.

In the present investigation, the isobaric rates of adsorption of hydrogen at different temperatures have been measured and the activation energies have been calculated for the respective temperature intervals. The surface area of the catalyst has been determined from the low temperature adsorption of nitrogen, by the application of both the Brunauer–Emmett–Teller and the Harkins–Jura equations.

Experimental

Apparatus.—The amount of gas adsorbed was determined volumetrically, employing a slight modification of the apparatus employed by Taylor and Williamson.[4] A manometer tube was attached to the buret for convenience in the measurement of the gas volume at atmospheric pressure. The evacuation of the system was carried out with a Leybold 4-stage mercury diffusion pump, backed by a Cenco Megavac pump.

(1) Taylor and Liang, *J. Am. Chem. Soc.*, **69**, 1306 (1947).
(2) Taylor and Ogden, *Trans. Faraday Soc.*, **30**, 1178 (1934).
(3) Taylor and Strother, *J. Am. Chem. Soc.*, **56**, 586 (1934).
(4) Taylor and Williamson, *ibid.*, **53**, 2169 (1931).

Preparation of the Catalyst.—The zinc oxide–molybdenum oxide catalyst was prepared by the method described by Taylor and Ogden.[2] The precipitate of zinc paramolybdate, obtained by the addition of ammonia dropwise to a mixed solution of ammonium paramolybdate and zinc nitrate, was washed, filtered and dried. It was then decomposed by heating in air at 150°; 3.175 g. of the decomposed product was placed in the catalyst tube and reduced in a stream of hydrogen at 400°. The reduced oxide in its final form was greenish black in color and had remarkable stability, as reported by Taylor and Ogden.

The catalyst tube after sealing off its outer end was attached to the adsorption apparatus. It was alternately evacuated and exposed to hydrogen at 400° and at atmospheric pressure, until reproducible values were obtained for the up-take of the gas. This procedure ensured that the catalyst suffered no further reduction during the adsorption measurements.

Preparation and Purification of the Gases Employed.—Hydrogen was prepared by the electrolysis of a 20% solution of caustic soda freed from oxygen by passing the gas over heated platinized asbestos and finally dried by passage over Drierite and phosphoric anhydride.

The helium used for the determination of the dead space in the catalyst tube and the nitrogen used in surface area measurements were the purest available commercial gases. Each had a purity of over 99.7%. The gases were freed from traces of oxygen by alkaline pyrogallol and dried with "Dehydrite" (anhydrous magnesium perchlorate).

All the above gases after purification were collected and stored over pure mercury in gas holders of glass.

Temperature Control.—Constant temperatures of 250° and below were obtained with the help of suitable vapor-baths. For temperatures above 250°, an electrically heated tube furnace was employed, its temperature being held constant to within 1° by means of an Energy Regulator (Sunvic–Type TYB).

Procedure.—The dead space in the catalyst tube was measured by filling it with helium at different pressures and temperatures and the mean value of the absolute dead space calculated from these measurements. The dead-space of the manometer section of the apparatus was determined by filling it with hydrogen at room temperature, at pressures ranging from 10 to 800 mm. Calibration charts were drawn (on an expanded scale) to read the volumes of the manometer section *vs.* the manometer readings. In the actual computation of adsorption, the volumes read from the chart were corrected for the prevailing ambient temperature and the pressure in the system. Similarly, the unadsorbed gas in the catalyst tube was calculated from its absolute volume, temperature and pressure.

Before each separate experiment, the catalyst was degassed for 10 hours at 400° under high vacuum, the McLeod gage attached to the system reading 10^{-6} mm. for at least 6 hours of the time.

Throughout the adsorption measurements, the pressure was maintained at that of the atmosphere, which varied between 683 and 689 mm. As the rate of adsorption was fairly slow, manual adjustment of the pressure was adequate and there was no need for any automatic device.

All the measurements reported in this paper were reproducible to within 0.02 cc.

For the determination of the surface area of the adsorbent, the adsorption isotherm of nitrogen at the temperature of liquid air (82°K.) was determined, adding 3% per 760 mm. pressure to the helium dead space to compensate for the deviation of nitrogen from the ideal gas laws, at this low temperature.

To determine the weight of the reduced catalyst, the catalyst tube was sealed off in the capillary tubulation at the end of the entire investigation, detached from the stop-cock, and weighed. It was then carefully cut in two and, after removing the adsorbent, the cut pieces were cleaned and weighed. The difference between the two weighings gave the weight of the reduced catalyst as 2.99 g. All adsorption results reported in this paper pertain to this weight of the reduced sample of zinc oxide–molybdenum oxide.

Results

Surface Area of the Catalyst.—The saturation pressure of liquid nitrogen at 82°K. was taken as 1279 mm. as found by Baly.[5] Eleven measurements of the adsorption of nitrogen on the catalyst at this temperature and at equilibrium pressures between 3 and 41 cm. gave straight-line graphs for $p/V(p_0 - p)$ *vs.* p/p_0 and for $-\log p/p_0$ *vs.* $1/V^2$, according to the equations of Brunauer, Emmett and Teller[6] and of Harkins and Jura,[7] respectively. The former equation gave $V_m = 2.59$ cc./g. (reduced), area = 11.62 sq. m./g. and $E_1 - E_L = 1042$ cal. and the latter 13.5 sq. m./g. for the area, taking k to be 4.06.

The Adsorption of Hydrogen.—In previous investigations[1,3] on a sample of this catalyst, it was reported that the adsorption of hydrogen thereon was practically nil below 200°. The present preparation, however, showed somewhat more active properties. The evacuated sample adsorbed in 24 hours 0.6, 0.64 and 0.75 cc. at 53°, 76° and 134°. In the neighborhood of 186°, there was a marked increase in the volume adsorbed.

Figure 1 depicts the observations made in a typical Taylor–Liang experiment in which the progress of adsorption was continually noted as the temperature was varied stepwise, in the order 134°, 186°, 250°, 340° and 375° and back to 134° in the reverse order.

The rates of adsorption were also determined separately at 186°, 250°, 300° and 350°, the catalyst having been evacuated for 10 hours at 400° prior to each experiment, at a given temperature. The rates of adsorption are shown graphically in Fig. 2.

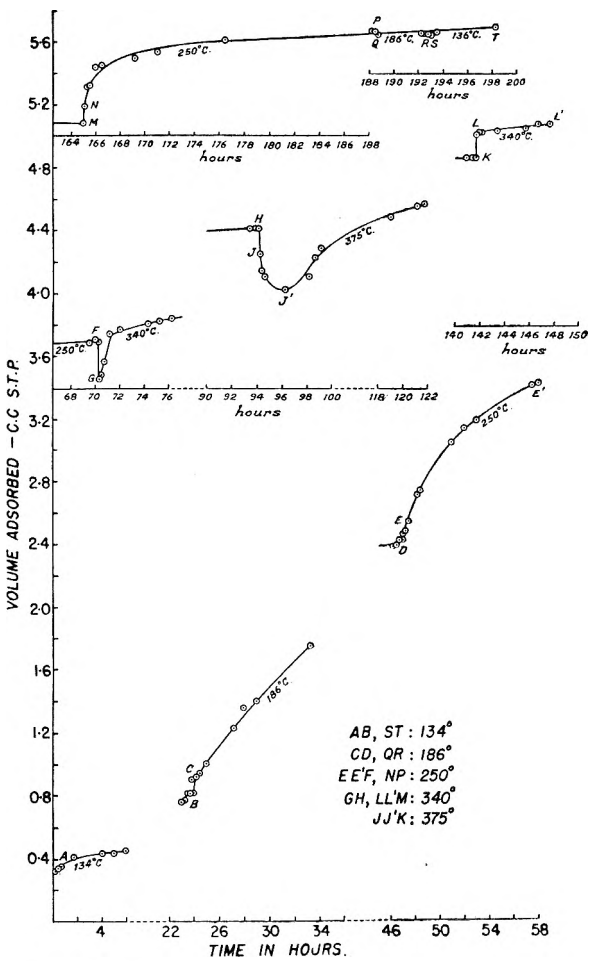

Fig. 1.

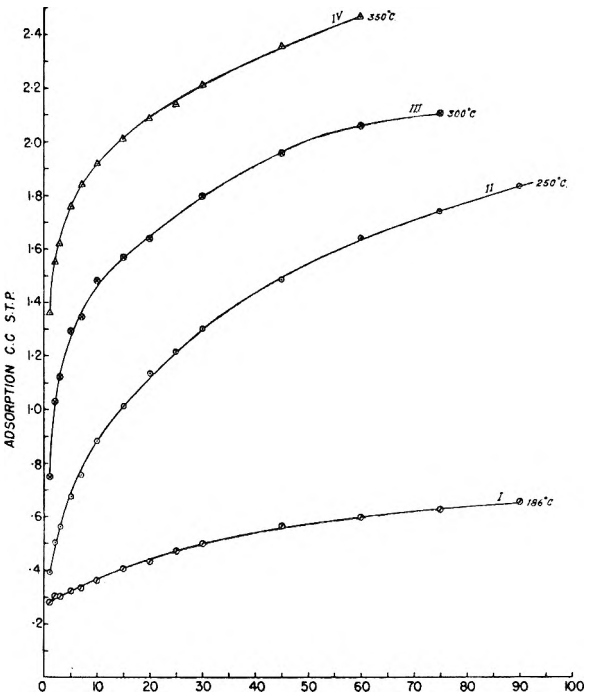

Fig. 2.

Discussion

It has been established by the earlier investigations of Taylor and his co-workers[2,3] that even at temperatures as low as 0°, van der Waals adsorption of hydrogen on zinc oxide–molybdenum oxide, as also on the relatively active zinc oxide and zinc oxide–chromium oxide catalysts, becomes almost negligible. In the present investigation therefore, it has been deemed unnecessary to prove experimentally that in the range of temperatures at which the measurements of hydrogen adsorption have been carried out, *viz.*, 134° to 375°, no adsorption by van der Waals forces is involved to any appreciable extent. The entire amount of gas adsorbed is to be considered as chemisorbed on the surface, with, as we shall see later, an activation energy of over 20 kcal. entering into the Boltzmann factor of the velocity of adsorption.

The amounts of gas desorbed at each increase of temperature and readsorbed on reversing this temperature change are deduced from Fig. 1 and presented in Table I. Below 250° no desorption was observed on increasing the temperature, there being only a smooth increase in adsorption. Correspondingly there was no increase in adsorption

(5) Baly, *Phil. Mag.*, **49**, 517 (1900).
(6) Brunauer, Emmett and Teller, *J. Am. Chem. Soc.*, **60**, 309 (1938).
(7) Harkins and Jura, *ibid.*, **66**, 1366 (1944).

on cooling from 250° downwards. Above 250°, on the other hand, every increase in temperature is attended by an instantaneous desorption, giving way subsequently to a readsorption. It is to be noted that each of the two cooling shifts between 375° and 250° is attended by a spurtive increase in adsorption.

TABLE I

AMOUNTS OF HYDROGEN DESORBED ON RAISING THE TEMPERATURE AND READSORBED ON LOWERING THE TEMPERATURE

Temperatures, °C. $T°_1$	$T°_2$	Volume desorbed on raising from T_1 to T_2, cc. S.T.P.	Volume adsorbed on lowering from T_2 to T_1, cc. S.T.P.
134	186	Nil	Nil
186	250	Nil	Nil
250	340	0.24	0.59
340	375	0.38	0.22

It is hard to conceive that a simple molecule like hydrogen can be chemisorbed in more than one way on the surface, within such a restricted range of high temperatures, or that chemisorbed hydrogen is both desorbed and readsorbed at the same temperature on one and the same group of adsorptive sites. The conclusion therefore seems inescapable that the desorption processes noticed on changing the temperature from 250° to 340° and from the latter to 375° (Fig. 1, FG and HJ′) occur on parts of the surface, different from those on which the subsequent slow adsorptions at 340° and 375° (GH and J′K) take place. Undoubtedly, the two processes proceed independently of each other. The hydrogen is adsorbed on separate groups of centers at the various temperature intervals, *viz.*, below 250°, 250° to 340°, and 340° to 375°, respectively, each group having its own characteristic temperature of maximum adsorption.

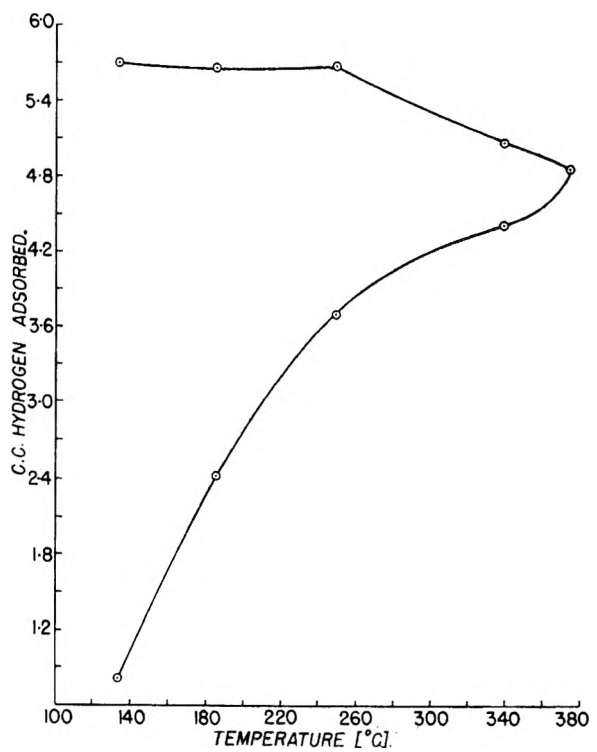

Fig. 3.

The increases in adsorption observed on decreasing the temperature from 375° to 340° and thence to 250° (KLL′M and MNP) represent a reversal of the desorption phenomena (FG and HJ′) and must have taken place on precisely those sites from which gas was desorbed immediately after the temperature was raised through each of these intervals. The absence of any desorption on changing from 134° to 186° and from the latter to 250°, coupled with the fact on the cooling range, the adsorption has remained constant from 250° to 134°, suggests that the active centers responsible for adsorption between 134° and 250° have fairly uniform characteristics.

The adsorption isobar in Fig. 3, drawn from the equilibrium values of adsorption at each of the temperatures between 134° and 375°, shows that as the temperature is increased the over-all adsorption increases, while on the cooling side, the adsorption increases only from 375° to 250°, and remains constant thereafter. This emphasizes the salient fact that only above 250°, desorption phenomena typical of surface heterogeneity are noticeable. The constancy of adsorption from 250° to 134° on the cooling branch, confirms the absence of any desorption on raising the temperature between these limits.

The main points of distinction among the various groups of sites must be with regard to their activation energies (E) and heats (λ). Taylor[8] has envisaged even in his earliest exposition on the theory of activated adsorption, the possibility of a considerable part of the surface remaining bare at a given temperature, as a direct consequence of the magnitude of $(E + \lambda)$. In another review,[9] he has shown schematically that, with increasing adsorptions, $(E + \lambda)$ could increase, or decrease, or pass through a minimum value, depending upon the relative slopes of E *vs.* adsorption and λ *vs.* adsorption.

Taylor and Liang[1] have endeavored to explain the desorption–readsorption phenomena, observed by them on zinc oxide surface, with the help of a simple picture of a hypothetical adsorbent surface, containing only two types of active centers, A and B, with E_a and E_b as their respective activation energies of adsorption, and with λ_a and λ_b, as their respective heats of adsorption.

The processes of desorption and adsorption, occurring independently on the sites A and B, and the net result emerging therefrom are illustrated clearly in Fig. 4. The values of E_a, E_b, λ_a and λ_b are such that at the lower temperature T_1, the site A becomes covered (curve A-1), while its counterpart B remains sensibly bare (curve B-1). Immediately on changing to a sufficiently higher temperature T_2 at constant pressure, the gas desorbs from A, more or less rapidly (curve A-2), while B becomes progressively covered (curve B-2). If at the higher temperature, the rate of desorption from A is initially faster than that of adsorption on B, the net effect observed on changing from T_1 to T_2 would be an immediate desorption, followed by a rise in adsorption (curve AB-2).

(8) Taylor, *J. Am. Chem. Soc.*, **53**, 578 (1931).
(9) Taylor, *Chem. Revs.*, **9**, 1 (1931).

Let V_a be the volume of gas adsorbed on the surface A at the temperature T_1 immediately before changing to T_2 and V_a'' the equilibrium adsorption on the same surface at the latter temperature. It is obvious that gas will desorb from A, on changing from T_1 to T_2, only if $V_a > V_a''$. In order that the surface B may remain relatively bare at the lower temperature T_1, $E_b \gg E_a$, since the rate of adsorption on a sparsely covered surface is given by

$$dv/dt = k_1 e^{-E/RT}$$

The resultant effect of desorption from A and simultaneous adsorption on B at the temperature T_2 (curve AB-2) is represented by

$$\frac{dv}{dt} = k_1 e^{-E_b/RT_2} - k_2 v_a e^{-(E_a + \lambda_a)/RT_2} \qquad (1)$$

where v_a denotes the adsorption on A at any instant of time. The first term on the right-hand side is the rate of condensation on B (curve B-2) and the second term is the rate of evaporation from A (curve A-2) at temperature T_2.

Equation 1 will give a minimum value for the net adsorption, when the volume of gas remaining on A is given by

$$V^* = \frac{k_1 e^{-E_b/RT_2}}{k_2 e^{-(E_a + \lambda_a)/RT_2}} \qquad (2)$$

Both the terms on the right, may be obtained from the experimentally determined kinetics of adsorption on the evacuated adsorbent (analogous to the curves of Fig. 2) at the temperatures T_1 and T_2. The numerator term may, without serious error, be taken as the x slope of the initial steep part of the rate curve at T_2. The denominator term can be calculated by applying the following equation 3, due to Taylor and Sickman,[10] to the rate of adsorption on the bare adsorbent at temperature T_1.

$$\log_e (V_a' - v_a) = \log_e V_a' - k_2 t e^{-(E_a + \lambda_a)/RT_1} \qquad (3)$$

or

$$\log (V_a' - v_a) = \log V_a' - 0.4343\, k_2 t e^{-(E_a + \lambda_a)/RT_1} \qquad (3a)$$

where V_a' is the equilibrium adsorption on A at T_1 and v_a the experimental value of the adsorption at time t. Assuming various values for V_a', $\log (V_a' - v_a)$ is plotted against time to see which value of V_a' gives a straight-line plot for the equation 3a. The slope of this straight line is given by

$$S_1 = 0.4343\, k_2 e^{-(E_a + \lambda_a)/RT_1} \qquad (4)$$

This gives the specific rate of desorption from A at T_1, whence one can calculate the corresponding rate at T_2, as

$$\text{If } S_2 = 0.4343\, k_2 e^{-(E_a + \lambda_a)/RT_2} \qquad (5)$$

then

$$\log S_2 = \log S_1 + 0.4343 \frac{(E_a + \lambda_a)}{R} \times \frac{(T_2 - T_1)}{T_1 T_2} \qquad (6)$$

whence S_2 and therefore $k_2 e^{-(E_a + \lambda_a)/RT_2}$ can be calculated, if the values of E_a and λ_a are known. Substituting in equation 2, V_a^* is obtained. The time taken for the gas on A to desorb from V_a to V_a^* can be found by integrating the equation for the rate of evaporation

$$dv_a/dt = -k_2 v_a e^{-(E_a + \lambda_a)/RT_2} \qquad (7)$$

(10) Taylor and Sickman, *J. Am. Chem. Soc.*, **54**, 602 (1932).

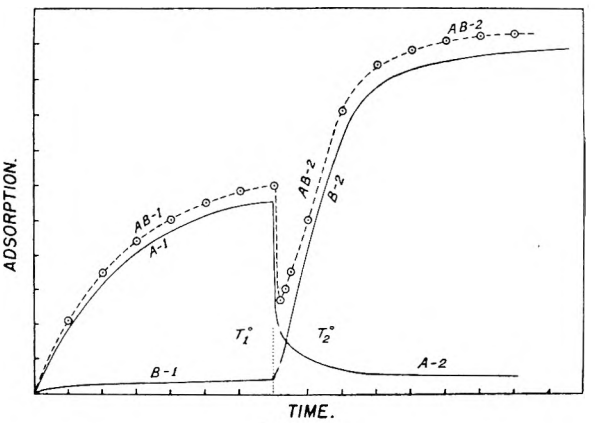

Fig. 4.

between the limits V_a and V_a^*. Thus

$$t = \frac{2.303 (\log V_a - \log V_a^*)}{k_2 e^{-(E_a + \lambda_a)/RT_2}} = \frac{\log V_a - \log V_a^*}{S_2} \qquad (8)$$

The net minimum value of the adsorption on the composite adsorbent AB is given by

$$V_{min} = V_a^* + t k_1 e^{-E_b/RT_2} \qquad (9)$$

Applying these equations to the observed kinetics of adsorption on the present sample of zinc oxide–molybdenum oxide at 250° and 350°, one can estimate the amount of desorption following an increase of temperature between these limits. Let A and B denote the parts of the surface which adsorb hydrogen at 250° and 350°, respectively.

$\log (4 - v_a)$ *vs.* time gives a straight line for the observed rate of adsorption at 250°; its slope $S_1 = 0.001$.

Therefore, $k_2 e^{(E_a + \lambda_a)/RT_1} = 0.0023$ where $T_1 = 523°$ K. From the rates of adsorption at 186° and 250°, it has been found (*vide* next section) that $E_a = 22{,}000$ cal. For the value of λ_a, Taylor and Ogden[2] have given a value of 22,300 cal. for the initial amount of adsorption at temperatures between 677° and 717° K. For adsorption approaching saturation at 523° K., one may reasonably assume $\lambda_a = 12{,}000$ cal., so that $E_a + \lambda_a = 34{,}000$ cal. By equations 6 and 5, for the desorption rate at 350°, $S_2 = 0.1845$ and $k_2 e^{-(E_a + \lambda_a)/RT_2} = 0.425$, where $T_2 = 623°$ K. The slope of the rate curve at 350° (Fig. 2, curve IV) for the first two minutes, *i.e.*, $k_1 e^{-E_b/RT_2} = 0.775$. Therefore, the gas remaining on A at the point of minimum adsorption, *i.e.*, $V_a^* = 0.775/0.425 = 1.82$ cc. by Eq. 2.

The time taken for minimum point to be reached after the change from 250° to 350° is $t = (\log 3.7 - \log 1.82)/0.1845 = 1.67$ min. by Eq. 8.

The gas adsorbed on B during this time, $V_b^* = 0.775 \times 1.67 = 1.29$, whence by Eq. 9, the total adsorption on the composite surface at the point of minimum adsorption at 350° is $V_{min} = 1.82 + 1.29 = 3.11$ cc.; the net desorption = 0.59 cc. This result may be compared with the experimental observation (Fig. 1) that within 5 minutes after changing from 250° to 340°, the adsorption fell from 3.70 to 3.46 thus desorbing 0.24 cc. and on reversing this change of temperature there was readsorption of 0.59 cc. This close agreement between the calculated and experimental values emphasizes the correctness of the theory on which

the calculation is based, in so far as it requires only a reasonable assumption of the value of λ_a to give a satisfactory check up on the experimental result.

The Activation Energy of Adsorption.—Table II shows the values of the activation energy of adsorption for the three temperature ranges, 186–250°, 250–300°, and 300–350°, calculated from the rates of adsorption (Fig. 2), using the simple formula

$$\log (t_1/t_2) = \frac{E}{2.303\ R}\left(\frac{1}{T_1} - \frac{1}{T_2}\right) \qquad (10)$$

where t_1 and t_2 are the times taken to adsorb specified amount of gas at the temperature, T_1 and T_2, respectively.

TABLE II

THE ENERGIES OF ACTIVATION OF ADSORPTION

Adsorption, cc. S.T.P.	Energies of activation, kcal. 186-250°	250-300°	300-350°
0.5	20.19		
0.6	20.81		
0.7	22.00		
1.2	...	21.37	
1.3	...	20.22	
1.4	...	17.81	
1.5	...	16.27	
1.6	...	14.46	26.80
1.7	...	13.01	24.84
1.8	...	12.36	22.87
1.9	...	...	20.42
2.0	...	...	17.58
2.1	...	...	17.60

It will be seen that the values of the energy of activation also reflect the sharp difference between the behavior of the adsorbent below 250° and that above this limit. While the values for the lowest range show the normal increase, with increase in adsorption, tending to attain constancy at *ca.* 22,000 cal., the values for each of the higher temperature intervals show a decrease, with increase in surface coverage. Normally, the latter type of variation of the activation energy would lead to the untenable inference that the first portions of surface to be covered at high temperatures are the least active ones. A similar abnormal variation was reported by Taylor and Ogden[2] on the same adsorbent for the temperature interval 300–450°, but was then ascribed to the high rate of desorption at the upper limit of temperature (especially for large values of adsorption) and to the consequent inapplicability of the approximate formula 10, which completely neglected the rate of desorption in the calculation. Such an explanation, though valid in itself, will not be adequate to account for the variations observed in the present experiments (Table II) where, it will be noticed, the values for the intermediate temperature range are much lower than those for the higher temperatures. If the increased rate of desorption provided the complete explanation for the observed abnormalities the reverse would be the case.

The evidence of surface heterogeneity, obtained from the temperature variation experiments (Fig. 1), provides a fundamentally different approach to the problem. While almost the same centers come into play at 186° and 250°, those that absorb at each of the higher temperatures, 300° and 350°, have very high average values for E and λ. The surface that gives, in Fig. 2, the curve II at 250° remains relatively bare at 300°, curve III being the rate of adsorption on a different set of sites. Similarly, the rate curve IV refers to a third group of centers. Thus, it would be logical to bracket only the rate curves for 186° and 250° to calculate the energy of activation. The other two curves pertain to different parts of the surface, each being independent of the other, and cannot therefore be used in any way, for this purpose. In general, if it is first established by the Taylor–Liang type of experiment that raising or lowering the temperature within a particular range, at constant pressure, gives no evidence of desorption or readsorption, kinetic measurements carried out on cleared surfaces at any two temperatures, within this range, can be employed to deduce the energy of activation of adsorption. A judicious combination of the two types of experiments may thus be fruitfully utilized to yield valuable information on the heterogeneous composition and the energetics of the adsorbent surface.

The Extent of the Active Surface.—The V_m of nitrogen for 2.99 g. of the adsorbent was 7.75 cc. by the B.E.T. method. Using the value of $\alpha_H/\alpha_N = 0.54$, given by Livingston[11] for the ratio of the sectional areas of adsorbed hydrogen and nitrogen, the volume of hydrogen required to form a complete unimolecular layer = 14.34 cc. By a separate experiment, it was found that the degassed catalyst adsorbed 4.6 cc. of hydrogen in 24 hours at atmospheric pressure and 375°, which is very nearly the temperature of maximum adsorption (*cf.* ref. 2). On the older views of the heterogeneity of catalyst surfaces, this upper limit for the adsorption on the bare surface would be taken to imply that only about 30% of the entire surface is really active. The examination of the surface by the Taylor–Liang technique, on the other hand, has revealed that the active part of surface extends to about 40% of the total, corresponding to 5.70 cc. of adsorption. Approximately one-fourth of the active area remains sensibly bare at 375°, because of a relatively high rate of desorption, though on the score of its lower activation energy of adsorption, it could be considered as more active than the area actually covered at the highest temperature.

Acknowledgment.—The authors are much obliged to Professor B. Sanjiva Rao for his kind interest in this investigation and his valuable advice in writing this paper and to Dean Hugh S. Taylor of Princeton University for kindly scrutinizing the original draft with keen interest.

(11) Livingston, *J. Colloid Sci.*, **4**, 447 (1949).

THE SPECTROPHOTOMETRIC DETERMINATION OF OVERLAPPING DISSOCIATION CONSTANTS OF DIBASIC ACIDS.[1] THE ACID CONSTANTS OF ISOPHTHALIC, TEREPHTHALIC AND CHLORANILIC ACIDS

BY B. J. THAMER[2] AND A. F. VOIGT

Institute for Atomic Research, Ames, Iowa

Received January 8, 1951

A spectrophotometric method is developed for determining overlapping dissociation constants for dibasic acids. The method is applied to the determination of the dissociation constants of isophthalic, terephthalic and chloranilic acids. The similar use of other properties is suggested as a possible alternative to the use of optical density.

Introduction

The ionization equilibria of a dibasic acid H_2A in solutions of constant ionic strength and fixed temperature may be represented in the following manner

$$k_1 = \frac{a \times [HA]}{[H_2A]} \text{ and } k_2 = \frac{a \times [A]}{[HA]} \qquad (1)$$

where a represents the hydrogen ion activity and brackets indicate concentrations. Charges are not attached to the symbols H_2A, HA and A because the "dibasic acid" H_2A may be a conjugate acid of an ampholyte or base instead of being a dibasic acid of the usual type. The thermodynamic dissociation constants, K_1 and K_2, can be estimated fairly accurately from the constants, k_1 and k_2, provided the value of the ionic strength is reasonably low. Thus

$$K_1 = \frac{\gamma_{HA}}{\gamma_{H2A}} \times k_1 \text{ and } K_2 = \frac{\gamma_A}{\gamma_{HA}} \times k_2 \qquad (2)$$

The constants, k_1 and k_2, are determined experimentally. They are related to the optical density

$$D = L[H_2A]\epsilon_1 + L[HA]\epsilon_2 + L[A]\epsilon_3 \qquad (3)$$

where L is the length of the absorption cell, and ϵ_1, ϵ_2 and ϵ_3 are the molar extinction coefficients of the forms H_2A, HA and A, respectively. Representing the total concentration of the acid in all its forms by c and combining equations 1 and 3, one can readily derive the relation

$$D = \frac{Lc\left[\epsilon_1 + \frac{k_1}{a}\epsilon_2 + \frac{k_1k_2}{a^2}\epsilon_3\right]}{1 + \frac{k_1}{a} + \frac{k_1k_2}{a^2}} \qquad (4)$$

If k_1 and k_2 differ greatly in magnitude they can be determined separately since then only one stage of ionization is operative at a given pH. However, if k_1/k_2 is less than 1000 the spectrophotometric determination of k_1 and k_2 is rendered more difficult by the fact that no more than 94% of the acid can be obtained in the intermediate form HA at any pH and the extinction coefficient ϵ_2 cannot be estimated accurately from the experimental data. For example, if $k_1/k_2 = 50$ the maximum obtainable value of $[HA]/c$ is 78%.

The quantities ϵ_1 and ϵ_3 can usually be obtained by direct measurement at low and high pH values, respectively. If k_1 and k_2 overlap and k_1/k_2 is therefore small, one can use optical density data and pH data with equation 4 to obtain ϵ_2, k_1 and k_2 by successive approximations. However, the calculations are very laborious. Vlès and Gex approached the problem by using a function $\phi = D'/D$ where D' and D were to be taken at the same pH but two different wave lengths.[3] Their method did not provide a means for calculating overlapping values of k_1 and k_2 without approximations. It should be noted also that a mistake was made in their derivation of the basic equations to be used in obtaining k_1 and k_2 for a dibasic acid having uncharged acidic groups. A derivation of the correct equations for their method has been placed in Appendix I. A correction to a similar mistake in their treatment of ampholytes has been made by Hughes, Jellinek and Ambrose.[4] A colorimetric method has been developed by Sacconi for the separate determination of k_1 and k_2 for a colored substance.[5] Although the effect of overlapping constants is minimized in his method it is liable to be a serious source of error for values of k_1/k_2 less than 50.

The method that is developed and used in the following sections is designed specifically for the case in which k_1/k_2 is less than 1000. The method is free of the approximations that are inherent in the previously published methods.

Theory

In this method buffered solutions of the acid are scanned at constant concentration of the dibasic acid and constant ionic strength, temperature and cell length. The measured optical density is corrected for absorption by the solvent and buffer and plotted against pH at various wave lengths. A wave length is selected at which the plot of optical density *versus* pH gives a decided maximum (or minimum) in the pH range in which the HA species predominates.

A synthetic example of the type of curve sought is shown for the case in which a maximum is exhibited (Fig. 1). The curve was calculated from equation 4. For any such curve showing a maxi-

(1) Contribution No. 136 from the Institute for Atomic Research and Department of Chemistry, Iowa State College, Ames, Iowa. Work was performed in the Ames Laboratory of the AEC.

(2) Abstracted from a part of the thesis submitted by B. J. Thamer to the Graduate Faculty of Iowa State College in partial fulfillment of the requirements of the degree of Doctor of Philosophy.

(3) F. Vlès and M. Gex, *Arch. Phys. biol.*, **6**, 69 (1927); *ibid.*, **9**, 171 (1931).

(4) E. B. Hughes, H. H. G. Jellinek and B. A. Ambrose, THIS JOURNAL, **53**, 414 (1949).

(5) L. Sacconi, *ibid.*, **54**, 829 (1950).

mum (or minimum) the pH at any point on the curve can be expressed as:

$$p\mathrm{H} = p\mathrm{H}_0 + \Delta \quad \text{and} \quad a = a_0 10^{-\Delta} \tag{5}$$

where $p\mathrm{H}_0 = -\log a_0$ is the pH at the maximum (or minimum) of the curve and a_0 is the hydrogen ion activity at that point. This pH is experimentally measurable as is the optical density D_m at this point. From equations 4 and 5

$$D_m = \frac{Lc\left[\epsilon_1 + \frac{k_1}{a_0}\epsilon_2 + \frac{k_1k_2}{a_0^2}\epsilon_3\right]}{1 + \frac{k_1}{a_0} + \frac{k_1k_2}{a_0^2}} \tag{6}$$

$$D = \frac{Lc\left[\epsilon_1 + \frac{k_1}{a_0}10^{+\Delta}\epsilon_2 + \frac{k_1k_2}{a_0^2}10^{+2\Delta}\epsilon_3\right]}{1 + \frac{k_1}{a_0}10^{+\Delta} + \frac{k_1k_2}{a_0^2}10^{+2\Delta}} \tag{12}$$

Combining this with equations 6 and 7 gives the following expression for k_1

$$k_1 = \frac{a_0}{(D_m - D)}\left[(D - D_1)10^{-\Delta} - D_m + D_1 + [(D - D_3)10^{+\Delta} - D_m + D_3]\frac{k_1k_2}{a_0^2}\right] \tag{13}$$

The substitution of equation 10 into 13 yields the expression

$$k_1 = \frac{a_0[(D_m - D_3)(D - D_1)10^{-\Delta} + (D_m - D_1)(D - D_3)10^{+\Delta} - 2(D_m - D_1)(D_m - D_3)]}{(D_m - D_3)(D_m - D)} \tag{14}$$

At the left-hand and right-hand limits of the curve the optical densities are, respectively

$$D_1 = Lc\epsilon_1 \quad \text{and} \quad D_3 = Lc\epsilon_3 \tag{7}$$

Putting dD/da equal to zero from equation 4 yields the following relation obtained at the maximum (or minimum)

$$\frac{\epsilon_1}{\epsilon_2} - 1 + \frac{k_1k_2}{a_0^2}\left(1 - \frac{\epsilon_3}{\epsilon_2}\right) + 2\frac{k_2}{a_0}\left(\frac{\epsilon_1}{\epsilon_2} - \frac{\epsilon_3}{\epsilon_2}\right) = 0 \tag{8}$$

The combination of equations 6, 7 and 8 leads to the following

$$(k_1k_2)^2 + a_0\left[k_1 + a_0\left(1 - \frac{D_m - D_1}{D_m - D_3}\right)\right](k_1k_2) - a_0^3\frac{D_m - D_1}{D_m - D_3}(k_1 + a_0) = 0 \tag{9}$$

Equation 9 can be factored to give the two roots and

$$k_1k_2 = a_0^2\frac{D_m - D_1}{D_m - D_3} \tag{10}$$

and

$$k_1k_2 = -a_0(k_1 + a_0) \tag{11}$$

Equation 11 has no physical meaning since k_1, k_2 and a_1 are all positive quantities. Equation 10 is physically valid since either a maximum or minimum will make $(D_m - D_1)/(D_m - D_3)$ a positive quantity.

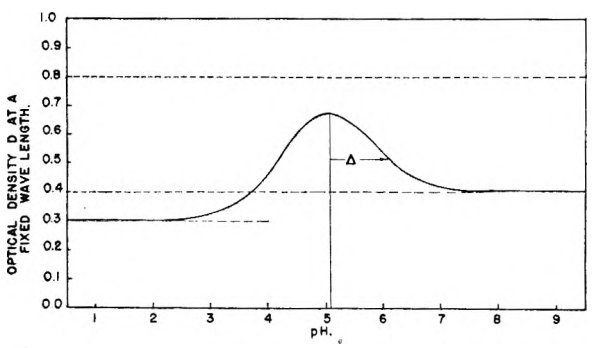

Fig. 1.—Plot of optical density *vs.* pH: $K_1 = 5 \times 10^{-5}$; $K_2 = 2 \times 10^{-6}$. The values of $Lc\epsilon_1$, $Lc\epsilon_2$, and $Lc\epsilon_3$ are 0.300, 0.800, 0.400, respectively, for which dotted horizontal lines have been drawn.

A combination of equations 4 and 5 gives the following expression for the optical density at any point on the curve

Since every quantity on the right-hand side of equation 14 is experimentally measurable, it can be used for the evaluation of k_1. Using equation 10, k_2 can then be determined.

If D_1 and D_3 are equal it can easily be shown that the curve of D *versus* pH is symmetrical about its maximum or minimum. In this case equations 10 and 14 can be put in the simpler forms

$$k_1k_2 = a_0^2 \tag{10'}$$

$$k_1 = \frac{2a_0}{(D_m - D)}[(D - D')\cosh(\Delta \ln 10) - (D_m - D')] \tag{14'}$$

where $D' = D_1 = D_3$.

Having obtained average values for k_1 and k_2 from the plot of experimental values of D *versus* pH, these average values can be used in the following two equations in order to calculate a curve through the experimental points

$$a_0 = \sqrt{\left(\frac{D_m - D_3}{D_m - D_1}\right)k_1k_2} \tag{15}$$

$$D = D_1 + (D_m - D_1)\left[\frac{\frac{k_1}{a_0} + 2 + \left(\frac{D_3 - D_1}{D_m - D_3}\right)10^{+\Delta}}{\frac{k_1}{a_0} + 10^{-\Delta} + \left(\frac{D_m - D_1}{D_m - D_3}\right)10^{+\Delta}}\right] \tag{16}$$

It sometimes happens that no single wave length can be found at which the plot of optical density *versus* pH gives a satisfactory maximum (or minimum). In such cases it is often advantageous to combine the data at different wave lengths into a composite, C, in the following manner

$$C = \sum_i g_iD_i \tag{17}$$

where i represents the wave lengths used and the g_i's are weighting factors arbitrarily chosen to give the most favorable maximum (or minimum) in the resulting plot of C *versus* pH. Such composites can be used in the same manner as optical densities to yield the equations

$$k_1k_2 = a_0^2\left(\frac{C_m - C_1}{C_m - C_3}\right) \tag{18}$$

$$k_1 = \frac{a_0[(C_m - C_3)(C - C_1)10^{-\Delta} + (C_m - C_1)(C - C_3)10^{+\Delta} - 2(C_m - C_1)(C_m - C_3)]}{(C_m - C_3)(C_m - C)} \tag{19}$$

Even if favorable maxima are obtained at several wave lengths, the use of a composite and equations 18 and 19 usually will afford the maximum accuracy in k_1 and k_2 for the least amount of calculating.

Experimental

Matched silica cuvettes were used in all measurements and the light path was 50 mm. except as otherwise noted. A Model 12 Cary Recording Spectrophotometer was used in all measurements except those at fixed wave lengths for terephthalic acid which were made on a Beckman Model DU Spectrophotometer. Each spectrophotometer was zero adjusted immmediately before each measurement. The *p*H measurements were made with a Beckman Model G *p*H Meter equipped with that company's No. 290 glass electrode and No. 270 calomel electrode. The *p*H values of scanned and unscanned portions of the same solution always fell within 0.02 *p*H unit of one another and the *p*H of the scanned portion was taken as the correct value. The standardization of the *p*H meter was checked before and after each measurement using a Beckman buffer of *p*H 4.00 or 10.00.

All solutions were prepared in conductance water. The determinations of the dissociation constants were made at constant ionic strength, the values of which are noted later. Formate and phosphate buffers were used in the study of isophthalic and terephthalic acids. Chloranilic acid was studied in unbuffered perchloric acid–lithium perchlorate solutions because its acid constants were desired entirely in terms of concentrations for use in other studies. All acids, salts and buffers were of at least C.P. grade. The stock solutions of these substances were filtered if necessary in order to remove slight turbidities or small amounts of foreign matter. For each solution measured correction was made for the optical density of the constituents other than the dibasic acid by means of a separate measurement.

A pure grade of isophthalic acid was obtained from the Genesee Research Corporation. Using the method of Baeyer and Villiger[6] it was further purified by metathesis with barium carbonate which produces the soluble salt of isophthalic acid and insoluble barium terephthalate. After removing the barium as barium sulfate, the isophthalic acid was finally precipitated from a 0.05 molar solution with dilute hydrochloric acid, thoroughly washed and dried at 105°. Eastman terephthalic acid was purified in a manner similar to that used by Scheurer and LeFave[7] except that the metathesis to barium terephthalate was accomplished with barium carbonate instead of barium chloride.

"Practical grade" chloranilic acid was obtained from the Eastman Kodak Company and purified in the following manner. Eight grams of the acid was dissolved in a liter of distilled water at the boiling point and filtered. The filtrate was extracted with two 200-ml. portions of benzene in a separatory funnel at 50°. The benzene phases, containing only a little chloranilic acid, were discarded. The aqueous phase was cooled in an ice-bath yielding bright red crystals of chloranilic acid which were filtered off and washed with three 10-ml. portions of water. The crystals were dried at 115° in order to expel the water of hydration.[8] The overall yield of chloranilic acid was approximately 50%. Its purity was determined by electrometric titration using carbonate-free sodium hydroxide, standardized against G. F. Smith potassium acid iodate.[9] The purities of two different preparations were found to be (99.8 ± 0.3%) by weight.

Isophthalic Acid.—Solutions of isophthalic acid are practically colorless but absorb strongly in the ultraviolet due to the presence of the benzene ring. Absorption curves (Fig. 2) indicated that the species HA (the predominant species of curve C) absorbed either more or less than the species H_2A (curve A) and A (curve B) only in the region of 2450–2500 Å. Consequently subsequent measurements were confined to this wave length interval.

The data have been summarized in Table I. The ionic strength was maintained at 0.0302. The corrections applied to the measured optical densities for absorption by the buffers were always less than 10% of the measured values. The band width was the same for each measurement at a given wave length. Its value was approximately 12 Å. The temperature during scanning and *p*H measurements was 25 ± 1°. "Spot" readings and automatic scanning gave the same values, thus indicating that the automatic scanning apparatus was functioning satisfactorily.

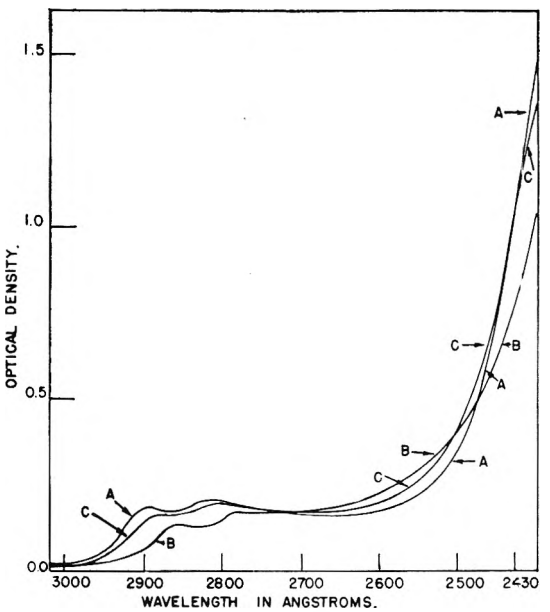

Fig. 2.—Absorption curves for 9.5×10^{-5} formal isophthalic acid in a 20.00-mm. cuvette: A, *p*H 1.92; B, *p*H 11.61; C, *p*H 4.10.

TABLE I

OPTICAL DENSITIES OF ISOPHTHALIC ACID

$c = 8.0 \times 10^{-4}$; $L = 50$ mm.

*p*H	*D* at 2476.0 Å.	*D* at 2460.0 Å.	Buffer
1.58	0.987	1.298	($HClO_4$)
1.585	.991	1.297	($HClO_4$)
1.585	.988	1.302	($HClO_4$)
2.49	1.007	1.318	Phosphate
2.725	1.016	1.324	Phosphate
3.03	1.063	1.365	Formate
3.12	1.076	1.375	Phosphate
3.175	1.081	1.383	Formate
3.37	1.109	1.408	Formate
3.37	1.108	1.412	Formate
3.56	1.134	1.435	Formate
3.575	1.141	1.436	Formate
3.75	1.158	1.451	Formate
3.96	1.160	1.447	Formate
3.96	1.167	1.451	Formate
3.96	1.165	1.440	Formate
4.18	1.152	1.421	Formate
4.33	1.142	1.395	Formate
4.34	1.136	1.391	Formate
4.515	1.110	1.341	None (NaCl)
4.535	1.107	1.350	Formate
4.55	1.104	1.346	Formate
4.715	1.078	1.294	Formate
4.91	1.056	1.256	Formate
5.095	1.036	1.233	Formate
7.90	0.982	1.149	Phosphate
7.98	.989	1.151	Phosphate
8.72	.982	1.146	Phosphate

(6) A. Baeyer and V. Villiger, *Ann.*, **276**, 256 (1893).

(7) F. G. Scheurer and G. M. LeFave, *J. Am. Chem. Soc.*, **72**, 3308 (1950).

(8) C. V. Graebe, *Ann.*, **263**, 26 (1891).

(9) I. M. Kolthoff and V. A. Stenger, "Volumetric Analysis," 2d. ed., Vol. 2, Interscience Publishers, Inc., New York, N. Y., 1947, pp. 100-101.

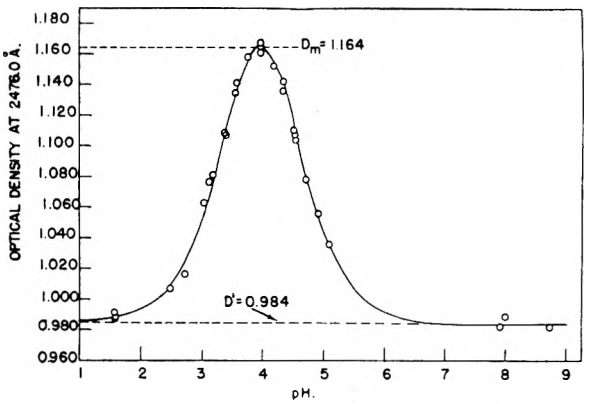

Fig. 3.—Isophthalic acid at 2476.0 Å.: circles, experimental points; solid curves, calculated as shown later.

Figure 3 shows the plot of optical density *versus* pH at 2476.0 Å. where $D_1 = D_3 = D' = 0.984$ and $D_m = 1.164$. Equations 10′ and 14′ were applicable. The quantity pH_0 probably could have been estimated to within 0.05 pH unit by an inspection of the points at the top of the curve. However, pH_0 was determined by the following method because it used more points for this purpose and appeared to be more accurate. The method is based upon the fact that the true value of k_1 should be independent of the value of Δ used in measuring it. The values of k_1/a_0 calculated from equation 14′ (or 14) are very sensitive to variations in pH_0 because of its direct effect on values of Δ. Hence if calculated values of k_1/a_0 are plotted against Δ for a trial value of pH_0, the best straight line through the points calculated by the method of least squares should have a definite slope if the trial value of pH_0 is in error, but zero slope if the trial value of pH_0 is the true value. Representing the equation of the least-squares straight line by

$$\frac{k_1}{a_0} = y = a + b\Delta$$

the formula for the slope is

$$b = \frac{n\Sigma(\Delta y_0) - \Sigma\Delta\Sigma y_0}{n\Sigma(\Delta)^2 - (\Sigma\Delta)^2}$$

where n is the number of points used, $\Sigma\Delta$ the sum of Δ overall of the points and y_0 is the value calculated for k_1/a_0 at each point that is used.[10] All reliable points are to be used for this purpose except those where dD/dpH has a low value as at D_m or near D_1 or D_3. A few trial values of pH_0 suffice to locate the best value of pH_0 within 0.005 pH unit. Hence for isophthalic acid at 2476.0 Å. the best value of pH_0 was found to be 3.9435. The resulting values for k_1, k_2 and their standard deviations were

$$k_1 = (3.24 \pm 0.56) \times 10^{-4}$$
$$k_2 = (4.00 \pm 0.69) \times 10^{-5}$$

Only points between $D = 1.036$ and $D = 1.158$ were used in calculating the above values. The other points appeared to be inaccurate or were too close to the limits (D_1, D_m or D_3) to be used.

The plotted data at 2460.0 Å. (Fig. 4) gave $D_1 = 1.295$, $D_m = 1.451$ and $D_3 = 1.149$. These values together with equations 10 and 14 and the above least-squares method yielded the following values:

$$pH_0 = 3.843$$
$$k_1 = (2.67 \pm 0.28) \times 10^{-4}$$
$$k_2 = (4.00 \pm 0.42) \times 10^{-5}$$

The grand mean values obtained from the values at these two wave lengths were

$$k_1 = (2.78 \pm 0.25) \times 10^{-4}$$
$$k_2 = (4.00 \pm 0.36) \times 10^{-5}$$

(10) A. G. Worthing and J. Geffner, "Treatment of Experimental Data," 1st ed., John Wiley and Sons, Inc., New York, N. Y., 1943, p. 239-40.

These values were used with equations 15 and 16 to calculate the solid curves shown in Figs. 3 and 4. The final values of k_1, k_2 and their standard deviations were taken as

$$k_1 = (2.8 \pm 0.4) \times 10^{-4}$$
$$k_2 = (4.0 \pm 0.6) \times 10^{-5}$$

thus giving $k_1/k_2 = 7.0 \pm 1.4$ where an additional error of 5% was added in order to take into account uncertainties in the values of pH_0.

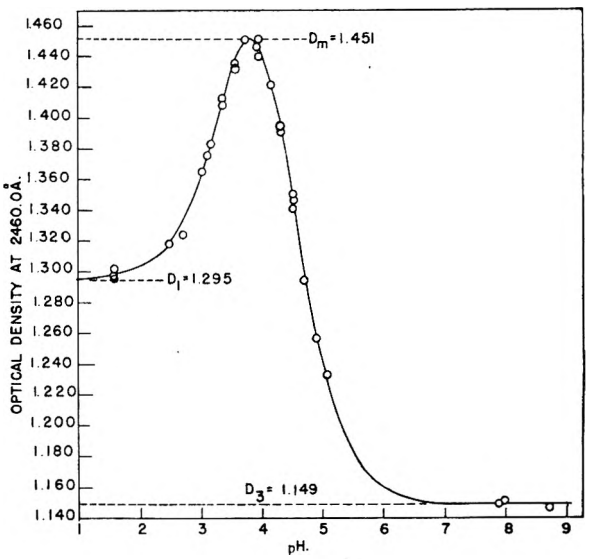

Fig. 4.—Isophthalic acid at 2460.0 Å.: circles, experimental points; solid curve, calculated as shown later.

The following form of the Hückel equation was used in estimating activity coefficients

$$\log \gamma_i = \frac{-0.509 z_i^2 \sqrt{\mu}}{1 + 0.330\, \text{å}\, \sqrt{\mu}} + C'\mu$$

where å was assumed to be 5 Å. for each ion and C' was assumed to be the same for each of the species H_2A, HA and $A^{=}$.[11] The values thus obtained for isophthalic acid at $\mu = 0.0302$ were

$$\frac{\gamma HA}{\gamma H_2A} = 0.854 \pm 0.014$$
$$\frac{\gamma A}{\gamma HA} = 0.622 \pm 0.030$$

where a 10% error was included in estimating the values of $\log \frac{\gamma HA}{\gamma H_2A}$ and $\log \frac{\gamma A}{\gamma HA}$. The estimated values of the thermodynamic dissociation constants and their standard deviations were therefore

$$K_1 = (2.4 \pm 0.3) \times 10^{-4}$$
$$K_2 = (2.5 \pm 0.4) \times 10^{-5}$$

thus giving

$$\frac{K_1}{K_2} = 9.5 \pm 2.0$$

Values of the first dissociation constant of isophthalic acid have been found to be 3.2×10^{-4} ($\mu = 2.5 \times 10^{-4}$) by Salm[12] using an auxilliary dye indicator and 2.87×10^{-4} (at low μ) by Ostwald[13] using conductance measurements. Their values probably would have approximated K_1 except that since the second ionization was ignored, they were probably too high. Chandler used Ostwald's value for k_1 and partition studies between water and diethyl ether to obtain $\frac{k_1}{k_2} = 10.8$ at $\mu = 0.001$ to 0.002.[14] One of the

(11) S. Glasstone, "Introduction to Electrochemistry," 1st ed., D. Van Nostrand Company, Inc., New York, N. Y., 1942, Ch. 5.

(12) E. Salm, *Z. physik. Chem.*, **63**, 105 (1908).

(13) W. Ostwald, *ibid.*, **3**, 376 (1889).

(14) E. E. Chandler, *J. Am. Chem. Soc.*, **30**, 694 (1908).

sources of error must have been the solubility of ether in the aqueous phase which amounted to 7.8% by volume. Maxwell and Partington determined k_1 and k_2 by means of electrometric titration. They obtained the following values: $k_1 = 2.0 \times 10^{-4}$ and $k_2 = 2.0 \times 10^{-5}$ at $\mu = 10^{-3}$ [15]; $k_1 = 3.5 \times 10^{-4}$ and $k_2 = 3.5 \times 10^{-5}$ at $\mu = 0.03$.[16] A source of error, particularly at $\mu = 10^{-3}$, was the effect of inconstant μ. If the same precision is assigned to the values of other investigators as is given to those of the present paper, the present values appear to agree with previous values within experimental error.

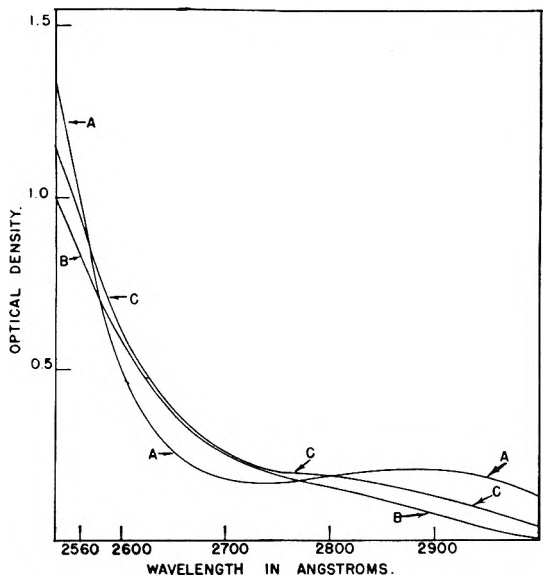

Fig. 5.—Absorption curves for 2.3×10^{-5} formal terephthalic acid in a 50.00-mm. cuvette: A, *p*H 1.60; B, *p*H 7.79; C, *p*H 4.06.

slight solubility in aqueous solution. Absorption curves (Fig. 5) indicated that the best wave lengths to use were from 2575 to 2625 Å. Measurements were made at six wave lengths in this range. The best single wave length appeared to be 2590.0 Å. and the data at the other five wave lengths (Fig. 6) were combined in a composite optical density by means of equation 17. Since the upper curves of Fig. 6 showed good values for the region between D_m and D_3 and the lower curves for the region D_1 to D_m a composite of all five curves was calculated. The weighting factors g of equation 17 were each taken as +1 in order to have favorable values for both $(C_m - C_1)$ and $(C_m - C_3)$.

The data have been summarized in Table II. The band

TABLE II

VALUES OF D AT 2590.0 Å. AND C FOR TEREPHTHALIC ACID

*p*H	D at 2590.0 Å.	C	Buffer
1.585	$2 \times 0.312 =$ 0.624	$2 \times 1.512 =$ 3.024	($HClO_4$)
1.62	0.622	3.025	($HClO_4$)
2.675	.642	3.108	Phosphate
3.025	.666	3.236	Formate
3.03	.662	3.2125	Formate
3.11	.675	3.271	Formate
3.38	.6915	3.341	Formate
3.58	.701	3.3995	Formate
3.76	.7105	3.4365	Formate
3.975	.712	3.453	Formate
4.19	.709	3.428	Formate
4.35	.700	3.384	Formate
4.54	.686	3.3235	Formate
4.73	.672	3.258	Formate
4.92	.659	3.2055	Formate
7.92	.637	3.094	Phosphate
7.92	.639	3.097	Phosphate

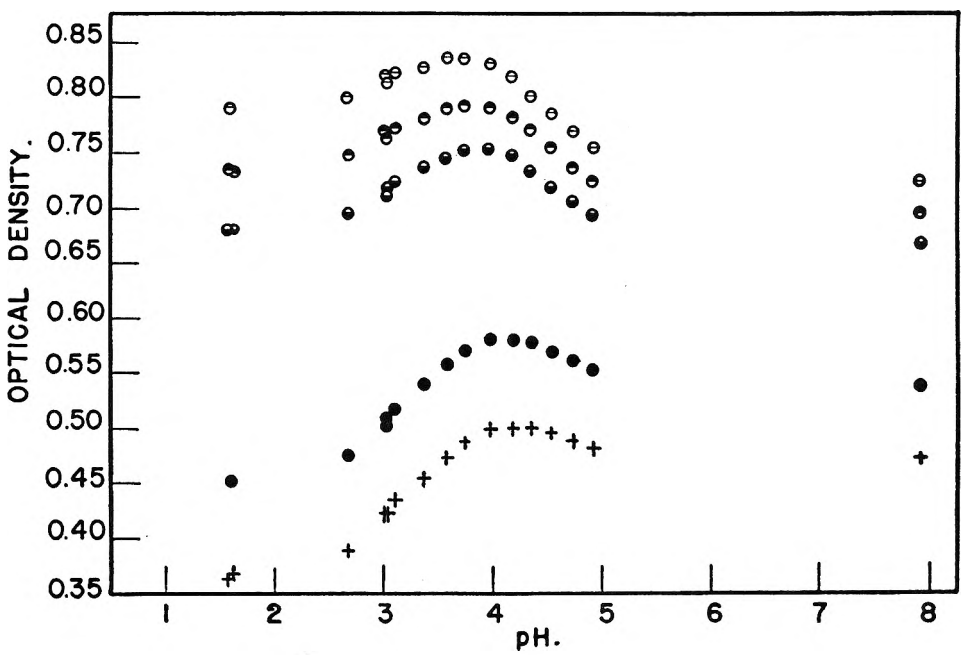

Fig. 6.—Terephthalic acid: ⊖, at 2575.0 A.; ⊖, at 2580.0 A.; ⊖, at 2585.0 A.; ●, at 2610.0Å.; + at 2625.0 Å.

Terephthalic Acid.—Terephthalic acid was studied at a concentration of 2.3×10^{-5} molar made necessary by its width was 30 A., the temperature 25 ± 1° and the ionic strength 0.0300. The solution at the lowest *p*H (1.585) was made up at half the usual strength of terephthalic acid. Its values of D and C when multiplied by two agreed well with those of the usual full-strength solution at *p*H 1.62, indicating that terephthalic acid was completely in solution

(15) W. R. Maxwell and J. R. Partington, *Trans. Faraday Soc.*, **31**, 922 (1935).

(16) W. R. Maxwell and J. R. Partington, *ibid.*, **33**, 670 (1937).

at pH 1.62. Since its solublity would be the least at the lowest pH values, it could be considered to be in solution at the other pH's as well.

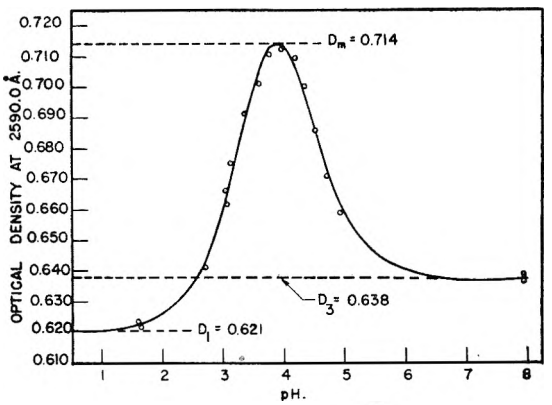

Fig. 7.—Terephthalic acid at 2590.0 Å.: circles, experimental points; solid curve, calculated as shown later.

The plot of the experimental data at 2590.0 Å. is shown in Fig. 7. Equations 10 and 14 were used with the previously described least-squares method and $D_1 = 0.621$, $D_m = 0.714$ and $D_3 = 0.638$ to give

$$pH_0 = 3.9028$$
$$k_1 = (3.43 \pm 1.04) \times 10^{-4}$$
$$k_2 = (5.59 \pm 1.70) \times 10^{-5}$$

The composite optical density data are plotted in Fig. 8.

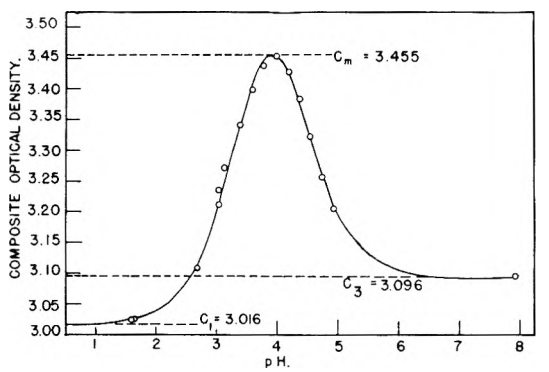

Fig. 8.—Use of composite optical density for terephthalic acid: circles, experimental points; solid curve, calculated as shown later.

Equations 18 and 19, the least-squares method, and $C_1 = 3.016$, $C_m = 3.455$ and $C_3 = 3.096$ gave the following values

$$pH_0 = 3.9038$$
$$k_1 = (3.46 \pm 0.87) \times 10^{-4}$$
$$k_2 = (5.51 \pm 1.38) \times 10^{-5}$$

The grand mean values obtained from D at 2590.0 Å. and C were

$$k_1 = (3.44 \pm 0.67) \times 10^{-4}$$
$$k_2 = (5.54 \pm 1.07) \times 10^{-5}$$

These values used with equations 15 and 16 and their C-analogs gave the solid curves shown in Figs. 7 and 8. The final values of k_1, k_2 and their estimated standard deviations were

$$k_1 = (3.4 \pm 1.0) \times 10^{-4}$$
$$k_2 = (5.5 \pm 1.6) \times 10^{-5}$$

where an additional 10% error was added in order to take into account uncertainties in the values of pH$_0$. The Hückel equation was used in the same manner as previously to give the values

$$\frac{\gamma HA}{\gamma H_2A} = 0.854 \pm 0.013$$
$$\frac{\gamma A}{\gamma HA} = 0.623 \pm 0.030$$
$$K_1 = (2.9 \pm 0.9) \times 10^{-4}$$
$$K_2 = (3.5 \pm 1.0) \times 10^{-5}$$

and

$$\frac{K_1}{K_2} = 8.5 \pm 3.5$$

The first dissociation constant of terephthalic acid has not previously been determined in aqueous solutions because of the very low solubilility of the undissociated form. Kuhn and Wasserman determined the second dissociation constant in aqueous solutions by potentiometric measurements.[17] Due to errors in measuring e.m.f.'s in the dilute solutions that were necessary, they did not claim much accuracy for the determination. They found k_2 to be approximately 3.5×10^{-5} at an ionic strength of 0.12 and a temperature of 16°. They calculated K_2 to be 1.5×10^{-5} at 16° but the expressions used for activity coefficients do not appear to be correct. For these reasons and others it is felt that the present value and that of Kuhn and Wasserman are in reasonable agreement, with the limits of error of the present value being somewhat less than theirs.

Chloranilic Acid.—The constants $k_1^* = \frac{[H^+][HA^-]}{[H_2A]}$ and $k_2^* = \frac{[H^+][A^{-2}]}{[HA^-]}$ for chloranilic acid were desired in connection with studies being conducted on the formation constants of zirconium chloranilate complexes.[18] These were being determined in terms of concentrations in perchloric acid–lithium perchlorate solutions of constant ionic strength in order to have constant activity coefficients. Consequently k_1^* and k_2^* were studied in perchloric acid–lithium perchlorate solutions of the same ionic strength, namely, 2.002 molar.

Chloranilic acid's absorption curves (Fig. 9) were quite favorable for the application of the method compared with those of isophthalic and terephthalic acids. The values of

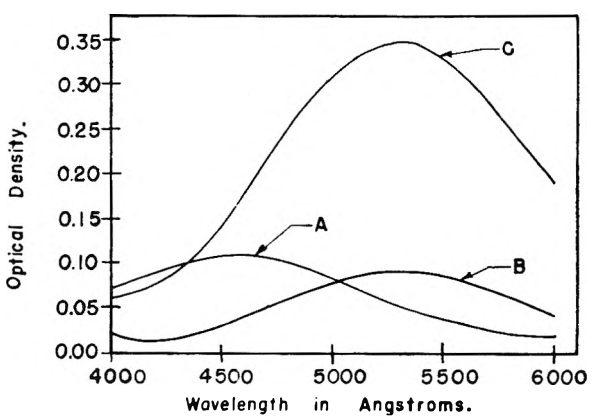

Fig. 9.—Absorption curves for 1.033×10^{-4} formal chloranilic acid in 50-mm. cuvettes: A, 2.00 M [H$^+$]; B, 5.0×10^{-11} M [H$^+$]; C, 2.00×10^{-2} M [H$^+$].

k_1^* and k_2^* were determined at 4960 Å. Control of the hydrogen ion concentration was obtained by including the appropriate amount of perchloric acid or lithium hydroxide in the preparation of the solutions. The data have been summarized in Table III. Equations 10 and 14 were used with the true hydrogen ion concentration in place of the quantity "a." A few successive approximations were required in correcting the hydrogen ion concentration for contributions from the chloranilic acid and in estimating the value of D_1 from the optical densities of the two most acidic solutions. The plot of optical density against $-\log$ (true [H$^+$]) is shown in Fig. 10. The values $D_1 = 0.075$, $D_m =$

(17) R. Kuhn and A. Wasserman, *Helv. Chim. Acta*, **11**, 44 (1928).

(18) B. J. Thamer and A. F. Voigt, *J. Am. Chem. Soc.*, **73**, 3197 (1951).

TABLE III

OPTICAL DENSITIES OF CHLORANILIC ACID

Concentration of Chloranilic Acid, 1.033×10^{-4}; T, 28°

Added [H⁺]	Added [OH⁻]	True [H⁺]	− log (true [H⁺])	D at 4960 Å.
2.002	....	2.002	− 0.3015	0.091
0.4004	....	0.4004	+ 0.3975	.126
.2002	....	.2002	.6985	.168
.08008	....	.08014	1.0962	.232
.04004	....	.04012	1.3966	.282
.01802	....	.01811	1.7421	.298
.01001	....	.01013	1.9944	.289
2.002×10^{-3}	....	2.169×10^{-3}	2.6637	.194
4.004×10^{-4}	....	5.928×10^{-4}	3.2271	.120
.....	0.0200	5.05×10^{-13}	12.297	.077

0.298 and $D_3 = 0.077$ were used with the points on the straight line portions on the side of the peak to calculate the value

$$-\log(\text{true } [H^+]_0) = 1.759$$

The points at optical densities of 0.282 and 0.289 were not used in calculating the average values of k_1^* and k_2^* because they were too close to the maximum optical density (0.298) to give accurate values. The values found for k_1^*, k_2^* and their standard deviations were

$$k_1^* = 0.082 \pm 0.004$$
$$k_2^* = 0.0038 \pm 0.0002$$

and

$$\frac{k_2^*}{k_1^*} = 21.6$$

The values of k_1^* and k_2^* were also calculated from the same data using the analog of equation 4 and a long series of successive approximations. The final values so obtained were

$$k_1^* = 0.084 \pm 0.004$$
$$k_2^* = 0.0038 \pm 0.0001$$
$$\frac{k_1^*}{k_2^*} = 22.1$$

$$Lc\epsilon_2 = 0.394,\ D_1 = 0.075 \text{ (and } D_3 = 0.077)$$

The latter values were used to calculate the solid curve shown in Fig. 10. The agreement of the latter values of k_1^* and k_2^* with the values calculated from equations 10 and 14 provided a check on the validity of the method employing these two equations.

Schwarzenbach and Suter[19] determined k_1 and k_2 of chloranilic acid by studying its reduction potential as a function of pH and also by spectrophotometric measurements. The values that they found were $k_1 = 0.14$ and $k_2 = 0.00066$. They did not specify the ionic strength but it was presumably less than two. In a resonating system such as chloranilic acid, it is difficult to predict the effect of large changes in ionic strength. Judgment on the disagreement between the results of Schwarzenbach and the present results is withheld until something more is known about this effect.

Discussion

If the acidic groups of an uncharged dibasic acid are equivalent and do not interact by means of resonance or hydrogen bonding, the following equation by Bjerrum[20] relates K_1/K_2 to the distance r (Å.) between the groups

$$\log \frac{K_1}{K_2} = \log 4 + \frac{3.08}{r}$$

The equation is based on electrostatic effects. Knowing r, an approximate value for K_1/K_2 can be calculated and, conversely knowing K_1/K_2, r can be estimated. For example, values calculated for r in isophthalic (I) and terephthalic acid (II) are thus (8.2 ± 2.0 Å.) and (9.4 ± 5.1 Å.) which are reasonably close to accepted values. Resonance interaction between the acidic groups in these examples do not appear greatly to affect the values of K_1/K_2.

(19) G. Schwarzenbach and H. Suter, *Helv. Chim. Acta*, **24**, 617 (1941).

(20) N. Bjerrum, *Z. physik. Chem.*, **106**, 219 (1923).

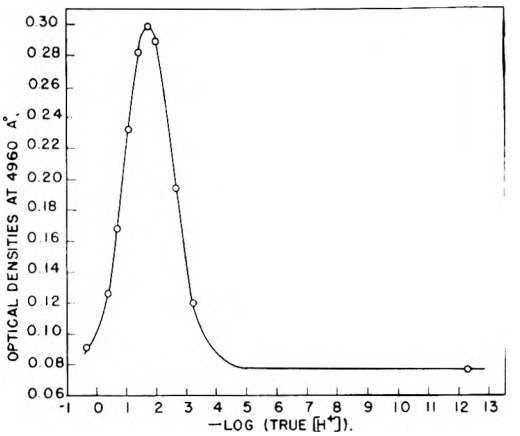

Fig. 10.—Optical densities of chloranilic acid at various acidities: circles, experimental points.

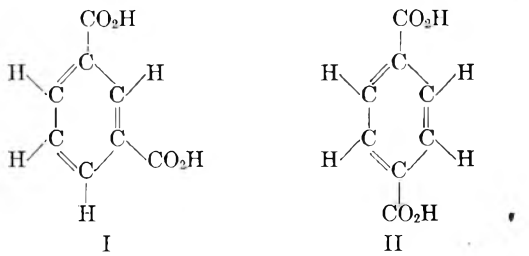

However, K_1/K_2 for chloranilic acid may be influenced by the relative resonance stabilization of the undissociated form (III), the singly dissociated form (IV) and the doubly dissociated form (V).

Since K_1/K_2, the ratio of the thermodynamic constants, would be larger than $k_1^*/k_2^* = 22$ observed at the ionic strength of 2, the value calculated for r would be less than 4.2 Å. Hence, if the application of the Bjerrum formula is valid in this case, the calculated value of r is definitely less than the true distance between the two para hydroxy groups (~ 6 Å.). It appears that the resonance effect preferentially stabilizes the intermediate species. This must be due partly to the fact that the right-hand resonance form of (IV) effectively reduces r and allows strong hydrogen bonding to the negatively charged oxygen atom.

The spectrophotometric method described in this paper is capable of yielding the most accurate results when the curve of optical density, or composite optical density, *versus* pH shows a maximum or minimum for which $|D_m - D_1|$ and $|D_m - D_3|$, or $|C_m - C_1|$ and $|C_m - C_3|$, have large

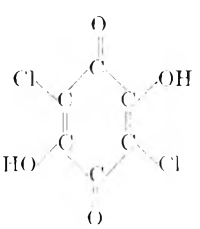

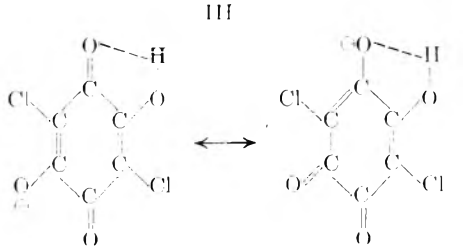

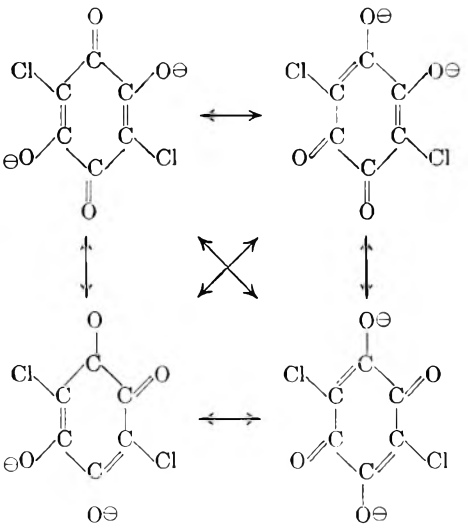

V

values. Errors in points close to D_1, D_m and D_3 give rise to inordinately large errors if they are used in calculating values for k_1 instead of only being used to estimate the values of D_1, D_m, D_3 and $p\mathrm{H}_0$. It seems advisable to use points near D_m only for estimating the values of D_m and $p\mathrm{H}_0$. With favorable absorption curves the accuracy of the determination of k_1 and k_2 should be limited only by the accuracy of the pH measurements.

There are many compounds having small values for k_1/k_2. Examples are crystal violet ($k_1/k_2 = 4$),[21] phenolphthalein ($k_1/k_2 = 4$)[22], p-dihydroxyglutacondianil ($k_1/k_2 = 0.316$),[23] 5-pyridinium-glutacondialdehyde-perchlorate ($k_1/k_2 < 1$)[24] and certain amino acids such as tyrosine[25] and l-dihydroxyphenylalanine.[26]

Any one of several other measurable properties such as optical rotation, intensity of fluorescence or magnetic susceptibility might be used in equations 10 and 14 in an analogous manner provided that the requisite maximum or minimum was obtained in the plot of the property *versus* pH. It is similarly possible to combine the same or different properties in a composite according to an analog of equation 17. Different properties would arbitrarily be brought to the same unit by choosing appropriate units for the weighting factors g_1, g_2, etc. The composite could be used in equations 18 and 19 provided that a maximum or minimum was obtained in the plot of the composite *versus* pH.

(21) E. Q. Adams and L. Rosenstein, *J. Am. Chem. Soc.*, **36**, 1452 (1914).

(22) L. Rosenstein, *ibid.*, **34**, 1117 (1912).

(23) G. Schwarzenbach and R. Sulzberger, *Helv. Chim. Acta*, **26**, 453 (1943).

(24) G. Schwarzenbach, *ibid.*, **26**, 418 (1943).

(25) G. Florence and G. Schapira, *Bull. Soc. Chim. biol.*, **27**, 293 (1945).

(26) G. Florence and G. Schapira, *ibid.*, **28**, 657 (1946).

Appendix I. Vlès and Gex's Method

Vlès and Gex[3] represented the ionization of a dibasic acid in the following manner

$$\begin{array}{ccc} \mathrm{H_2A} & \rightleftharpoons & \mathrm{H^+} + \mathrm{HA^-} \\ 1 - \alpha_1 & & \alpha_1(1 - \alpha_2) \\ \mathrm{HA^-} & \rightleftharpoons & \mathrm{H^+} + \mathrm{A^{-2}} \\ \alpha_1(1 - \alpha_2) & & \alpha_1\alpha_2 \end{array}$$

Their first equation involving pk_1, namely

$$p\mathrm{H} = pk_1 + \log \frac{\alpha_1}{1 - \alpha_1}$$

should have been

$$p\mathrm{H} = pk_1 + \log \frac{\alpha_1(1 - \alpha_2)}{1 - \alpha_1}$$

Consequently their equations for ϕ, k_1 and k_2 were incorrect and unnecessarily complicated.

From equation 4 their ϕ function should have been

$$\phi = \frac{D'}{D} = \frac{\epsilon_1' + \frac{k_1}{a}\epsilon_2' + \frac{k_1k_2}{a^2}\epsilon_3'}{\epsilon_1 + \frac{k_1}{a}\epsilon_2 + \frac{k_1k_2}{a^2}\epsilon_3}$$

Putting the latter equation in the form

$$\phi = \frac{\epsilon_1' 10^{pk_1 - p\mathrm{H}} + \epsilon_2' + \epsilon_3' 10^{p\mathrm{H} - pk_2}}{\epsilon_1 10^{pk_1 - p\mathrm{H}} + \epsilon_2 + \epsilon_3 10^{p\mathrm{H} - pk_2}}$$

and rearranging terms, one obtains

$$10^{pk_1}(\epsilon_1' - \phi\epsilon_1)10^{-p\mathrm{H}} + 10^{-pk_2}(\epsilon_3' - \phi\epsilon_3)10^{p\mathrm{H}} = \phi\epsilon_2 - \epsilon_2'$$

The latter equation is valid at any measured value of ϕ. Hence at values ϕ_1 and ϕ_2 corresponding to $p\mathrm{H}_1$ and $p\mathrm{H}_2$, one has the equations

$$10^{pk_1}(\epsilon_1' - \phi_1\epsilon_1)10^{-p\mathrm{H}_1} + 10^{-pk_2}(\epsilon_3' - \phi_1\epsilon_3)10^{p\mathrm{H}_1} = \phi_1\epsilon_2 - \epsilon_2'$$

$$10^{pk_1}(\epsilon_1' - \phi_2\epsilon_1)10^{-p\mathrm{H}_2} + 10^{-pk_2}(\epsilon_3' - \phi_2\epsilon_3)10^{p\mathrm{H}_2} = \phi_2\epsilon_2 - \epsilon_2'$$

On solving the latter pair of equations for $10^{pk_1} = 1/k_1$ and $10^{-pk_2} = k_2$, one obtains

$$k_1 = \frac{(\epsilon_2' - \phi_1\epsilon_1)(\epsilon_3' - \phi_2\epsilon_3)10^{-p\mathrm{H}_1 + p\mathrm{H}_2} - (\epsilon_1' - \phi_2\epsilon_1)(\epsilon_3' - \phi_1\epsilon_3)10^{-p\mathrm{H}_2 + p\mathrm{H}_1}}{(\phi_1\epsilon_2 - \epsilon_2')(\epsilon_3' - \phi_2\epsilon_3)10^{p\mathrm{H}_2} - (\phi_2\epsilon_2 - \epsilon_2')(\epsilon_3' - \phi_1\epsilon_3)10^{p\mathrm{H}_1}}$$

$$k_2 = \frac{(\epsilon_1' - \phi_1\epsilon_1)(\phi_2\epsilon_2 - \epsilon_2')10^{-p\mathrm{H}_1} - (\epsilon_1' - \phi_2\epsilon_1)(\phi_1\epsilon_2 - \epsilon_2')10^{-p\mathrm{H}_2}}{(\epsilon_1' - \phi_1\epsilon_1)(\epsilon_3' - \phi_2\epsilon_3)10^{-p\mathrm{H}_1 + p\mathrm{H}_2} - (\epsilon_1' - \phi_2\epsilon_1)(\epsilon_3' - \phi_1\epsilon_3)10^{-p\mathrm{H}_2 + p\mathrm{H}_1}}$$

The latter pair of equations can be used to calculate k_1 and k_2 provided that the extinction coefficients are obtainable. As previously implied, successive approximations would be necessary if k_1/k_2 were small and the extinction coefficients ϵ_2 and ϵ_2' could not be estimated accurately.

THE PREPARATION AND PURIFICATION OF OF_2 AND DETERMINATION OF ITS VAPOR PRESSURE

BY J. G. SCHNIZLEIN, J. L. SHEARD, R. C. TOOLE AND T. D. O'BRIEN

School of Chemistry, University of Minnesota, Minneapolis, Minnesota

Received January 19, 1951

OF_2 was prepared and purified. Iodometric and infrared analyses showed substantially 100% purity. The vapor pressure of OF_2 was measured from −195 to −145° and its boiling point shown to be −145.3°

The preparation and purification of oxygen fluoride was undertaken to obtain the pure compound whose physical properties could be determined. The method of purification used by early workers[1,2] was repeated as a preliminary step, but further purification followed.

Experimental

Fluorine was generated in a Harshaw low temperature cell[3] at a rate of 2–6 liters of gas per hour. This gas was passed through a 3% solution of NaOH which had been previously cooled in an ice-bath. The basic solution was continuously changed in the reaction vessel at the rate of 1–2 liters/hour (Fig. 1). The gaseous products were passed through a series of bubblers and traps and the partially enriched OF_2 was finally collected in a transfer ampoule (K in Fig. 2). These ampoules were then inserted into the vacuum line at C (Fig. 3) for transfer to the storage bulbs 1–6.

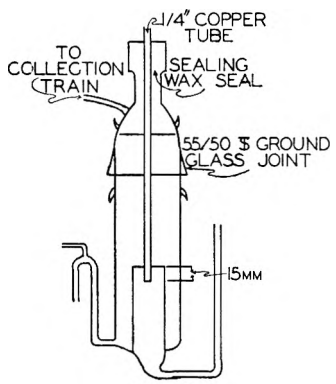

Fig. 1.

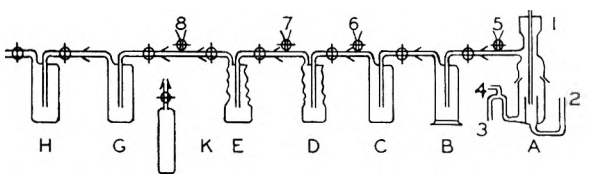

Fig. 2.—A, Sodium hydroxide solution bubbler (see Fig. 1); 1, fluorine inlet (copper tube); 2, sodium hydroxide solution inlet; 3, sodium hydroxide solution outlet; 4, siphon interrupter; 5, analysis outlet; B, water wash bubbler; C, carbon dioxide-acetone trap (−78°); 6, analysis outlet; D, column trap (approx. −130°), 7, analysis outlet; E, column trap (approx. −160°); 8, outlet for collection in ampoule K; G, liquid nitrogen trap (−196°); H, liquid nitrogen trap (−196°); K, transfer ampoule.

Preliminary purification was carried out by cooling the storage bulbs in liquid nitrogen and then aspirating with a water-pump. Iodometric analysis of the residual gas showed 96% purity.

Final purification was achieved by distilling through a 3-ft. glass column tightly packed with 1/8-in. single turn glass helices, and surrounded by a strip silvered evacuated jacket. The temperature of the distillation vessel was controlled by surrounding it with an asbestos jacket containing a nichrome heating element of 10 ohms resistance. This system was then surrounded by a large glass test-tube and the whole assembly then immersed in liquid nitrogen in a dewar flask. The top of the column was surrounded by a hollow copper head which was automatically cooled by liquid nitrogen.

In practice the still was allowed to come to equilibrium and the OF_2 was distilled until the temperature became constant at −144°. Approximately 1/4 of the remaining liquid was distilled at −144° and discarded. About 1/2 of the remaining liquid was distilled and collected. Finally, most of the remaining liquid was distilled at −144° and collected, and the residue discarded. Two iodometric analysis of the "middle cut" showed 99.60% and 100.02% purity, respectively.

The infrared spectrum (Fig. 4) of this sample showed less than 0.1% SiF_4 (probably from the reaction of OF_2 with glass) and 0.002% CF_4 as the only impurities.

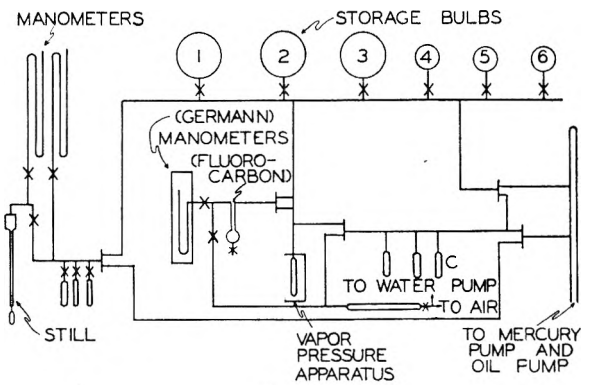

Fig. 3.

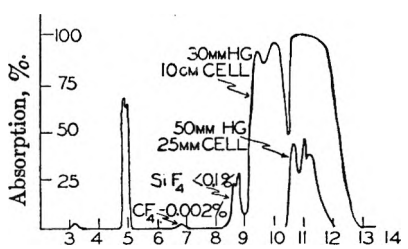

Fig. 4.

Vapor Pressure Apparatus.—The purified sample was condensed in an ampoule (Fig. 5) with a centered thermocouple well and a magnetic stirrer. A nichrome wire heater around the ampoule immersed in liquid nitrogen controlled the temperature to ±0.2°. Temperatures were measured with a 5-junction copper–constantan thermocouple and a Leeds and Northrup potentiometer with a supplementary galvanometer.

Pressures on the manometer were observed with a cathetometer, and were held constant 5–12 minutes for each point recorded in Table I. Purity of the sample was checked several times during the vapor pressure measurements by

(1) Lebeau and Damiens, *Compt. rend.*, **185**, 652 (1927); *ibid.*, **188**, 1253 (1929).

(2) Ruff and Menzel, *Z. anorg. chem.*, **190**, 257 (1930); *ibid.*, **198**, 39 (1931).

(3) Pinston, *Ind. Eng. Chem.*, **39**, 255 (1947).

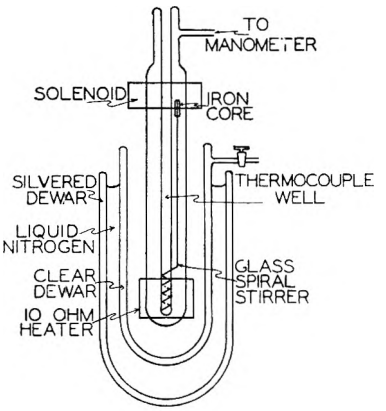

Fig. 5.

distilling off portions of the liquid and redetermining the vapor pressure at various temperatures. In no case was there any change.

Results

Vapor pressure data for pure OF_2 are listed (Table I) and shown graphically (Fig. 6). Plotting the logarithm of the vapor pressure against the reciprocal of the absolute temperature (Fig. 7) indicates a linear relationship for pressures greater than 15 mm. Calculation of the constants by the method of least squares gives the relation

$$\log P_{mm.} = 7.2242 - \frac{555.42}{T, °A.}$$

This equation gives −145.3° as the boiling point of OF_2.

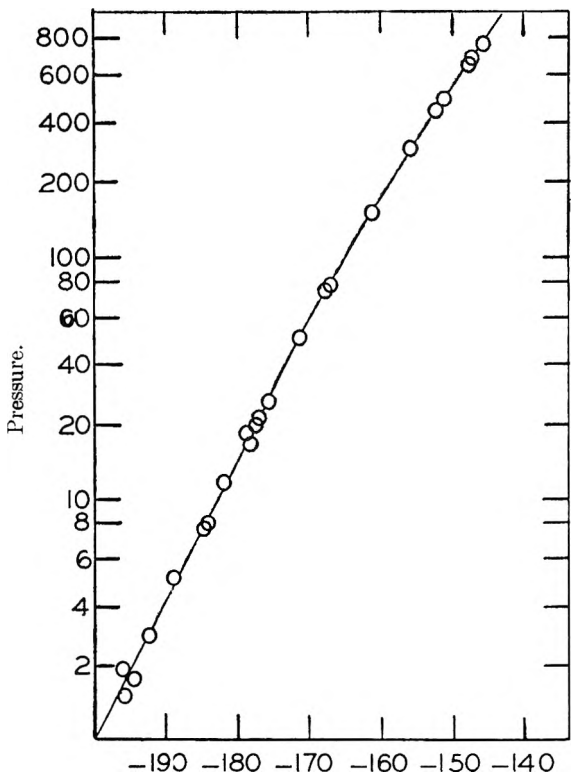

Fig. 6.

TABLE I

VAPOR PRESSURES OF OF_2

Temp., °C.	Pressure, mm. Corr. obsd.	Calcd.	Deviations, % (Exptl.-Calcd.	Temp., °C.	Pressure, mm. Corr. obsd.	Calcd.	Deviations, % (Exptl.-calcd.)
−195.4	1.4			−169.6	72.2	72.1	+0.14
−195.3	2.1			−169.6	73.0	72.1	+1.25
−193.9	1.7			−169.5	73.5	73.0	+0.68
−192.1	2.9			−169.5	73.9	73.0	+1.37
−190.1	4.7			−169.5	75.0	73.0	+2.74
−185.7	7.6			−163.2	140.2	148.0	−4.59
−185.6	8.0			−163.2	142.8	148.0	−3.51
−185.5	8.1			−157.3	273.0	267.8	+1.94
−184.0	11.6			−157.0	279.1	275.6	+1.27
−181.7	14.3			−152.0	422.7	434.3	−2.68
−181.3	15.4	14.9	+3.35	−152.0	424.4	434.3	−2.28
−180.9	16.3	15.9	+2.52	−151.4	471.9	457.5	+3.15
−179.9	18.3	18.4	−0.54	−151.4	472.9	457.5	+3.37
−179.8	18.5	18.7	−1.07	−151.2	471.3	465.5	+1.25
−179.3	19.4	20.1	−3.48	−148.4	577.0	591.5	−2.46
−179.1	20.6	20.7	−0.48	−147.9	618.8	615.2	+0.59
−178.1	24.1	23.9	+0.84	−146.0	735.0	715.0	+2.80
−172.7	47.3	49.2	−3.87	−145.3	740.0	755.5	−2.05

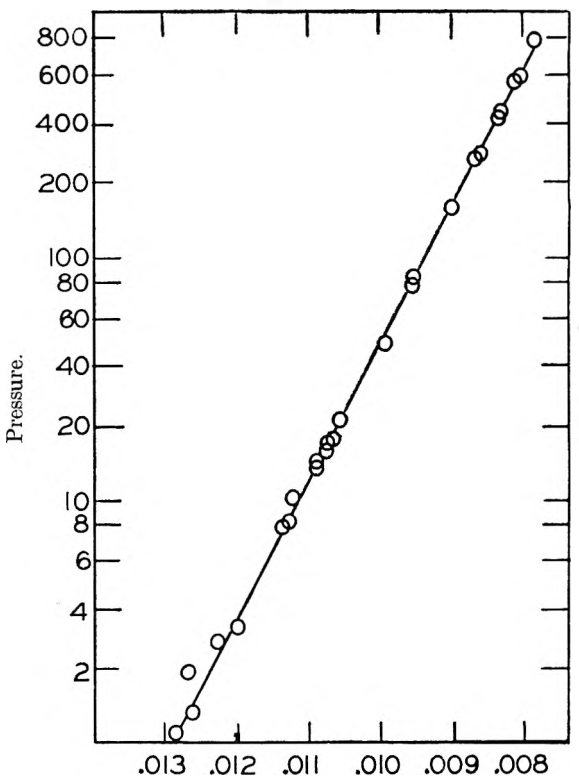

Fig. 7.

DIFFUSION COEFFICIENTS AND SOME RELATED PROPERTIES OF THE BUTYL ALCOHOLS IN AQUEOUS SOLUTIONS

BY H. NEAL DUNNING[1] AND E. ROGER WASHBURN

Avery Laboratory, University of Nebraska, Lincoln, Nebraska

Received January 24, 1951

Values of densities and equilibrium surface tensions for solutions of the butyl alcohols in water, have been determined at intervals of concentration throughout the solubility ranges of these alcohols. The viscosities of various aqueous solutions of these alcohols have been determined. An attempt has been made to correlate the data from these studies and to show that the variations of these physical properties are in mutual agreement. The validity of a new experimental method for the determination of diffusion coefficients has been tested. Experimentally determined values of the diffusion coefficients of the butyl alcohols are in close agreement with calculated values and of the same order as values recorded in the literature.

A new method for the determination of diffusion coefficients in solution has been described recently.[2] Data used in the calculations were based on studies of *n*-butyl alcohol in aqueous solutions. In an extension of this study the diffusion coefficients, and some other physical properties, of the other butyl alcohols have been determined.

In this method for the determination of diffusion coefficients the solute particles diffuse through a column of liquid contained in the calibrated capillary of a manometric capillarimeter. As shown in the preceding article, an approximate expression for the diffusion coefficient is

$$D = (m^2 \times dc/dt)/2(C_0 - C_h)$$

where

C_0 = concentration at end of capillary (g./cm.^{3})
C_h = concentration at the hypothetical plane (g./cm.^{3})
m = distance of the hypothetical plane from the end of the capillary in direction of diffusion (cm.)
D = diffusion coefficient.

It was shown that the value of the diffusion coefficient calculated from this expression was the same as that calculated with the series solution of an analogous problem in heat flow as derived by Ingersoll and Zobel.[3]

Certain other properties of these solutions were also determined.

Instruments.—For all measurements the temperature was controlled by immersion of the apparatus in a water-bath having opposing plate-glass windows. When the mechanical stirrer was in operation the temperature was maintained at 25.00 ± 0.01°. All temperatures reported in this paper are based on comparisons with thermometers calibrated by the United States Bureau of Standards.

The values of equilibrium surface tension were determined with a closed capillarimeter constructed by Transue.[4]

The diffusion studies were conducted with a modified form of the manometric capillarimeter described by DeWitt and Roper.[5] The instrument was modified as follows for the diffusion studies: (a) The capillary was calibrated throughout its length so that any desired length of capillary could be used and was incorporated into its container so that the capillary and container were replaceable at a ground glass joint to facilitate cleaning and to make it possible to have the entire pressure system submerged in the water-bath. (b) The pressure was controlled by raising and lowering a bob in a U-tube filled with water. The bob was powered by motor for gross adjustments and by hand crank for delicate control.

The radius of the capillary as determined by measuring the capillary rise of purified water was 0.02515 ± 0.00003 cm. The radius determined by the rise of purified benzene was 0.02517 ± 0.00003 cm. The radius of the capillary determined by the method of weighing mercury threads was 0.0251 ± 0.0002 cm.

For dilute aqueous solutions, using water in the manometer, keeping h_{cap} small, and using 0.0012 g./cm.^{3} as the density of vapor above the liquid phases, an expression for surface tension is

$$T = 12.28\,(h_{man} - h_{cap}) + 0.1$$

where

T = surface tension (dynes/cm.)
h_{man} = difference in levels of manometer arms (cm.)
h_{cap} = distance of large meniscus above capillary meniscus (cm.).

The use of this instrument in the determination of diffusion coefficients has been discussed in the preceding article.

Materials.—Eastman Kodak Co. best grade of butyl alcohols were purified by drying, fractional distillation, azeotropic distillation, and in the case of *t*-butyl alcohol by fractional crystallization. The physical constants of these alcohols appear in Table I.

TABLE I

SOME PHYSICAL PROPERTIES OF THE PURIFIED BUTYL ALCOHOLS

Alcohol	Density$^{25}_4$	Ref. index $n^{25}D$	Surf. tension (dynes/cm.)	Freezing point, °C.
n-Butyl	0.8058	1.3974	23.7	
i-Butyl	.7982	1.3939	22.4	
s-Butyl	.8024	1.3950	23.0	
t-Butyl	.7806	1.3851	20.1	25.53

Experimental and Results

The densities of various dilute aqueous solutions of the four butyl alcohols were determined.

It was observed that the density–concentration curves were nearly linear in dilute solutions and showed positive deviations from the corresponding curves calculated on the basis of additivity of densities in weight per cent. solutions. These positive deviations indicate a small volume decrease when a given alcohol is mixed with water.

Equilibrium values of surface tensions of aqueous solutions of the butyl alcohols, at intervals of concentration throughout the solubility ranges of these alcohols, were measured with the closed capillarimeter. The results of these measurements are recorded in Table III.

To ensure that values of surface tension determined with the manometric capillarimeter corresponded to values determined with the closed capillarimeter, the surface tensions of the solutions of *s*-

(1) E. I. du Pont de Nemours Fellow, 1948–1949; Standard Oil Co. Fellow, 1949–1950.

(2) Washburn and Dunning, *J. Am. Chem. Soc.*, **71**, 1311 (1951).

(3) Ingersoll and Zobel, "Heat Conduction," McGraw-Hill Book Co., Inc., New York, N. Y., 1948, p. 127.

(4) Transue, Washburn and Kahler, *J. Am. Chem. Soc.*, **64**, 274 (1942).

(5) DeWitt and Roper, *ibid.*, **54**, 445 (1932).

TABLE II

THE DENSITIES OF AQUEOUS SOLUTIONS OF BUTYL ALCOHOLS

Wt. % alcohol	d^{25}_4	Wt. % alcohol	d^{25}_4
(a) *n*-Butyl Alcohol		(b) *s*-Butyl Alcohol	
0.00	0.9971	0.00	0.9971
0.87	.9957	0.83	.9959
1.59	.9946	2.43	.9935
2.78	.9929	3.73	.9916
3.96	.9910	5.04	.9897
4.46	.9903	6.39	.9879
5.29	.9891	7.65	.9862
6.22	.9878	8.42	.9852
6.99	.9867	10.26	.9828
7.32	.9862	10.72	.9822
(c) Isobutyl Alcohol		(d) *t*-Butyl Alcohol	
0.00	0.9971	0.00	0.9971
0.36	.9966	0.66	.9960
0.89	.9958	1.66	.9943
1.79	.9944	1.97	.9936
2.13	.9939	2.92	.9921
2.83	.9928	4.12	.9904
3.89	.9912	5.67	.9881
5.03	.9896	6.75	.9866
6.01	.9882	7.41	.9856
6.72	.9872	9.19	.9832
7.84	.9857	10.58	.9813

TABLE III

EQUILIBRIUM SURFACE TENSIONS OF AQUEOUS SOLUTIONS OF THE BUTYL ALCOHOLS (DYNES/CM.)

Wt. %	Surface tension	Wt. %	Surface tension
n-Butyl alcohol		*s*-Butyl alcohol	
0.00	72.1	0.00	72.1
.25	64.7	.25	65.6
.45	59.8	.50	61.1
.87	53.0	1.11	54.3
1.59	45.8	1.48	51.5
2.78	38.6	2.37	46.5
3.96	33.3	3.20	43.3
5.29	29.4	4.32	39.4
6.22	27.4	6.35	33.5
6.99	25.8	8.86	29.2
Isobutyl alcohol		*t*-Butyl alcohol	
0.00	72.1	0.00	72.1
.25	64.4	.25	65.7
.51	58.1	.55	60.4
1.00	51.0	1.66	51.6
1.95	43.6	3.00	45.9
2.55	40.1	4.12	42.8
3.54	35.8	6.48	37.8
4.22	33.8	9.72	33.0
5.03	31.1	15.65	27.3
6.10	28.7	23.22	24.3
8.10	25.2	35.44	23.1
		54.94	22.4
		65.53	22.0
		72.76	21.8
		78.62	21.5
		82.08	21.4
		85.82	21.2
		89.52	20.9
		94.60	20.5
		100.00	20.1

butyl alcohol listed above were measured with the manometric capillarimeter. In all cases the values of surface tension determined by the two methods corresponded within 0.1 dyne/cm.

With the manometric capillarimeter, using a length of capillary of 0.5 cm. or less, the equilibrium values of surface tension were established in less than ten seconds. Using the closed capillarimeter, a period of about 12 hours was required for the establishment of the equilibrium values of surface tension.

The alcohols have similar surface tension–concentration curves. A noteworthy difference in degree is that, in order of increasing effectiveness in reducing the surface tension of water, the alcohols may be arranged: tertiary < secondary < iso < normal. Thus, the most soluble alcohol is least effective in decreasing the surface tension of water. The surface activity of a butyl alcohol appears to be a reciprocal function of its solubility since in order of increasing solubility the alcohols may be arranged: normal < iso < secondary < tertiary.

As an example of the effect of increasing alcoholic concentration on the viscosity of aqueous solutions the viscosities of aqueous solutions of *n*-butyl alcohol, at intervals of concentration throughout the solubility range of this alcohol, were determined with an Ostwald-type viscometer. The results of these measurements appear in Table IV.

TABLE IV

THE VISCOSITIES OF AQUEOUS SOLUTIONS OF NORMAL BUTYL ALCOHOL

Weight % alcohol	Viscosity, poise
0.00	0.008937[6]
0.70	.00921
1.21	.00941
1.48	.00949
1.99	.00970
2.26	.00981
3.25	.01021
3.88	.01048
4.92	.01096
5.35	.01114
5.95	.01141
6.51	.01166
6.99	.01185

It was observed that the viscosity–concentration curve was nearly linear and that there was a positive deviation from the curve calculated on the basis of additivity of viscosities in weight per cent. solutions.

The viscosities of solutions of the four butyl alcohols at a concentration of 1.482 weight per cent. were determined. The values (in poise) observed were: normal 0.009494, iso 0.009517, secondary 0.009532 and tertiary 0.009639. Since the concentration of alcohol varies throughout the column in the diffusion experiments, there is some doubt as to the correct value of viscosity to use for a given solution. For this reason values of diffusion coefficients will be calculated both by using the viscosities listed above and by using the viscosity of water in the Stokes–Einstein equation. This will give the limits within which the values of diffusion coefficients, calculated by this equation, should fall.

TABLE V

DATA AND CALCULATIONS INVOLVED IN DETERMINATION OF THE DIFFUSION COEFFICIENTS OF ISO-, *s*-, AND *t*-BUTYL ALCOHOL

	Iso	Secondary	Tertiary
	(a) Experimental values		
Surface tension of water (dynes/cm.)	72.1	72.1	72.1
Slope of surf. tension–concn. curve, dc/dT (g./cm.^{2} dyne $\times 10^{-4}$)	3.21	3.89	3.85
Length of diffusion column, m (cm.)	0.50	0.50	0.50
Concn. of bulk soln., C_0 (g./cm.^{3})	0.01482	0.01482	0.01482
Surface tension after diffusion for reference time (dynes/cm.)	66.8 (at 60 min.)	67.7 (at 56 min.)	67.7 (at 56 min.)
Slope of surf. tension–time curve, dT'/dt (dynes/cm. sec. $\times 10^{-3}$)	2.63	2.05	1.98
	(b) Calculated values		
Concn. at hypothetical plane at ref. time, $C_h = \Delta T' \times dc/dT'$ (g./cm.^{3}) (at 60 min.)	0.00170	(at 56 min.) 0.00171	(at 56 min.) 0.00169
Average concn. throughout capillary (g./cm.^{3})	0.0082	0.0082	0.0082
$dc/dt = dc/dT' \cdot dT'/dt$ (g./cm.^{3} sec. $\times 10^{-7}$)	8.44	7.97	7.62
Diffusion Coefficient, $D = (m^2 \cdot dc/dt)/2(C_0 - C_h)$ (cm.^{2}/sec. $\times 10^{-5}$)	0.80	0.76	0.73

The data necessary for calculation of the diffusion coefficients of the butyl alcohols, both from an experimental method with our equation and from the classical Stokes–Einstein equation, has now been determined. The diffusion coefficients of iso-, *s*- and *t*-butyl alcohol were calculated using our equation. Pertinent data and calculations appear in Table V.

For purposes of comparison, the diffusion coefficients of the butyl alcohols were also calculated from the Stokes–Einstein equation

$$D = (kH)/(6\pi nr)$$

where

k = Boltzmann's constant, 1.380×10^{-16} (erg/deg.)
H = temperature, degrees absolute
n = viscosity (poise)
r = radius of particle (cm.)

Since this equation presupposes spherical particles, tertiary butyl alcohol should be best adapted to application of the equation with the other butyl alcohols as a close approximation. The equation also presupposes large particles so that the solvent appears as a continuous medium. However, the results may be of interest in a qualitative way. The value of "r" used in each case was obtained by averaging the values determined by many measurements of Hirschfelder models, Pauling's bond distances, molar volume assuming cubic packing, and molar volume assuming hexagonal packing. The values of the diffusion coefficients of the butyl alcohols calculated from this equation and from other sources are recorded in Table VI.

The positive deviations observed in the various physical properties from calculated values based on the additivity of these properties in weight per cent. solutions are indicative of an increase in complexity of the alcohol molecules when they are dissolved in water. The order of arrangement in increasing the viscosity of water, as well as in the arrangement in increasing diffusion coefficients in water, indicates that the particles of *t*-butyl alcohol in solution are the most complex and that the complexity of particles decreases until those of *n*-butyl alcohol, the least complex, are reached. Since this order of change in complexity is the same as the solubility of the alcohols, it might be postulated that the increase in complexity of molecules, evidenced by these various physical properties, is due to varying degrees of association with the solvent molecules, water.

TABLE VI

COMPARISON OF THE VALUES OF THE DIFFUSION COEFFICIENTS OF THE BUTYL ALCOHOLS, FROM SEVERAL SOURCES

A, Experimental values at average concentration 0.0082 g./cm.^{3} B, Calculated from the Stokes–Einstein equation using "n" = viscosity of solution of concentration 1.482 wt. %, and using the following values of "r" = av. radius: *n*-butyl 2.85×10^{-8}, isobutyl 2.87×10^{-8}, *s*-butyl, 2.87×10^{-8}, and *t*-butyl 2.92×10^{-8} (cm.). C, Calculated from the Stokes–Einstein equation using "n" = viscosity of water,[6] and above values of radii. D, Listed by Stearn, Irish and Eyring.[7] E, Calculated by Stearn, Irish and Eyring[7]. F, Other literature.[8]

Alcohol	Diffusion coefficient (cm.^{2}/sec.) $A \times 10^{-5}$	$B \times 10^{-5}$	$C \times 10^{-5}$	$D \times 10^{-5}$
n-Butyl[2]	0.81	0.81	0.86	0.88
Isobutyl	.80	.80	.85	
s-Butyl	.76	.80	.85	
t-Butyl	.73	.78	.84	
	$E^{\times 10-5}$	$F^{\times 10-5}$		
n-Butyl	.34	(.77 ± 0.05)		

(6) Bingham and Jackson, *Bull. Bur. Standards*, **14**, 75 (1918).
(7) Stearn, Irish and Eyring, THIS JOURNAL, **44**, 990 (1940).
(8) Thovert, *Ann. Phys.*, **2**, 369 (1914).

CATAPHORESIS STUDY IN HYDROCARBON OIL BY RADIOACTIVE AND MICROSCOPIC METHODS

BY ANDREW GEMANT

Research Department, The Detroit Edison Company, Detroit, Michigan

Received January 24, 1951

Cataphoresis of a few organic and inorganic suspensions in a hydrocarbon oil of medium viscosity was investigated. Beside the standard microscopic method a novel technique utilizing radioactive tracers (C-14) was developed and used. Labelling was effected by adsorption of the tracer substance from the oil phase. The two techniques, while basically in agreement, complement each other in a useful manner. The chief results among others are as follows: The charge of the particles is negative, occasionally both signs are simultaneously present. Acids tend to reverse the sign of negative particles. The cataphoretic mobility increases somewhat with the electric field. The order of magnitude of the ζ-potential is frequently between 150 and 200 millivolts. In general, a distinct deposit was formed on the electrodes. In oil of increased ionic conductivity the zeta-potential is markedly reduced, probably owing to compression of the double layer.

This paper describes the results of a study of cataphoresis of various organic and inorganic suspensions in hydrocarbon oil. The available quantitative information in this field, which might be of value in understanding ionic processes in insulating liquids, is rather limited; the study was undertaken in order to enlarge this knowledge.

Experimental Technique

Two independent experimental techniques were used. One was the direct, visual microscopic method and the other a novel technique utilizing a radioactive tracer. The results obtained from both methods are, as was expected, basically in agreement, yet in certain instances each supplies some information not obtainable by the other; thus, the two methods complement each other in a useful manner.

The microscopic method was the same that the author had described in an earlier study.[1] A flat glass cell is used, containing the suspension to be studied and two suitably formed wires as electrodes. The cell is observed under a microscope which is focused at the point of closest approach of the electrodes where the electric field is approximately parallel. The movement of the particles is directly observable, and their electrophoretic velocity is measured by means of a scale in the ocular lens. Frequent reversal of the electric field permits many single observations.

The radioactive method employs an assembly shown in diagram form in Fig. 1. The cell consists of a cylindrical body C, made of bakelite, to which a metal plate, M, is cemented. A glass dish, G, receives the overflow of the radioactive suspension, S, poured into the cell. The high-voltage lead, H, is connected to M which is one of the electrodes. The other electrode is F, an aluminum foil about 0.001-cm. thick, which is placed on top of the suspension, trapping of air bubbles being avoided. A metal ring, R, keeps the foil in position, a thin window Geiger–Mueller tube G–M being placed on top of this ring; GR is the grounded lead of a d.c. voltage generator. Figure 2 is a photograph of the assembly.

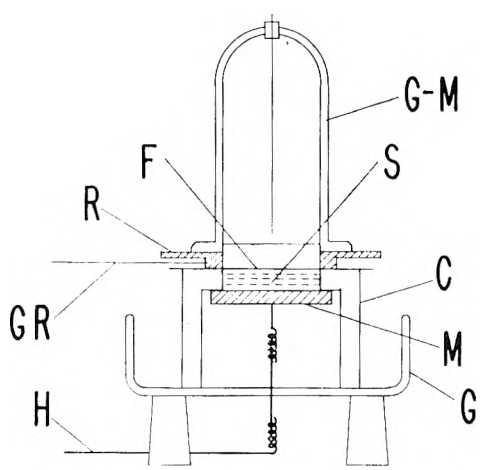

Fig. 1.—Diagram of cataphoresis cell using radioactive tracers.

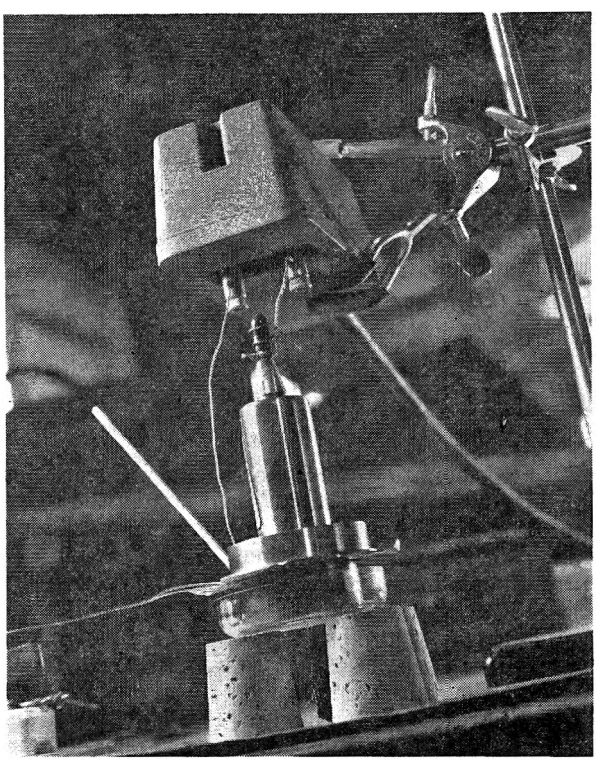

Fig. 2.—Photograph of tracer cataphoresis cell.

The particles of the suspensions used in this cell are labelled by a radioactive substance. The counts as registered initially by the G–M Counter are used as zero-value for the subsequent measurements. D.c. voltage is applied between M and F. If the polarity is such that cataphoresis takes place in an upward direction, reduced absorption causes an increase of counts with time. The counts *vs.* time are plotted, and from the curve the cataphoretic velocity computed as will be shown. The method is applicable only if a deposit of the suspension is formed on the top electrode; in certain instances the particles do not adhere to the electrode and no increase of counts is observed.

Reversal of the voltage causes the particles to migrate downward and the counts then decrease until the original zero-value is reached. There are suspensions in which both positive and negative particles are present; in such cases reversal of the voltage produces first a dip in the counts followed by an increase.

The hydrocarbon oil was a transformer type, having a viscosity of 0.14 poise at 25° and a dielectric constant of

(1) Andrew Gemant, THIS JOURNAL, **43**, 745 (1939).

2.18. Labelling of the suspension can be done in two ways. Either the tracer is introduced chemically into the solid material, or the tracer is dissolved in the liquid from which it passes onto the solid by adsorption. In this latter case the tracer technique yields not only the cataphoretic velocity, but also quantitative information on the adsorption of the solute upon the suspended particles. It is this latter technique that was used in the present study.

The following substances were used as suspensions: silver myristate, potassium tridecanoate, potassium acid tridecanoate, magnesium oxide, and graphite. Labelling was done by tridecanoic acid containing carbon-14 in the carboxyl group.[2]

Outline of Interpretation of Results.—Before presenting experimental results, it will be useful to review a few basic relations that were used in evaluating test data.

The electrophoretic potential ζ at the solid–liquid boundary responsible for cataphoresis is given by the Helmholtz equation.[3]

$$\zeta = \frac{4\pi\eta v}{\epsilon E} \qquad (1)$$

where η = viscosity of liquid, v = cataphoretic velocity, ϵ = dielectric constant of liquid, E = electric field intensity. Of these, η and ϵ are usually known; E is given as the ratio of applied voltage to electrode separation. The velocity v remains to be measured. It has been mentioned previously how this is done in the microscopic method. The measurement of v in the tracer technique is now explained by means of two typical counts *vs.* time curves shown in Fig. 3. The counts increase linearly, then a more or less sharp bend follows, and finally the counts seem to attain a constant value. This is what one would expect theoretically. The particles in the electric field are swept to one of the electrodes and when all particles are deposited, the counts reach their maximum value. The initial straight slope is extended until it crosses the horizontal branch of the curve. The abscissa of the crossing point marks the time needed for a particle to move at constant velocity across the entire gap. Since the latter is known (0.32 cm.), the velocity is known too, and the zeta-potential can be computed.

The mobility m is given by

$$m = v/E \qquad (2)$$

The two different methods yielded values of m that are in fair agreement. Absolute agreement cannot be expected since the field distribution differs considerably in the two cells. The field in the tracer cell is actually more free from disturbances than in the microscopic cell. Another reason will be mentioned in a later section.

The thickness δ in cm of the electric double layer at the boundary is for a hydrocarbon oil approximately[1]

$$\delta = 0.5 \times 10^{-8}/\sqrt{c} \qquad (3)$$

if c, the ion concentration, is measured in mole per liter. An increase of the ion concentration in the oil compresses the double layer so that its tail end in the liquid, representing the ζ-potential, is considerably reduced; this is the cause of the reduction of m with increasing concentration in aqueous suspensions.[4] Experimental evidence will be presented to indicate a similar effect in hydrocarbon oil.

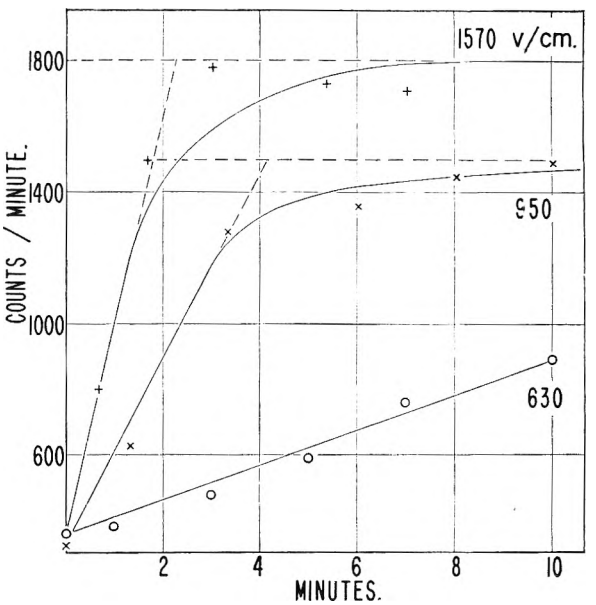

Fig. 3.—Counts/min. *vs.* time for labeled silver myristate in oil. KOH: 0.6 milliequivalent/g. Ag salt; tridecanoic acid, 0.01 *N*.

It was mentioned that the radioactive cataphoresis technique permits an estimate of the amount of adsorbate on the suspended particles. Let a designate the number of grams of radioactive substance per gram of suspended particles and σ the counts/min. for 1 g. of radioactive substance located directly below the top foil electrode. If D is the final value of the deposited amount and B is the final value of counts/min., then $B = \sigma a D$, or

$$a = B/(\sigma D) \qquad (4)$$

This equation may be used for evaluating the amount of adsorbate. The values derived for a are approximate for reasons explained in the following sections which present the experimental results.

Silver Myristate Suspensions.—The silver myristate was prepared by precipitation from alcoholic solutions and subsequent washing in a Gooch filter. Its suspension in hydrocarbon oil is not very stable but sufficient for measurements of cataphoresis. The particles are irregularly shaped and judging from the microscopic picture, have an average linear dimension of about 1.3×10^{-3} cm.

The results from both the microscopic and tracer technique are presented in Table I. The samples for the microscopic tests were prepared with nonradioactive tridecanoic acid; a few comparative observations with the radioactive acid showed that the cataphoretic velocity was unaffected by the presence of C-14. Each horizontal row of the table refers to a different solution in the oil phase, as specified. The first four solutions contained an increasing concentration of acid, and show a corresponding small decrease of mobility and ζ-potential. The values for the latter are somewhat higher

(2) Edward Hines and Andrew Gemant, *Science*, **110**, 19 (1949).

(3) Samuel Glasstone, "Textbook of Physical Chemistry," D. Van Nostrand Co., Inc., New York, N. Y., 1947, p. 1220.

(4) Herbert Freundlich, "Kapillarchemie," Akad. Verl. Ges. Leipzig, 1930.

than those encountered in aqueous systems. The particles are negative which is also the prevalent sign in aqueous suspensions and colloids.

TABLE I

SILVER MYRISTATE SUSPENSIONS IN HYDROCARBON OIL (MIGRATION NEGATIVE)

KOH, milliequivalent per g. Ag salt	Normality of Tridecanoic acid	Tributyl amine	o-Cresol	Mobility 10^{-4} cm./sec. per v./cm. ζ microscopic	tracer	mv.	Acid adsorbed, milliequivalent per g. Ag salt
0	0	0	0	3.9	..	280	..
0	0.01	0	0	2.9	..	210	..
0	.02	0	0	2.0	..	150	..
0	.07	0	0	2.0	..	150	..
0	0	.08	0	2.4	..	170	..
0	.07	.08	0	2.4	..	170	..
0	0	0	.15	1.8	..	130	..
0	.07	.08	.15	0.23	..	17	..
0.3	.01	0	0	1.9	1.1	110	0.2
0.6	.01	0	0	2.7	1.5	150	.6
1.2	.01	0	0	2.2	1.8	150	.8
0.6	.05	0	0	..	2.4	170	.35
0.6	.07	.08	.15	0.42	..	31	..

The next four lines refer to the combination acid–amine–phenol which, as the author found,[5] produce markedly high ionic conductivities in hydrocarbon oil. While neither an amine, nor a phenol in itself affects the cataphoresis of Ag myristate, the three in combination lower the mobility markedly, as may be seen. Although no final conclusion can be drawn from this observation, it appears to be the analog of similar observations made in aqueous colloidal solutions, and explainable on the basis that the electric double layer is compressed with increasing ion concentration.

The next solutions listed in Table I were prepared with radioactive tridecanoic acid. If such a suspension is introduced into the tracer cell (Fig. 2), no effect is observed. The counts remain the same, whatever voltage is applied across the cell. The reason is that the adsorption of the acid by the suspended particles is insignificant. In order to produce a measurable adsorption, a small amount of potassium hydroxide was added to the Ag myristate particles prior to their mixing with the oil by bathing them in a drop of alcoholic KOH solution until the alcohol evaporated. In this manner large effects in the tracer cell were obtained. The approximate amounts of milliequivalent KOH per gram silver salt are listed in Table I. The mobility figures deduced from the tracer experiments are somewhat lower, but of the same order of magnitude as the microscopically determined figures. The microscopic mobility figures show that the presence of KOH does not noticeably affect the cataphoretic process.

Figure 3 shows the results from the tracer experiments for one particular solution: counts per min. are plotted *vs.* time in minutes. The three curves refer to three different electric fields. Two anomalous features appear on the graph. One is that the slope of the lowest curve (630 v./cm.) is too small relative to the others. Another is that the final values of the two upper curves are not identical as might be expected. Both these anomalies are caused by the settling due to gravity of the suspended particles. The velocity due to gravity v_g can be calculated from the equation

$$v_g = \frac{0.22\, g(\rho - \rho_0)r^2}{\eta} \qquad (5)$$

(g = gravitational constant, ρ = density of particle, ρ_0 = density of oil, r = equivalent radius of particle.) With $\rho = 2.7$, $\rho_0 = 0.9$, $r = 0.65 \times 10^{-3}$ $\eta = 0.14$, one has $v_g = 1 \times 10^{-3}$ cm./sec. The velocities for the two upper curves calculated from the intersection of the dotted lines, as explained in the previous section, are, respectively, 2.4×10^{-3} and 1.3×10^{-3} cm./sec. It can be seen that the settling rate must have interfered rather seriously with the lowest curve, causing it to be too flat. Only the two upper curves were used, therefore, for evaluations. Even these two are, of course, influenced by the settling of particles which causes the 950 v./cm. curve, corresponding to a lower cataphoretic velocity, to reach a lower final value. The same effect is probably responsible for the fact that the values of m are altogether lower than those derived microscopically; in this latter technique gravity does not affect the data.

The last solution of the series in Table I contains the highly conducting combination acid–amine–phenol with KOH added to the suspensed particles. The microscopically measured mobility is again markedly reduced, by a factor of 1:5. The tracer test, accordingly, showed a small effect only: in the first 2 minutes the counts/min. rose by about 60, as compared with 500 with the preceding sample of low ion content.

The last vertical column gives the amounts of acid adsorbed, as estimated from Equation 4. The data are approximate, chiefly because the total amount D of Ag salt deposited at the electrode is not exactly known. The amount of Ag salt present in the cell was somewhat over 2 mg., and it may be estimated that half of this escaped deposition because of settling, hence $D = 10^{-3}$ g. The value of σ was known by calibration to be 10 counts/min. per μg. Hence $a = 10^{-4}\, B$. The figures derived in this manner divided by 214, the molecular weight of the acid, are listed in Table I. It can be seen that these figures increase with the amount of KOH added, as would be expected.

TABLE II

SILVER MYRISTATE SUSPENSIONS IN OIL

KOH, milliequivalent per g. Ag salt	Tridecanoic acid, normality	Field intensity, v./cm.	Mobility, 10^{-4} cm./sec. per v./cm.	Method used
0	0	390	3.4	Microscopic
0	0	580	3.9	Microscopic
0	.01	390	2.6	Microscopic
0	.01	580	2.9	Microscopic
0	.02	220	1.5	Microscopic
0	.02	410	2.0	Microscopic
.6	.01	940	1.4	Tracer
.6	.01	1570	1.6	Tracer
1.2	.01	940	2.1	Tracer
1.2	.01	1570	1.6	Tracer

The mobilities as listed in Table I show only little variation with field intensity. A few data il-

(5) Adalbert Farkas, "Physical Chemistry of Hydrocarbons," Vol. I, Academic Press, Inc., New York, N. Y., 1950, Chap. 6.

TABLE III

POTASSIUM TRIDECANOATE SUSPENSIONS

KOH, milliequivalent per g. K salt	Normality of Tridecanoic acid	Tributylamine	o-Cresol	Polarity of particles	Mobility 10^{-6} cm./sec. per v./cm. Microscopic	Tracer	ζ, mv.	Acid adsorbed, milliequivalent per g. K salt
0	0.01	0	0	Positive	2.7	1.4	200	0.04
.3	.01	0	0	Positive	3.2	2.0	190	.3
.6	.01	0	0	Positive	2.3	1.1	120	.25
1.2	.01	0	0	Pos. and neg.	..	..	..	..
0	.15	.17	.30	Positive	0.15	..	11	..

lustrating this behavior are given in Table II for both techniques used. As a rule, the mobility increases somewhat with increasing electric field.

Potassium Tridecanoate Suspensions.—Results obtained from these suspensions are summarized in Table III and shown for two particular instances in Figs. 4 and 5. The polarity of these suspensions is generally positive. The tracer test can be carried out even without the addition of KOH, although the amount of acid adsorbed (final value of net counts) is very little. The mobility as deduced from the two tests is of the same order of magnitude.

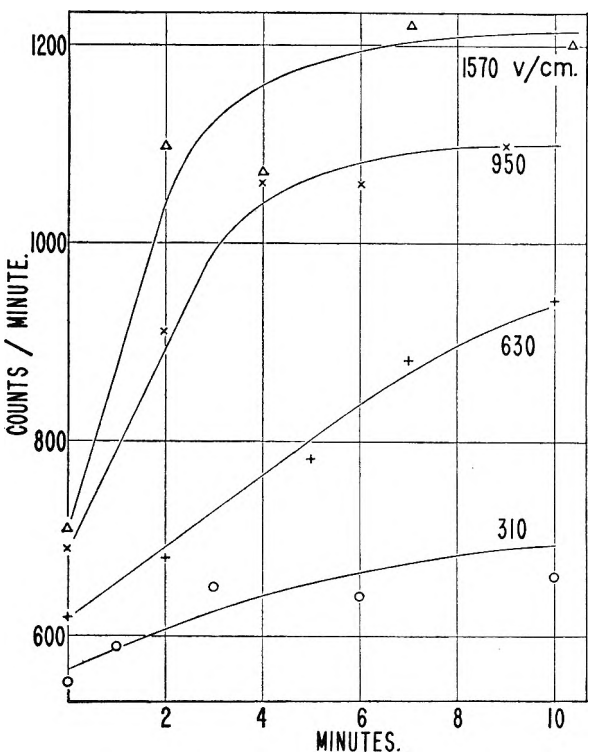

Fig. 4.—Counts/min. *vs.* time for labeled potassium tridecanoate in oil. KOH: 0.6 milliequivalent/g. K salt; acid, 0.01 *N*.

An interesting effect takes place when the added KOH exceeds a certain amount: under the microscope both positive and negative crystallites are observed and an accurate determination of the velocity is not possible. This is in agreement with the known reversal by OH ions of positive colloids in aqueous systems. If the suspension containing 1.2 mg. of KOH is studied by the tracer technique, a result shown in Fig. 5 is obtained. Negative voltages (the sign refers to the high-voltage electrode) produce marked rises in the counts, whereas reversed voltages cause first a sharp drop and then a slow rise. This behavior clearly indicates that both polarity particles are present with negative ones prevailing.

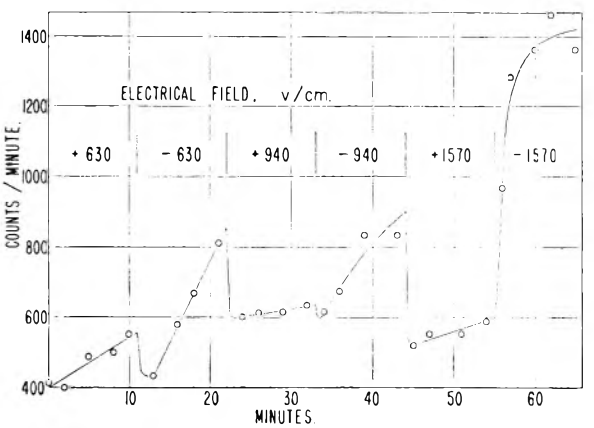

Fig. 5.—Counts/min. *vs.* time for potassium tridecanoate in oil. KOH: 1.2 milliequivalents/g. K salt; acid, 0.01 *N*.

The last solution in Table III was of the conducting type, acid–amine–phenol, and the cataphoretic velocity is again markedly reduced. This reduction is thus observed with both negative (Ag salt) and positive (K salt) systems; this is further proof that the effect is not a discharge process but a compression of the double-layer due to the high ion concentration, as explained.

Table IV presents results obtained from potassium acid tridecanoate suspensions. These particles, in contrast to the neutral salt, are negative. Apart from this difference the two compounds behave similarly, the tracer test showing a measurable effect without any added KOH. Figure 6 gives the tracer test results with 0.01 *N* tridecanoic acid. The conducting solution markedly reduces the ζ-potential, as in the previous suspensions. The tracer test with such solutions indicated no measurable increase of counts.

TABLE IV

POTASSIUM ACID TRIDECANOATE SUSPENSIONS
(MIGRATION NEGATIVE)

KOH, milliequivalent per g. K salt	Normality of Tridecanoic acid	Tributyl amine	o-Cresol	Mobility 10^{-6} cm./sec per v./cm. microscopic	tracer	ζ mv.	Acid adsorbed milliequivalent per g. K salt
0	0	0	0	2.0	..	150	..
0	.05	0	0	1.4	..	100	..
0	.01	0	0	..	2.3	170	0.05
0	.05	.06	.10	0.40	..	29	..
.6	.05	0	0	2.6	..	190	..
.6	.01	0	0	..	1.2	88	0.35

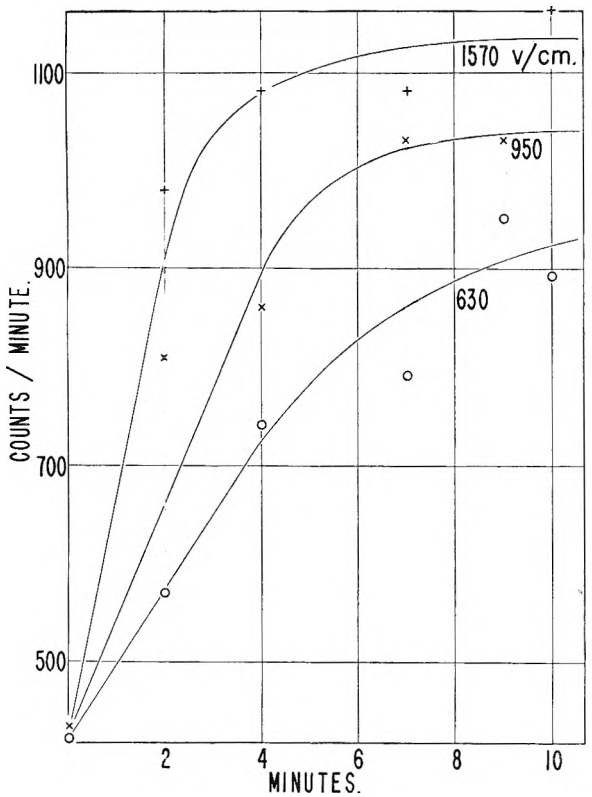

Fig. 6.—Counts/min. *vs.* time for potassium acid tridecanoate in oil. KOH: 0.6 milliequivalent/g. KH salt; tridecanoic acid, 0.01 *N*.

Magnesium Oxide Suspensions.—In contrast to the organic compounds discussed up to now, an inorganic substance, MgO, is dealt with in this section. The results are summarized in Table V. The migration is negative throughout. The suspension is remarkably stable and the settling rate low, probably because of the fluffy structure of the crystallites. Since the material is basic, the addition of KOH is unnecessary for labelling with the radioactive acid. Figure 7 shows the results of the tracer test with 0.05 *N* tridecanoic acid. In spite of the scattering of the counts, the sharp bend of the curve is conspicuous.

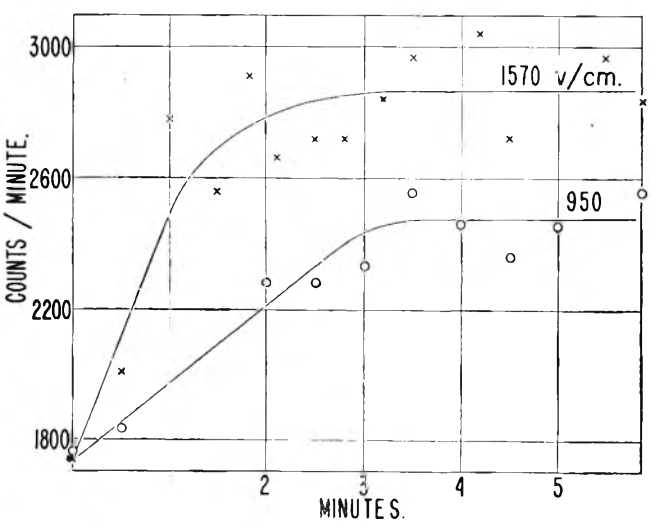

Fig. 7.—Counts/min. *vs.* time for labeled magnesium oxide; acid, 0.05 *N*.

TABLE V

MAGNESIUM OXIDE SUSPENSIONS (MIGRATION NEGATIVE)

Normality of Tridecanoic acid	Tributyl amine	*o*-Cresol	Mobility 10^{-6} cm./sec. per v./cm. Microscopic	Tracer	ζ, mv.	Acid adsorbed milli-equivalent per g. MgO
0	0	0	1.8	..	130	..
.01	0	0	1.9	2.0	140	0.5
.05	0	0	2.9	1.7	210	.55
.05	.04	.20	0.80	..	58	..
.15	.17	.30	.47	..	34	..

Using the conducting combination acid–amine–phenol, the reduction of the ζ-potential is again noticeable. In spite of this reduction, the tracer test should have shown an effect, even if reduced in magnitude. There was, however, no increase in counts observed. After disassembly of the cell, no deposit upon the foil was found, whereas in the solutions containing the acid alone a white deposit formed on the aluminum foil. This shows that the absence of an effect in this case was caused by a non-adherence of the magnesium oxide particles at the electrode.

The magnitude of the ζ-potential is very similar with such dissimilar substances as Ag myristate and MgO. This again is in keeping with observations in aqueous systems where the potential is often around 50 mv. independent of the nature of the solid phase. The reason of this is that the ζ-potential is determined by the structure of the double layer in the liquid phase, hence it is frequently independent of the chemical nature of the solid, except, of course, for its sign.

Graphite Suspensions.—Colloidal graphite contained in Oildag[6] was used after separation from the liquid phase by repeated washing with toluene and centrifuging. The average particle size of this graphite is about 1 micron. The polarity of these particles in hydrocarbon oil is negative, but the sign is easily reversed by acids. The migration of the particles under the microscope is somewhat turbulent. When the vicinity of the negative electrode has been cleared of particles, their motion stops altogether, probably because of distortion of the electric field. For this reason the tracer test cannot be used for quantitative evaluations.

Table VI gives the data of the microscopic observations. The cataphoretic mobilities are lower than with the other suspensions investigated. This is an instance in which the chemical nature of the solid markedly influences the potential. Acid in higher concentrations reverses the polarity, as may be seen. In the highly conducting solution the motion was regular, without signs of turbulence.

The results from tracer tests are shown in Fig. 8, taken at a field intensity of 950 v./cm. The lowest curve has no potassium hydroxide added, the other two in the amount indicated. While the total increase of the lowest curve is only about 40 counts/min., this figure reverts to a rather small amount of

(6) Acheson Colloids Corp., Port Huron, Michigan.

TABLE VI

GRAPHITE SUSPENSIONS (MICROSCOPIC OBSERVATIONS)

KOH	Normality of Tridecanoic acid	Normality of Tributyl amine	o-Cresol	Polarity of particles	Mobility 10^{-6} cm./sec. per v./cm.	ζ mv.
None	0.01	0	0	Negative	0.48	35
None	.05	0	0	Positive	.66	48
None	0	.08	0	Negative	.95	69
None	.05	.05	.10	Positive	.47	34
Present	0	0	0	Negative	.95	69
Present	.01	0	0	Negative	.54	39
Present	.05	0	0	Positive	.66	48

graphite; the total amount present in the cell was only about 0.5 mg., and of this only a small fraction was deposited because of the incompleteness of the cataphoretic motion. From the writer's study[7] on diffusion of tridecanoic acid in oil, a figure of 0.2 milliequivalent of acid adsorbed per g. graphite can be derived. From this $a = 0.04$, and from Equation 4 with $B = 40$, $D = 10^{-4}$ g. follows. This means that about 20% of the graphite was deposited by cataphoresis. While this figure could not be determined experimentally, it appears of the right order of magnitude, judging from the microscopic observations.

The amphoteric nature of carbon, as found in this study, is in agreement with corresponding observations from aqueous systems.

(7) Andrew Gemant, THIS JOURNAL, **54**, 569 (1950).

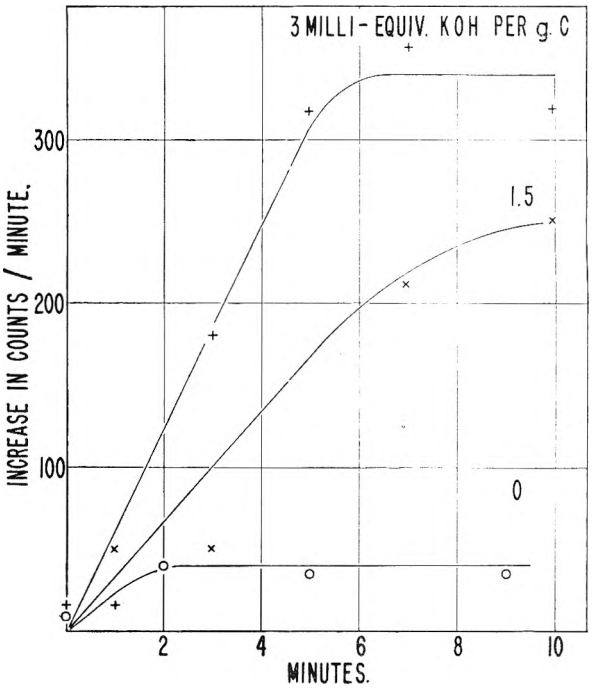

Fig. 8.—Counts/min. *vs.* time for labeled graphite in oil; acid, 0.01 normal; field, 950 v./cm.

STUDY OF THE FISCHER–TROPSCH REACTION USING DEUTERIUM GAS[1]

BY SYDNEY O. THOMPSON, JOHN TURKEVICH AND A. P. IRSA

Department of Chemistry, Brookhaven National Laboratory, Upton, Long Island, New York

Received January 30, 1951

A description is given of an apparatus for the production of deutero carbons from deuterium and carbon monoxide. The various deutero carbons and waxes are examined for their mass spectrum patterns and infrared spectra.

Introduction

The Fischer–Tropsch reaction is important not only from an industrial point of view but also from the scientific viewpoint in that it offers in its complex but flexible features a challenge to the theory of heterogeneous catalysis.

In this paper we shall present the study of the interaction of deuterium and carbon monoxide over a Fischer–Tropsch cobalt catalyst and the infrared and mass spectral data of the deuterated products.

Apparatus.—The apparatus (Fig. 1) was designed to study the reaction both under straight flow conditions and under conditions in which the exit gas was recycled. The latter procedure was used in the work with deuterium in order to conserve this gas. For the flow experiments the apparatus consisted of a gas mixing section (not shown in the figure), a reactor (1), a series of traps (2), (3), (5) and a circulating system consisting of a pump (7) and ballast chamber (6) and (8).

For the recycle experiments the gas mixture was introduced from the storage bulb (9) and recycled by the pump (7) using ballast chambers (6) and (8). The pressure was determined by mercury manometers, the flow rate by rotameters; and the temperature was monitored by thermocouples placed in the heating jacket and in the catalyst bed.

The reactor was a glass tube 35 mm. diameter and about 30 cm. long. Two wells extending from the top to the midpoint of the catalyst bed were used for a bimetallic thermoregulator and a chromel–alumel thermocouple. The reactor was charged with 20.5 g. of catalyst and occupied a space of 65 cc., the actual volume of the catalyst being 42 cc.

The trap system consisted of one at 0° (2), another at Dry Ice temperature (3), and a third one (5) at liquid air temperature. The first two were constructed so that one could syphon off the liquid products without opening the system to air. The contents of the liquid air trap, when brought to room temperature, were stored over water in a gas reservoir. A gas pipet (4) was used for intermittent sampling of the recycled gas.

The recycling pump was constructed of bronze sylphon bellows and valves of stainless steel ball bearings.[2] The pump was driven by a 0.1 horsepower Boston Ratio Motor Type MB and gave a displacement of approximately 90 liters per hour. A 5-liter ballast bulb before the pump and the 3-liter bulb after the pump was used to increase the gas capacity of the system and to even out the pressure variations during the pumping cycle. An 18-liter reservoir tank

(1) Research carried out under the auspices of the Atomic Energy Commission. Presented at symposium on the Use of Tracers in the Petroleum Industry at the Chicago Meeting of the ACS, September, 1950.

(2) B. B. Corson and W. J. Cerveny, *Ind. Eng. Chem., Anal. Ed.*, **14**, 899 (1942).

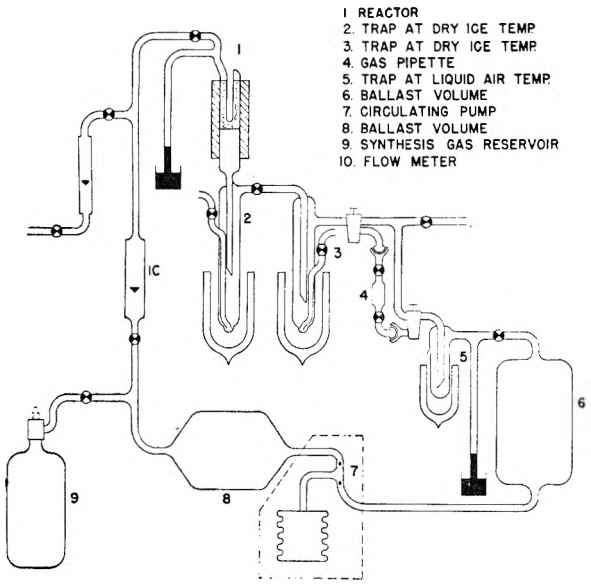

Fig. 1.—Apparatus used in the Fischer-Tropsch process.

was used to introduce the synthesis gas through a bleeder valve into the recycling system to maintain atmospheric pressure within the system. The drop in pressure of the tank was used as a measure of the progress of the reaction.

Materials.—Tank hydrogen and tank carbon monoxide were used directly. The carbon monoxide gas has the following impurities: 0.36% CO_2, 0.97% H_2, 1.0% N_2, 0.9% saturated hydrocarbons, 1.9 mg. per liter of iron and 0.32 mg. per liter of sulfur. The deuterium gas was obtained from the Atomic Energy Commission and its deuterium value fluctuated from 98.5 to 99.4% D_2.

The catalyst was the standard cobalt-thoria-magnesia kieselguhr material.[3]

In the initial stages of the investigation the deuterium gas was generated by electrolysis of heavy water.

Procedure.—The reduction schedule used to activate the catalyst was identical to that described by the Bureau of Mines group.[3] For the deuterium work the reduction was carried out with deuterium on a catalyst that had been previously evacuated at 250°.

For the operating conditions a space velocity of 150 per hour and a temperature of 200° was used with protium synthesis. For deuterium synthesis two temperatures, 192 and 227°, were used, and products were discarded until the analysis of the water produced indicated a light hydrogen impurity of less than 2%. A typical run consisted of eight hours of synthesis followed by 16 hours of standing in deuterium gas at the synthesis temperature. When the rate of product formation fell off, the catalyst was purged with deuterium at a space velocity of 2000 per hour for eight hours.

The products obtained from the various traps were distilled either through a Podbielniak low temperature column or a highly efficient high temperature fractionation column. The gaseous products were examined in a General Electric Mass Spectrometer. Infrared spectra were obtained on all products with the Baird Double Beam Recording Infrared Spectrometer.

Results

Typical data on the process are given in Table I, while Table II gives the distribution of the converted deuterium between the liquid, gaseous and aqueous phases.

The gas phase was analyzed during the course of reaction by an Orsat apparatus. Typical results are presented in Table III. The residual gas from the Orsat was dried, examined in the infrared spectrometer and found to be primarily deuteromethane. Gases obtained from run to run were collected and separated into C_1, C_2, C_3 and C_4 cuts by

TABLE I

FISCHER-TROPSCH DATA FOR DEUTERIUM AND CARBON MONOXIDE (2:1 VOL.) ON COBALT CATALYST

Run no.	Time, hr.	Temp., °C.	No. of moles[a] of synthesis gas used	No. of moles of product Water	Deutero-carbon	Gas	Input, moles deuterium	Output, moles, deuterium
1	36.5	190.2	3.11	1.26	0.045	0.22	1.97	2.20
2	57.	192.	1.78	0.69	.036	.06	1.07	2.21
3	45	192.	1.32	.56	.027	.035	0.79	0.93
4	42	192	1.37	.52	.038	.085	0.85	1.09
5	63	227	2.48	.96	.045	.20	1.65	1.86
6	20	227	1.67	.58	.031	.13	1.1	1.17
7	24	225	1.62	.47	.030	.20	1.1	1.20
8	30	225	1.64	.48	.033	.13	1.1	1.1
9	20	227	1.64	.19	.035	.17	1.1	0.91
10	53	227	1.63	.36	.014	.32	1.1	1.15
11	56	232	1.64	.42	.029	.13	1.1	1.0

[a] Synthesis gas is deuterium and carbon monoxide (2:1 vol.).

TABLE II

YIELDS[a] OF FISCHER-TROPSCH PRODUCTS FOR DEUTERIUM AND CARBON MONOXIDE INPUT

Run	Liquid, %	Gas, %	Aqueous, %
1	23	20	57
2	33	10	57
3	38	7	55
4	53	30	17
5	27	22	52
6	28	22	49
7	28	33	39
8	30	24	46
9	42	37	21
10	13	55	32
11	32	26	42

[a] Based on input D_2.

TABLE III

ANALYSIS OF GAS PRODUCTS

Temp., °C.	CO_2, %	CO, %	Deutero carbon	D_2, %	Sat., %	Unsat., %
190	7.0	11.5	81.5	1.0	75.5	6.0
192	14.9	25.0	59.9	...	54.0	5.9
192	11.5	25.7	61.8	2.0	58.0	3.8
227	9.2	26.4	61.6	1.9	57.2	4.6
227	13.4	21.1	63.2	2.3	63.2	6.0
227	9.2	27.8	62.5	0.2	54.5	8.0

(3) R. B. Anderson, A. Krieg, B. Seligman and W. O'Neill, *Ind. Eng. Chem.*, **39**, 1548 (1948).

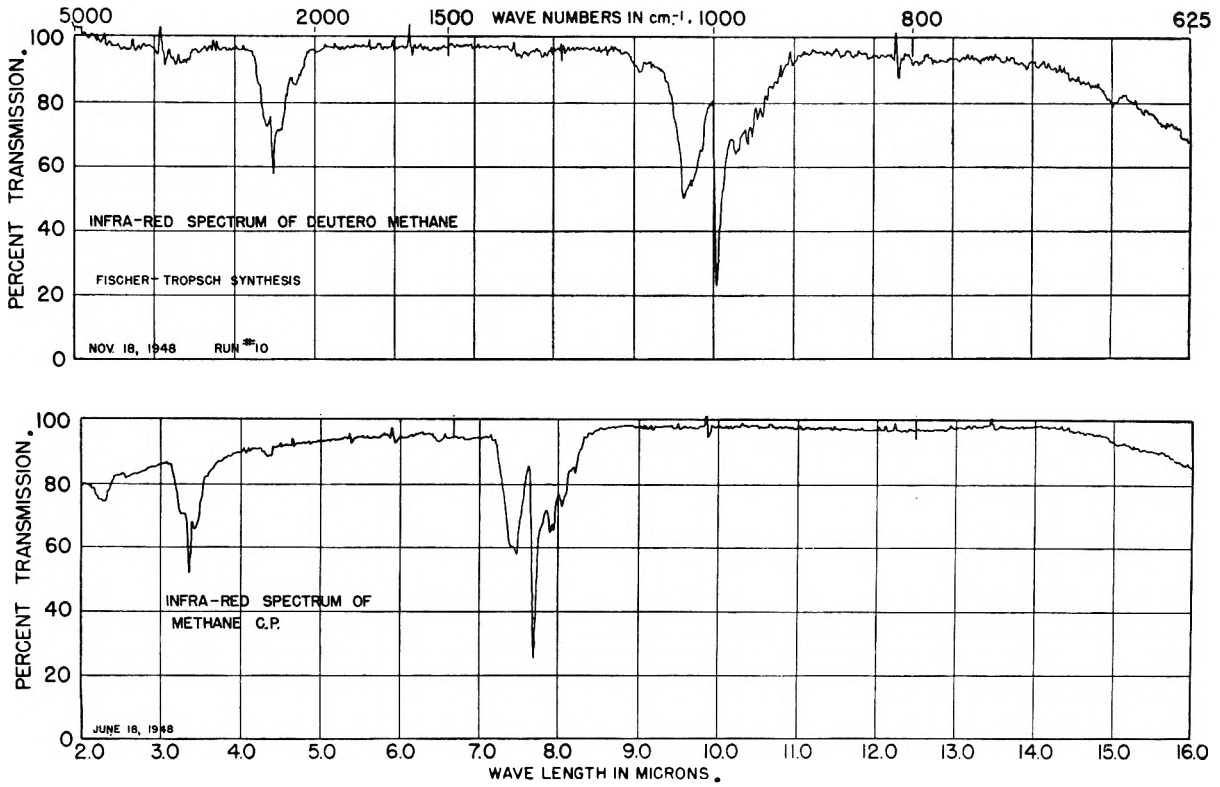

Fig. 2.—Infrared spectra of methane-d_4 and methane.

distillation in a Podbielniak column. The degree of unsaturation was determined either by catalytic deuteration or by absorption in fuming sulfuric acid. Table IV gives typical analyses. It is seen that methane is the main gaseous product and the per cent. unsaturated in the C_2 and C_3 fractions is between 20–30%.

TABLE IV

ANALYSIS OF THE DEUTEROCARBON GAS PRODUCTS

C_1, %	C_2, %	C_3, %	C_4, %
87.5	5.5	6.7	0.3
94.5	2.4	2.8	0.3
90.0	4.8	4.7	0.5
90.5	3.8	3.8	2.4

DEGREE OF UNSATURATION IN FISCHER–TROPSCH PRODUCT

C_2 Sat., %	Unsat., %	Sat., %	C_3 Unsat., %
79	21	69	31

The infrared spectrum of deuterated methane is given in Fig. 2 and Table V. The mass spectrum is substantially the same as that of CH_4 after due allowance is made for the change in masses. The sample contained 5.4% CD_3H indicating a 1.3% protium impurity in the product.

TABLE V

INFRARED ABSORPTION DATA FOR METHANE-d_4

Sample Wave length in cm.$^{-1}$	Literature reference[a]
2250 strong	2258.2
2215 weak	
2095 weak	
995 strong	995.6
968 weak	
960 weak	

[a] G. Herzberg "Molecular Spectra," Vol. II, D. Van Nostrand Co., New York, N. Y., p. 307.

TABLE VI

MASS SPECTRUM OF METHANE

m/e	Methane-d_4	m/e	Methane-d_4	Methane
20	100.0	16	7.8	100.0
19	5.4	15	0.3	80.9
18	81.5	14	3.5	10.3
		13	...	4.7
17	2.4	12	1.3	1.5

TABLE VII

INFRARED ABSORPTION DATA (WAVE LENTGH, CM.$^{-1}$) FOR ETHYLENE-d_4 AND ETHANE-d_6

Ethane-d and ethylene-d	Ethane-d	Ethylene-d	Ethane-d^b	Ethylene-d^b
2345 shoulder		2345 shoulder		2345
2200 strong	2200 strong	2200 strong	2236	2200
			2110	
2080 medium	2080 medium		2087	
2060 medium	2060 medium			
			1907 weak	
			1654 weak	
				1595
1510 weak		1510 weak		1510
1480 weak		1480 weak		1495
1470 weak		1470 weak		1480
1090 medium	1095 medium		1102	
1080 strong	1073 strong	1080 strong	1072	1079
1045 medium	1045 medium			
993 strong[a]	993 strong[a]			
718 strong		718 strong		723
				720

[a] Absorption wave length for methane-d. [b] G. Hertzberg, "Infrared and Raman Spectra," p. 344, ethane-d_6; p. 326, ethylene-d_4.

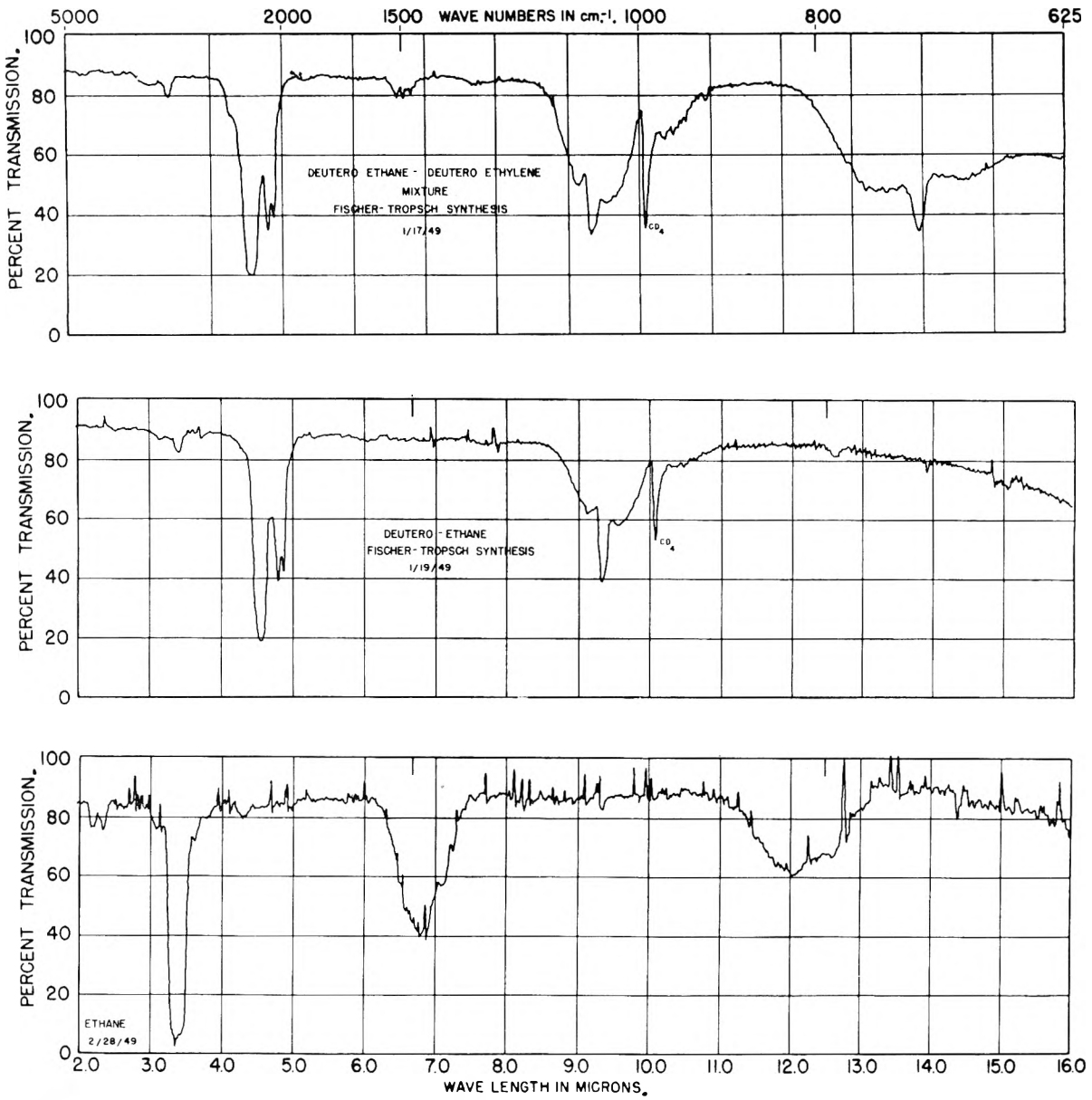

Fig. 3.—Infrared spectra of ethane-d_6, ethane and ethylene-d_4.

The infrared spectra of the deuteroethane–ethylene, deuteroethane and protium ethane are presented in Fig. 3 and in Table VII. The agreement with published data is satisfactory. The mass spectrum of the deuterated ethane is given in Table VIII. The light ethane is given for comparison. It is seen that there is about 8.2% C_2D_5H in the product corresponding to 1.3% protium impurity.

TABLE VIII

MASS SPECTRUM OF ETHANE AND DEUTEROETHANE

m/e	Deuteroethane	m/e	Deuteroethane	Ethane
36	100.0	30	147.9	100.0
35	8.2	29	11.9	92.4
34	88.6	28	95.8	441.8
33	16.3	27	11.1	143.6
32	561.3	26	27.0	95.8
31	25.2	25	0.1	19.2
		24	0.3	4.1

The agreement between the C_2D_6 spectrum and the C_2H_6 spectrum after due allowance is made for mass changes, is satisfactory except for the case of the removal of two hydrogen atoms giving ions of masses 32 and 28, respectively.

The deuterated propane–propylene mixture, the deuterated propane and ordinary propane infrared spectra are given in Fig. 4 and Table IX. It is seen that the completely deuterated propane has two bands in the 2–16 μ region, one at 4.6 μ and another at 9.3 μ, both corresponding to an isotopic shift from 3.4 and 6.8 μ, respectively. The completely deuterated propylene spectrum is characterized in part by a band at 6.3 μ and a broad band from 13 to 15 μ which definitely disappear on bromine treatment and distillation of the deuterated propane–propylene mixture. The mass spectrum of the deuterated propane is given in Table X. The concordance between the mass spectra of the C_3D_8 and C_3H_8 is not as good as in the case of the ethanes

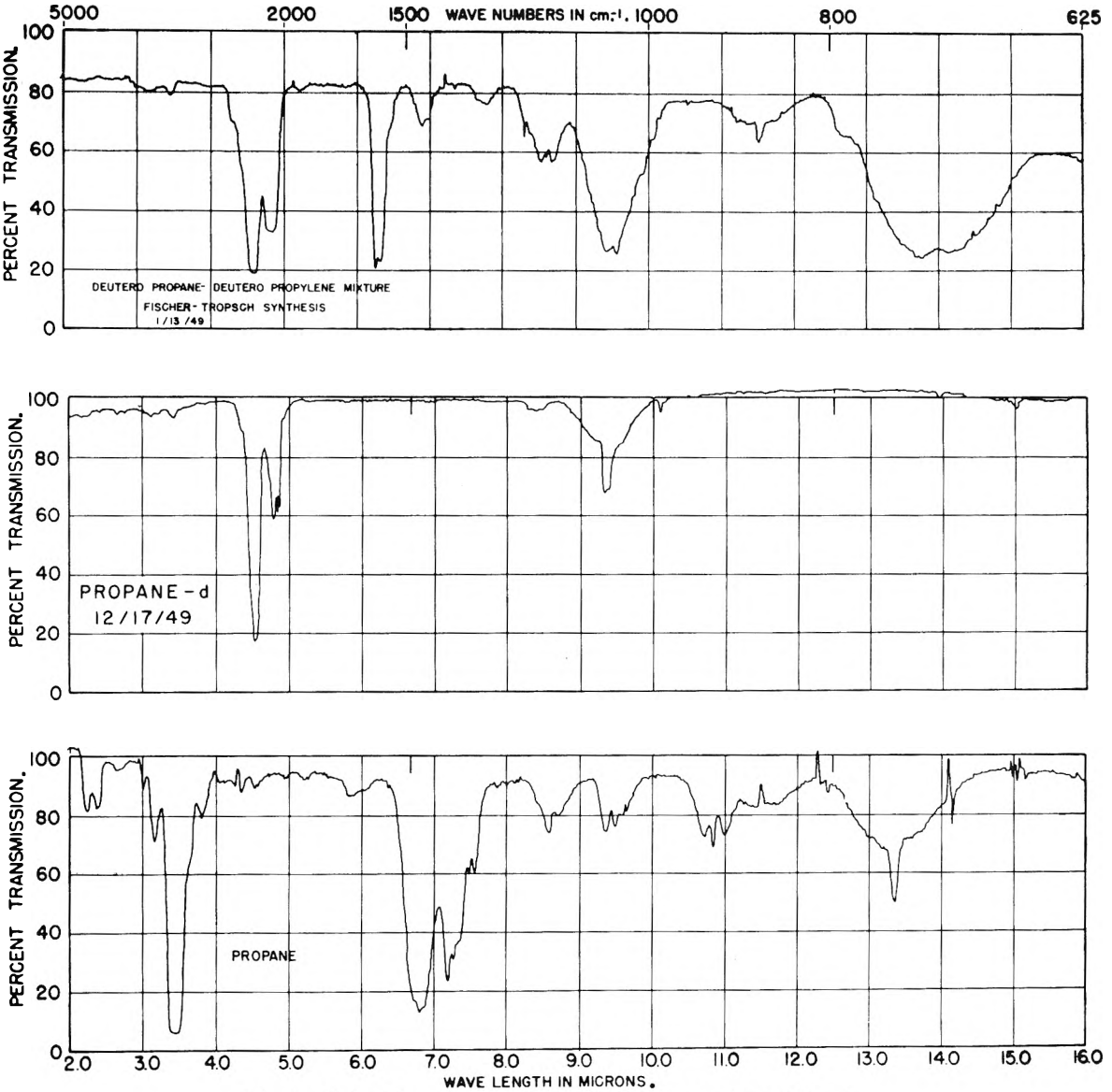

Fig. 4.—Infrared spectra of propane-d_8, propane and propylene-d_6.

TABLE IX

INFRARED ABSORPTION DATA (WAVE LENGTH, CM.$^{-1}$) FOR PROPANE-d_8 AND PROPYLENE-d_6

Propane-d and propylene-d	Propane-d	Propylene-d (partial spectrum)
2860 weak		
2320 shoulder		
2180 strong	2220 strong	
2070 medium	2094 medium	
	2085 medium	
	2070 medium	
1590 strong		
1580 strong		1580[a]
1450 medium		
1430 medium		
1380 weak		
1175 medium	1200 weak	
1145 medium		
1055 strong[a]	1073 medium	
1043 strong[a]		
	992 weak[b]	
868 medium		868
783 shoulder		783 shoulder
730 strong	720 weak	730
705 strong		705
	668 weak	

[a] Absorption frequencies for ethane-d_6. [b] Absorption frequency for methane-d_4.

and methanes, particularly for the positive ions of masses 34, 32 and 28. This is undoubtedly due to either an air contribution to masses 32 and 28 or to C_2D_6 and C_4D_{10} components not completely removed by fractional distillation.

The deuterated butane was recovered by the stabilization of the liquid product to give a gas boiling -9 to $0°$. The butenes were separated by bromine treatment. The infrared spectrum shows three bands at 4.6, 4.8 and 9.5 μ as shown in Fig. 5 and Table XI. The mass spectra are given in Table XII. The concordance between the protium and deuterium spectra is reasonably good among the C_4 fragments. However, in the C_3 and C_2 region the deuterium compound shows considerably higher

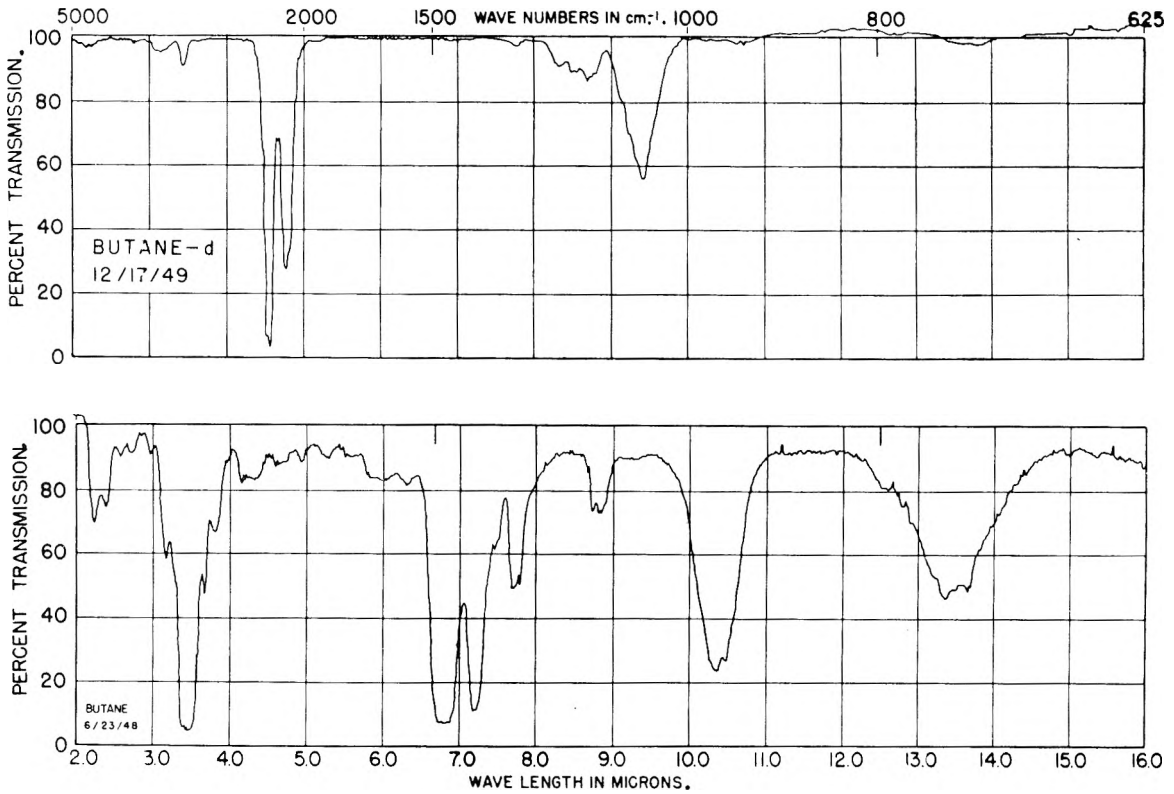

Fig. 5.—Infrared spectrum of butane-d_{10} and butane.

currents which may be due either to impurities or greater ease of fragmentation of the deuterated butane.

The infrared spectra of the liquid phase deutero carbons before stabilization, after stabilization at room temperature to remove dissolved gaseous products, and after catalytic deuterization are given in Fig. 6. Figure 7 gives the spectra of the hydrocarbons for comparison. It is seen that removal of dissolved gases clears up the spectrum considerably

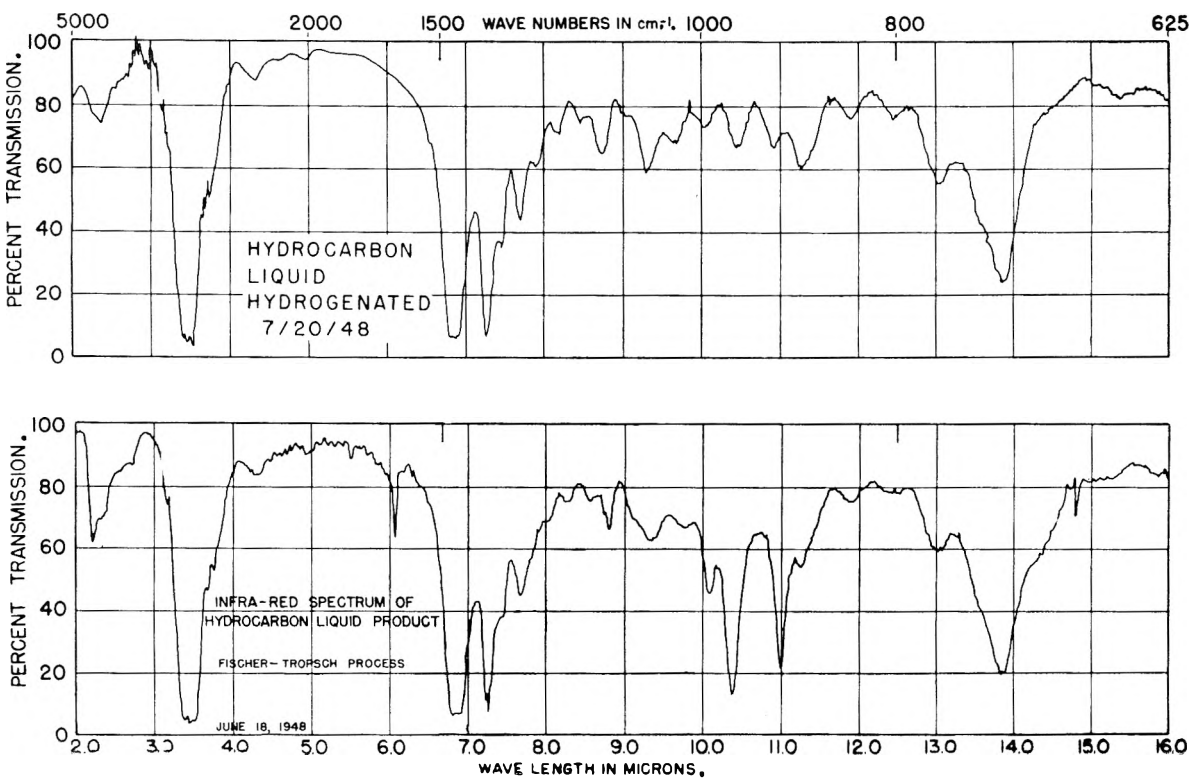

Fig. 6.—Infrared spectra of liquid hydrocarbon product.

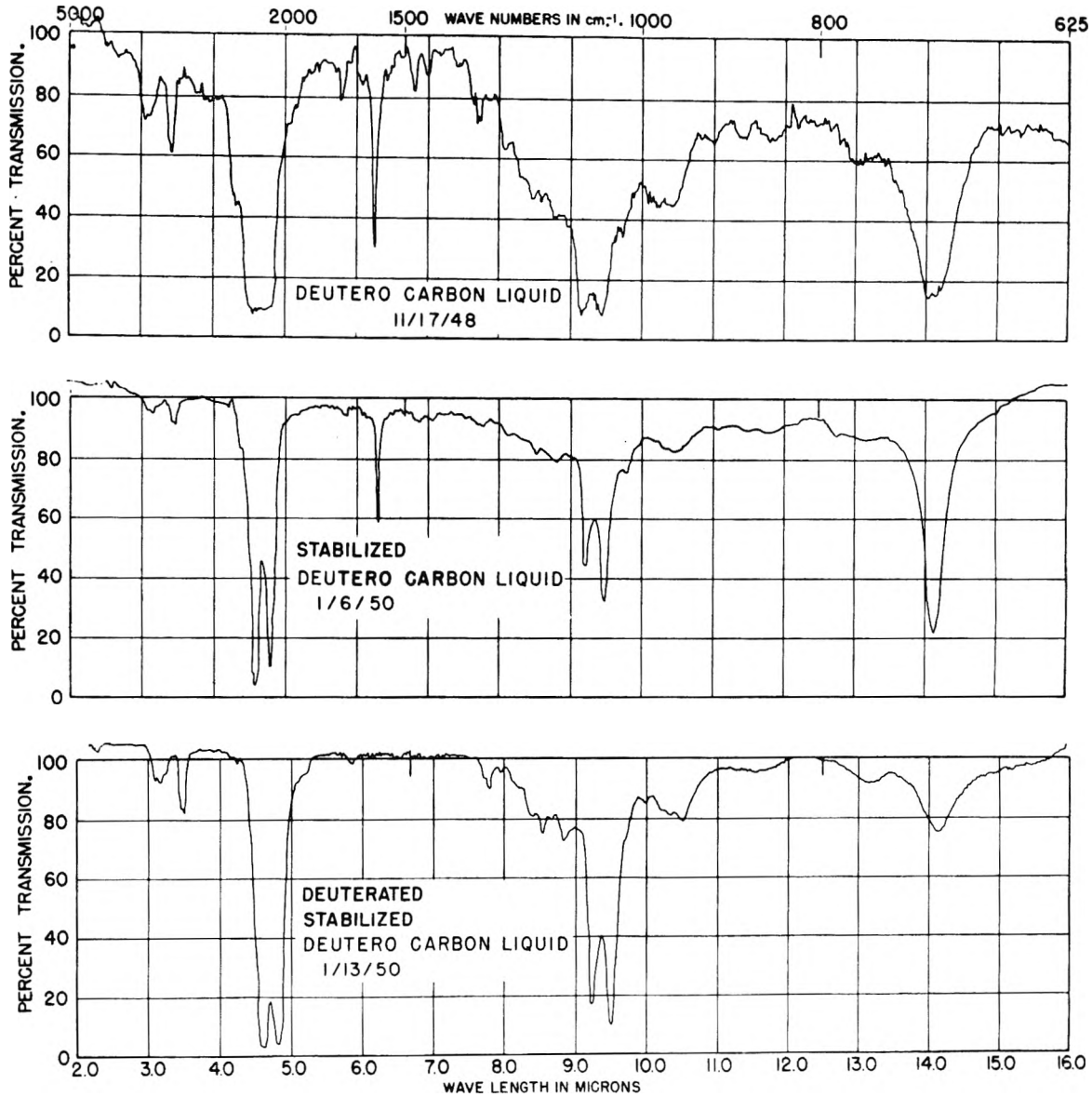

Fig. 7.—Infrared spectra of the liquid deutero deuterocarbon product.

TABLE X

MASS SPECTRA OF DEUTERATED PROPANE AND PROPANE (GENERAL ELECTRIC MASS SPECTROMETER)

m/e	Deuterated propane	Propane	m/e	Deuterated propane	Propane
52	100.0		33	30.4	
51	9.9		32	446.8	
50	86.6		31	19.0	
49	5.2		30	208.2	
48	15.9		29	5.0	403.0
47	2.0		28	71.4	242.0
46	47.1		27	2.5	146.5
45	1.8		26	9.5	33.0
44	19.6	100.0	25	...	4.6
43	3.0	102.0	24	1.4	1.0
42	52.7	17.9			
41	2.6	55.1	20	3.2	
40	14.3	9.2	19	0.4	
39	1.0	67.1	18	23.9	
38	8.3	20.7	17	2.9	
37	...	13.6	16	12.7	
36	26.7	2.1	15	1.7	12.5
35	11.7		14	4.5	5.0
34	472.1		13	...	1.6
			12	2.6	0.8

TABLE XI

INFRARED ABSORPTION DATA (WAVE LENGTH CM.$^{-1}$) FOR BUTANE-d_{10} AND ISOBUTANE-d_{10}

Butane-d and isobutane-d^a	Butane-d and isobutane-d^a
2230 shoulder	1210 weak
2200 strong	1180 weak
2150 weak	1150 weak
2115 shoulder	1095 shoulder
2090 strong	1065 medium strong
2050 shoulder	

[a] Product is mixture of butane and isobutane.

while deuterization removes the bands at 6.3 μ and 14.2 μ due to deutero unsaturateds.

The wax products obtained both as solids during synthesis and from distillation of the liquid were

TABLE XII

MASS SPECTRUM OF DEUTEROBUTANE AND BUTANE

m/e	Deutero-butane	Butane	m/e	Deutero-butane	Butane
68	100.0		43	8.0	905.0
67	10.9		42	214.0	134.0
66	16.3		41	7.3	321.8
65	1.5		40	48.1	16.2
64	4.6		39	1.9	126.2
63	0.4		38	27.2	21.4
62	4.5		37	35.2	14.5
61	....		36	4.0	1.3
60	0.4		35	26.4	
59	....		34	1162.0	
58	4.0	100.0	33	78.6	
57	....	19.2	32	994.0	
56	0.9	6.8	31	51.9	
55	0.8	8.9	30	741.0	9.4
54	4.6	1.6	29	26.2	457.0
53	4.0	6.7	28	180.0	291.6
52	19.7	2.3	27	7.3	310.0
51	59.0	10.5	26	25.0	54.3
50	1521.0	13.9	25	....	5.2
49	111.2	3.9	24	4.0	0.8
48	235.4	0.5	20	10.5	
47	29.8		19	3.4	
46	501.0	0.8	18	59.8	
45	21.8	...	17	....	
44	12.8	28.7	16	....	

white in color and amounted to about 5–6% of the liquid product. Their infrared spectrum showed bands at 4.6, 4.8, 9.15 and 9.4 and the spectrum was similar to that of the catalytically deuterated liquid deutero carbons. This is taken to indicate that they were relatively free of unsaturation.

Density determinations on the aqueous phase indicated 98% deuterium, and about 1% organic constituents. The latter were partially identified by distillation of the liquid between 60–100°, extraction of the various fractions with carbon tetrachloride and examination of the infrared spectra of the extract. Indications were obtained of the presence of OD and C=O bands.

Acknowledgments.—We wish to express our appreciation to Dr. Richard Dodson and Dr. Lewis Friedman for advice during the course of this investigation.

APPLICATION OF THE CATHODE-RAY OSCILLOSCOPE TO POLAROGRAPHIC PHENOMENA. I. DIFFERENTIAL CAPACITY OF THE ELECTRICAL DOUBLE LAYER

BY J. WEST LOVELAND AND PHILIP J. ELVING

Department of Chemistry, The Pennsylvania State College, State College, Pennsylvania

Received February 2, 1951

A detailed description of an electronic circuit has been given whereby the differential capacity *vs.* potential curve may be obtained on the screen of an oscilloscope. The capacity current pattern consists of a charging current trace and a discharging current trace. Comparison of calculated capacity values with known values agree favorably for the five solutions investigated. The potentials of certain distinguishing points on the curves likewise are in agreement with known values. The time required is a fraction of that needed with other methods. The application of the circuit is useful for studying charging currents at a streaming mercury electrode. Adsorption phenomena can be easily followed by the technique.

The application of the cathode-ray oscilloscope (CRO) to the measurement of polarographic phenomena has been reported by many investigators. A few have shown how the CRO may be used to study capacity phenomena at the mercury capillary electrode. Heyrovsky[1] employed a sine wave voltage alternately to charge and discharge negatively a mercury capillary electrode. The voltage output from the polarographic cell was placed on the vertical deflection plates of a CRO. The horizontal sweep was synchronized with the frequency of the applied potential to give on the face of the oscilloscope a potential–time trace consisting of the charging and discharging branches. Reversible depolarization processes are accompanied by definite kinks or time-lags situated symmetrically on the two arms of the potential–time curve. Similar kinks result when various non-electrolytes are adsorbed and desorbed at the electrode. On adsorption of the non-electrolyte film the capacity of the film-electrode layer becomes smaller than that of the aqueous double layer, whereas, on desorption the film suddenly breaks up at a certain charge density of the polarized electrode.

Delahay[2] developed an electronic saw-tooth voltage sweep for the purpose of studying reduction processes at the dropping electrode. The horizontal sweep of the CRO is proportional to the applied potential; the vertical deflection is proportional to the current flowing at the electrode. Because of the high rate of voltage change, *ca.* 20 volts per second, a considerable capacity current flows. Delahay measured the capacity currents of a 0.5 molar sodium sulfate solution on both the positive and negative branches of the electrocapillary curve, the observed and calculated values of which differed by 12 and 17%, respectively.

Bieber and Trumpler[3] described a method for studying polarographic phenomena using an isosceles triangular voltage sweep to polarize the dropping mercury electrode (D.M.E.) alternately,

(1) J. Heyrovsky, F. Sorm and J. Forejt, *Collection Czechoslov. Chem. Commun.*, **12** 11 (1947).

(2) P. Delahay, THIS JOURNAL, **53**, 1279 (1949).

(3) R. Bieber and G. Trumpler, *Helv. Chim. Acta*, **30**, 971 (1947).

negatively and then positively. With depolarizers in solution, the potential–time relationship obtained on the screen of the CRO shows reduction on one arm of the sweep and oxidation on the other. The polarographic behavior of formaldehyde was studied in this manner. A similar triangular voltage sweep was applied by Sevcik[4] to other systems to obtain current–voltage oscillograms. In the absence of depolarizers, the i–E patterns show the charging and discharging capacity current curves as a function of the applied potential. Sevcik demonstrated this with a photograph of the current–voltage oscillogram of an "empty" electrolyte solution (one normal potassium hydroxide solution).

The most recent and most comprehensive investigation on differential capacity at the mercury electrode has been reported by Grahame.[5] His method of measuring differential capacity of the electrical double layer with great accuracy at any applied potential involves the use of an impedance type capacity bridge with a CRO as a null-point indicator. A synchronized timing mechanism indicates the age of the mercury drop at the instant the null-point is reached. From the age of the drop and the rate of flow of mercury, the area of the drop is calculated.

The present paper describes a circuit for producing i–E oscillograms similar to those of Sevcik and demonstrates the usefulness of such oscillograms for studying electrocapillary phenomena.

Theory of Method

The equation relating differential capacity, C, to the surface charge density of the electrical double layer, Q, and applied potential, E, is

$$C = \mathrm{d}Q/\mathrm{d}E \qquad (1)$$

Under the conditions of the experiment where a linearly increasing and decreasing potential sweep is applied to the D.M.E., the rate of change of voltage with respect to time, t, is equal to a constant, K, *i.e.*

$$\mathrm{d}E/\mathrm{d}t = K \qquad (2)$$

Substituting the value of $\mathrm{d}E$ of equation 2 into equation 1, we have

$$C = \frac{1}{K} \times \frac{\mathrm{d}Q}{\mathrm{d}t} \qquad (3a)$$

or

$$\mathrm{d}Q/\mathrm{d}t = KC = i_c \qquad (3b)$$

In the latter equation, $\mathrm{d}Q/\mathrm{d}t$ is the rate of flow of charge equal to the capacity current, i_c, which is proportional to the differential capacity of the electrical double layer. Thus, as the applied potential increases linearly, the capacity current is proportional to the differential capacity over the potential range covered. The assumption is made that the differential capacity as a function of applied potential is independent of the rate at which the voltage sweep is applied. Since the electrical double layer is formed in a microsecond or less (ref. 7, p. 496) and sweep frequencies of much less than 100 c.p.s. are used, this assumption is considered to be valid.

Method of Measurement

Principle (Fig. 1).—To obtain a linear voltage sweep a square wave voltage is fed from a square wave generator (Block A) into an integrating circuit (Block B). The output from the integrator is a triangular voltage wave which after amplification (Block C) provides the potential sweep to the polarographic cell (P). The same sweep is used to deflect the cathode-ray electron beam horizontally after passing through the amplifiers of the oscilloscope (Block D). The current which passes through the cell also passes through the current-measuring resistance (R). The voltage developed across R is proportional to the current passing through it. This signal is amplified (Block E) before being led to the CRO vertical amplifier (Block F). The output from Block F is used to deflect the oscillographic trace vertically so that the resulting trace has an i–E relationship. A permanent record of the trace is obtained by photographing the oscillographic pattern on 35 mm. Eastman Kodak Panatomic X film using a Du Mont 271-A camera.

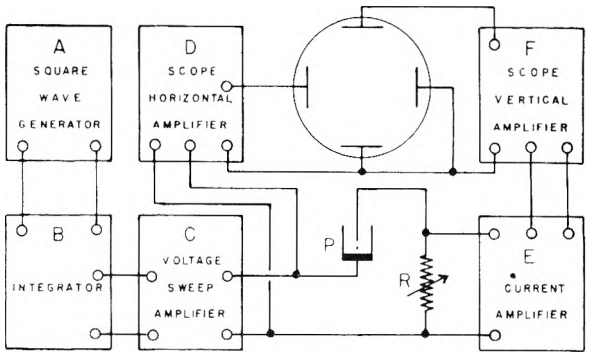

Fig. 1.—Block diagram of the electronic apparatus.

Circuit Description (Fig. 2).—An 185-A Du Mont electronic switch and square wave generator capable of giving 30-volt square waves covering a frequency range of 7.5 to 500 c.p.s. was used. A square wave signal of low frequency is fed through a d.c. blocking capacitor, C_1, to the grid of one-half of a duo-triode, T_1, where it is integrated by a circuit having a negative condenser feedback (through C_2) which gives the amplifier great stability. By using resistive regeneration (through R_4) practically perfect integration can be obtained. The amplitude of the integrated signal is increased or decreased by varying the integration resistor R_1. The coupling components C_3 and R_5 provide a large time constant for passing the low frequency signal without noticeable distortion to the grid of tube T_3. The potential sweep applied to the polarographic cell, P, is taken from the cathode follower resistor R_6. The resistance of R_6 is low to provide an ample current supply for charging the D.M.E. without altering the shape of the voltage signal. To ensure exact reproduction of the applied potential on the horizontal axis of the CRO, the same potential which is applied to the cell is also applied to the horizontal d.c. amplifiers of the CRO. All leads to the cell and oscilloscope are shielded. A 304-H Du Mont oscilloscope was used.

In addition to the alternating voltage occurring across R_6 a direct voltage exists which must be compensated before connections are made to the cell. A bucking voltage is supplied by the battery, B_2, and potentiometer, R_8, circuit. The starting potential of the voltage sweep is determined by the position of R_8. The plate B^+ supply of 250 volts for tubes T_1, T_2, and T_3 is supplied by a voltage regulated power supply having an a.c. ripple of about 0.01 volt. Filaments are heated by a 6 volt battery.

The current passing through the cell, P, also passes through the current measuring resistance, R_9, which is a Leeds and Northrup No. 4748 decade box. The small voltage of about 0.001 volt developed across R_9 is amplified by a pentode, T_4. Because very small voltages are being amplified about 10^4 times, a plate and screen B^+ supply with no ripple is required for the amplifier. For this purpose two 45-volt batteries, B_4 and B_5, are used.

The voltage output of the pentode amplifier is transferred through shielded leads to the vertical amplifier of the oscilloscope where, after further amplification, the signal is impressed across the vertical deflection plates. The sensitivity of the Du Mont 304-H oscilloscope with the preamplifier is 0.001 volt per inch. Although there was complete shielding of leads a small a.c. signal of about 10 microvolts was picked up; however, the slight 60 c.p.s. fluctuations did not hinder observation of the traces.

Calibration.—Calibration marks are superimposed on the differential capacity curves by multiexposures. To

(4) A. Sevcik, *Collection Czechoslov. Chem. Commun.*, **13**, 349 (1948).
(5) D. C. Grahame, *J. Am. Chem. Soc.*, **71**, 2975 (1949).

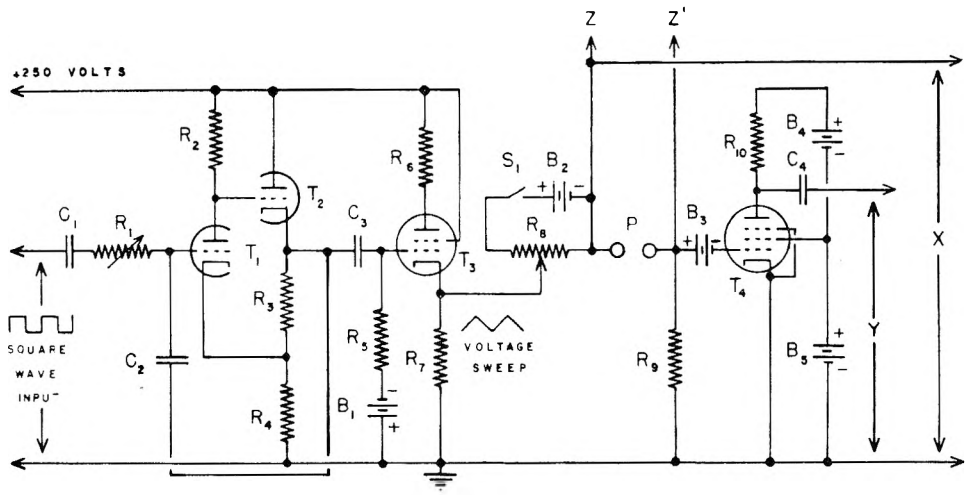

Fig. 2.—Circuit diagram of the electronic apparatus, square wave integrator, voltage sweep generator, and "polarographic current" amplifier: B_1, 15 volt dry cell, C supply; B_2, 4.5 volt dry cell, B supply; B_3, 3 volt dry cell, C supply; B_4, B_5, 45 volt dry cell, B supply; C_1, C_4, 0.5 microfarad paper condenser; C_2, 0.2 microfarad paper condenser; C_3, 1.0 microfarad paper condenser; P, polarographic cell; R_1, 3 megohm potentiometer; R_2, R_5, 1 megohm, 1 watt; R_3, 200,000 ohms, 2 watt; R_4, 2,700 ohms, 1 watt; R_6, 3,600 ohms, 20 watt; R_7, 85 ohms, 2 watt; R_8, 30 ohm potentiometer; R_9, 0 to 10,000 ohm Leeds and Northrup decade box, No. 4748; R_{10}, 150,000 ohms, 1 watt; S_1, single pole, single throw switch; T_1, T_2, 1/2 6SL7; T_3, 6V6 or 6L6; T_4, 6SJ7; X, voltage sweep output to horizontal amplifiers of oscilloscope; Y, polarographic current signal output to vertical amplifier of oscilloscope; Z–Z', connections to potentiometer for measuring cell potential.

bring out the detail of the traces against the plastic grid screen of the CRO, the following procedure is followed. After an exposure of the capacity trace, the trace is deflected off the tube screen, the intensity turned up to give a slight glow to the tube and an exposure made for about five seconds.

To measure the applied potential, the square wave signal is disconnected from the apparatus which results in the cessation of the voltage sweep to the cell and to the CRO. A spot appears on the screen of the scope, the horizontal position of which is indicative of the applied potential relative to a pool of mercury. The applied potential is measured on a potentiometer at points Z and Z' (Fig. 2) to an accuracy of 1 millivolt and an exposure of the spot taken. The applied potential is changed to a new setting by potentiometer R_9, and another reading is made, and the spot is exposed again. Since d.c. amplifiers are used for the voltage sweep deflection, the distance between the two spots is proportional to the difference in potential between the two settings. Thus, two points are obtained from which the total voltage span may be calculated as well as the potential of the starting voltage sweep with respect to the reference electrode. The drift of the d.c. amplifiers is negligible during the time interval required to make the potential calibrations.

A method for calculating the differential capacity from observed capacity current *vs.* potential curves involves the use of equation 3b as indicated previously. The constant, dE/dt, is determined by the frequency and the voltage span of the sweep. The capacity current is easily found by calibration of the vertical axis of the CRO in microamperes. The differential capacity may then be calculated by

$$C = \frac{i_c}{(dE/dt \times A)} = \text{microfarads per square cm.} \quad (4)$$

where A is the area of the mercury drop at the instant of exposure. This method was the one first used. It gave values of differential capacity accurate only for a small portion of the curve due, in part, to the slight non-linearity of the vertical amplifiers as well as the varying vertical sensitivity of the oscillographic trace at the outer round portions of the CRO tube.

An improved calibration procedure of the vertical axis employs the use of a known capacitor in place of the polarographic cell. The same potential sweep conditions as employed at the cell are maintained so that charging and discharging current traces are obtained, the distance between the two being proportional to the size of the capacity at a definite setting of R_9. By increasing or decreasing the sensitivity, *e.g.*, by varying R_9 at constant capacity, the distance between the two calibration lines may be made to coincide with those of the differential capacity lines. The calculation of differential capacity then involves (1) the ratio of the sensitivity settings of R_9, and (2) the ratio of the distance between the charging and discharging curves for the standard capacity and the distance between the same curves for the differential capacity. All calibrations were made with a 0.261 ± 0.001 microfarad capacitor previously calibrated on an impedance bridge. In all cases two sets of calibration lines were made, one to coincide as closely as possible to the lowest portions of the differential capacity lines and the other to correspond to the highest portion of the differential capacity lines, as may be seen in Figs. 3 and 4. In this manner any error due to the curvature of the CRO tube becomes negligible. Also, since amplification characteristics are identical for both the differential capacity and calibration curves, any error due to non-linearity in amplifier response over the potential range covered becomes negligible.

The time interval from the moment the mercury drop begins to form to the time of exposure of the capacity pattern was measured by a stopwatch. The timing was accurate to $\pm$ 0.1 second. An exposure for less than 0.2 second was sufficient to give good detail of the trace. The calculation of the area of the drop may be in error due to timing and exposure by 0.5 to 1% depending on the age of the drop; the longer the drop time, the less the error. To obtain a long drop time a capillary of 10 inches length was used. The application of such a long capillary resulted in large cell resistances of about 400 ohms with about one-half of this resistance being due to the solution and the other half to the thin thread of mercury in the capillary. In ordinary polarography a cell resistance of 400 ohms produces a negligible iR drop across the cell because only a few microamperes are passed by the cell. However, in oscillographic polarography where charging currents are of the order of 10 or more microamperes depending on the rate of voltage change, the iR drop across the cell can be appreciable. To minimize the resistance of the cell as much as possible, a low resistance electrode and fairly concentrated electrolyte solution, *e.g.*, 1 *N*, should be used. A low resistance electrode was made from the long capillary without changing any of its characteristics by sealing into the capillary a platinum electrode about one-half inch from the tip. The resistance between the platinum electrode and the mercury in contact with the solution was 9 ohms.

In order to test the applicability of our method for determining differential capacity tenth normal solutions were used since the most recent data available for comparison cover solutions of this concentration. The resistance of the cell with tenth normal solutions was approximately 200 ohms. (To calculate the iR drop more accurately the re-

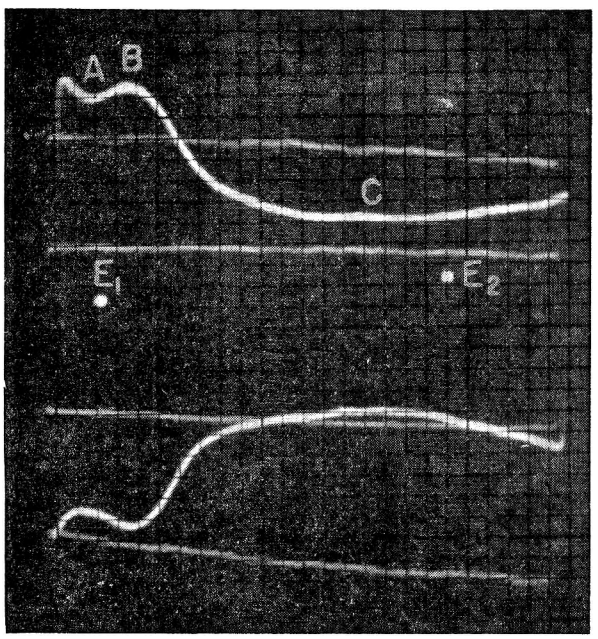

Fig. 3.—0.1 N KCl; $E_1 = -0.293$ v.; $E_2 = -1.429$ v.; exposure time, 10.7 seconds; mass per second, 0.291 mg.; calibrating capacity, 0.261 μf.; sensitivity resistance, R_9, for differential capacity curve, 60 ohms; for calibration, 60 and 150 ohms; sweep frequency, 7.5 c.p.s.

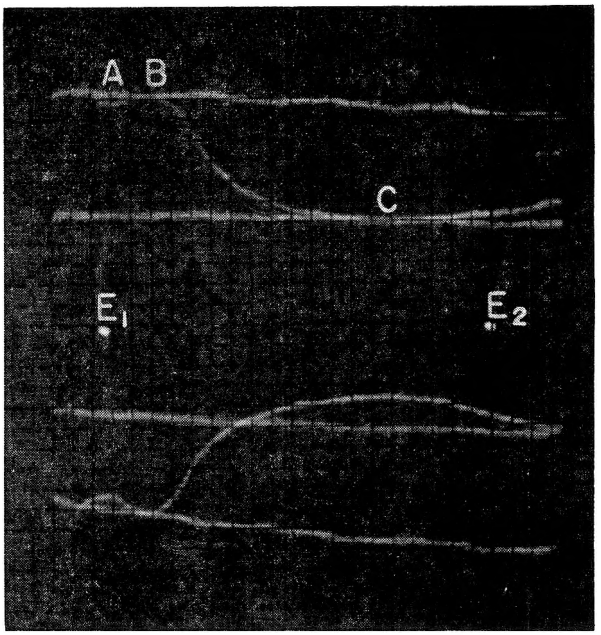

Fig. 4.—0.1 N $MgCl_2$; $E_1 = -0.264$ v.; $E_2 = -1.559$ v.; exposure time, 11.9 seconds; mass per second, 0.291 mg.; calibrating capacity, 0.261 μf.; sensitivity resistance, R_9, for differential capacity curve, 50 ohms; calibration, 70 and 150 ohms; sweep frequency, 7.5 c.p.s.

sistance of the current measuring resistance should also be added to the resistance of the solution.) The iR drop across the cell of this resistance is noticeable in all the i–E capacity current patterns observed. In Figs. 3 and 4, for example, the top differential capacity current or charging current produces an iR drop which shifts the potential sweep to more negative values while the bottom, or discharging current curve, shifts the potential sweep to more positive values. A position midway between the two curves corresponds to zero current flow so that at this point there is no shift in the applied potential.

Discussion of Results Obtained

To determine the applicability of this technique to the measurement of differential capacity, five solutions were studied, all of which had been carefully investigated by Grahame.[6] These were tenth normal solutions of the chlorides of potassium, lithium, barium, magnesium and aluminum. All solutions were degassed for 15 minutes or until no oxygen wave interfered. All solutions were investigated at a temperation of 25 ± 1°. For each solution two exposures were made on different drops with all necessary calibration marks. The differential capacity was calculated at three specific points on the capacity current *vs.* potential oscillogram, represented by A, B and C in Figs. 3 and 4, where A and C are minima and B is a maximum in all of the curves analyzed. The calculated capacities at the three specific points are tabulated in Table I under the appropriate headings of A, B and C, respectively. Adjacent to each of these columns are the corresponding averages of the two calculations for each solution and, for comparison, the values found by Grahame. The average deviation of the combined calculated values with respect to those of Grahame is 0.9%, with the largest individual deviation being 2.0%.

(6) D. C. Grahame, Office of Naval Research Technical Report No. 1 (1950).

TABLE I

DIFFERENTIAL CAPACITY OF 0.1 N SOLUTIONS IN MICROFARADS PER SQUARE CENTIMETER

0.1 N solution	C_A			C_B			C_C		
	Calcd.	Av.	Grahame	Calcd.	Av.	Grahame	Calcd.	Av.	Grahame
LiCl	37.5	38.1	38.1	39.6	39.9	39.8	15.2	15.6	15.4
	38.6			40.2			15.9		
KCl	37.7	37.4	38.0	39.5	39.1	39.9	16.3	16.1	16.0
	37.1			38.7			15.9		
$BaCl_2$	38.4	38.3	38.5	40.2	40.2	40.2	16.3	16.2	16.3
	38.2			40.1			16.1		
$MgCl_2$	38.4	38.2	38.4	40.7	40.4	39.9	15.7	15.8	15.7
	37.9			40.0			15.8		
	38.0	38.1	38.7	39.8	39.8	40.4	16.5	16.2	16.1
$AlCl_3$	38.2			39.8			15.9		

A further test of the validity of the method was made by comparing the observed potentials at which the maximum, C_B, and minima, C_A and C_C, capacities occur with respect to those of Grahame. Potentials were obtained by drawing a straight line between corresponding maxima and minima points on the charging and discharging curves. The location where the mid-point or zero current point of this line cuts the potential axis, was taken to represent the potential of the particular maximum or minimum capacity under consideration. These observed potentials are given in the first column under the corresponding headings of E_A, E_B and E_C in Table II. The average values for each solution are given in the second column and those of Grahame in the third. All voltages given are referred to the mercury pool in the same electrolyte solution, *i.e.*, 0.1 N chloride ion. In no case is there any large difference between the average observed potentials and those found by Grahame. The individual values never deviated more than 0.03 volt from the given values.

The authors believe that the method and appara-

TABLE II

APPLIED POTENTIALS RELATIVE TO THE MERCURY POOL AT WHICH MINIMA C_A AND C_C, AND MAXIMUM C_B OCCUR

0.1 N solution	E_A Calcd.	E_A Av.	E_A Grahame	E_B Calcd	E_B Av.	E_B Grahame	E_C Calcd.	E_C Av.	E_C Grahame
LiCl	0.26	0.27	0.28	0.41	0.41	0.41	1.22	1.23	1.24
	.27			.41			1.23		
KCl	.28	.27	.28	.42	.41	.41	1.22	1.21	1.20
	.25			.40			1.20		
$BaCl_2$	.28	.28	.29	.44	.44	.41	1.16	1.17	1.16-
	.28			.44			1.18		1.18
$MgCl_2$	.28	.28	.28-	.42	.42	.41	1.18	1.21	1.20-
	.28		.29	.42			1.23		1.24
$AlCl_3$	.28	.27	.28-	.43	.42	.40	1.16	1.18	
	.26		.29	.41			1.19		

tus described, which originally was designed to follow oxidation–reduction reactions at the D.M.E. has definite application to the study of capacity phenomena. Although the method may be somewhat less accurate than the most accurate procedures for calculating the capacity of the electrical double layer, it is well suited for obtaining an overall picture of the relationship of differential capacity to the applied potential at the dropping mercury electrode. Moreover, the complete capacity spectrum may be observed during the formation of each individual mercury drop. The time required is very much less than with other procedures.

The method is not limited to the use of the D.M.E. Figure 5 shows the type of capacity current pattern obtained with a streaming mercury electrode (S.M.E.) of the general nature described by Heyrovsky.[1] The S.M.E. consists of a capillary of about 0.1 mm. inner diameter, the tip of which is pointing upward at an angle of about 45° and at a point about 5 mm. below the surface of the solution. The mercury issues forth in a fine unbroken stream, making an interface with the solution of constant area. The actual area can only be roughly estimated since the amount of solution adhering to the stream of mercury as it breaks the surface of the solution is not known. The symmetry of the charging and discharging curves obtained with the D.M.E. has completely disappeared in the case of the S.M.E. The potentials corresponding to points B′ and C′ (Fig. 5) where changes of slope are most noticeable are almost identical to the potentials of maximum B and minimum C in the case of the D.M.E. (B' = −0.45 volt and C' = −1.23 volts). The shape of the i–E curve for the S.M.E. may be explained on the basis that the mercury stream carries away most of the surface charge accumulated at the mercury–solution interface so that additional current is required to keep the electrode fully charged. If the surface charge is carried away as fast as it accumulates, then the current required to charge the S.M.E. at any potential should be proportional to the surface charge density of the electrode at that potential over the potential span covered. In this case the current–potential oscillogram will appear to have the same general shape as a plot of the surface charge density *vs.* potential. This is found to be the case upon comparison of the observed curve with known surface charge density curves.[7]

The technique also may be applied to the study of film formations at the mercury electrode. This is exemplified by the capacity pattern obtained on a 0.5 molar sodium sulfate solution saturated with octyl alcohol (Fig. 6). The two peaks on the charging curve or top trace, indicate the formation of the alcohol layer about the electrode at a low applied negative potential and the desorption of the layer at a higher applied negative potential, while those on the lower or discharge curve,

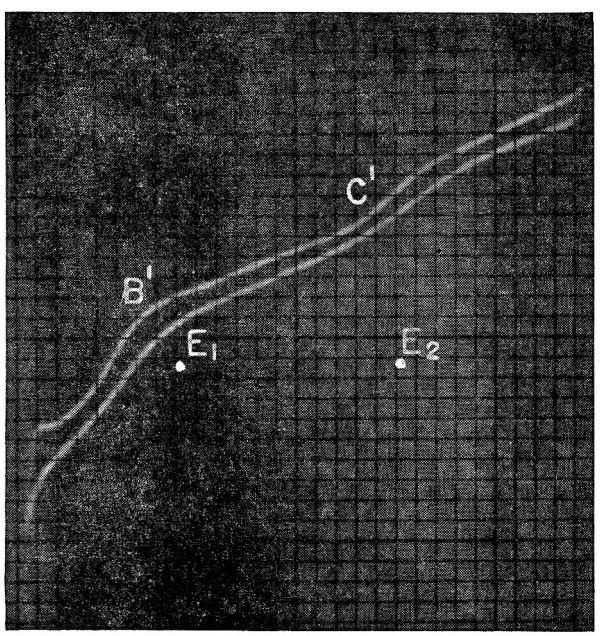

Fig. 5.—0.1 N KCl; capacity curve for streaming mercury electrode; E_1 = −0.578 v.; E_2 = −1.369 v.; sweep frequency, 7.5 c.p.s.

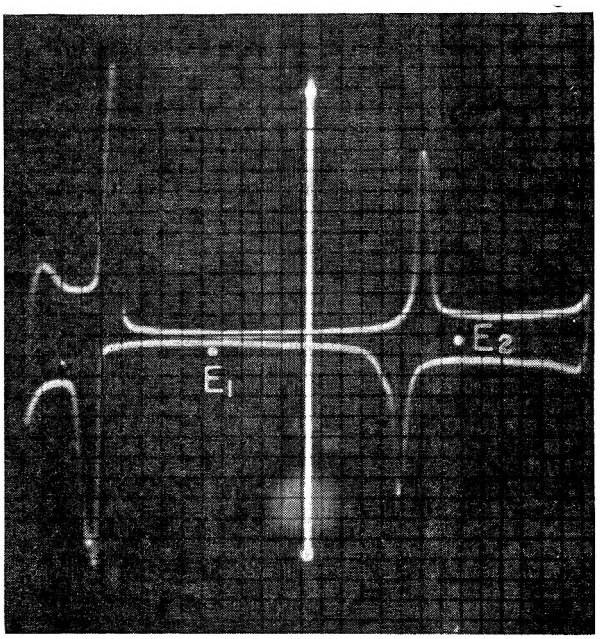

Fig. 6.—Capacity effects of octyl alcohol in 0.5 M Na_2SO_4; E_1 = −0.300 v.; E_2 = −1.240 v.; exposure time, 11.0 seconds; mass per second, 0.291 mg.; vertical sensitivity, 25.8 μa. per division; sweep frequency, 15 c.p.s.

(7) D. C. Grahame, *Chem. Revs.*, **41**, 441 (1947).

indicate the desorption of the film layer at a low negative potential and the adsorption at a higher negative potential. The voltage difference between the two peaks is 1.20 volts corresponding closely to Grahame's value of 1.23 as measured from Fig. 21 of reference[7] which is a plot of differential capacity *vs.* E.

The authors wish to thank the Office of Naval Research for their support of the research project upon which the work described was done.

APPLICATION OF THE CATHODE-RAY OSCILLOSCOPE TO POLAROGRAPHIC PHENOMENA. II. SURFACE CHARGE DENSITY OF THE ELECTRICAL DOUBLE LAYER

BY J. WEST LOVELAND AND PHILIP J. ELVING

Department of Chemistry, The Pennsylvania State College, State College, Pennsylvania

Received May 3, 1951

Through the use of an additional amplifier and integrator circuit with a circuit described in a previous paper, differential capacity currents are integrated to give a surface charge density trace on the face of an oscilloscope. The accuracy obtainable is good when the values found are compared to those obtained by graphical integration. The method is rapid; a complete surface charge density relation can be observed and recorded on one mercury drop. Application of the technique is found in the study of film formation. The use of an additional integration circuit to the arrangement described will provide a means of obtaining the electrocapillary curve on the screen of an oscilloscope.

In a previous paper[1] a description was given of an electronic circuit which produces on the screen of a cathode-ray oscilloscope (CRO) a complete spectrum of the differential capacity of the electrical double layer at a mercury solution interface as a function of applied potential. Basically, an isosceles triangular potential sweep is applied to a mercury microelectrode, and the charging and discharging capacity current traces as a function of applied potential are observed on the face of the CRO. Comparison of the distance between the two traces with the distance between the traces obtained with a known capacity, permits evaluation of the differential capacity at any applied potential.

In the present paper a method is described for converting the differential capacity current *vs.* potential pattern obtained for a mercury–solution interface into a surface charge density *vs.* potential curve on the CRO screen. A further method is indicated for converting the latter curve to a plot of the electrocapillary curve relating surface tension and potential.

Theory of Method

The differential capacity, C, of the electrical double layer is related to the surface charge density, q, and applied potential, E, by the differential expression

$$C = \mathrm{d}q/\mathrm{d}E \qquad (1)$$

Integration of equation 1 results in equation 2

$$q = \int_{E_{max}}^{E_d} C\,\mathrm{d}E \qquad (2)$$

where the limits of integration are taken from the potential of the electrocapillary maximum (E_{max}) since the charge on the mercury surface at that potential is zero with respect to E_d, which is the applied potential.

The capacity current has been shown[1] to be equal to

$$i_c = \frac{\mathrm{d}q}{\mathrm{d}t} = C\frac{\mathrm{d}E}{\mathrm{d}t} = KC \qquad (3)$$

where $\mathrm{d}E/\mathrm{d}t$ was a constant, K, for the experimental arrangement. Comparison of this capacity current with that for a known standard capacity current provided a means of calculating the differential capacity.

Upon integration of the capacity current equation 3, q is obtained as a function of time, t

$$q = K\int_{t_1}^{t_2} C\,\mathrm{d}t + k \qquad (4)$$

However, since t is a known function of E, it is possible by calibration procedures, described subsequently, to obtain q as a function of voltage as in equation 2, *i.e.*

$$q = K\int_{E_1}^{E_2} C\frac{\mathrm{d}E}{K} + k \qquad (5)$$

$$q = \int_{E_1}^{E_2} C\,\mathrm{d}E + k \qquad (6)$$

Circuit.—The apparatus used to obtain differential capacity patterns[1] is employed in its entirety. For integration of the differential capacity current, an integrating circuit identical to that composed of tubes T_1 and T_2 in Fig. 2 (reference 1) was constructed. The integrated output signal voltage was found to produce too small an oscillographic trace. An additional 6SJ7 amplifier, similar in all respects to the circuit of T_4 (ref. 1, Fig. 2) was adequate to amplify the capacity "current" signal output of T_4. The output signal of this second amplifier is then fed through the integrating circuit just mentioned; the output from the integration circuit is then passed on to the vertical deflection amplifiers of the CRO. The triangular voltage sweep applied to the polarographic cell is used for producing the horizontal sweep of the CRO in the same manner as for differential capacity current patterns. The resulting oscillogram has a surface charge density *vs.* potential relationship.

The solution–electrode arrangements used were the same as those previously described.[1]

Calibration.—The horizontal or voltage axis of the CRO screen is calibrated, as previously described,[1] by photographing on the voltage axis of the oscilloscope two spots, the potentials of which *vs.* a pool of mercury are known to ± 1 millivolt. This permits the calculation of the voltage span used as well as the starting potential of the sweep. For calibration of the vertical or surface charge density axis the trace obtained by the integration of the charging–discharging currents of a known capacitor is used; the latter is inserted in place of the solution–electrode system. The total charge represented by the vertical height of the calibration trace may be found from the relationship

$$Q_c = C_c V \qquad (7)$$

which holds for any capacitor of constant capacity, C_c, when a charge, Q_c, accumulates due to a voltage, V, being

(1) J. W. Loveland and P. J. Elving, THIS JOURNAL, **56**, 250 (1952.)

impressed across the capacitor's terminals. The value of V used is equal to the applied potential span. The capacity of C_c was 0.261 microfarad in all of the calibration experiments of the work described in the present paper. Once the voltage span is calculated, Q_c is readily determined.

Exposures of the surface charge density (S.C.D.) trace were made at a known age of the mercury drop from which the area of the drop of mercury could be calculated. Long drop times of about ten seconds were used and exposures of 0.1 to 0.2 second were made. The error involved in the calculation of the area of mercury due to timing and length of exposure was of the order of 1%. The total change in the S.C.D. of the electrical double layer, as indicated by the vertical length of the trace, is calculated according to the equation

$$Q_t = \frac{D_1 R_2 Q_c}{D_2 R_1 A} \qquad (8)$$

where Q_t is the difference in S.C.D. as represented by the points at the beginning and the end of the trace. R_1 and R_2 are the resistance sensitivity settings for the surface charge and calibration curves, respectively, and D_1 and D_2 are the vertical distances between the ends of the S.C.D. and calibration traces, respectively. Q_c is determined from equation 7 and A is the area of the mercury surface at the time of exposure of the surface charge density trace.

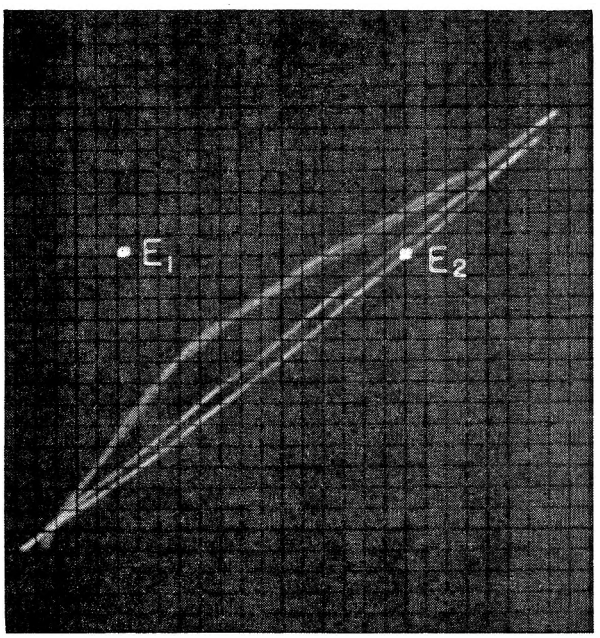

Fig. 1.—Surface charge density relation for 0.1 N LiCl: $E_1 = -0.488$ v.; $E_2 = -1.538$ v.; exposure time, 10.4 seconds; mass per second, 0.291 mg.; calibrating capacity 0.261 μf; sensitivity resistance for surface charge density curve, 80 ohms; for calibration, 120 ohms; sweep frequency, 7.5 c.p.s.

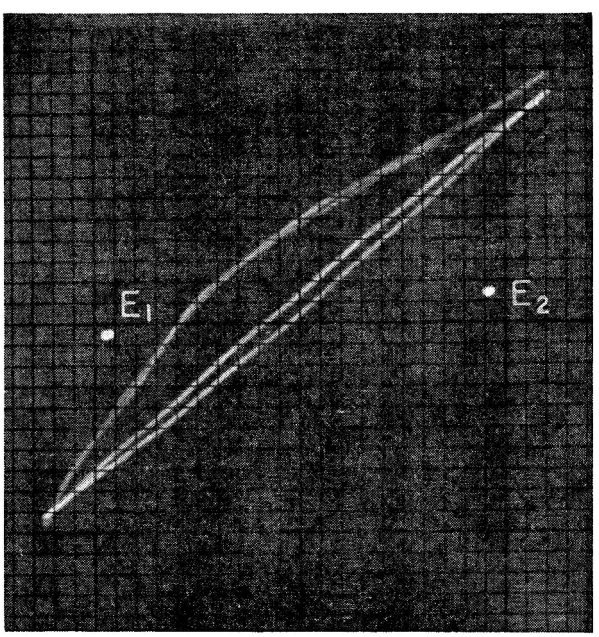

Fig. 2.—Surface charge density relation for 0.1 N $BaCl_2$: $E_1 = -0.277$ v.; $E_2 = -1.533$ v.; exposure time, 10.8 seconds; mass per second, 0.291 mg.; calibrating capacity, 0.261 μf; sensitivity resistance for surface charge density curve, 90 ohms; for calibration, 150 ohms; sweep frequency, 7.5 c.p.s.

Discussion of Results Obtained

Surface charge density oscillograms were obtained in duplicate for tenth normal solutions of the chlorides of lithium, potasssium, barium, magnesium and aluminum. Typical S.C.D. curves with calibration traces and potential marks are shown in Figs. 1 and 2.

Due to a very small alternating voltage which could not be filtered out of the electronic circuit, the charging and discharging S.C.D. traces are not exactly superimposed on each other at all times. In the calculations made on the oscillograms, the points of measurement were made from a line which was the average of the two traces.

For a preliminary test of the applicability of the method to the determination of S.C.D., the total S.C.D. difference represented by the vertical length of the trace was calculated; the values obtained are compared with Grahame's[2] results in Table I. Since Grahame's values of S.C.D. are given for potential intervals of 0.05 and 0.10 volt, the values of S.C.D. used for comparison were obtained by interpolation in many cases. In the case of aluminum chloride solution, the S.C.D. was calculated at an applied potential of -1.00 volt relative to 0.1 normal calomel since Grahame's values for the solution were only given up to this potential. In every case except one, lithium chloride solution, the agreement between the present and Grahame's values of S.C.D. is within 1 microcoulomb per square centimeter.

TABLE I

TOTAL SURFACE CHARGE DENSITY CHANGE FROM BEGINNING TO END OF APPLIED POTENTIAL SWEEP IN MICROCOULOMBS PER SQUARE CENTIMETER

0.1 N solution	Found	Grahame[2]
LiCl	40.7	38.9
	39.6	40.2
KCl	40.7	40.3
	37.1	37.5
$BaCl_2$	39.6	39.4
	41.1	42.0
$MgCl_2$	40.9	41.1
	41.5	41.4
$AlCl_3$	27.0	26.5
	26.8	26.5

A more critical examination of the validity of the method was carried out by calculating absolute

(2) D. C. Grahame, Office of Naval Research, Technical Report No. 1 (1950); D. C. Grahame, *Chem. Revs.*, **41**, 441(1947).

values of S.C.D. at −0.20 and −1.50 volts relative to the mercury pool after locating the point of zero charge from knowledge of the potential of the electrocapillary zero. The potential of the zero charge was taken to be −0.559 volt for the tenth normal solutions of lithium and potassium chloride, and −0.558 volt for the tenth normal solutions of barium, magnesium and aluminum chloride, both values being referred to the mercury pool in the tenth normal solutions. The values of S.C.D. obtained in this manner for the five solutions are given in Table II as are the corresponding averages for each solution and, for comparison, the values obtained by Grahame. The largest deviation of the average value at low applied potential is 0.5 microcoulomb while at the higher applied potential the largest deviation is 0.3 microcoulomb. The average value of 18.1 microcoulombs obtained for aluminum chloride solution at −1.50 volts is probably high by about 0.5 microcoulomb on the basis of other S.C.D. values.

TABLE II

SURFACE CHARGE DENSITY AT −0.20 AND −1.50 VOLTS RELATIVE TO THE MERCURY POOL IN MICROCOULOMBS PER SQUARE CENTIMETER

0.1 *N* solution	At −0.20 volt[a] Found	Average	Grahame[2]	At −1.50 volts[a] Found	Average	Grahame[2]
LiCl	13.5	13.5	13.6	17.0	16.5	16.8
	13.4			15.9		
KCl	13.2	13.1	13.6	17.6	17.5	17.3
	12.9			17.4		
$BaCl_2$	13.6	13.7	13.7	18.3	18.0	17.9
	13.8			17.6		
$MgCl_2$	14.2	14.0	13.6	17.2	17.4	17.5
	13.8			17.6		
$AlCl_3$	14.0	13.8	13.7	17.7	18.1	..
	13.6			18.5		

[a] S.C.D. values at −0.20 volt are positive and at −1.50 volts are negative.

The presence of non-electrolytes in solution has appreciable effect on the surface charge density curve. Figure 3 shows the type of surface charge density curve obtained when a 0.5 molar solution of sodium sulfate is saturated with octyl alcohol (a saturated aqueous solution is about 4.5 millimolar in octyl alcohol). The formation of a film layer of the alcohol about the mercury drop produces a sharp increase in the S.C.D. at a low applied potential designated at A in Fig. 3. This sudden increase is a result of the charging of the very high capacity encountered during the formation of the film layer. From potential A to potential B the mercury–film interface which exists is of much lower capacity than that of the mercury–solution interface. Because of this small differential capacity due to film formation, the surface charge density increases only a small amount as indicated by the relatively flat portion of the curve between points A and B. At potential B where the film is desorbed, the S.C.D. increases rapidly to the value it assumes for the aqueous solution alone. On the discharge cycle, potential B corresponds to film formation while potential A is indicative of film disruption. This surface charge density oscillogram may be compared with the charge-potential

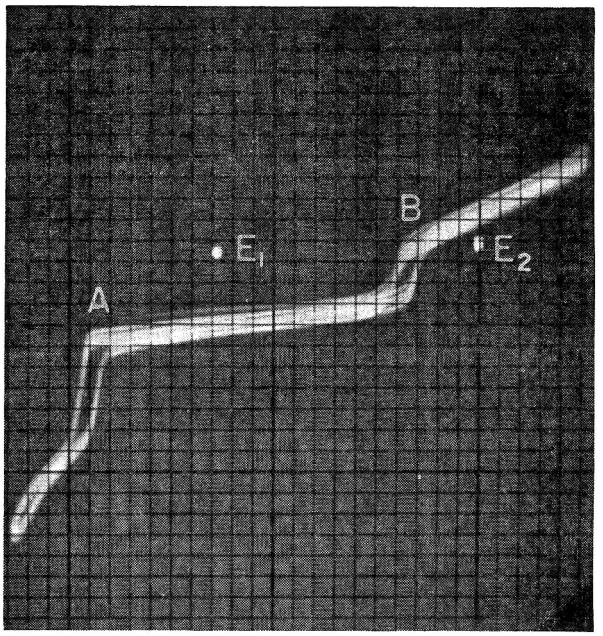

Fig. 3.—Effect of octyl alcohol on the surface charge relation of 0.5 *M* Na_2SO_4: E_1 = −0.356 v.; E_2 = −1.305 v.; exposure time, 11.0 seconds; mass per second, 0.291 mg.; resistance sensitivity, 15 ohms; sweep frequency, 15 c.p.s.

curve estimated by Grahame[3] for octyl alcohol in potassium nitrate solution.

An oscillogram of the capacity current trace obtained with a streaming mercury electrode is similar in shape[1] to the S.C.D. curves obtained with D.M.E.

Integration of the capacity current traces of a streaming electrode results in a pattern characteristic of the electrocapillary curve, Figure 4, where the maximum occurs approximately at the elec-

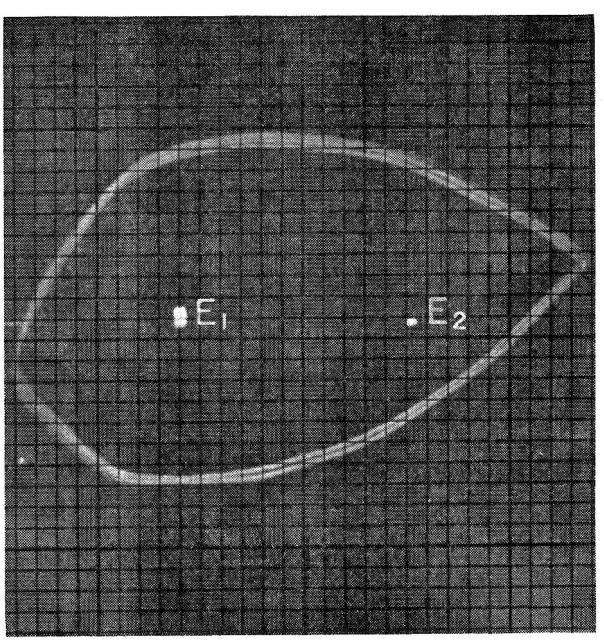

Fig. 4.—Integration curve of capacity current using a streaming mercury electrode in 0.1 *N* KCl: E_1 = −0.578 v.; E_2 = −1.369 v.; sweep frequency, 7.5 c.p.s.

(3) D. C. Grahame, *J. Am. Chem. Soc.*, **68**, 301 (1946).

trocapillary curve. This suggests the use of an additional integration circuit to integrate the S.C.D. curves obtained with a D.M.E. to secure electrocapillary curves. Such curves have been observed for chloride solutions. However, the curves are somewhat distorted and of small magnitude due to the fact that the amplification available was non-linear and insufficient in magnitude. Work on this aspect is being continued.

The time required to obtain S.C.D. curves by the method described is a fraction of that required by the method of graphical integration; the information obtainable is comparable.

The authors wish to thank the Office of Naval Research for their support of the research project upon which the work described was done.

HYDROGEN EXCHANGE REACTIONS OVER IRON SYNTHETIC AMMONIA CATALYSTS AT −195°

BY J. T. KUMMER AND P. H. EMMETT

Gulf Research & Development Company's Multiple Fellowship, Mellon Institute, Pittsburgh 13, Pa.

Received February 5, 1951

The behavior of singly promoted and doubly promoted iron catalysts has been compared for the ortho–para hydrogen interconversion and for the hydrogen–deuterium exchange reaction at −195°. The work of Emmett and Harkness[1] on the ortho–para conversion over the doubly promoted catalyst has been confirmed by showing that the ortho–para exchange occurs rapidly on such a catalyst at −195° but is very strongly poisoned by the presence of hydrogen chemisorbed at or about 100°. The hydrogen–deuterium exchange over the doubly promoted catalyst has been found to be very slow at −195°. Singly promoted iron catalysts, unlike the doubly promoted catalysts, rapidly catalyze the hydrogen–deuterium exchange at −195° as well as the ortho–para hydrogen conversion. Furthermore, the latter reaction is not poisoned by hydrogen put on the catalyst at 100°. The existence of a third type of activated adsorption of hydrogen on a singly promoted catalyst is suggested by the high velocity for the H_2–D_2 exchange and by the appearance of the low-temperature adsorption isotherms and the adsorption isobar.

During the past twenty years, two reactions have been used very extensively in studying hydrogenation catalysts. One of these involves the interconversion of ortho and para hydrogen according to the reaction

$$H_{2\text{para}} \rightleftarrows H_{2\text{ortho}} \qquad (1)$$

The other is the reaction of hydrogen and deuterium to form HD

$$H_2 + D_2 \rightleftarrows 2HD \qquad (2)$$

The only published work for these two reactions on iron catalysts[1] showed that the ortho–para hydrogen reaction at −195° over the surface of a reduced, doubly promoted iron catalyst proceeded rapidly, and that the reaction at −195° was poisoned to a large extent by the chemisorption of hydrogen on the catalyst surface at about 100°.

Continuing our study of iron catalysts, we have recently made some observations on the rate at which reactions 1 and 2 take place both on doubly promoted catalysts of the type studied by Emmett and Harkness[1] and on singly promoted catalysts containing aluminum oxide as promoter. These measurements have revealed a very unexpected difference between the singly and doubly promoted catalyst that makes presentation of the results at this time seem desirable.

Experimental

The sample of doubly promoted catalyst No. 931 that we employed was from the same supply from which samples used by Emmett and Harkness were taken. In addition to iron oxide, the doubly promoted catalyst contained 1.59% K_2O and 1.3% Al_2O_3; the singly promoted catalyst contained 2.26% Al_2O_3, 0.2% SiO_2, and 0.21% ZrO_2.

The experimental setup for studying the ortho–para-hydrogen conversion was similar to that employed previously[1] and need not be described in detail. The hydrogen–deuterium reaction was studied by mixing pure hydrogen and pure deuterium[2] in known proportions and passing the mixture over the catalyst at about −195°. The exit gas was analyzed by means of a mass spectrometer.

The iron catalysts were reduced in all cases at 500° in a stream of pure hydrogen at 1,000 to 5,000 space velocity. The samples were then evacuated at 500° and cooled to −195° in the presence of a few mm. pressure of helium unless otherwise noted. The rate of reaction 2 was critically dependent upon how well the sample was reduced, the rate being greatly retarded by any remaining trace of oxide.

Results

Doubly Promoted Iron Catalysts.—The conversion of ortho to para hydrogen according to reaction 1 over the doubly promoted catalyst was found to be similar to that observed on the sample employed by Emmett and Harkness.[1] As can be seen from Table I, the reaction is rapid at −195°, the time of half conversion being approximately 0.4 second. Furthermore, in agreement with the work of Emmett and Harkness, hydrogen adsorbed at about 100° was found to act as a strong poison for reaction 1 at −195°. In the experiment recorded in Table I, the addition of hydrogen slowed down the rate by a factor of about 20.

TABLE I

	Time for ½ conversion, sec. Singly promoted catalyst	Doubly promoted catalyst
Reaction (1) sample cooled in He	0.06	0.4
Reaction (1) sample cooled in H_2	0.06	8.0
Reaction (2) sample cooled in He	3–10	~100 min.

(1) P. H. Emmett and R. W. Harkness, *J. Am. Chem. Soc.*, **57**, 1628 (1935). E. Ogawa, M. Tada and T. Okuno studied the conversion at 73 and 112° over an iron synthetic ammonia catalyst but no details were given as to promoter content or the extent of prior exposure to chemisorbed hydrogen. See *J. Soc. Chem. Ind. Japan*, **45**, 387 (1945).

(2) The hydrogen was freed of traces of O_2 and N_2 by slow passage through a large tube of baked-out charcoal at −195°. The deuterium was passed over hot Pt to remove traces of O_2.

In view of the fact that reaction 1 with this doubly promoted catalyst is generally assumed[3] to take place as a result of a magnetic perturbation of the molecules by the ferromagnetic iron, it was not surprising that the hydrogen–deuterium reaction was very slow at −195°. Previous studies had indicated that activated adsorption of hydrogen on this doubly promoted catalyst did not take place at temperatures lower than about −100°.[4] It was therefore understandable that the hydrogen–deuterium reaction involving, as is generally assumed, the dissociative or activated adsorption of hydrogen on the catalyst would necessarily have to be very slow at −195°. As can be seen from the last column in Table I, the time for half conversion of reaction 2 over this doubly promoted catalyst at −195° was about 100 minutes. In other words, the rate of reaction was slower by a factor of about 10^4 than the ortho–para hydrogen interconversion.

Singly Promoted Iron Catalysts.—The results obtained on catalyst No. 423 which contained irreducible oxides but did not contain any potassium oxide were unexpectedly very different from those obtained on the doubly promoted catalyst. The only point of resemblance between the behavior of the singly and the doubly promoted catalysts was the fact that each of them was active toward the ortho–para interconversion at −195°. However, the singly promoted catalyst differed from the doubly promoted catalyst in two important respects. In the first place, the adsorption of hydrogen at 100° had no detectable poisoning effect on the ortho–para hydrogen interconversion at −195°. Thus, as pointed out in Table I, the time for half conversion over the singly promoted catalyst was approximately 0.06 second when the sample was cooled from 500° either in hydrogen or in helium.

The striking difference between the singly and the doubly promoted catalysts was discovered when measurements were made for the hydrogen–deuterium exchange. The singly promoted catalyst, unlike the doubly promoted catalyst, was extremely active for the reaction at −195°. Thus the time of half conversion over the singly promoted catalysts for reaction 2 was 3 to 10 seconds compared to about 6000 seconds for the doubly promoted catalyst.

The very rapid hydrogen–deuterium exchange over the singly promoted catalyst at −195° raised the question as to the type of activated adsorption that was involved. In similar work on tungsten, Eley[5] and Rideal[6] had proposed that the conversion of a H_2–D_2 mixture to HD at −195° took place as a result of gaseous D_2 molecules striking the bare tungsten surface adjacent to very strongly chemisorbed H atoms that had been left on the surface during the exposure of the tungsten catalyst to hydrogen at high temperature. The D_2 molecules were then postulated to interact with the adjacent H atoms to form adsorbed D atoms and gaseous HD. Previous adsorption work[4] on iron catalysts had suggested that two types of activated adsorption existed. One of them, called Type A adsorption, became appreciable at about −100° and continued to occur at an increasing rate but in lower equilibrium quantities as the temperature was raised. At about 100° a second type of activated adsorption had been found to occur. This was designated as Type B adsorption. In the present work it became of interest to ascertain whether either Type A or Type B adsorption could account for the rapid hydrogen–deuterium exchange observed at −195° by analogy with the mechanism proposed for tungsten catalysts by Eley and by Rideal.

To establish this point, a large 25.2-g. sample of the singly promoted catalyst was reduced and evacuated at 500° and cooled slowly to −195° in hydrogen. It was then evacuated with a collection pump at −195°. The difference between the amount of hydrogen added to the system and the amount removed by pumping was 31.1 cc. This presumably was held on the catalyst surface as a combination of Type A and Type B activated adsorption. The catalyst was next exposed at −195° to 8.39 cc. of deuterium for about 40 minutes. The gas phase was then analyzed for the total content of light hydrogen. It was found that no increase in the light hydrogen content of the gas phase occurred. Thus the original deuterium sample contained 4% light hydrogen and the sample removed from the catalyst after 40 minutes contained 3.8% light hydrogen. It therefore appeared that deuterium was unable to remove Type A or Type B hydrogen from the surface of the iron catalyst at −195°.

To avoid the possibility that this result might be interpreted as due to an isotope effect, the experiment was repeated in the reverse order. The catalyst was cooled in an atmosphere of deuterium, and then after evacuation at −195°, the sample with its layer of chemisorbed deuterium was exposed to an atmosphere of light hydrogen. An analysis of the hydrogen after one hour's circulation showed no deuterium content. Presumably, therefore, neither Type A nor Type B activated adsorption is capable of reacting with gaseous hydrogen or deuterium at −195° to form HD. However, at the end of both of these experiments, the catalyst was found to be very active for reaction 2, being capable of rapidly converting 50 cc. of a 50–50 hydrogen–deuterium mixture into one containing nearly the equilibrium amount of HD in a period of about 5 minutes.[7]

Since the rapid H_2–D_2 exchange at −195° apparently did not involve either Type A or Type B activated adsorption, it seemed likely that for this singly promoted catalyst some new type of chemisorption was involved. Accordingly, adsorption isotherms at −195° and an isobar in the tempera-

(3) A. Farkas, "Light and Heavy Hydrogen," Cambridge University Press, 1935, Chapter IV.

(4) P. H. Emmett and R. W. Harkness, *J. Am. Chem. Soc.*, **57**, 1631 (1935).

(5) D. Eley, *Proc. Royal Soc. (London)*, **A178**, 452 (1941).

(6) E. K. Rideal, *Proc. Camb. Phil. Soc.*, **35**, 130 (1939).

(7) At the time this experiment was done the flow runs reported in Table I had not yet been made. Hence the exact value for the time of half conversion at this point cannot be given. Actually, there was some indication that the rate of reaction 2 was less (conversion was 80% of equilibrium in 5 min.) in this experiment in which the catalyst was covered with Type A and Type B hydrogen adsorption than in runs in which the catalyst was cooled to −195° in helium after reduction and evacuation at 500°. (Conversion was ~100% of equilibrium in 5 minutes in this latter case.)

ture range −195 to −78° were measured on the singly promoted catalyst. At the same time, a low temperature adsorption isotherm was made at −195° on the sample of doubly promoted iron catalyst at −195°. The results of these adsorption measurements are shown in Figs. 1, 2 and 3.

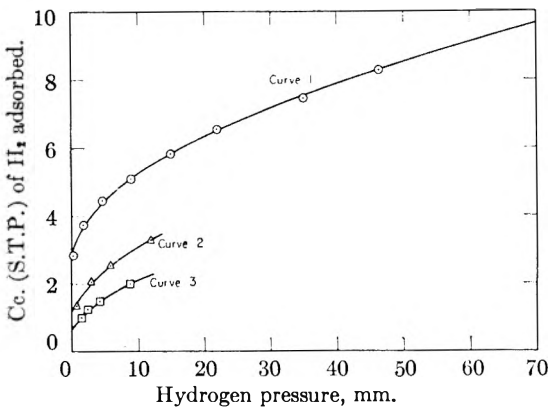

Fig. 1.—Hydrogen adsorption at −195° on 25.2 g. of sample of singly promoted iron catalyst 422. The CO chemisorption was 25 cc. and the volume of nitrogen for a monolayer was 85 cc. on this sample. Curve 1, original adsorption, sample cooled in He; curve 2, adsorption made after sample evacuation for 1.5 hr. at −195° immediately following the run given in curve 1; curve 3, adsorption made after the iron sample was saturated with 13.2 cc. of hydrogen at 100°.

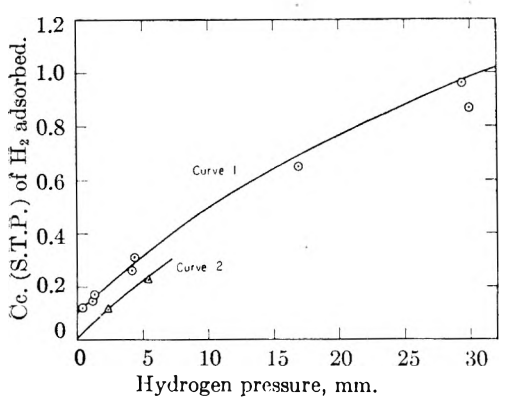

Fig. 2.—Hydrogen adsorption at −195° on 12 g. of doubly promoted iron catalyst 931. The chemisorption of CO was 3.2 cc., and the volume of nitrogen in a monolayer was 10 cc. Curve 1, original adsorption on sample cooled in He; curve 2, adsorption made after sample evacuation for one hour at −195° immediately following the isotherm given by curve 1.

Curve 1 of Fig. 1 gives the hydrogen adsorption isotherm on the sample of singly promoted catalyst cooled, after evacuation, from 500 to −195° in helium. Curve 2 represents a repeat isotherm on the same sample after an evacuation of the hydrogen at −195° following a completion of the run shown in curve 1. It is evident from the two isotherms that some type of activated adsorption of hydrogen is occurring at very low pressures even at −195°. The presence of such an activated adsorption on the singly promoted catalyst was further confirmed by the one-atmosphere adsorption isobar shown in Fig. 3. Clearly, all of the low-temperature chemisorbed hydrogen does not desorb from the surface before a temperature is reached at which one of the known

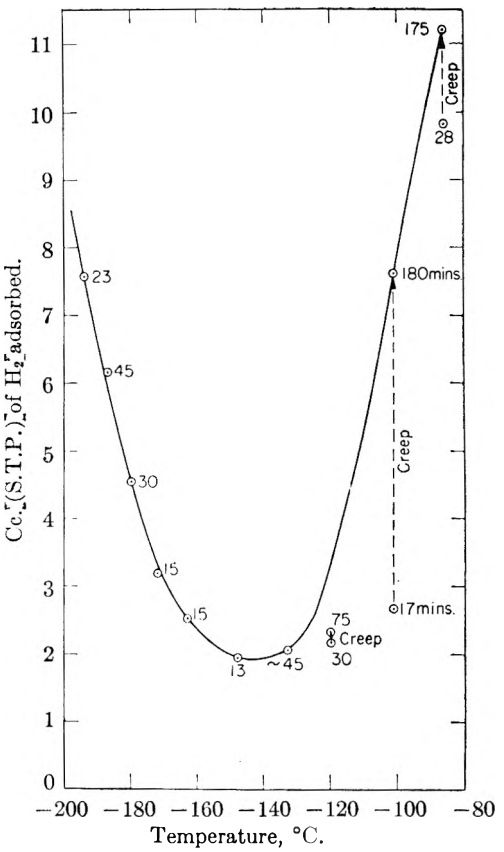

Fig. 3.—Isobar for the adsorption of hydrogen on singly promoted iron catalyst 422 (25.2 g.) at 69 mm. pressure. The numbers opposite the points are the times in minutes allowed for equilibration.

types of activated adsorption (Type A) begins to occur.

It is interesting to note in curve 3 of Fig. 1 that a definite detectable amount of low-temperature activated adsorption of hydrogen occurs at −195° even on a catalyst on which a considerable amount of activated adsorption has already been allowed to occur at or above 100°. These adsorption measurements on the singly promoted catalyst all indicated, then, the existence of a type of activated adsorption of hydrogen at −195° that probably is responsible both for part of the interconversion of para to ortho hydrogen over this catalyst and also of the hydrogen–deuterium reaction.

The adsorption measurements on the doubly promoted catalyst showed a very small amount of activated adsorption at −195°. However, all of this activated adsorption was apparently rather tightly bound as evidenced by the fact that after the catalyst was evacuated at −195° following a low-temperature adsorption isotherm measurement, a repeat isotherm showed substantially no chemisorption of hydrogen. It is therefore not surprising that the low-temperature hydrogen–deuterium reaction over this doubly-promoted catalyst is extremely slow at −195°.

It remained to establish in one final experiment that if the catalyst sample is cooled to −195° in helium, and is then exposed to an atmosphere of hydrogen and later evacuated for a short time at −195°, some of the hydrogen that remains on the

surface is capable of exchanging with the gas phase to form HD. To prove this point it was convenient to use tritium[8] instead of deuterium. Accordingly, 16 cc. of hydrogen containing a small amount of tritium as HT was added to a 252.2-g. sample of reduced, evacuated and helium-cooled singly promoted catalyst at −195°. The original activity of the gas was 15400 counts per minute per cc. Eight cc. was adsorbed leaving 8 cc. in the gas phase. The latter had an activity of 10700 counts per minute per cc. The sample was then evaluated for 1.5 hours at −195° after which 15.5 cc. of hydrogen was added and left in contact with the catalyst for 28 minutes. The gas phase then analyzed 2400 counts per minute per cc. Because of the large isotope effect in runs involving tritium, it is not possible to make accurate calculations as to the exact amount of tritiated hydrogen retained in the catalyst and exchanged with the added hydrogen at −195°. The data do, however, unmistakably indicate that the several cc. of the sample of tritiated hydrogen left on the surface after evacuation were able to exchange with the added gas-phase hydrogen.

From these results it is evident that the hydrogen which we consider to be chemisorbed at −195° on the sample cooled in helium does not behave the same as the hydrogen chemisorbed at the higher temperature. The former will exchange rapidly with the gas-phase hydrogen at −195°, whereas both Types A and B hydrogen placed on the catalyst at a higher temperature will not react at −195° with gaseous hydrogen. As a matter of fact, the experimental data show that the high-temperature chemisorption of hydrogen inhibits chemisorption of the type that is capable of taking place at −195° (curve 3 Fig. 1 compared to curve 1).

Discussion

The data recorded in Table I for the doubly promoted catalyst are not in the least surprising. The observations on the ortho–para hydrogen interconversion merely confirm the earlier work of Emmett and Harkness.[1] The extremely slow rate of the hydrogen–deuterium interchange is consistent with the indications of the adsorption isotherm to the effect that very little if any readily reversible chemical adsorption of hydrogen occurs on the doubly promoted catalyst at −195°. Presumably the rapid ortho–para hydrogen conversion over this doubly promoted catalyst at this low temperature is, therefore, to be attributed to a magnetic perturbation and not to a dissociative adsorption of hydrogen.

The experimental data on the singly promoted catalyst, unlike those on the doubly promoted catalyst, appear to show the existence of a third type of activated adsorption of hydrogen on the singly promoted catalyst at −195°. Little can be said as yet about the nature of this third type of activated adsorption except to point out that its heat of binding is apparently considerably greater than that of the heat of adsorption of physically adsorbed hydrogen, but at the same time is considerably smaller than the heat of adsorption of either Type A or Type B hydrogen adsorption. These conclusions as to the heat of adsorption can be drawn from the adsorption isotherms in Fig. 1. The heat of binding is high enough to cause a considerable adsorption at a very low partial pressure of hydrogen. At the same time, it is low enough to permit approximately one half of the tightly bound hydrogen to be removed by pumping for 1.5 hours at −195°. If one makes the usual assumption that the hydrogen–deuterium exchange is catalyzed only under those conditions in which dissociative adsorption of hydrogen occurs on a catalyst, then one must conclude that this new third type of activated adsorption is a dissociative type of adsorption, just as it is believed Type A and Type B adsorption are dissociative adsorptions.

It is well recognized that from a theoretical standpoint, the conversion of ortho to para hydrogen over a metallic catalyst at −195° would not necessarily have the same rate as that observed for the hydrogen–deuterium exchange. The zero point energy difference between deuterium and hydrogen is such as to lead one to expect that the hydrogen–deuterium reaction at a given low temperature might be considerably slower than the ortho–para hydrogen conversion, even though each of these reactions is assumed to take place as a result of the dissociative adsorption of hydrogen on the surface of the catalyst. Accordingly, the fact that the hydrogen–deuterium exchange reaction at −195° on the singly promoted catalyst is approximately one hundredth as fast as the ortho–para hydrogen interconversion is not unexpected. However, such a difference in zero point energy probably would not account for the observed factor of 15,000 between the half time for reaction 2 as compared to reaction 1 over the doubly promoted catalyst.

In conclusion it may be pointed out that the present differences between the singly promoted and doubly promoted iron catalysts merely add one more example to the many differences that have already been noted between these two types of catalysts. It is already well known that in ammonia synthesis and decomposition[9] and also in Fischer–Tropsch synthesis the singly and doubly promoted catalysts have very different properties.[10] In the present work, as in most of the previous work,[11] the cause for the difference between the singly and doubly promoted catalysts is unknown; its elucidation will have to await further experimental work.

(8) The tritium must be introduced into the counter tube in order to be counted since its radiation is so weak. A very satisfactory counting procedure consisted of filling the counter tube with 90 mm. partial pressure of hydrogen containing the tritium, 20 mm. partial pressure of isobutane and 50 mm. partial pressure of helium. The threshold voltage was −1200 volts in the tube used (cathode with 1 inch inside diameter) and the plateau was flat for 200 volts.

(9) K. Love and P. H. Emmett, *J. Am. Chem. Soc.*, **63**, 3297 (1941).

(10) H. Koch and R. Billig, *Brennstoff Chem.*, **21**, 157 (1940).

(11) S. Brunauer and P. H. Emmett, *J. Am. Chem. Soc.*, **62**, 1732 (1940).

THE REACTION OF FORMIC ACID WITH CARBOHYDRATES. I. THE REACTION OF FORMIC ACID WITH SUGARS[1]

BY HAROLD TARKOW AND ALFRED J. STAMM

United States Department of Agriculture, Forest Service, Forest Products Laboratory,[2] Madison 5, Wisconsin

Received February 5, 1951

A simple method for following the reaction of formic acid with alcohols is described. It is based on the conversion of unreacted acid to carbon monoxide by means of acetic anhydride. Formic acid is shown to react only with the hydroxyls in positions 4 and 6 in glucose. It is pointed out that, wherever preferential reactivity has been reported for hydroxyls in positions 1, 2 and 3, alkaline activation was required.

Introduction

The reaction between formic acid and acetic anhydride (equation 1) was shown by Schierz[3] to go to completion in a relatively short time at room temperature when catalyzed with tertiary amines.

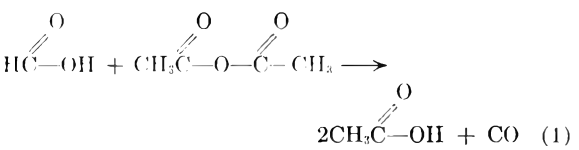

$$HC(=O)-OH + CH_3C(=O)-O-C(=O)-CH_3 \longrightarrow 2CH_3C(=O)-OH + CO \quad (1)$$

He, as well as Behal,[4] noted an evolution of heat on mixing, and suggested that the two reactants first form the mixed anhydride (equation 2) which then decomposes according to equation 3.

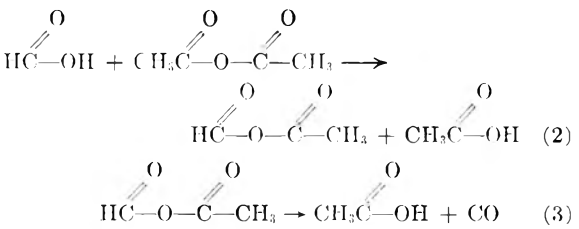

$$HC(=O)-OH + CH_3C(=O)-O-C(=O)-CH_3 \longrightarrow HC(=O)-O-C(=O)-CH_3 + CH_3C(=O)-OH \quad (2)$$

$$HC(=O)-O-C(=O)-CH_3 \rightarrow CH_3C(=O)-OH + CO \quad (3)$$

The over-all reaction (equation 1) has been found to go to completion in a relatively short time in the absence of a catalyst when carried out at the reflux temperature (~143°). However, if an alcohol is added to the formic acid before the anhydride is added, the volume of carbon monoxide collected is less than that equivalent to the weight of acid used. Evidently, some of the formic acid is consumed in esterifying the alcohol. It is only the unreacted formic acid that is converted to carbon monoxide by the anhydride. The possibility of a transesterification reaction (equation 4) occurring, followed by the decomposition of the mixed anhydride (equation 3), is ruled out by the absence of carbon monoxide when methyl formate is treated with the anhydride. Thus, the volume of carbon monoxide collected when an excess amount of acetic anhydride is added to the mixture of alcohol and formic acid is a quantitative measure of the amount of unreacted acid in the mixture. If the amount of acid originally added is known, one can calculate the weight of formic acid that has reacted with the alcohol. Based on this analytical procedure, the interaction of formic acid with a number of hydroxyl-containing compounds has been studied at the Forest Products Laboratory. These have included alcohols, simple sugars and polysaccharides. The results suggest a marked specificity in reactivity of hydroxyl groups in sugars. They also suggest a rapid, simple method for determining the amount of readily accessible material in polysaccharides (see Part II of this report).

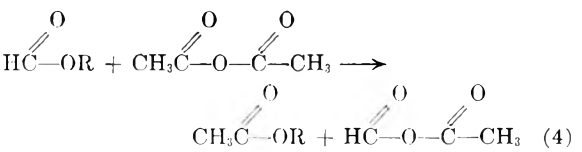

$$HC(=O)-OR + CH_3C(=O)-O-C(=O)-CH_3 \longrightarrow CH_3C(=O)-OR + HC(=O)-O-C(=O)-CH_3 \quad (4)$$

Experimental Procedure

The substance whose reactivity with formic acid is to be measured is weighed out (0.1 to 0.2 g.) into a 7-cubic centimeter round-bottom flask (blown from the neck of a 19/24 S.T. glass joint). If the substance is hygroscopic the flask and contents are set in a vacuum oven at 65° for 2 hours before weighing to get the oven-dry weight. A weighed amount of formic acid is added. The flask is stoppered and the reaction allowed to come to equilibrium. Before the acetic anhydride is added, the bulb of the flask is cooled in ice-water to reduce the loss of formic acid that may occur on removal of the stopper. The flask is almost completely filled with acetic anhydride, a small boiling chip is added, and a connector is inserted that leads through a short length of capillary tubing to a gas-displacing buret. The flask is immediately lowered into an oil-bath thermostated at 146 ± 1°. The gas collected is transferred to an Orsat gas analyzer and analyzed for carbon monoxide.

The weight of formic acid equivalent to the measured volume of carbon monoxide (equation 1) is calculated with the help of the ideal gas law. Subtraction of this weight from the weight of formic acid originally added gives the weight of formic acid that has reacted with the hydroxylic compound. The degree of esterification is expressed as grams of formic acid combined with 100 g. of original material.

Materials.—Materials used in these experiments were: *d*-glucose, sucrose C.P. grade, rhamnose, α-methyl glucoside, cellobiose, 2,3,4 - trimethyl - α - methylglucoside,[5] menthol glucuronide (free acid) used as purchased from a commercial manufacturer without further purification, ethyl alcohol (absolute grade), anhydrous formic acid shown by analysis to be 99% pure. All calculations were corrected for the 1% impurity.

Results

Ethyl Alcohol.—Kailin[6] has shown that, in the absence of a catalyst, formic acid reacts more than 10,000 times as fast with alcohols as does acetic acid. Forest Products Laboratory research has

(1) Presented at the American Chemical Society, Chicago, Ill., September 3-8, 1950.

(2) Maintained at Madison, Wis., in cooperation with the University of Wisconsin.

(3) E. R. Schierz, *J. Am. Chem. Soc.*, **45** 455 (1923).

(4) A. Behal, *Compt. rend.*, **128**, 1460 (1899).

(5) The authors are indebted to Prof. C. B. Purves, McGill University, for a sample of the crystalline material, having a melting point of 94°.

(6) A. Kailin, *Monatsh.*, **62**, 284 (1933).

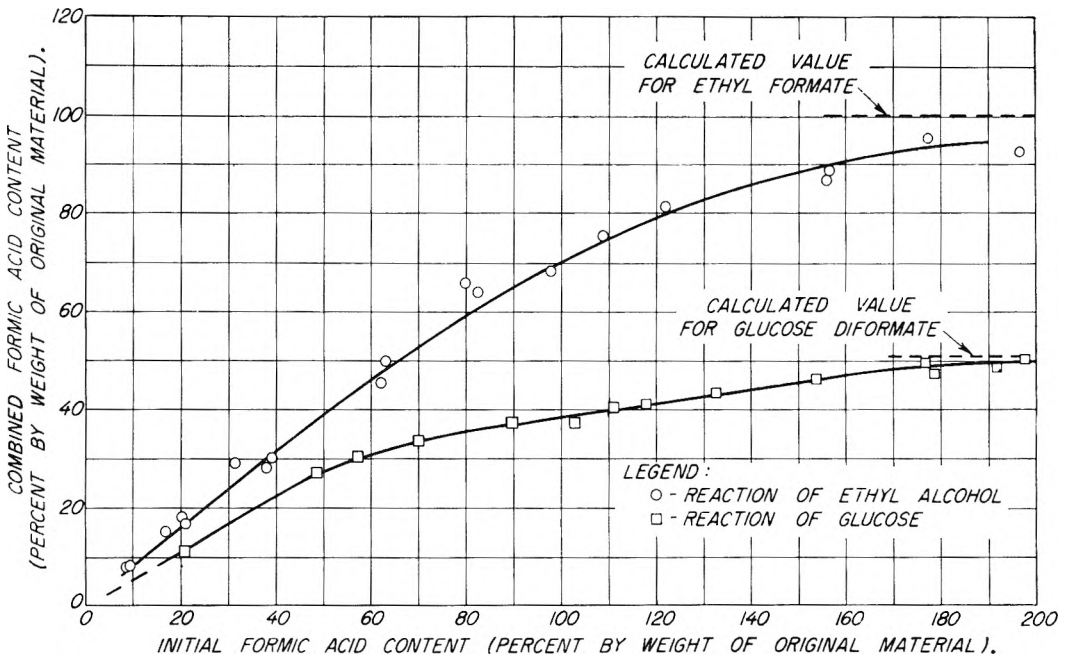

Fig. 1.—Reaction of ethyl alcohol and glucose with formic acid.

shown that formic acid comes to equilibrium rapidly with ethyl alcohol by the fact that, if the reaction mixture is kept at 25° for 2 hours before the anhydride is added, the resulting values are indistinguishable from those obtained after the system is allowed to stand for 3 days. In the Forest Products Laboratory's work with alcohol, however, reaction mixtures were kept overnight at room temperature. The following day acetic anhydride was added to determine the amount of unreacted formic acid. Figure 1 shows the relationship (reaction curve) between the initial concentration of formic acid in the acid–alcohol mixture and the corresponding combined formic acid content at equilibrium. The curve is of the type one would expect for an equilibrium reaction. Note that the combined formic acid rapidly approaches the value of 100%, which is the theoretical value for the monoformate.

Under the conditions used, the small amount of alcohol that did not react with formic acid may have reacted with the acetic anhydride at the reflux temperature. However, the carbon monoxide collected measures directly the amount of formic acid that did not react with the alcohol, and, therefore, indirectly the amount of formic acid that did react. It is not believed that the addition of anhydride upsets the equilibrium, since, if it did, all the formic acid originally added (if less than that required for complete reaction) would have reacted. This, according to Fig. 1, did not occur. The reaction is not novel. It is presented to illustrate the method of following the reaction between formic acid and hydroxylic compounds.

Sugars.—To aid in understanding the reaction between formic acid and polysaccharides, the reaction with simple sugars and derivatives was studied. As with the alcohol, the mixture was kept in the small flask until equilibrium was obtained. It was shown that the degree of esterification is independent of temperature, at least in the range 35 to 55°, with overnight treatment (Fig. 2). Reaction mixtures of sugars and formic acid were kept overnight at 55° before the acetic anhydride was added.

d-**Glucose.**—Figure 1 shows the reaction curve for *d*-glucose. With increasing concentration of formic acid, the resulting combined formic acid increases and finally approaches the value of 57%. This is also the calculated value for the diformate. Thus, only two of the five hydroxyl groups in *d*-

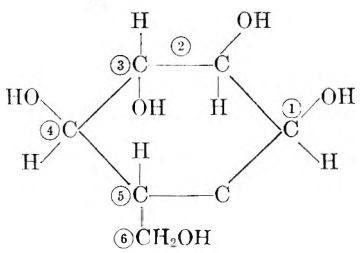

glucose are capable of reacting with formic acid under the conditions previously described.

Rhamnose.—Rhamnose is a derivative of mannose in which the primary alcohol group has been reduced to a methyl group. It forms the monoformate, as is shown in Fig. 3. This fact, when

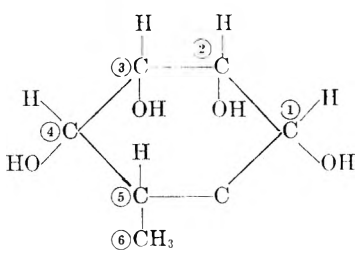

considered with the results for *d*-glucose, suggests that in *d*-glucose the primary hydroxyl is capable of reacting with formic acid.

2,3,4-Trimethyl-β-methylglucoside.—To confirm the finding that the primary hydroxyl does

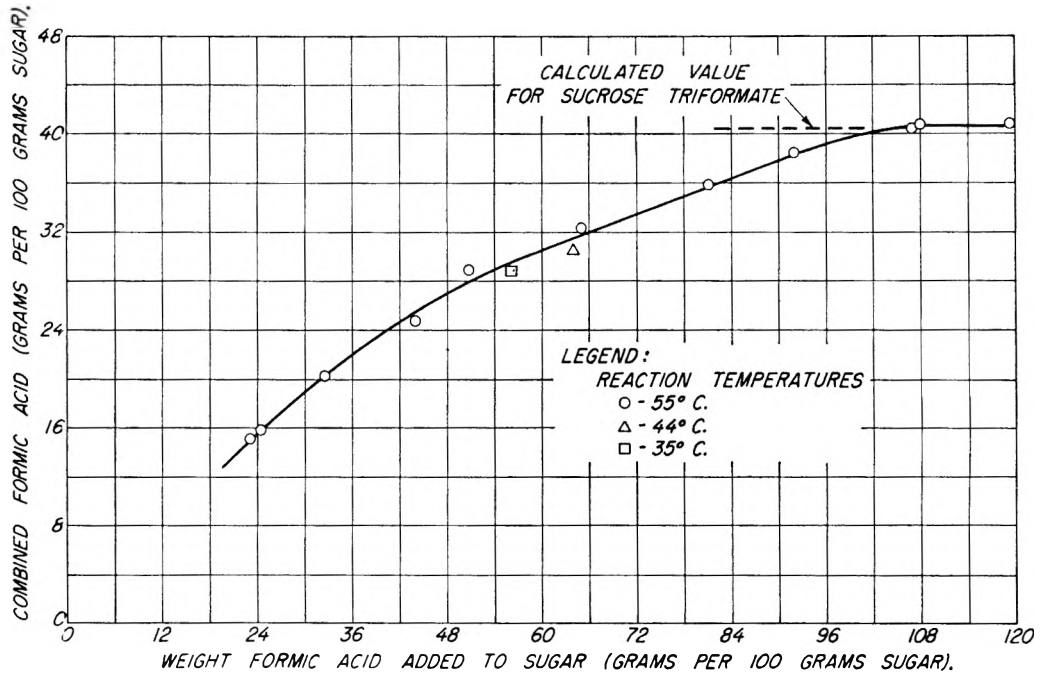

Fig. 2.—Reaction of sucrose with formic acid.

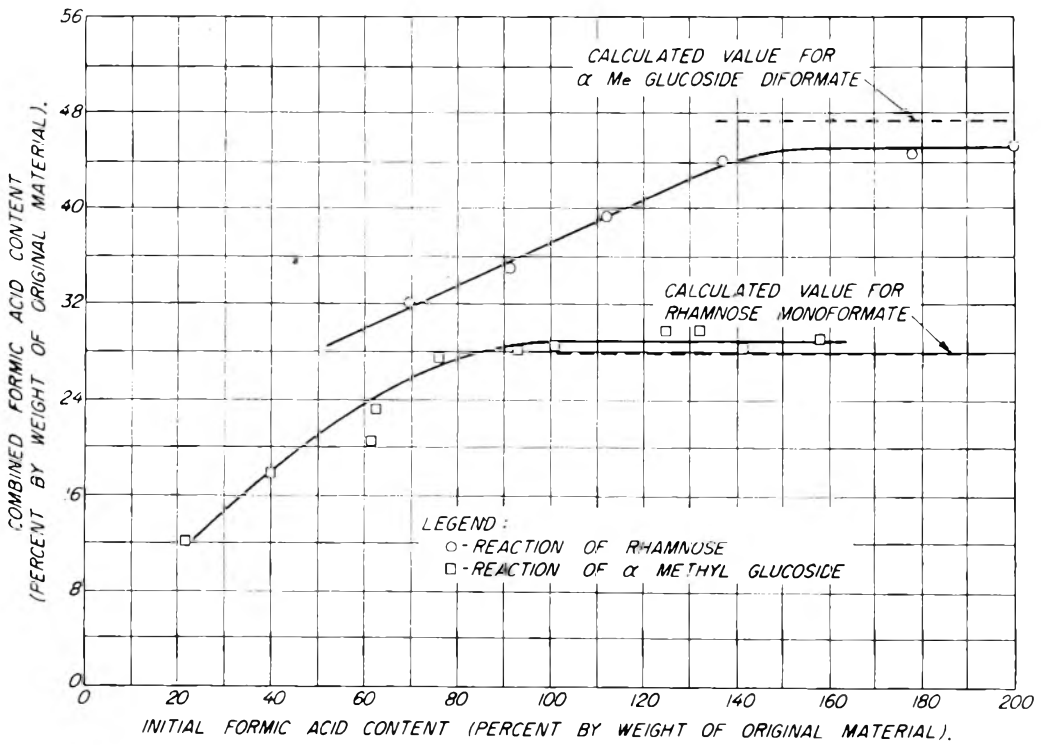

Fig. 3.—Reaction of rhamnose and α-methyl glucoside with formic acid.

react with formic acid, a glucose was used in which all but the primary hydroxyl was methylated.

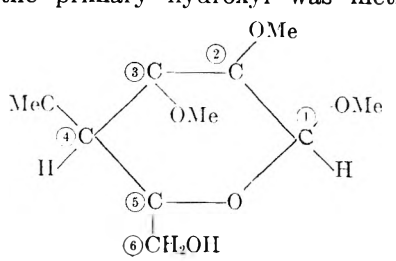

Unfortunately, there was insufficient material to obtain a complete reaction curve. It was observed, however, that when 102 g. of formic acid per 100 g. of this sugar derivative was used, the combined formic acid content was 19.4 g. per 100 g. of sugar derivative, and when 124 g. of formic acid per 100 g. of derivative was used, the combined formic acid content was 18.9 g. The curve was therefore at the plateau. The theoretical value for the monoformate is 19.5 g. per 100 g. of sugar. Therefore, the free primary hydroxyl group of 2,3,4-

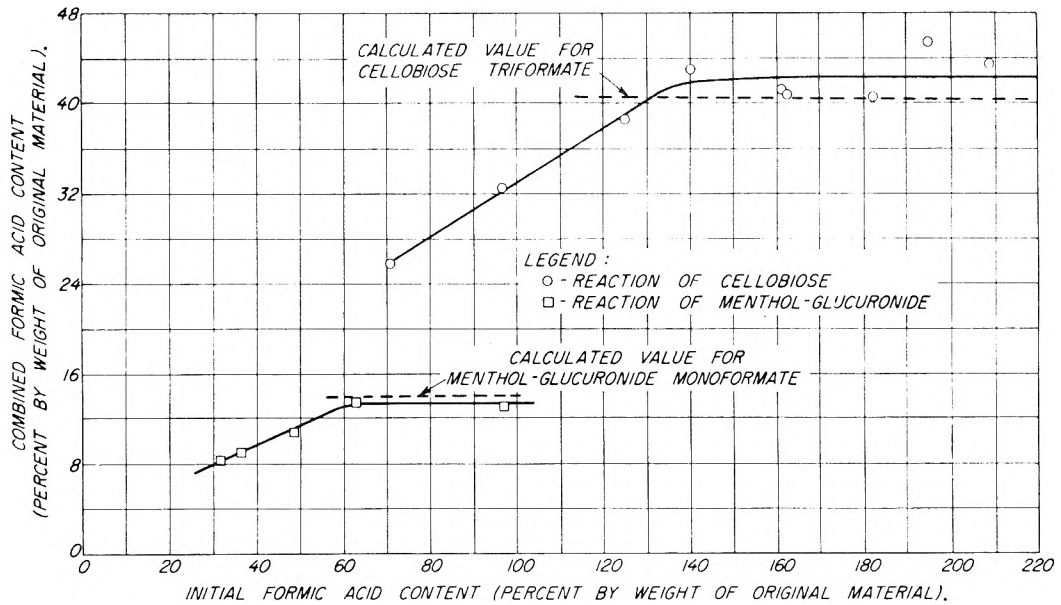

Fig. 4.—Reactions of cellobiose and menthol glucuronide with formic acid.

trimethyl-β-methylgucoside does react with formic acid. Thus, of the two hydroxyls in *d*-glucose capable of reacting with formic acid, one of them is definitely the primary hydroxyl.

α-Methyl-*d*-glucoside.—The maximum combined formic acid content of this sugar derivative corresponds to the diformate (Fig. 3). Considering this together with the result for *d*-glucose, it can be concluded that the hemiacetal hydroxyl (position 1) does not react with formic acid. Thus the remaining hydroxyl group capable of reacting with formic acid, other than the primary, must be attached to position 2, 3 or 4.

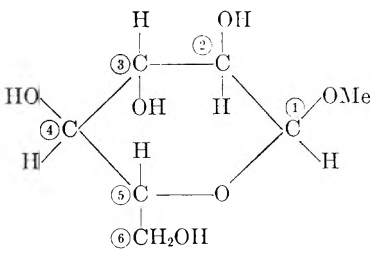

Menthol-*d*-glucuronide.—The observed maximum combined formic acid content of this derivative corresponds to a monoformate (Fig. 4). Again, when considered with the data for *d*-glucose,

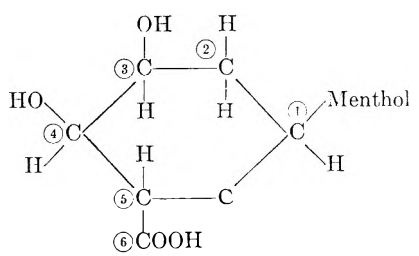

it is concluded that in *d*-glucose, the reactive hydroxyl, other than the primary one, must be attached to position 2, 3 or 4.

Cellobiose.—The maximum combined formic acid content of cellobiose corresponds to the triformate (see Fig. 4). It has been shown that the primary hydroxyl in *d*-glucose reacts with formic

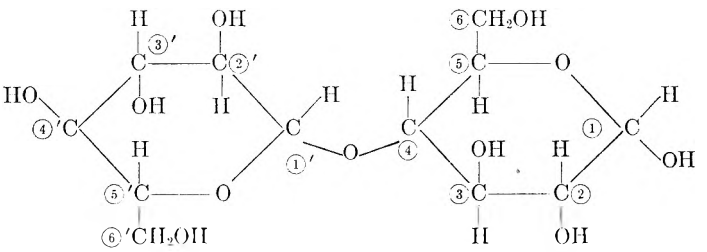

acid. Thus it is quite likely that two of the three reactive hydroxyls in cellobiose are the two primary groups. It has been shown that the hemiacetal hydroxyl does not react. Since the hydroxyls in each of the pairs 2,2′ and 3,3′ would be expected to have similar properties, it is improbable that hydroxyls in these positions react with formic acid; that is, the third hydroxyl in cellobiose capable of reacting with formic acid would not be expected to be found among these two pairs. It is suggested that the free hydroxyl in position 4 of the nonreducing residue is the one capable of reacting with formic acid. It will be shown in the second paper that the hydroxyls in positions 2 and 3 in starch do not react with formic acid.

Carrying these results over to *d*-glucose, it can be concluded that the two hydroxyls in *d*-glucose capable of reacting with formic acid are those in positions 4 and 6.

Sucrose.—Sucrose is shown in Fig. 2 to form a triformate. Sucrose has a furanoid fructose resi-

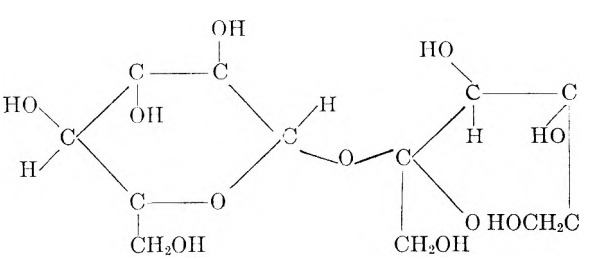

due. The reaction of furanoid fructose and suitable derivatives with formic acid was not studied. Therefore, it is not possible to state which of the hydroxyls in the fructose residue of sucrose do react. That the two primary groups in the fructose residue have different reactivities is shown by recent work on the alkaline hydrolysis of sucrose octaacetate.[7] It would be predicted that the hydroxyls in positions 4 and 6 of the glucose residue do react, leaving one hydroxyl in the fructose residue capable of reacting with formic acid.

Discussion

The reaction of glucose with formic acid has been shown to involve hydroxyls in positions 4 and 6. The literature contains some references to work done on the relative reactivity of the hydroxyls in glucose. The reactions concerned, however, were generally those carried out under alkaline conditions: methylation in the presence of NaOH,[8] and xanthation in the presence of NaOH.[9] The evidence is strong that under such controlled alkaline conditions only those hydroxyls in positions 1, 2 and 6 react.[10] Occasionally, reference is made to a similarity in reactivity of hydroxyls in positions 2 and 3.[8,11] The reactivity of the hydroxyls in positions 1, 2 and possibly 3, under alkaline conditions may be associated with their slightly acidic character.[12,13] The reactivity of the primary hydroxyl, on the other hand, is general and may be attributed to the greater reactivity of such groups in contrast to that of secondary groups. Because of this general reactivity, the primary hydroxyl would be expected to react with formic acid. On the other hand, since the hydroxyls in positions 1, 2 and possibly 3 require alkaline activation for reaction, it is not surprising that they do not react with formic acid.

There are a few references in the literature suggesting the occasional similarity in reactivities of groups in positions 4 and 6. Thus, although tosylation of methylglucoside under mild conditions leads to the formation of the tetra derivative, under more drastic conditions 2,3-ditosyl-4,6-dichloromethylglucoside is formed.[14] Sulfuryl chloride reacts with α-methylglucoside to form the 2,3-sulfuryl-4,6-dichloro derivative.[15] It is of interest to point out that reducing disaccharides containing aldose residues generally contain 1,4 or 1,6 linkages.

With simple sugars there is no question concerning the accessibility of formic acid to the reactive hydroxyls. In the case of polysaccharides, this factor of accessibility is of great importance; it is considered in Part II of this study.

(7) B. Rabinowitch and A. Alexander, *J. Am. Chem. Soc.*, **72**, 293 (1950).

(8) E. G. Percival, *J. Chem. Soc.*, 1160 (1934); 249 (1939).

(9) T. Lieser, *et al.*, *Ann.*, **495**, 235 (1932); **511**, 121 (1934).

(10) T. Temell, 'Studies on Cellulose Reactions," Esselte Aktiebolag, Stockholm, 1950.

(11) E. J. Lorand, *Ind. Eng. Chem.*, **31** 891 (1939).

(12) P. Hirsch and R. Schlags, *Z. physik. Chem.*, **141A**, 387 (1929).

(13) S. P. Sari and P. K. Schonfield, *Proc. Roy. Soc.*, **185A**, 431 (1946).

(14) K. Hess, *Ann.*, **507**, 48 (1933).

(15) B. Helferich, G. Sprock and E. Besler, *Ber.*, **58**, 889 (1925).

THE REACTION OF FORMIC ACID WITH CARBOHYDRATES. II. POLYSACCHARIDES: A NEW METHOD FOR DETERMINING ACCESSIBILITY[1]

BY HAROLD TARKOW AND ALFRED J. STAMM

United States Department of Agriculture, Forest Service, Forest Products Laboratory,[2] Madison 5, Wisconsin

Received February 5, 1951

The maximum degree of interaction of a polysaccharide with formic acid is shown to be a measure of the accessibility of the material. It is shown that the initial formic acid content at which the combined formic acid becomes constant is a measure of the fiber-saturation point. For different polysaccharides, the moisture adsorption at a given relative humidity is proportional to the accessibility. On extrapolating these curves, the moisture adsorptions for 100% accessible cellulose are calculated. Analysis of the moisture adsorptions for such a theoretical cellulose, shows that the adsorption of 3 molecules of water per available glucose residue is not complete even at 90% relative humidity.

The work described in the previous paper[3] showed that only those hydroxyls in positions 4 and 6 of glucose are capable of reacting with formic acid. In the formation of polysaccharides (polyanhydroglucose), the hydroxyl in position 4 is usually eliminated, while the one in position 6 (primary) usually remains free. Although it is free in the sense that it can be identified by chemical analysis, owing to the existence of crystalline and amorphous zones, the primary groups within the crystalline zones may not be reached by mild reagents. It has been shown that different polysaccharides do react to different extents with formic acid and that the variation in degree of reaction can be attributed to variations in the degree of accessibility.

Experimental Procedure

The experimental procedure was similar to that described in the previous paper.[3] The material in the reaction flask was vacuum dried at 65° for 2 hours. After the material was cooled and weighed, anhydrous formic acid was added from a microburet. The flask was then set in an oven at 55° for about 15 hours. It was shown (Fig. 1) that equilibrium is attained under these conditions. After cooling and weighing, the flask was almost completely filled with

(1) Presented at the American Chemical Society, Chicago, Ill., September 3–8, 1950.

(2) Maintained at Madison, Wis., in cooperation with the University of Wisconsin.

(3) H. Tarkow and A. J. Stamm, THIS JOURNAL, **56**, 262 (1952).

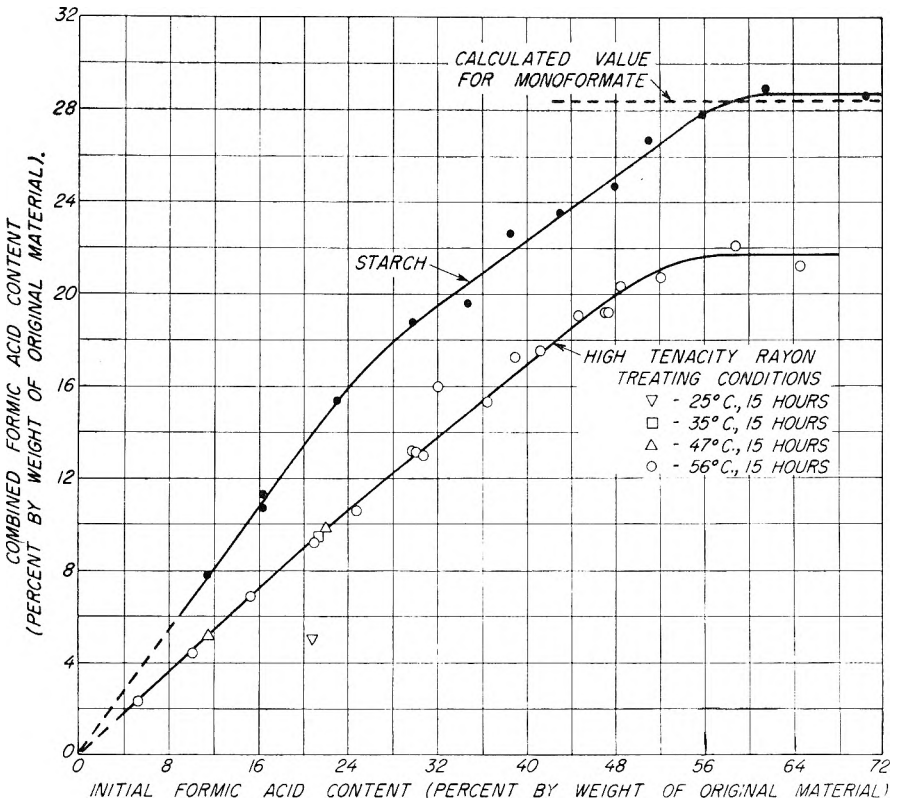

Fig. 1.—Reaction curves for starch and high-tenacity rayon with formic acid.

acetic anhydride and set in an oil-bath at 146° and the gas was collected and analyzed for carbon monoxide.

Materials.—Starch, a commercial, purified starch; cotton, mercerized cotton, flax, high-tenacity rayon; fiber G: These were similar to those used previously in this Laboratory in acid-hydrolysis studies; Cellophane, non-moisture-proof cellophane was thoroughly washed and air dried; Wood, sugar maple cross sections 1 millimeter thick were cut up into 2- by 2-millimeter squares; formic acid, 99% pure. All calculations were corrected for the 1% impurity; acetic anhydride, C.P. grade.

Results

Starch.—Figure 1 shows the reaction curve for starch. The maximum combined formic acid content is 28.7%. This agrees well with the value of 28.4% calculated for the monoformate. Since the previous paper[3] showed that in glucose only those hydroxyls in positions 4 and 6 react, it can be concluded that in starch only the primary hydroxyl reacts with formic acid. Hixon[4] has shown that starch reacts with formic acid to form only a monoformate. On the basis of the amount of periodic acid consumed by the ester, he showed that the formyl group is attached in the primary position. The fact that the observed maximum combined formic acid content agrees reasonably well with the calculated value indicates that starch contains very few, if any, primary hydroxyl groups which cannot react with formic acid.

High-tenacity Rayon.—Figure 1 shows the reaction curve for a high-tenacity commercial rayon. The maximum combined formic acid content is about 21.8%. The fact that this value is smaller than the theoretical value (28.4%) suggests the presence of regions into which formic acid cannot enter, or in which the primary hydroxyls are involved in hydrogen bonding of such intensity as not to be broken by formic acid. The ratio 21.8/28.4 × 100, or 77%, is, therefore, the per cent. of all the primary groups in this rayon accessible by formic acid.

Flax.—The maximum combined formic acid content is shown in Fig. 2 to be 8.4%. Evidently only a small fraction of the primary hydroxyls is accessible; that is, only 8.4/28.4 × 100, or 30%.

Cotton, Rayon and Cellophane.—Figures 2, 3 and 4 present reaction curves for native and mercerized cotton, Fiber G (a rayon), and cellophane.

If it is assumed that for every available primary group a glucose residue is made available, then the accessibilities of the primary groups are also the accessibilities of the glucose residues. It is not likely that chain degradation occurs. This is suggested by the inability of formic acid to break the glycosidic bonds in α-methylglucoside and in cellobiose.[3] Furthermore, no harmful effect on toughness is observed on treating wood with anhydrous formic acid. In the absence of chain degradation,[5] recrystallization very likely does not occur. Table I lists the accessibilities of the various carbohydrates that were tested. Since the method depends on the reaction between formic acid and primary hydroxyl groups in pyranose residues, some doubt arises in the interpretation of the data for carbohydrates containing appreciable amounts of pentosans, polyuronides and lignin. For this reason, the value obtained for maple is not included in the table.

(4) D. Gottlieb, C. G. Caldwell and R. M. Hixon, *J. Am. Chem. Soc.*, **62**, 3342 (1940).

(5) V. J. Brenner, J. A. Frilette and H. Mark, *ibid.*, **70**, 877 (1948).

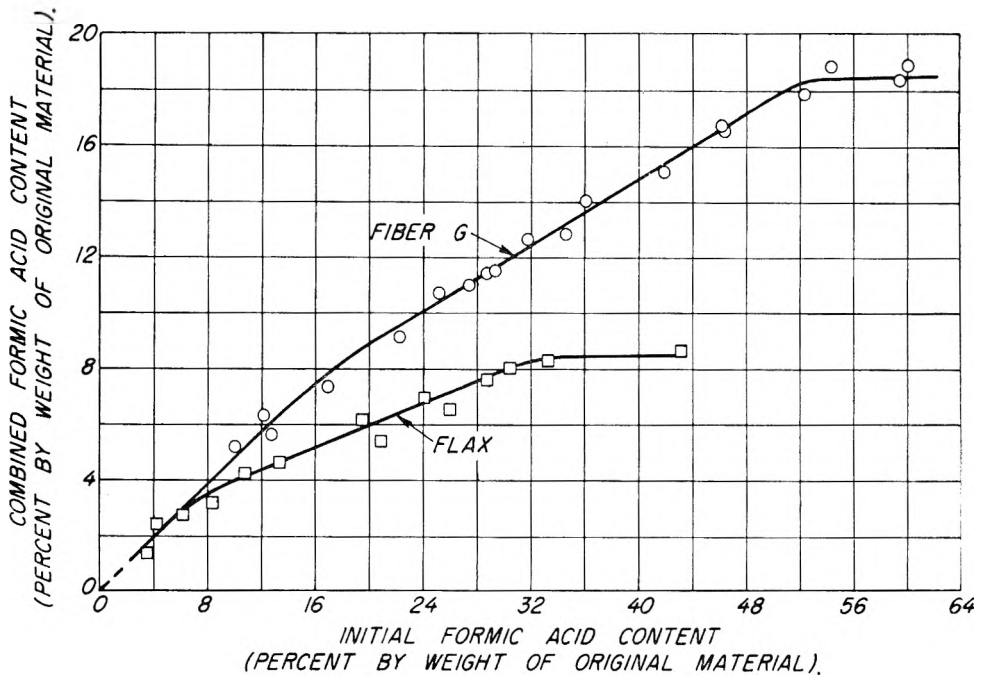

Fig. 2.—Reaction curves for flax and Fiber G with formic acid.

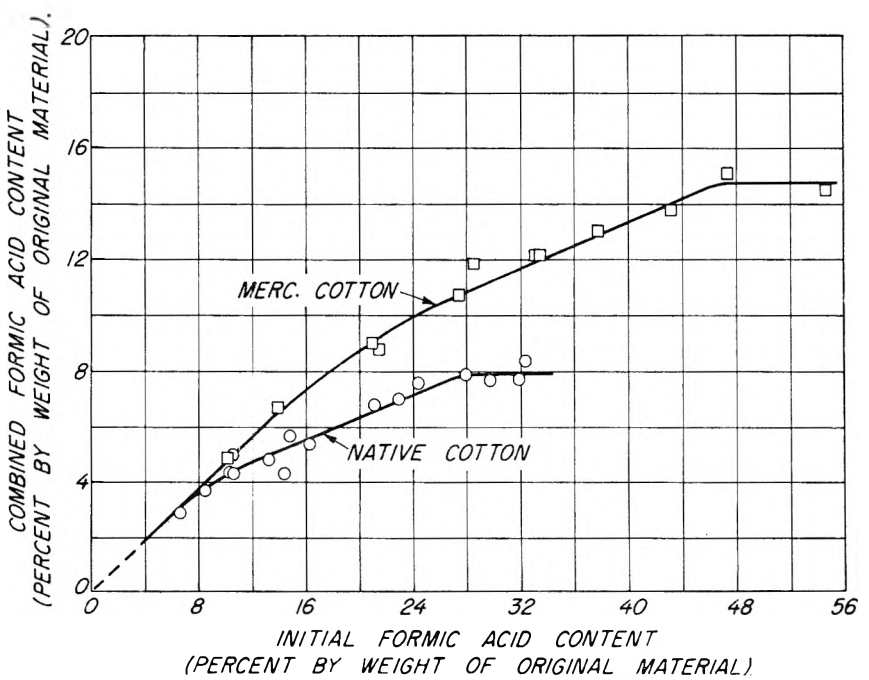

Fig. 3.—Reaction curve for native and mercerized cotton with formic acid.

TABLE I

ACCESSIBILITIES OF VARIOUS CARBOHYDRATES AS DETERMINED FROM FORMIC ACID REACTIVITY

Material	Accessibility, %
High-tenacity commercial rayon	77
Cellophane	72
Fiber G	65
Mercerized cotton	52
Douglas fir holocellulose	48
Alpha pulp No. 1	47
Alpha pulp No. 2	35
Flax	30
Native cotton	28

No attempt was made to convert these accessibilities to per cent. crystallinities since there is doubt about the size of the crystallites.[6] Timell[7] has recently summarized and critically reviewed the various physical and chemical methods for measuring accessibilities. He concludes that native cotton is 30 to 40% accessible, while rayons are 60 to 70% accessible. The good agreement with the values in Table I is interesting in view of the fact that formic acid swells polysaccharides more than water does.

(6) J. Howsmon, *Text Res. J.*, **19**, 152 (1949).

(7) T. Timell, "Studies on Cellulose Reactions," Esselte Aktiebolag, Stockholm, 1950.

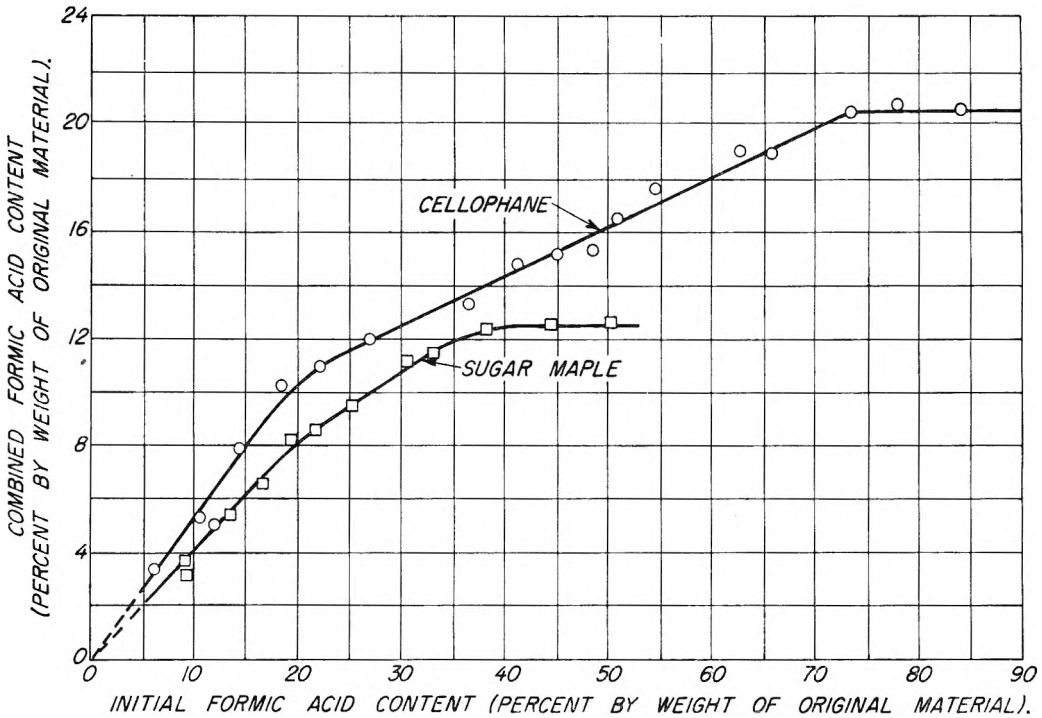

Fig. 4.—Reaction curve for cellophane and sugar maple with formic acid.

(It swells cellophane in the "cross-machine" direction 1.9 times as much as water, and it swells maple in the tangential direction 1.8 times as much as water does.) This suggests that beyond a certain degree of swelling in formic acid, no more primary hydroxyl groups are made available. This is clarified in the following discussion.

Consider the reaction curve for maple (Fig. 4). Unlike the reaction between formic acid and an alcohol, where all hydroxyls are immediately available, the hydroxyls in polysaccharides become increasingly available as more formic acid is added; that is, as the wood swells. The curve shows that, when at least 38 g. of formic acid has been added to 100 g. of wood, the combined formic acid becomes constant even though the wood is capable of taking up more than 38 g. of formic acid into its cell walls. This weight corresponds to 31 cubic centimeters if it is assumed that the initially adsorbed formic acid has its normal density. The wood substance can be assumed to swell by 31 cubic centimeters for this degree of adsorption. This, of course, is a rough approximation, as any adsorption compression is neglected.[8] It assumes the absence of submicroscopic voids within the cell wall[9] and it neglects the small amount of formic acid vapor in the dead space of the flask.

As swelling continues beyond 31 cubic centimeters, no additional reactive groups are exposed. It is of great interest that this value, 31 cubic centimeters, is approximately the generally accepted value for the fiber-saturation point of wood; that is, it is the volume by which 100 g. of extractive-free wood swells under stress-free conditions in water.[10] It is therefore concluded that the maximum number of primary hydroxyl groups are made available when the degree of swelling in formic acid is equal to that by which the original wood swells in water. Swelling beyond this volume exposes no more primary groups. This means that either formic acid does not penetrate the crystalline regions, or that if it does, it does not break those hydrogen bonds involving primary groups. For polysaccharides composed of native cellulose, it may be the former, as the X-ray diffraction pattern of wood treated with formic acid is similar to that of untreated wood.

Further evidence that the abscissa of a reaction curve corresponding to the beginning of the plateau is a measure of the fiber-saturation point was shown in another manner. Consider the curve for cellophane in Fig. 4. The combined formic acid content becomes constant when 73 g. or 60 cubic centimeters of formic acid has been added to 100 g. of cellophane. From the previous discussion, it would be concluded that 100 g. of cellophane would swell by 60 cubic centimeters in water; that is, it would adsorb about 60 g. of water at 100% relative humidity.

A sheet of wet cellophane was suspended in a 97% relative humidity room and weighed every 10 minutes (Fig. 5). During the first 50 minutes the rate of evaporation was constant. The rate then decreased continuously and presumably would have reached the value of zero, when the equilibrium moisture content for these conditions was reached. The linear portion is interpreted as being due to the evaporation of free water. When the free water has evaporated, further evaporation occurs from the swollen material. The point of intersection represents the weight of water in 100 g. (dry basis) of swollen cellophane containing no free surface water. This value, 65 g., agrees

(8) A. J. Stamm and R. M. Seborg, THIS JOURNAL, **39**, 133 (1934).

(9) P. H. Hermans, "Contribution to Physics of Cellulose Fibers," Elsevier Publishing Co., Amsterdam, 1946.

(10) A. J. Stamm, *Ind. Eng. Chem., Anal. Ed.*, **1**, 94 (1929).

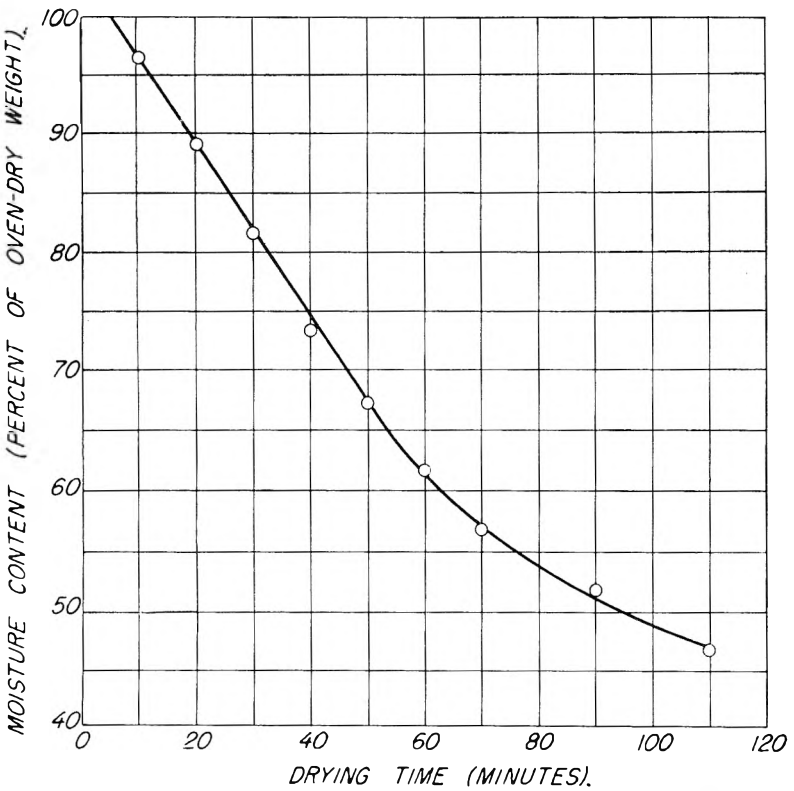

Fig. 5.—Determination of the fiber-saturation point of cellophane by measuring the rate of loss of moisture from the initially water-logged condition as a function of time at 97% relative humidity.

reasonably well with the value determined from the formic acid reaction curve.

swollen to make available all the non-hydrogen-bonded primary hydroxyl groups.

Relationship between Accessibility and Moisture Adsorption.—Howsmon[6] has shown that a linear relationship exists between accessibility and moisture adsorption at 58% relative humidity. He implied that other humidities could have been used. This is confirmed in Fig. 6 which shows the relationship between accessibility and moisture adsorption at 50 and 90% relative humidity. Considering the variety of carbohydrates, it can be concluded that moisture adsorption at some arbitrary relative humidity is a relative measure of accessibility.

The exact mechanism whereby this water is held is not clear. Purves[11] believes that at 50% relative humidity, every available glucose residue can adsorb 3 molecules of water. Hermans[9] also postulates direct interaction and even proposes the structure of the two hydrates which, he claims, cellulose can form under certain conditions. One difficulty in the elucidation of the mechanism arises from the existence of accessible and non-accessible regions in carbohydrates. This difficulty can be avoided by extrapolating the curves to 100% accessibility to determine the moisture adsorption of a completely accessible cellulose. This

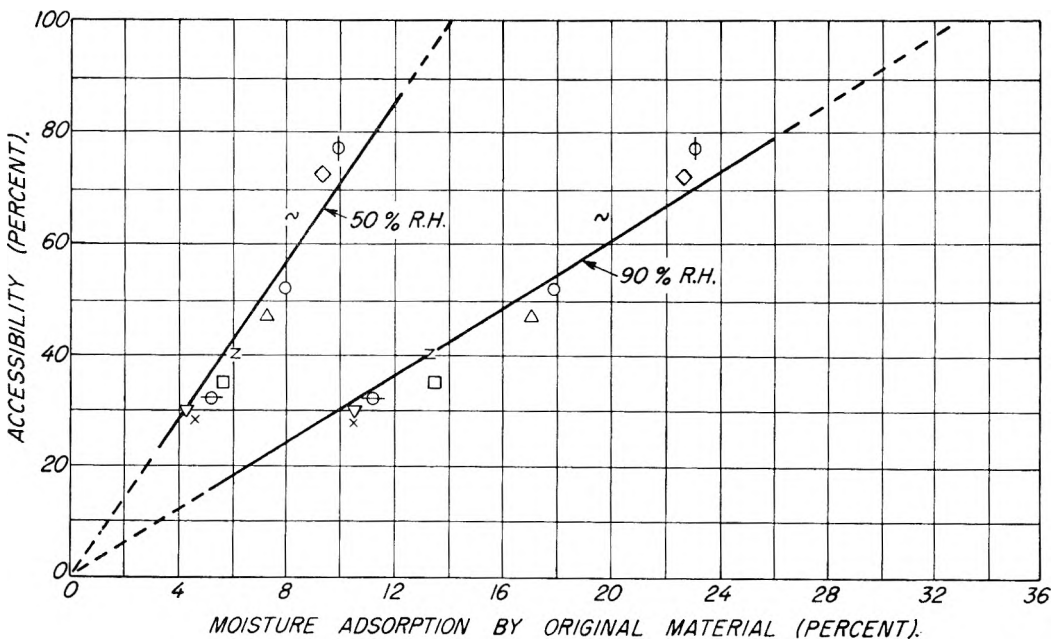

Fig. 6.—Relationship between accessibility and moisture adsorption of the original material at 50 and 90% relative humidity: high-tenacity rayon, ⓘ; fiber G, ~; Cellophane, ◊; alpha pulp No. 1, □; alpha pulp No. 2, Δ; native cotton, x; mercerized cotton, ○; flax, ▽; cotton linter, ⊖; highly beaten linter, z.

The term fiber-saturation point can thus be given a chemical interpretation: It is the minimum volume by which 100 g. of polysaccharide must be

(11) A. C. Assaf, R. H. Haas and C. B. Purves, *J. Am. Chem. Soc.*, **66**, 66 (1944).

has been done in Fig. 6. It will be noted that at 50 and 90% relative humidity such a theoretical cellulose would adsorb 14 and 33% moisture, respectively. It is not known what fraction is held directly on hydroxyl groups and what fraction is held as water of condensation; however, it is reasonable to assume that a large fraction of the water adsorbed at 50% relative humidity is held directly by hydroxyl groups. Assume all of it is held this way; then, according to the extrapolated value in Fig. 6, each glucose residue would adsorb $1^1/_3$ molecules of water at 50% relative humidity. This throws doubt on Purves' contention that at this humidity, each available glucose residue adsorbs 3 molecules of water. At 90% relative humidity, some of the adsorbed water very likely is held as water of condensation. According to Fig. 6, 100% accessible cellulose should adsorb 33% moisture at this humidity; therefore, the amount of water held directly on hydroxyl groups is somewhat less than 33 g. per 100 g. of cellulose or somewhat less than 3 molecules of water per glucose residue. The remainder of the sorbed water is present as capillary condensed water. Perhaps only at 100% relative humidity will each available glucose residue have adsorbed directly 3 molecules of water. This seems reasonable, considering the fact that swelling in water with its resultant exposure of new surface is completed only at 100% relative humidity.

Acknowledgment.—The authors are indebted to Prof. M. L. Jackson of the University of Wisconsin Soils Department who placed at their disposal his department's X-ray diffraction equipment.

Addendum

A recent paper by Nickerson[12] on the accessibility of cellulose determined by formic acid esterification has just come to our attention. His values are appreciably lower than ours. He obtained a rapid initial rate of esterification, followed by a slow but continued reaction with time, even beyond the monoformate stage at room and slightly elevated temperatures. At a given temperature and for various reaction times, he measures the ratio of combined formic acid in a cellulose to that in starch. On extrapolating these ratios to zero time, he gets an instantaneous ratio which he calls the accessibility of the cellulose. This ratio of reaction rates, however, increases with time and eventually seems to level off. Roughly speaking, our work differs from Nickerson's in that, we were interested in the final value of the ratio, whereas he was interested in the initial value. Several questions can be raised concerning his treatment. His method assumes that the rate of reaction of starch with formic acid is equal to that of accessible cellulose. Starch is an α-glucoside with a zigzag chain. Celluloses are β-glucosides with straight chains. Do these have similar rates of reaction? Starch contains branched chains which make for a highly open structure. (A comparison of the densities of starch and highly amorphous cellulose might show this.) Would not the rate of diffusion of formic acid through the starch be greater than through the amorphous cellulose? Water is a reaction product and its accumulation would tend to retard esterification. Would not the more open structure of starch permit the water to diffuse out faster than out of cellulose? Some doubt is thus raised about identifying the initial ratio of the rate of reaction of a cellulose to that of starch as a measure of the accessibility of the cellulose.

In Nickerson's work, the ratio of formic acid to carbohydrate was high, about 50 to 1. In our work it was relatively low (generally less than 1 to 1). When the combined formic acid (in our procedure) begins to level off, the activity coefficient of the formic acid is still appreciably less than unity. (The cellulose is not in the completely formic-acid-swollen state.) Perhaps only when a large excess of formic acid is present so that the activity coefficient is unity does the reaction with secondary hydroxyls become significant.

(12) R. F. Nickerson, *Text. Res. J.*, **21**, 195 (1951).

BROWNIAN MOVEMENT AND ELECTRICAL EFFECTS[1]

BY MAX BENDER[2] AND HENRY MOUQUIN

Department of Chemistry, New York University, New York, N. Y.

Received February 6, 1951

1. Brownian activity stops in the Taggart shallow cell when the electrolyte changes from alkali to acid, because the particles become attracted to the glass walls as a result of the changes in electrostatic forces. 2. In this connection a means of estimating the sign and intensity of electrical charge on a glass surface in the presence of different solutions of electrolytes is presented. 3. Even though a suspension is at the isoelectric point, flocculation may not happen. For instance, with sphalerite, flocculation did not occur in acid medium (even 0.1 *M* H_2SO_4) or in concentrated NaCl, the suspensions being close to the isoelectric point. With aluminum chloride, flocculation occurred only in alkaline solution, not in distilled water or acid. 4. The Brownian movement of sphalerite particles was found to be different in one electrolyte medium compared with another. It was lowest in the alkaline aluminum chloride flocculating medium, the activity being $^1/_3$ that predicted by Einstein's theory. In alkaline medium only, it was somewhat over $^1/_2$ that of Einstein, and in acid medium only, almost $^2/_3$. 5. The displacement due to Brownian movement of sphalerite particles in 0.001 *M* Na_2CO_3 medium is about $^1/_3$ greater when measured in a shallow cell than when in a deep cell. 6. This enhanced displacement of sphalerite in the shallow cell along with the observations of Henri and Lucas indicates that the shallow cell serves to accentuate the effect of electrical charge on Brownian movement, for the walls of the cell are close to the particles. Thus, the variations in Henri's results might be explained. 7. In samples of suspension of low electrolyte content and near the isoelectric point, particles (in the deep cell) were observed to have markedly different Brownian motion, as well as different cataphoretic velocities. Those particles with higher Brownian activities generally had a higher cataphoretic velocity (or zeta potential). 8. Likewise, qualitative observations in the shallow cell point to electrical environment affecting pedesis. Attraction forces or repulsion forces or a combination of both are seen to be involved with the Brownian activity, the effects acting over a relatively "long range." 9. A reasonable agreement was found between the time-displacement data observed for sphalerite and the Einstein expression which theoretically relates time and displacement. Comparison of the data with that obtained by Henri for latex shows still closer correlation even though the systems and conditions under consideration are markedly different. 10. This research indicates that electrical forces influence the Brownian movement. Nevertheless, molecular collisions (density fluctuations) must be considered, and the Einstein relationships between the displacement and the time, the viscosity, the temperature and the radius hold at least roughly. But allowance should be made for the ionic content of the medium, and the zeta potential of the particles and nearby walls.

Introduction

Reliable data on the quantitative aspects of Brownian movement are rare. The early experimenters largely concentrated their efforts in demonstrating the validity of the Einstein equation.[3] Occasionally, however, there have appeared results which seemed to indicate that factors other than those envisaged in the classical equation might influence the amplitude of the Brownian movement, notably the possible effect of electrolytes on aqueous suspensions.

Unfortunately, none of the previous workers in this field have published data giving simultaneous measurements of size, charge and amplitude of Brownian movement on given particles under known conditions. The experimental part of this paper is an attempt to remedy this lacuna.

Admittedly, much more information is necessary before arriving at any final explanation. Nevertheless, a very brief analysis of the various theoretical possibilities has been appended herein.

Henri[4,5] in 1908, claimed that the pedesis of rubber latex globules varied in intensity depending on the presence and nature of electrolyte dissolved in the suspending medium. His particles were spherical, having a relatively uniform radius of about one micron. The greatest displacement was in distilled water. This activity was practically four times that calculated with the Einstein formula. When the medium was alkaline, Henri observed a displacement one-half that which he found in distilled water and when acidic, it was one-ninth. Henri used a shallow cell.[6]

Henri's experimental technique, involving cinematography, appears to have been above any real important criticism. Actually, there was in his work an approximate check of the classical displacement–time relationship and the acknowledgment of this by Perrin,[7] Chaudesaigues,[8] and Svedberg[9] indicates approval of Henri's methods. Burton,[10] refers to Henri's "very reliable results of the motion in pure solvents and also in these solvents after impurities were added."

Despite the great amount of work by Perrin and his collaborators and by Svedberg,[11] which tended to conform with the classical theory, Henri's work was not actually disproven and we have Duclaux[12] as late as 1938 in his extensive review on Brownian movement pointing out in no uncertain terms the contradictions in the literature regarding the possible effect of electrical charge on pedesis.

A recent disagreement with the classical ideas of Brownian movement was voiced by Taggart and

(1) The data cited in this paper are from M. Bender, "Brownian Movement—Electrical Charge—Flocculation," Ph.D. Dissertation, New York University, 1949. See also this thesis for a comprehensive survey on Brownian movement literature relative to this work.

(2) Calco Chemical Division, American Cyanamid Company, Bound Brook, New Jersey.

(3) A. Einstein, *Ann. Phys.*, **17**, 549 (1905); **19**, 371 (1906); translations by A. D. Cowper, in "Investigations on the Theory of the Brownian Movement," Methuen Co., Ltd., London, 1926.

(4) V. Henri, *Compt. rend.*, **146**, 1024 (1908)

(5) V. Henri, *ibid.*, **147**, 62 (1908).

(6) Distinction should be made between shallow cell (generally prepared by placing a drop of the suspension being examined between microscope glass slide and cover-glass) and deep cell. From observations, the shallow cell usually has an inside height no greater than 35μ. Very often this height is considerably less depending on the investigator's technique. The deep cell, on the other hand, has an inside height of over 100μ.

(7) J. Perrin, *Ann. Chim. Phys.*, **18**, 1 (1909).

(8) Chaudesaigues, *Compt. rend.*, **147**, 1044 (1908).

(9) T. Svedberg, "Colloid Chemistry," 2nd Ed., The Chemical Catalog Co., Inc., New York, 1928.

(10) E. F. Burton, "The Physical Properties of Colloidal Solutions," 3rd Ed., Longmans, Green, and Co., London, 1938, p. 68.

(11) T. Svedberg, Nova Acta Regiae Societatis Scientiarum Upsaliensis Ser. IV, **2**, NI (1907), or "Studien zur Lehre von den Kolloiden Lösungen," Dissertation, 1907; translation in Ion, **1**, 373 (1909).

(12) J. Duclaux, "Traité de Chimie Physique," Tome II, Hermann & Cie, Paris, Chapitre V (1937) and Chapitre VI (1938).

his collaborators[13-16] in connection with studies pertaining to ore flotation. The claims were that the Brownian activity (of mineral particles like quartz, galena, sphalerite and pyrite, etc.) could be stopped or revivified at will by the addition of given electrolytes to the aqueous suspension, and that there was a region of solubility of the surface compound on the particle (*i.e.*, between 1 and 40 mg. per liter) only within which, Brownian movement occurred. In this work Taggart took care to keep the suspension sufficiently dilute so that there would not be a variation in actual particle size. His observation cell was shallow.

In 1945, Kellogg[17] criticized Taggart's viewpoints. This was based on qualitative experiments including comparative observations in both deep (500 μ) and shallow cells, the correlations he found between slime-coating and lack of Brownian movement in a shallow cell or at the bottom of a deep cell, and his observations of Brownian activity where the "surface compounds" were outside the limits of Taggart's Brownian movement-solubility curve.

Finally, one more disagreement with classical theory can be given. Lucas[18] in 1938 mentioned *retarding* the Brownian motion of Hevea rubber globules by diluting the latex with 7% sodium chloride solution. He made use of this effect in his ultraviolet photographic work. Since the particles were caused to be in *subdued* movement, he was able to obtain clear photographic images. The observation cell was shallow, it being prepared by placing a quartz cover-glass over a drop of the suspension on a quartz slide, and blotting out excess liquid. Spence,[19] in 1908, had made similar observations of reduced Brownian movement activity of Hevea latex in saline solution.

Experimental and Discussion

Although most of this literature is consistent in the sense of pointing out the inadequacies of the classical theory of Brownian movement, nevertheless, it is difficult to deduce interconnecting theory (at least on a general basis) between the different authors. Much of it, as outlined above, is qualitative, and more quantitative displacement and electrical charge data are now attempted to the solution of this problem.

The experiments in this work are grouped in several sections. First, a resumé of qualitative observations and tests made along the lines of previous workers is given. Second, the electrical charges were measured on particles and on cell walls under a variety of conditions. From these it also was possible to establish the necessary conditions of electric neutrality on the particles. Third, the amplitude of Brownian movement and the particle size were measured simultaneously. Finally, qualitative experiments were carried out in order to help more fully develop the theoretical implications. One series of these observations shows connections between the zeta potential of particles and their Brownian activity. Another series indicates how attraction forces and repulsion forces become interrelated with the Brownian movement.

I. **Preliminary Observations and Tests.**—These were carried out in verification and extension of the work both of Taggart and of Kellogg. Preliminary tests showed that the finely divided particles of sphalerite conformed well to Taggart's predictions; accordingly, this material was used in the later and quantitative parts of this research.

Numerous attempts showed that Taggart's results could not be duplicated in deep cells. For example the Brownian movement of sphalerite particles could not be stopped under deep cell conditions by addition of dilute sulfuric acid—quite different to what is observed in shallow cells. The solubility criterion advanced in the Taggart hypothesis fell down when applied to such simple suspensions as silver iodide or calcium sulfate, both having a solubility range outside the critical region. Furthermore, the typical adhesion to the glass bottom (and top) of a cell could be demonstrated both by a simple flow technique and even by micromanipulation. Finally, it was observed that chemical treatment with diethyl germanium oxide[20] of the glass cell surface delayed stopping of Brownian movement in the Taggart cell thus proving that the cell surface was involved in the reaction.

II. **Electrokinetics. a. Particle Charge and Wall Charge.**—Although the above observations point quite conclusively that adherence to cell walls (glass) is the cause for Taggart's particles having ceased their Brownian movement, the phenomena involved can be better understood as well as confirmed if the electrical charge data are known for the particles and surface(s) under consideration.

It was decided to use the Northrup–Kunitz rectangular cell in this connection because not only could it be employed to measure particle electric charge, but also hydrodynamic theory (see Abramson)[21] predicts that data pertaining to glass wall charge can be obtained by an analysis of the electro-osmotic flow occurring in such a cell. The direction and amount (or velocity) of the electro-osmotic flow naturally depends on the cell wall. By algebraically adding the true particle cataphoretic velocity (*i.e.*, that observed at the usual Smoluchowski levels in the cell, which levels are at or near $^1/_5$ and $^4/_5$ the cell height) and the velocity of the particles when they are close to the glass cell surfaces, it becomes possible to evaluate the direction and velocity of the liquid (electro-osmotic flow) at the walls, and accordingly obtain a relative idea of the sign and amount of charge on the glass. The direct values of these liquid velocities were used and no attempt was made to translate them to zeta potentials by means of any of the standard equations such as the Helmholtz equation.

After preliminary experiments showed that the usual hydrodynamics of a rectangular cataphoresis cell were being obeyed and that the amount of bow in the curve of a cell height *vs.* particle velocity was affected by the acidity of the suspension, it was considered valid to calculate velocity data of liquid at the glass surface due to electroendosmosis, and use this liquid velocity to show relative charge of the cell walls. The results of such calculations are given in Table I for six suspensions[22] of sphalerite in alkaline (*p*H 10.1, 8.9), distilled water (*p*H 6.6), and acid (*p*H 4.3, 2.9, 2.6) media. True average cataphoretic velocity (C.V.) is given for these six suspensions and also for two additional ones of greater acidity, namely, 0.01 and 0.1 *M* H_2SO_4. Zeta potential data are also contained therein.

Figure 1 represents a graph of this C.V. and liquid velocity data as a function of *p*H. Note how markedly the

(13) T. C. Fitt, "The Brownian Movement and the Reactions at the Surface of Zinc Sulfide Particles in Solutions of Sodium Arsenate," Doctoral Thesis, Columbia University (194-).

(14) T. C. Fitt, A. W. Thomas and A. F. Taggart, A.I.M.E. Tech. Pub. No. 1575 (1943).

(15) A. F. Taggart, *J. Phys. Chem.*, **36**, 130 (1932).

(16) A. F. Taggart, T. C. Taylor and A. F. Knoll, Transactions, A.I.M.E., **87**, 217 (1930); or A.I.M.E. Tech. Pub. No. 312 (1930).

(17) H. H. Kellogg, A.I.M.E. Tech. Pub. No. 1841 (1945).

(18) F. F. Lucas, *Ind. Eng. Chem.*, **30**, 146 (1938).

(19) D. Spence, *India Rubber Journal*, **36**, 233 (1908).

(20) This material was contributed by Dr. H. H. Anderson of the Chemistry Department, N.Y.U., 1949.

(21) H. A. Abramson, "Electrokinetic Phenomena, and Their Application to Biology and Medicine," The Chemical Catalog Company, Inc., New York, N. Y., 1934.

(22) All the suspensions employed in the research, contained 0.0125% by weight of sphalerite in given electrolyte solution of given concentration. This gave an optimum number of particles in the field of the microscope for observing cataphoresis or Brownian movement displacement. Also, this concentration of particles was sufficient to clearly display flocculation phenomena.

In preparation, the 0.0125% suspension was formed by dilution of 0.025% suspension in distilled water volumetrically in half with the requisite electrolyte solution. The distilled water suspension was obtained by grinding that weighed out quantity of powdered sphalerite necessary for 1 liter, in the "Diamonite" mortar and pestle with a few drops of water. More water was gradually added and grinding continued. Then the slurry was transferred to a volumetric flask and the balance of the water gradually added with shaking.

TABLE I

AVERAGE C.V.,[a] ZETA POTENTIAL AND AVERAGE LIQUID VELOCITY[a] AT DIFFERENT *p*H

*p*H	10.1	8.9	6.6	4.3	2.9	2.6	2.2	(1.45)[b]
Concn.	(0.001 *M*)	(0.0001 *M*)		(0.00006 *M*)	(0.001 *M*)	(0.002 *M*)	(0.01 *M*)	(0.1 *M*)
Electrolyte	(Na_2CO_3)	(Na_2CO_3)	(Dist. H_2O)	(H_2SO_4)	(H_2SO_4)	(H_2SO_4)	(H_2SO_4)	(H_2SO_4)
C.V. av. (true)	− 2.11	− 2.09	− 1.51	− 2.10	− 1.12	−0.08	−0.44	(0)
ζ (mv.)	−27.5	−27.2	−19.6	−27.3	−14.6	−1.0	−5.8	(0)
Velocity H_2O[c] at glass	− 2.95	− 3.54	− 2.71	− 2.48	− 0.38	+1.28		

[a] μ/sec./volt/cm. at 25°. [b] The *p*H value given is probably approximate. [c] + or − sign means that the glass is charged that way.

TABLE II

CHANGES IN PARTICLE C.V. (TRUE) AND LIQUID VELOCITY AT THE GLASS SURFACE AS 0.002 *M* H_2SO_4 IS ADDED TO SPHALERITE IN 0.001 *M* Na_2CO_3

	% H_2SO_4	Molarity H_2SO_4	Molarity Na_2CO_3	Molarity Na_2SO_4	C.V. true[a]	ζ (mv.)	Liquid[a,b] velocity
1	0	0	0.001000	0	−2.11	−27.5	−2.95
2	20.0	0	.000400	0.000400	−2.31	−30.0	−3.98
3	33.3	0	0	.000667	−1.86	−24.2	−1.12
4	50.0	0.000500	0	.000500	−0.76	− 9.9	+0.83
5	66.7	.001000	0	.000333	−1.49	−19.4	+1.09
6	100.0	.002000	0	0	−0.08	− 1.0	+1.28

[a] μ/sec./volt/cm. [b] Positive or negative sign means that the glass is charged that way.

charges of both sphalerite particles and glass cell wall decrease in negativity with increasing acidity below *p*H 4. Cell wall charge decreases faster than particle charge and even becomes positive while the particles still remain somewhat negative. This immediately suggests electrostatic attraction forces at at least certain regions of H_2SO_4 acidity which forces are capable of causing particles to adhere and stop their Brownian movement.

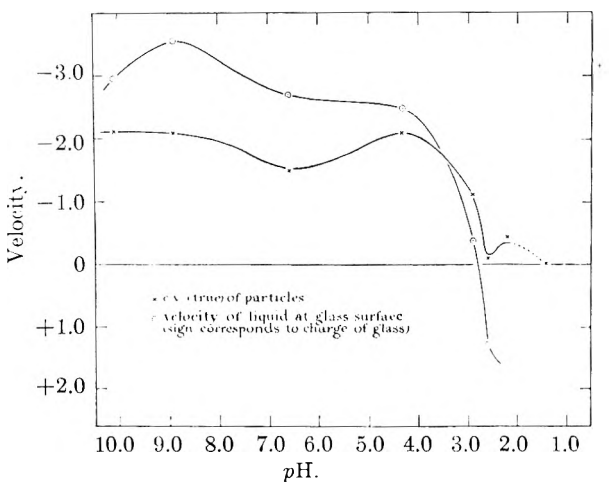

Fig. 1.—C. V. (true) of particles and velocity of liquid at glass surface *vs.* *p*H.

Yet another series of C.V. and cell surface liquid velocity determinations was carried out. This time the electrolyte content of each sphalerite suspension considered was representative of given proportions of 0.002 *M* H_2SO_4 to 0.001 *M* Na_2CO_3, thus duplicating conditions at different times in the original Taggart cell where the Brownian movement of particles in alkaline medium was stopped by addition of acid. The data are given in Table II and are plotted in Fig. 2. Note how the wall charge becomes positive, the particle charge still remaining negative, when the suspension has 50% or more of 0.002 *M* H_2SO_4, the balance being 0.001 *M* Na_2CO_3. There was no appreciable flocculation for any of the six suspensions and Brownian motion was vigorous for all.

Thus, Taggart's results can be explained by the fact that in acid medium the negative particles become attached to the positive glass upon coming close to it as a result of their normal settling. Revivification occurs when alkali solution is added to the cell because the glass surface becomes negative again and repels the particles, the smaller ones becoming resuspended (in the vicinity of the glass surface).

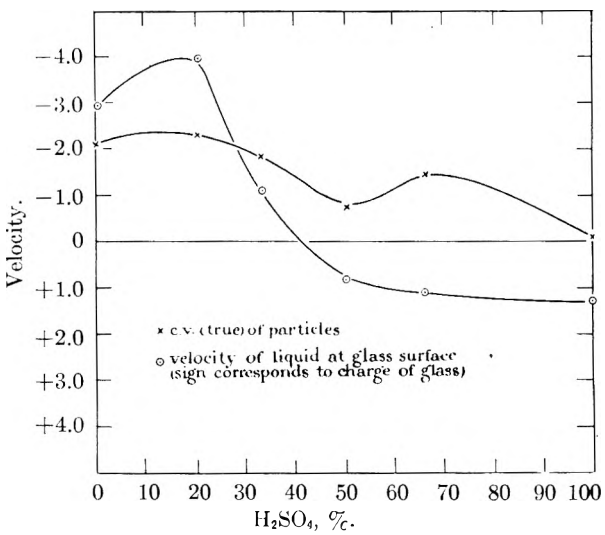

Fig. 2.—Particle C.V. (true) and liquid velocity at the surface for different mixtures of 0.001 *M* Na_2CO_3 and 0.002 *M* H_2SO_4.

b. Isoelectric Point.—With evidence at hand that the Brownian movement is not stopped by given electrolytes, the next step is to prove whether pedesis at least varies with the electrical environment. In making the comparison, it should be of advantage to consider at least one suspension where the particles are not charged, *i.e.*, they are at the isoelectric point (I.P.). Furthermore this system should be one where there is a tendency toward flocculation[23] so that the differences in the suspensions being compared will represent extremes (more than is the case if a non-flocculated isoelectric were used). Also, the presence of floccules would be a check on the isoelectric point having been determined correctly by the cataphoretic measurements technique used in this work.

None of the sulfuric acid suspensions considered so far (Tables I and II) showed flocculation. This was true even

(23) Flocculation (coagulation) is defined in all this work as the grouping together of the majority of the "individual" particles of a suspension, which are no greater than 1 micron in diameter and mostly submicroscopic in size, to become macroscopic in size. Actually the "individual" particles of all the suspensions were mostly aggregates judging from high resolution dark field microscope observations. In the work, care was taken to consider those particles only whose dark field haloes (at the lower microscope resolution where cataphoresis and Brownian displacement were measured) showed them to be fairly regular in shape.

when the particle charge was practically zero as for 0.002 M and 0.1 M H_2SO_4. Likewise, NaCl used by Lucas[18] (see Introduction) to decrease the Brownian activity of Hevea rubber latex, did not flocculate the sphalerite particles even at the high concentration of 1 N where the suspension was practically at the isoelectric point.

Aluminum chloride then was studied as a possible flocculent for the 0.0125% sphalerite. Various aluminum concentrations were tried in basic medium (0.001 N Na_2CO_3), in distilled water and in acid medium (0.001 M H_2SO_4), the true cataphoretic velocity being measured each time. No flocculation was evident in distilled water or in acid solution at any of the aluminum concentrations tried including those which brought the suspensions to the isoelectric point. It was only in alkaline medium that flocculation was apparent and this occurred sharply and only at the isoelectric point determined from the cataphoretic measurements, namely, 0.000400 N $AlCl_3$. Data pertaining to the Na_2CO_3–$AlCl_3$ suspensions are given in Table III and C.V.–N $AlCl_3$ points line up as depicted in Fig. 3.

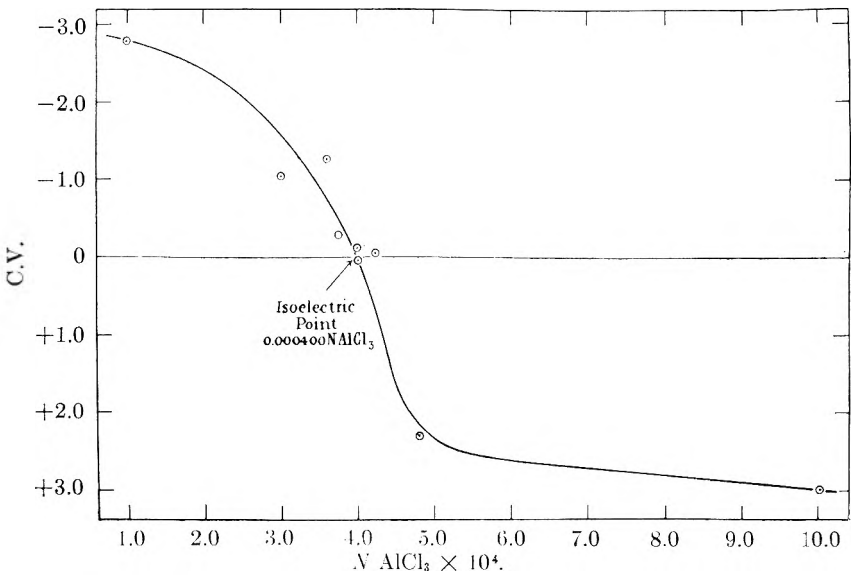

Fig. 3.—C.V. vs. N $AlCl_3$ in 0.001 N Na_2CO_3 (Sphalerite).

TABLE III

C.V. (TRUE) *vs.* NORMALITY $AlCl_3$ IN ALKALINE[a] SOLUTION

Normality $AlCl_3$	pH	C.V. (μ/sec./volt/cm.)	ζ (mv.)
0.000100	9.5	−2.79	−36.3
.000300	8.5	−1.04	−13.6
.000360	7.9	−1.29	−16.8
.000375	7.9	−0.30	− 3.9
.000399	7.8	−0.12	− 1.5
.000400	7.7	+0.02	+ 0.3
.000425	7.6	−0.06	− 0.8
.000480	6.9	+2.31	+30.0
.001000	5.3	+3.00	+39.0

[a] 0.001 N Na_2CO_3.

From a practical viewpoint the flocculated $AlCl_3$–Na_2CO_3 suspension was suitable for observations because an appreciable proportion of the sphalerite was in the form of "individual"[23] particles. Also, shaking tended to temporarily break up the floccules (which were loose in structure) and form more of these "individual" particles. This made it possible to compare Brownian movement displacement of particles in a flocculating medium with those in a nonflocculating medium as will be described in the next experimental section on pedetic displacements.

III. Brownian Movement Displacement.—According to Einstein[3] the intensity of Brownian movement can be represented in terms of the mean displacement D in a given direction (Dx in the x direction) of a particle from its original position for a given time t. He gives the following formula which relates the displacement with the time t, the absolute temperature T, the viscosity of the suspending medium η and the particle radius r, if the particles are small rigid spheres

$$D^2 = \frac{RTt}{N3\pi r\eta} \qquad (1)$$

R and N are the gas constant and Avogadro number, respectively.

This equation does not take into consideration any possible effect of electrical charge on the absolute displacement.

In this work the displacement which particles underwent in a given time, was measured and used as a criterion of Brownian movement intensity. All the data were placed on a comparative basis of the same temperature, viscosity and particle radius by using the proportionalities of equation (1) for D and T, η, r. It was considered justifiable to make corrections in this manner even in the face of the possibility of electrical environment influencing pedesis and altering equation (1). First, the correcting ratios obtained from the equation represent the best available approximations. Second, they have been checked experimentally by Perrin and his collaborators,[7,8] Henri[4] and others. And third, the range in temperature (viscosity) and particle size over which the adjustments were made was not too great.

Most of the displacement measurements were made in the deep Northrup–Kunitz cell where the particles are well removed from the walls. This eliminates wall effects (electrical), which, it has already been shown, may complicate Brownian movement studies. Also, with the particles being too small for their size to be determined by direct microscopy, it was at least possible in the deep cell to follow the settling of each with the microscope fine adjustment and determine its rate of fall. The rate of fall could then be converted to particle size by employing Stokes' law.

Particle size was chosen small enough to obtain measurable Brownian movement displacement in the period of time t. But the particle had to be large enough so that its displacement, as considered in an up or down vertical direction was relatively small compared to the distance fallen. Otherwise too great an error creeps into the rate of fall and therefore into the radius which is evaluated from it.

In order to study the effect of a continuously charged surface (glass) on the Brownian movement of particles which are close to the glass but are repulsed by it because they bear the same sign of charge, shallow cell[24] displacement measurements were made in alkaline medium and compared with the deep cell data.

Since under these last circumstances, there was no appreciable cell depth in which to measure the rate of fall of a particle, individual particle sizes could not be determined as in the case of the deep cell and therefore displacements could not be adjusted for comparison on an individual particle basis. Accordingly, an average radius was obtained for all the shallow cell particles and this along with the average temperature and average viscosity for the shallow cell observations, was used to bring an average of the observed shallow cell displacements on to a comparative basis with the deep cell data. The average radius obtained was based on actual rate of fall data for particles of the same suspension in a deep cell, the particles in both deep and shallow cells having dark field haloes of about the same intensity. Light field (Leitz dark-and-light field condenser) filar micrometer measurements were also made on the particles for estimation of the average size.

Displacement measurements were made on sphalerite particles in three different media, namely, in 0.000400 N $AlCl_3$–0.001 N Na_2CO_3 which is flocculating, the particles

(24) Cover-glass sealed with paraffin over a drop of the suspension on a microscope slide.

TABLE IV

BROWNIAN MOVEMENT DISPLACEMENT OF SPHALERITE PARTICLES (INDIVIDUAL) IN A FLOCCULATED[a] SYSTEM: 30 SECONDS

	Distance fallen in 300 sec. (μ)	Radius (μ)	T, °K.	Dx or y Calc. at T^0 (μ)	Observed (μ) Dx	Dy	Dx Obsd./ Dx Calcd.	Dy Obsd./ Dy Calcd.	Obsd. D Stdized. to $r = 0.1\mu$; $T = 298°K$ Dx	Dy
1	52.0	0.155	296.0	9.44	2.7	3.4	0.28	0.36	3.4	4.4
2	46.0	.146	296.0	9.74	4.0	2.1	.41	.22	5.0	2.6
3	61.3	.168	296.0	9.06	3.2	2.5	.36	.27	4.3	3.3
4	55.3	.160	296.0	9.30	4.0	4.2	.43	.45	5.2	5.5
5	113.3	.230	295.5	7.70	3.1	2.1	.40	.27	4.8	3.3
6	146.5	.260	296.0	7.30	4.4	2.7	.60	.37	7.3	4.4
7	32.7	.123	296.0	10.61	3.1	2.5	.29	.23	3.5	2.8
8	26.7	.111	296.0	11.18	3.6	3.8	.33	.34	3.9	4.1
9	118.8	.234	296.0	7.67	4.8	1.3	.62	.18	7.6	2.1
10	114.5	.230	296.0	7.75	2.9	3.4	.37	.44	4.5	5.4
11	217.0	.324	294.0	6.35	3.4	2.7	.54	.42	6.5	5.1
12	80.6	.197	294.5	8.21	5.5	3.4	.68	.42	8.2	5.1
13	73.2	.187	294.5	8.42	4.0	3.3	.48	.39	5.8	4.7
14	92.0	.210	294.5	7.95	5.0	2.9	.63	.36	7.6	4.4
15	132.5	.252	294.5	7.24	3.1	3.6	.42	.50	5.1	6.1
16	72.7	.187	294.5	8.45	2.1	1.2	.25	.14	3.0	1.7
17	109.6	.229	294.5	7.61	4.0	2.7	.53	.35	6.4	4.2
18	39.3	.137	294.5	9.83	1.9	1.7	.19	.18	2.4	2.1
19	78.0	.195	294.0	8.20	2.1	2.1	.26	.26	3.1	3.1
20	30.0	.120	294.5	10.52	1.7	1.5	.16	.15	2.0	1.8
21	58.6	.168	294.5	8.90	3.4	2.9	.39	.32	4.7	3.9
22	271.0	.362	294.0	6.01	4.8	2.7	.80	.44	9.6	5.4
23	67.0	.179	294.5	8.61	1.9	2.5	.22	.29	2.7	3.5
24	52.3	.158	294.5	9.15	3.4	3.1	.38	.33	4.5	4.0
25	60.0	.168	295.0	8.93	2.5	2.5	.28	.28	3.4	3.4
26	124.7	.242	295.0	7.45	4.8	3.4	.64	.46	7.8	5.6
27	182.0	.293	295.0	6.77	3.1	3.1	.45	.45	5.5	5.5
28	59.3	.168	295.0	8.95	1.5	1.3	.17	.15	2.1	1.8
29	128.6	.246	295.0	7.38	5.9	5.9	.80	.80	9.7	9.7
30	108.7	.227	295.0	7.70	5.0	4.0	.65	.52	7.8	6.3
31	90.5	.207	295.0	8.06	3.6	3.1	.45	.38	5.5	4.6
32	73.9	.187	295.0	8.48	3.8	3.1	.45	.37	5.5	4.5
33	32.6	.124	295.0	10.40	1.9	3.4	.18	.33	2.2	4.0
34	73.2	.186	295.0	8.49	1.5	2.3	.18	.27	2.2	3.3
35	118.2	.236	295.0	7.53	5.0	2.9	.66	.38	8.0	4.6
36	46.6	.149	295.0	9.50	1.9	2.9	.20	.30	2.4	3.6
37	56.6	.164	295.0	9.07	3.1	3.1	.34	.34	4.1	4.1
38	54.6	.161	295.0	9.14	2.1	3.6	.23	.40	2.8	4.8
39	254.0	.346	295.0	6.23	4.5	1.9	.72	.31	8.8	3.7
40	85.5	.202	295.0	8.17	4.6	4.8	.56	.59	6.8	7.1
Avg.							0.42	0.35	5.1	4.2
Avg.							0.39		4.7	

[a] 0.000400 N $AlCl_3$; 0.001 N Na_2CO_3.

being at the isoelectric point; in 0.001 M Na_2CO_3 which is alkaline and non-flocculating (Taggart); and in 0.001000 M H_2SO_4 and 0.000333 M Na_2SO_4[25] which is acidic and non-flocculating (Taggart). Displacements of particles in all these three suspensions were taken in the deep cell. Only the alkaline non-flocculated suspension was used for shallow cell data as well as deep cell data.

Two different times, 30 seconds and 300 seconds, were used in evaluating displacements. Both the flocculated suspension and the alkaline non-flocculated suspension were considered at each of these two displacement times. The acid suspension was measured for a time of 30 seconds only and shallow cell measurements were taken for the period of 300 seconds

In the 30-second displacement measurements, the position of particles was located with the aid of a "100 square" reticule in a 25× ocular.[26] About 40 particles in each suspension were followed for exactly 5 minutes, thus giving 11 positions per particle or 10 horizontal displacements (x) and 10 vertical displacements (y). These data, in each direction, were averaged for each particle to give Dx and Dy observed. Timing was accomplished with the aid of a mechanism which clicked every 30 seconds.

For the 300-second displacement measurements the position of particles was located with a Zeiss filar micrometer ocular,[27] it being possible only to make displacement measurements in the x direction. About 20 particles in each suspension were followed exactly for 20 minutes, thus giving 5 positions per particle or 4 horizontal displacements. These data were averaged to give Dx observed. An ordinary laboratory timer graduated in intervals of 15 seconds magnitude was used for these measurements, filar micrometer (and microscope fine adjustment) readings being taken after each 5 minutes elapsed.

Temperature was that of the room, at which all suspensions and apparatus were in equilibrium. One temperature was recorded for each particle when displacements were 30

(25) This acidic suspension is No. 5 in Table II.

(26) At 210-mm. tube length with the Leitz U.M. 4 objective the side of a reticule square was 19.1μ.

(27) At 210-mm. tube length with the Leitz U.M. 4 objective, a single division of the filar was 0.35μ.

TABLE V

SUMMARY OF BROWNIAN MOVEMENT DISPLACEMENT RESULTS

Suspension	Cel.	t = 30 sec. D Obsd./D Calcd.	t = 30 sec. D obsd. (μ) $r = 0.1\mu$, $T = 25°$	t = 300 sec. D Obsd./D Calcd.	t = 300 sec. D obsd. (μ) $r = 0.1\mu$, $T = 25°$
0.000400 N $AlCl_3$ .001 N Na_2CO_3 (flocculated)	Deep	0.39	4.7	0.32	12.2
.001 M Na_2CO_3 (non-flocculated)	Deep	0.57	7.0	0.51	19.4
.001000 M H_2SO_4 .000333 M Na_2SO_4 (non-flocculated)	Deep	0.66	7.9	..	..
.001 M Na_2CO_3 (non-flocculated)	Shallow	..	..	0.67	25.7

seconds duration. When they were 300 seconds, the temperature was recorded at the beginning and end of following a given particle and averaged. Variations during this 20 minutes usually were no greater than 0.5° if at all. During any over-all period of making measurements, the room temperature varied but slightly.

Table IV represents as an example the observational data and calculations relative to one of the series of Brownian movement displacement measurements, as labeled. From the distance fallen by the particle in a given time (rate of fall) the radius has been calculated and from this the displacement which the particle should have according to the Einstein formula (1) at the temperature of measurement. This calculated displacement is then divided into (compared with) the observed displacement. Some further comparison is also made by multiplying this ratio by the Einstein displacement for a particle of 0.1 μ radius at 25°, which is 12.1 μ when the time interval is 30 seconds and 38.2 μ when the interval is 300 seconds. It may be mentioned here that the greatest possible error in calculated displacement (Dx or y calcd.) due to actual Brownian movement displacement on the rate of fall data for all the particles considered, was 17%. But in the great majority of particles it was well under 10%.

In the various experiments, the ratios of D observed to D calculated were averaged for each set of data and also, averages were obtained for values of the observed displacement adjusted to 0.1 μ and 25°. Besides, x and y averages were averaged together. Table V summarizes and compares the final figures.

According to these results:

1. The observed values are all considerably lower than those predicted by the Einstein formula.

2. Displacement is not the same in the different electrolyte media studied. It is about one-third the Einstein value in flocculating medium where the particles are at the isoelectric point, and somewhat over half the Einstein value in alkaline non-flocculating medium. The acidic suspension showed greater Brownian movement than the alkaline (non-flocculating) suspension even though it is less negative in zeta potential.[28]

3. Shallow cell displacement is about 30% greater than deep cell displacement for the same alkaline (non-flocculating) sphalerite suspension.

4. The Einstein time relation $(D_1/D_2)^2 = t_1/t_2$ is reasonably fitted by the data obtained for each of the two different sphalerite suspensions studied at the two displacement times which, incidentally, differed as much as tenfold.[29]

IV. Further Qualitative Observations.—The experimental evidence presented, indicates strongly that electrical environment affects the degree of Brownian activity of a particle. Additional qualitative observations favor this view.

For instance, in the deep cell, sphalerite suspensions of low electrolyte concentration at or near the isoelectric point, were seen not to have either consistent cataphoretic velocity[30] or Brownian activity from particle to particle, there being a correlation in these two properties, namely that the particles of low or zero zeta potential showed sluggish pedesis as compared to those of relatively high electrical charge whether + or −. This was especially true in the flocculating medium 0.000400 N $AlCl_3$–0.001 N Na_2CO_3.

Meanwhile, Brownian activity seemed to be consistently vigorous when the electrolyte content of the suspending medium was high, for example in 0.1 M H_2SO_4 or 1 N NaCl, even though the non-flocculated suspensions were close to or at the isoelectric point. In this case, the cataphoretic velocity, although low, was practically the same in sign and amount from particle to particle. Such constancy of cataphoretic velocity was also observed when particle charge was relatively high (either + or −) in low concentrations of electrolyte.

A glance at the displacement data for the flocculated sphalerite suspension in Table IV shows the great nonuniformity in displacement values for a system of low electrolyte concentration at the isoelectric point. This being the case, one may infer that the mean displacement of particles at the isoelectric point (in the $AlCl_3$–Na_2CO_3 flocculating medium under consideration) is still lower than one-third the Einstein displacement, for in the measurements presented, the particles were randomly chosen, whether they were sluggish or active.

Other qualitative observations which point to electrical environment affecting pedesis have been in the shallow cell. Here the neighboring electrically charged glass surface should represent an intensification of effects due to ions or charged particles in the vicinity of the particle under consideration. Attraction and repulsion forces become involved with the Brownian movement activity:

(1) If the shallow cell mount of 0.0125% sphalerite in 0.001 M H_2SO_4 is kept under observation while the liquid between slide and cover glass is drying, air-liquid interface lines are seen to move across the field because the liquid is diminishing in quantity. But, particles, as large as 4 μ although apparently attracted fast to the slide and not in Brownian activity, are not left behind in the air. They are carried in the liquid, for which they evidently have high affinity, as the interface shifts.

The fact that the particles readily leave their "anchorage" as the liquid evaporates indicates that they are not actually touching the glass and therefore the forces of attraction, previously shown to involve electrostatics, are acting over "long range" and are sufficiently strong not only to keep a particle in one place but also stop its Brownian activity.

The idea of a particle in liquid medium adhering to a plate and still not touching it (no Brownian movement evident) is not unusual. A. von Buzágh[32] calculates this to be so on the basis of his "adhesion-number" and "adhesion-angle" experiments. Similarly, the individual particles of floccules often do not appear to be in contact as seen under the mi-

(28) It should be mentioned here, that in this acid suspension the sphalerite (zinc sulfide) undergoes some decomposition. The odor of H_2S was apparent.

(29) Let the relationship between the displacement (D) and the time (t) be written as $(D_1/D_2)^n = t_1/t_2$. Then according to the Einstein theory the exponent "n" equals 2. Calculations based on the data of this paper result in n = 2.42 for the $AlCl_3$-Na_2CO_3 (flocculated) suspension and n = 2.27 for the Na_2CO_3 suspension. If Henri's displacement data in distilled water are considered, n amounts to 2.38.

This agreement of the present results on sphalerite with Henri's results on rubber is very interesting considering that (a) the suspended particles were altogether different in chemical and physical composition; (b) the time periods involved were so far apart, *i.e.*, 4/20/: 1/20 seconds for Henri and 300: 30 seconds for the present data; (c) Henri worked with a shallow cell whereas the sphalerite data in consideration were obtained from deep cell measurements; and (d) the comparison covers three aqueous media of different electrolyte content.

(30) Some particles were fast and others even opposite in charge (to the majority). Sun[31] mentions that he had noticed this for low zeta potential slimes (low electrolyte concentration) including sphalerite.

(31) S. Sun, A.I.M.E. Tech. Pub. No. 1580 (1943).

(32) A. von Buzágh, "Colloid Systems," (English translation), The Technical Press, Ltd., London, 1937.

croscope. These particles remain side by side without evident pedesis. Perrin[7] states that he saw this in clusters of mastic granules The individual particle size was 10–12 μ and the flocccules had formed when he added a coagulant to the system. This has been observed by the authors in sphalerite flocculles.

(2) A shallow cell mount of sphalerite in 0.002 M Na_2CO_3 was completely sealed with paraffin and observed periodically. Pedesis persisted even after three days although the particles were large enough to settle out within an hour according to Stokesian calculations. It has already been shown that the particles and the glass are appreciably negative charged in an Na_2CO_3 solution and therefore repulsion forces are operative between particles and the cell floor.

These forces, which evidently help maintain a distribution against normal sedimentation forces, apparently play a part in the difference in displacement already observed between the shallow cell and the deep cell. They should be contrasted with the attraction forces just described.

(3) Finally, attraction forces and repulsion forces can act together in affecting pedesis. For instance, it was observed in mounts of sphalerite in 0.001 M or 0.002 M Na_2CO_3 that small particles of about 1 μ in diameter and less maintained vigorous pedesis while never leaving the side of larger particles to which they seemingly were attached. The large particle, often over 4 μ in diameter remained on the microscope slide showing Brownian vibrations with no appreciable displacement while the smaller particle remained at arm's length, a distance away of over 1 μ dancing very actively but keeping within the same range of distance and even the same side of the large particle never leaving it as should be true for a particle in random motion due to Brownian activity.

Since the particles, large and small, are apart from each other and it has already been shown that in the alkaline medium they have negative charges of appreciable magnitude, repulsion forces must be assumed. Meanwhile forces of attraction, acting over a relatively long distance, are sufficiently strong to prevent the small particle from wandering away. Yet this attraction is not so strong that the pedetic oscillations are halted as is the case in acid medium.

A similar phenomen has been described by von Buzágh.[32] He observed small particles to be in vivid Brownian activity, although they seemingly adhered to a plate. Their movement was two-dimensional since they were not able to move out of the plane into which they originally sedimented owing to the attractive force which the base plate exerts on them. The distance between base plate and particles was said to be appreciable, *i.e.*, many molecular dimensions.

It is quite possible that Henri's results (obtained in a shallow cell) of different Brownian activities for latex globules in different media might be explained in terms of these electrical forces involving the particle and the cell surface. For instance, in distilled water, where Henri obtained his highest displacement values, Hauser and Bender[33] report that the cataphoretic velocity of Hevea rubber latex can be as negative as -7.7 μ/sec./volt/cm., which corresponds to a zeta potential of -97 millivolts. But in 0.1 N NaOH the C.V. of the latex globules is much less negative, namely, -3.0 μ/sec./volt/cm. In HCl solution ($^1/_{32}$ N), zeta potential of the rubber can become still less negative as has been observed for sphalerite. Meanwhile, the charges on the glass surface exposed to these various electrolyte media should be quite similar to the observations for sphalerite already discussed.

Lucas' remarks[18] and those of Spence[19] pertaining to the decreasing of the pedesis of Hevea latex in NaCl electrolyte might also be explained in this manner since the zeta potential of the rubber (and probably the quartz or glass) becomes much less negative in saline solution of appreciable concentration. For instance, Hauser and Bender[33] found a C.V. of -1.1 μ/sec./volt/cm. for a given latex in 7% NaCl.

It is now opportune to reconsider in the light of the experimental findings, the literature discussed at the beginning of this paper. First, Taggart stopped the Brownian activity of mineral particles with an appropriate electrolyte, only in the sense of having created sufficient affinity between particle and cell surface, to render the particles visibly immobile. However, there definitely appear to be variations in pedesis of *suspended* particles depending on the electrolyte medium. The "abnormal" shallow cell observations of Henri, Lucas and Spence might be explained in terms of the effect of the cell surface on the particle as the present shallow cell displacement measurements and observations indicate.

General Considerations

The fact that the amplitude of Brownian movement can be influenced by the electrical double layer (as measured by cataphoresis) suggests a number of interesting implications. Pedesis is not only a manifestation of kinetic energy, but at the same time is a measure of the degree of asymmetry of the molecular bombardment involved. From this viewpoint, in a case such as the one presented here, namely, a relatively large particle surrounded by the close-packed molecular structure of liquid water, the collisions involved may or may not possess the non-statistical character required to produce visible motion. In very general terms these concepts resolve themselves into two categories:

(a) The direct bombardments of the particles by the kinetic units of the suspension medium are too uniformly distributed to create visible Brownian movement. Any observed movement (or variation thereof) must be caused by some intermediate mechanism. The ionic interchange mechanism suggested by Taggart, freed from some of its original postulated limitations, is a distinct possibility. Of historical interest, at least, is the amicronic theory. Based on the contention "natura non facit saltum," it postulated the presence of small invisible particles, amicrons, normally in Brownian movement, which, in turn, communicated their activity to the larger particles.

(b) Assuming that the normal Brownian movement as described by the simple kinetic theory applies, then in terms of amplitudes (as contrasted to kinetic energy) the experimental values may be either diminished or enhanced by a change in surface conditions, which in turn may influence the non-uniformity characteristic in the distribution of molecular collisions across the dineric interface. Degree of hydration, including dipole orientation, as well as adsorbed layers, whether electrical or otherwise, so profoundly influence the behavior of colloidal systems that it is conceivable that they may also alter the nature of the kinetics across the interface.

(33) E. A. Hauser and M. Bender, "Survey of the Electrokinetics of Rubber Latex," Paper No. 43, Proceedings of the Rubber Technology Conference, London (1938).

ON THE REACTION OF HYDROGEN PEROXIDE WITH DONOR PARTICLES

By John O. Edwards

Department of Chemistry, Cornell University, Ithaca, N. Y.

Received February 15, 1951

Data on the rate laws, energetics and other factors concerning the reactions of hydrogen peroxide with electron donors are considered. The conclusions are reached that many of the reactions are general acid-catalyzed, and that the oxygen-oxygen bond of the peroxide is broken at the same time that a bond is being formed between the electron donor and an oxygen.

The existence of two independent rate laws for the reaction of hydrogen peroxide with iodide,[1,2] bromide,[2] chloride,[2,3] iodate,[4] thiosulfate[5,6] and hypoiodite[7] ions in aqueous acid has been demonstrated. The reaction with hypochlorite ion[8-10] has been shown to proceed by at least three separate mechanisms, and it is possible to calculate rate constants for the kinetic paths analogous to those for the other six anions. The rate equation for these reactions is

$$\frac{-d[H_2O_2]}{dt} = k_1[H_2O_2][B^-] + k_2[H_2O_2][B^-][H^+]$$

where B^- is the donor particle (anion) and brackets denote concentrations. A mechanism consistent with these observed rate laws will be developed in this article.[11]

The reactions of hydrogen peroxide with bromate ion[12-14] and hypobromite ion[13,15-18] have been investigated in a limited range of acidity and the observed rate laws show only a value corresponding to the k_2 term. Further study of these reactions is necessary before the presence or absence of a k_1 term is proved.

The oxidation of hydrazine by hydrogen peroxide was studied in concentrated aqueous solution, and the rate was found to be first order in each of the molecular species. Addition of either acid or base causes a lowering of the rate of reaction, which has been interpreted by the investigator as a result of the formation of $N_2H_5^+$ or O_2H^-, respectively.[19]

(1) H. A. Liebhafsky and A. Mohammed, *J. Am. Chem. Soc.*, **55**, 3977 (1933).
(2) A. Mohammed and H. A. Liebhafsky, *ibid.*, **56**, 1680 (1934).
(3) E. A. Budge, *ibid.*, **54**, 1769 (1932).
(4) H. A. Liebhafsky, *ibid.*, **53**, 896, 2074 (1931).
(5) E. Abel, *Monatsh.*, **28**, 1239 (1907).
(6) K. Sandved and J. B. Holte, *Kgl. Norske Videnskab. Selskabs, Forh.*, **11**, 189 (1938); *C. A.*, **33**, 4856 (1939).
(7) H. A. Liebhafsky, *J. Am. Chem. Soc.*, **54**, 1792, 3499, 3504 (1932)
(8) R. E. Connick, *ibid.*, **69**, 1509 (1947).
(9) B. Makower, Thesis, Univ. of California (1932).
(10) B. Makower and W. C. Bray, *J. Am. Chem. Soc.*, **55**, 4765 (1933).
(11) The reaction of ozone with chloride ion was found to have a similar rate equation (L. R. B. Yeatts, Jr., and H. Taube, *ibid.*, **71**, 4100 (1949)).
(12) W. C. Bray and P. R. Davis, *ibid.*, **52**, 1427 (1930).
(13) H. A. Young, *ibid.*, **72**, 3310 (1950).
(14) H. A. Young and W. C. Bray, *ibid.*, **54**, 4284 (1932).
(15) Balint, Thesis, Budapest (1910).
(16) W. C. Bray and R. S. Livingston, *J. Am. Chem. Soc.*, **45**, 1251 (1923); **50**, 1654 (1928).
(17) J. A. Christiansen, *Z. physik. Chem.*, **117**, 453 (1925); **128**, 430 (1927).
(18) R. S. Livingston, *J. Am. Chem. Soc.*, **45**, 1251 (1923).
(19) A. S. Gordon, "Third Symposium on Combustion, Flame and Explosion Phenomena," Williams and Wilkins Press, Baltimore, Md., 1949, p. 493.

The data under consideration are presented in Table I. Numerical values for rate constants were obtained directly from the indicated references or were computed from the work of the investigators. It will be noted that the value of log k_2 lies close to that of log k_1, but it does not show any significant correlation with K_D which is the dissociation constant for the acid from which the donor particle is formed. This trend would be expected if the reactions were general acid-catalyzed. The evidence for this type of catalysis will now be summarized.

TABLE I

RATE AND DISSOCIATION CONSTANTS AT 25°

Donor	log k_1[a]	log k_2[b]	log K_D[c]	Ref.[d]	log k_0
$S_2O_3^=$	− 1.61	0.22	− 1.57	5, 21	−1.0
Cl^-	− 6.96	− 4.30	6.11	2, 22	−0.8
Br^-	− 4.64	− 1.85	∼ 8	2, 23	∼3
I^-	− 0.16	1.02	∼ 9	1, 23	∼7
IO_3^-[e]	− 5.36	− 3.67	− 0.80	4, 24	−4.3
OCl^-	3.64	6.40	− 7.46	8, 8	0.8
OI^-	12.95	15.70	−12.35	7, 25	6.8
OBr^-	.....	15.23	− 8.70	13, 26	9.0
BrO_3^-	.....	− 1.58	.....	14	...
N_2H_4	− 1.73	.....	− 8.24	19, 27	−3.6

[a] Units of k_1 are liters/mole/sec. [b] Units of k_2 are liters²/mole²/sec. [c] K_D is the dissociation constant for the acid which forms the donor particle. [d] The first reference number refers to the rate constants and the second to the dissociation constants. [e] Rate data for iodate reaction at 50°.

1. Calculation of the correlation coefficient r from the seven samples of log k_2 and log k_1 gives a value of 0.99,[20] while the value of r for a 1% level of significance with 5 degrees of freedom is 0.874. One concludes from this correlation that the relation between the rate constants for the two independent reaction mechanisms is very significant.

2. A least squares evaluation of log k_2 against log k_1 gives a line whose equation is

$$\log k_2 = 1.022 \log k_1 + 2.23$$

(20) The equation

$$r = \frac{\Sigma(x \times y)}{(\Sigma x^2 \times \Sigma y^2)^{1/2}}$$

where x and y are the deviations of log k_1 and log k_2 from their means, respectively, has been used for this calculation. Although the number of samples is small for this type of a correlation, little doubt remains concerning the existence of a significant relationship.
(21) N. Yui and H. Hagisawa, *Bull. Inst. Phys. Chem. Research (Tokyo)*, **21**, 597 (1942); *C. A.*, **43**, 2074 (1949).
(22) R. A. Robinson, *Trans. Faraday Soc.*, **32**, 743 (1936).
(23) J. Bjerrum, *Chem. Revs.*, **46**, 381 (1950).
(24) R. M. Fuoss and T. Shedlovsky, *J. Am. Chem. Soc.*, **71**, 1496 (1949).
(25) A. Skrabal, *Ber.*, **75**, 1570 (1942).
(26) L. Farkas and M. Lewin, *J. Am. Chem. Soc.*, **72**, 5766 (1950).
(27) W. S. Hughes, *J. Chem. Soc.*, 491 (1928).

A slope of one would be expected for general acid catalysis involving a similar mechanism for every case.

3. In Table II, data are presented on frequency factors (A) and activation energies (E) for four cases from the literature. The difference, $E_1 - E_2$, is nearly constant (3600 ± 800 cal.) which is a further indication of the relationship between the two simultaneous mechanisms. There is a large increase in the frequency factor as the activation energy increases, but the values are too scattered to characterize the function. Hender and Robinson[28] discuss the reaction between hydrogen peroxide and iodide ion in terms of the collision theory; their calculations of Arrhenius constants for aqueous salt solutions are consistent with the presence of a water molecule in the activated complex.

TABLE II

ARRHENIUS CONSTANTS FOR FOUR REACTIONS[a]

Donor	Log A_1'[b]	Log A_2	E_1[c]	E_2	Ref.
IO_3^-	11.41	12.14	27,500	23,500	4
Cl^-	8.59	10.85	23,600	20,740	2
Br^-	9.08	10.38	21,100	16,700	2
I^-	7.95	8.66	13,400	10,450	1,2

[a] Less complete thermal data are recorded for the reactions with hypochlorite,[8] thiosulfate[6] and hydrazine.[19] [b] Corrected for concentration of water in k_1, units of A_1' and A_2 are liters²/mole²/sec. [c] Units of E_1 and E_2 are calories.

4. Connick[8] and Makower[9] observed that acetic acid–acetate buffers cause a 20- to 30-fold increase in the rate constant for the hypochlorite reaction. In the absence of any other explanation, this is good evidence of general acid catalysis.

5. It has been estimated that the oxidation of iodide by D_2O_2 in heavy water proceeds only 60% as fast as the oxidation by H_2O_2 in regular water.[29] According to the postulates of Wynne-Jones,[30] this is indicative of general acid catalysis if the O–D bond in the peroxide is not broken in the transition state.

6. In the rate of thiosulfate oxidation by peroxide, there are inconsistencies[5,6] which are most easily explained in terms of a general acid catalysis by the acetate buffers used in the experiments.

Having established the existence of a linear relationship between the logarithms of the two rate constants for the independent mechanisms and having presented the evidence for general acid catalysis, it is important to consider the parameters a and α in the equation of Brönsted[31]

$$k_i = aK_i^{\alpha}$$

where k_i is the rate constant for the reaction with the i^{th} acidic component and K_i is the dissociation constant for the acid. Employing 2.24 as the average difference between log k_1 and log k_2 and including the correction for the concentration of water in k_1, it was calculated that α equals 0.23. For a comparative check, it was found that the value of α for the general acid catalysis of the mutarotation of α-D-glucose is 0.18.[32]

Swain[33] has recently discussed acid–base catalysis in terms of a concerted push-pull mechanism. The reactions here considered are believed to have this type of mechanism, but it is thought that the chemical reactivity of the donor particle is an important factor in determining the rate. The large rate constants for the hypohalite reactions compared with those of the less basic anions are in the expected direction for a basic catalysis, whereas the relative rates of oxidation of the halide ions are in the direction of their reducing ability. The interpretation of the parameter a is dependent on these factors and the value of it is different for each reaction. While no comparative values from the literature may be advantageously discussed, a comparison can be made in the present series of reactions.

From the theories of Brönsted[31] and Swain,[33] a linear combination of logarithmic terms is indicated for a concerted acid-base catalysis. This deduced equation

$$\log k_{ij} = \log k_0 + \alpha \log K_i - \beta \log K_j$$

where k_{ij} is the observed rate constant, K_i is the dissociation constant of the acid catalyst, K_j is the dissociation constant of the acid from which the basic catalyst is formed and α and β are the usual exponents from the equations of Brönsted, will enable separation of the two main rate factors. Moelwyn-Hughes[34] has shown that $\beta - \alpha$ is 0.44 in several cases, so an estimate for β is 0.67. Using these coefficients, the dissociation constants given in Table I, the dissociation constants for water and hydronium ion and the rate constants, log k_0 for each reaction is calculated. The values, which are averages of two values (for hydronium ion and water catalyses) except for the hypobromite and hydrazine cases, are also present in Table I. These numerical results, which should be sensibly independent of catalytic factors, may be interpreted as relative rates of reaction. In accordance with expectation, the values decrease as the activation energy increases for the four reactions in Table II.

The mechanism of these reactions is still subject to some question. The rate step may be thermolecular or there may be an equilibrium before the rate step. A prior equilibrium involving a hydrogen ion and any other particle is ruled out by the argument of Wynne-Jones[30] on general acid catalysis. An intermediate complex between hydrogen peroxide and a donor particle is possible; however, if present, it should exist only in small quantities, for both normally act as donors in their complexes. Despite the improbability of its existence, the possibility of such a complex being the kinetically important species must be considered.

In all of the reactions, the breaking of the peroxide bond plays a significant part. Presumably the donor particle causes a shift in the electron distribution of the peroxide away from the oxygen near the particle. The role of the acid is to enhance this

(28) W. C. K. Hender and R. A. Robinson, *Trans. Faraday Soc.*, **29**, 1300 (1933).

(29) T.-L. Chang and Y.-C. Wei, *J. Chinese Chem. Soc.*, **7**, 138 (1940).

(30) W. F. K. Wynne-Jones, *Chem. Revs.*, **17**, 115 (1935).

(31) J. N. Brönsted, *ibid.*, **5**, 231 (1928).

(32) E. A. Moelwyn-Hughes, "Kinetics of Reactions in Solution," 2nd Edition, Oxford University Press, London, 1947, p. 309.

(33) C. G. Swain, *J. Am. Chem. Soc.*, **72**, 4578 (1950).

(34) E. A. Moelwyn-Hughes, "Kinetics of Reactions in Solutions," 2nd Edition, Oxford University Press, London, 1947, p. 331.

shift by donating a proton to the oxygen farthest from the donor particle. In the transition state, the donor particle displaces a hydroxyl ion from hydrogen peroxide, thereby forming the molecule HOB.

There is a certain amount of chemical evidence for this reaction scheme. Trialkyl amines form amine oxides in good yield when treated with H_2O_2 while dialkyl amines are oxidized to dialkyl hydroxylamines.[35] In their discussion of the oxidation of hydrazine, Kirk and Browne[36] showed that hydrogen peroxide acted as a di-delectronator and explained the formation of ammonia and hydrazoic acid through the dimerization of the unsymmetrical intermediate $N{\cdot}NH_2$. The dimer then decomposes to give the observed products.

In a recent communication, Winter and Briscoe[37] describe experiments on the reaction of sodium sulfite with peroxide in water containing heavy oxygen. Their results show that direct transfer of one oxygen from the peroxide to the sulfite occurs, although the peroxide does not exchange with water under the conditions of their experiments.

The chemical evidence is consistent with the concept of a nucleophilic attack by the reducing agent on the peroxide with the concurrent displacement of a hydroxyl ion. The kinetic evidence supports this theory for the rate laws are indicative of a concerted acid–base catalyzed reaction, in which the role of the general acid is to donate a proton to the hydroxyl ion being displaced. Derbyshire and Waters[38] have interpreted certain reactions of peroxide in acid solution from the standpoint of the concept of cationic intermediates (OH^+ or $H_3O_2^+$). In view of their lack of kinetic substantiation, it is the opinion of this writer that their results are merely an extension of the present mechanism into concentrated acid solutions.

(35) W. R. Dunstan and E. Goulding, *J. Chem. Soc.*, **75**, 1005 (1899).

(36) R. E. Kirk and A. W. Browne, *J. Am. Chem. Soc.*, **50**, 337 (1928).

(37) E. R. S. Winter and H. V. A. Briscoe, *ibid.*, **73**, 496 (1951).

(38) D. H. Derbyshire and W. A. Waters, *Nature*, **165**, 401 (1950).

CRYOSCOPIC STUDIES OF SOLUTIONS OF POTASSIUM AND AMMONIUM CHLORIDES, AND ACETIC, PROPIONIC AND BENZOIC ACIDS IN FORMAMIDE

BY LYLE R. DAWSON AND EDWARD J. GRIFFITH

Department of Chemistry, University of Kentucky, Lexington, Kentucky

Received February 15, 1951

The molal freezing point depression for formamide has been redetermined and has been found to be 3.56$_6$°. The degrees of dissociation of potassium and ammonium chlorides, and acetic, propionic and benzoic acids in formamide have been determined. Activity coefficients of these solutes have been calculated in the range from 0.02 to 0.15 molal.

Although the properties of formamide as a solvent are of interest because of its striking similarity to water, it has been used in few cryoscopic studies.[1,2,3] It is a colorless liquid having a high dielectric constant, which dissolves readily many substances that are soluble in water.

Wide disagreement as to the values for the physical constants of formamide may be found in the literature. It is difficult to prepare in the pure state and equally difficult to preserve, thus preventing the accumulation of large quantities of pure solvent. According to recent data[4] its dielectric constant is approximately 109 at room temperature.

The purpose of the present investigation was to obtain, by cryoscopic methods, information concerning the properties of both strong and weak electrolytes in formamide, which might permit comparison with aqueous solutions. It was believed that cryoscopic data in conjunction with other physico-chemical data would be of value in studying the nature of the solute particles in a solvent having a large dielectric constant. A redetermination of the cryoscopic constant for formamide was undertaken also in an effort to establish a more accurate value.

(1) F. H. Getman, *Rec. trav. chim.*, **55**, 231 (1936).

(2) J. E. Mackenzie and S. Ghosh, *Proc. Roy. Soc., Edinburgh*, **35**, 22 (1914).

(3) E. N. Vasenko, *J. Phys. Chem. (U. S. S. R.)*, II, **22**, 999 (1948).

(4) G. R. Leader, *J. Am. Chem. Soc.*, **73**, 856 (1951).

Experimental

The cryostat was constructed to accommodate a sample of approximately fifty grams. It consisted of a two-liter dewar flask employed to house the unit, and an inner jacket containing the freezing tube, which in turn contained the sample, stirrer and a platinum resistance thermometer; thus, the freezing tube was suspended in the dead air space of the freezing jacket. The temperature of the air space was measured with an alcohol thermometer. A modified Wheatstone bridge, fitted with a mercury-switch commutator, was used in conjunction with the resistance thermometer. All stirring was done manually.

Reagent grade potassium chloride was recrystallized from water and fused in a platinum crucible. Reagent grade ammonium chloride was recrystallized from water and dried in a vacuum desiccator. Eastman Kodak Co. white label propionic and reagent grade acetic acids were purified by static crystallization, the best one-third being retained in each case. The best commercial grade of benzoic acid obtainable was purified further by sublimation.

Purified formamide was prepared from the commercial product by repeated distillation from calcium oxide under reduced pressure at from 52 to 60°. Usually it was allowed to stand over calcium oxide several hours before distilling. It was found advisable also to store the formamide in the dark as a precaution against possible photochemical effects. All samples of the solvent used in this research froze at 2.45° or higher.

The solutions were prepared on a weight basis, all transfers being accomplished in a dry-box. The freezing temperature of the pure solvent was obtained by cooling about fifty grams in a salt–ice-water-bath until two or three grams

of solid had formed. Then the stoppered freezing tube was transferred to the cold cryostat and the resistance thermometer and stirrer inserted. An equilibrium temperature that persisted for more than 15 minutes when the environment temperature was below the temperature of the solvent was accepted as the freezing point of the solvent.

Prior to the measurement of the freezing temperature of a solution about one gram of pure formamide was frozen in the freezing tube. The solution to be tested was cooled in a refrigerator to a temperature just above the expected freezing point and then transferred to the freezing tube with the frozen seed of pure formamide. Then the sample was treated in the same manner as the pure solvent except that equilibrium temperature could not be maintained quite as long.

For the redetermination of the cryoscopic constant of formamide, neither the method used by Getman[4] nor the Lewis method[5] seemed applicable. The former appears to be quite arbitrary in nature and there exist insufficient thermal data for formamide to use the Lewis method satisfactorily. An alternate procedure was adopted.

Solutions of varying concentrations of urea and of sugar in formamide were prepared and their freezing points observed. The purest solutes obtainable were used and the resulting data were related to the equation

$$\Delta t = \lambda_f m \qquad (1)$$

where

λ_f is the molal freezing point lowering
Δt is the experimental freezing point lowering
m is the molality of the solute

Equation (1) is of the slope intercept form for a straight line with an intercept of zero. A plot of Δ *versus* m was constructed, and the result was a straight line with an intercept at the origin. Small variations were eliminated by applying the method of least squares to the data, and the calculated value for the slope was accepted as the molal freezing point constant. Its value, determined in this way, was 3.56$_6$ degrees/mole/1000 g. of solvent

The results are given in Tables I–V.

TABLE I

STOICHIOMETRICAL ACTIVITY COEFFICIENT AND DEGREE OF DISSOCIATION OF POTASSIUM CHLORIDE IN FORMAMIDE

Molality	F.p., °C., solution	F.p., °C., solvent	Δt	γ	α
0.0398	2.182	2.448	0.266	0.926	0.95
.0634	2.038	2.457	.419	.901	.89
.1043	1.781	2.458	.677	.871	.85
.1206	1.665	2.449	.784	.870	.86
.1584	1.459	2.458	.999	.840	.80

TABLE II

STOICHIOMETRICAL ACTIVITY COEFFICIENT AND DEGREE OF DISSOCIATION OF AMMONIUM CHLORIDE IN FORMAMIDE

Molality	F.p., °C., solution	F.p., °C., solvent	Δt	γ	α
0.0511	2.151	2.473	0.322	0.943	0.88
.0717	2.011	2.473	.462	.917	.84
.0906	1.888	2.473	.585	.885	.84
.1120	1.772	2.473	.701	.877	.79
.1188	1.715	2.473	.758	.870	.82
.1314	1.647	2.473	.826	.870	.80
.1475	1.548	2.473	.925	.855	.79

Discussion

Treatment of Data.—The data were treated from two different viewpoints. Activity coefficients were calculated for the strong electrolytes by the method of Lewis and Randall[5] employing the conventional approach, but this treatment was modified for the weak electrolytes. The degree of

(5) G. N. Lewis and M. Randall, "Thermodynamics," McGraw-Hill Book Co., Inc., New York, N. Y., 1923.

TABLE III

FUNCTIONAL ACTIVITY COEFFICIENT AND DEGREE OF DISSOCIATION OF ACETIC ACID IN FORMAMIDE

Molality	F.p., °C., solution	F.p., °C., solvent	Δt	γ	α
0.0329	2.370	2.510	0.140	0.585	0.196
.0442	2.285	2.469	.184	.546	.164
.0475	2.291	2.483	.192	.532	.136
.0589	2.238	2.469	.231	.500	.100
.0714	2.208	2.469	.261	.465	.027
.0937	2.193	2.510	.317	.425	− .051
.1062	2.138	2.505	.366	.418	− .034
.1107	2.128	2.505	.377	.410	− .046
.1333	2.051	2.505	.454	.394	− .039
.1522	1.916	2.425	.509	.377	− .063

TABLE IV

FUNCTIONAL ACTIVITY COEFFICIENT AND DEGREE OF DISSOCIATION OF PROPIONIC ACID IN FORMAMIDE

Molality	F.p., °C., solution	F.p., °C., solvent	Δt	γ	α
0.0262	2.396	2.505	0.109	0.543	0.172
.0506	2.317	2.505	.188	.448	.044
.0536	2.254	2.505	.251	.441	.046
.0707	2.244	2.505	.261	.415	.037
.0905	2.147	2.483	.336	.394	.040
.1243	2.063	2.493	.430	.355	− .030

TABLE V

FUNCTIONAL ACTIVITY COEFFICIENT AND DEGREE OF DISSOCIATION OF BENZOIC ACID IN FORMAMIDE

Molality	F.p., °C., solution	F.p., °C., solvent	Δt	γ	α
0.0295	2.356	2.485	0.129	0.592	0.228
.0419	2.294	2.469	.175	.541	.174
.0531	2.273	2.485	.212	.505	.122
.0636	2.244	2.483	.239	.472	.052
.0779	2.186	2.469	.283	.440	.018
.0955	2.159	2.493	.334	.415	− 018
.1299	2.014	2.469	.455	.388	− .017

dissociation was calculated for both strong and weak electrolytes by the equation

$$\alpha = \frac{i - 1}{\nu - 1} \qquad (2)$$

where

α is the degree of dissociation
i is the ratio of the observed freezing point lowering to the calculated freezing point lowering
ν is the number of ions into which the solute dissociates

In the calculation of activity coefficients of the solutes by the method of Lewis and Randall the correction terms were omitted because sufficiently accurate thermal data were not available, and because the systems were not completely stable. Thus the equation employed was

$$\ln \gamma = -2 \int_0^m J/m^{1/2}(dm^{1/2} - J) \qquad (3)$$

where

γ is the activity coefficient
J is the Lewis and Randall divergency factor
m is the molality of the solution

The integral was evaluated by graphical methods.

When this equation is used for a weak electrolyte the solute is treated in the same manner as if it were a strong electrolyte, and the activity coefficient thus obtained is intrinsically different from

the conventional activity coefficients for electrolytes in which attention is focused on ionic behavior. The value obtained in this way has been called the functional activity coefficient because it is concerned not with ionic behavior only, but with the colligative behavior relative to a standard state in which the solute would be completely dissociated, irrespective of the particle aggregates at finite concentrations. Although such values cannot be used in quantitative thermodynamic relationships, they are useful in comparing the states of aggregation of the particles of various solutes in a given solvent. Of course, it is to be admitted that both dissociation and solvolysis may be important factors in determining the nature of the solute particles.

The ultimate objective of the majority of freezing point studies centered around conventional activity coefficients, is to compare cryoscopic data with similar data obtained by electrochemical methods. Treatments of this type generally ignore the undissociated portion of the solute and yield a distorted picture where the total solute behavior of a weak electrolyte is used.

The results of this work were reproducible with a probable error of less than 1%.

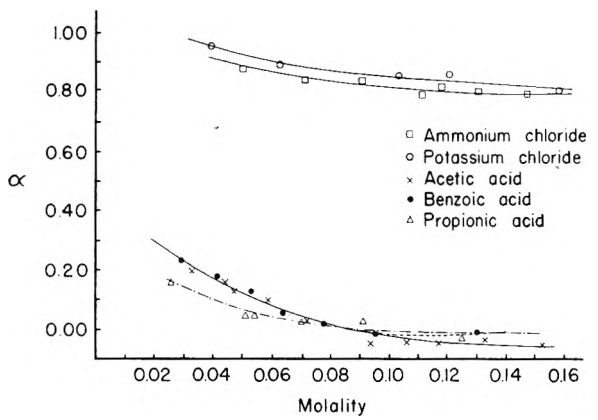

Fig. 1.—Influence of concentration on the degree of dissociation of solutes in formamide.

Properties of the Solutions.—Ammonium chloride behaved much like it does in water solutions; the apparent degree of dissociation as determined by croscopic methods is approximately 0.88 in both solvents at a concentration of 0.05 molal. Some evidence of a greater degree of dissociation of potassium chloride in formamide appeared. In 0.05 molal solution, the value is 0.93, while in the corresponding water solution it is approximately 0.89.[6] The difference of about 2.5° in the freezing points of the solutions would be expected to have little effect on the data.

The degree of dissociation of benzoic, acetic and propionic acids was found in this work to be from 2–15% greater in formamide than the accepted values for water solutions. Probably this apparently larger dissociation results from the difference in the activity coefficient of the undissociated molecules in formamide as compared to water. Verhoek[7] found by electrical methods that both benzoic and propionic acids dissociated to a lesser extent in formamide than in water.

The acidity of the benzoic acid solutions increases with time. When brom thymol blue is added to a fresh 0.05 *m* solution of benzoic acid and formamide the initial color is blue, but upon standing for several hours the color turns to green and subsequently to straw-yellow. It is known that at elevated temperatures acetamide and benzoic acid react to form benzamide and acetic acid, and it is believed that a very slow reaction may take place between formamide and benzoic acid to form benzamide and formic acid. However, additional experimental data would be required to establish this point.

Values of the activity coefficients calculated for potassium chloride and ammonium chloride (Fig. 2) are approximately 8% higher than the values reported for water solutions at the same molalities.[5]

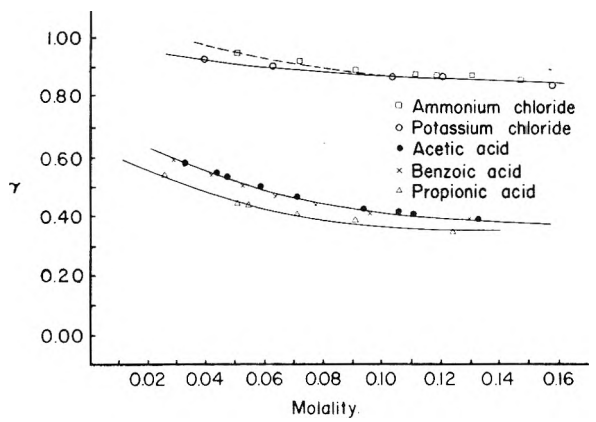

Fig. 2.—Influence of concentration on the activity coefficient of solutes in formamide.

The functional activity coefficients calculated for the weak electrolytes are of the order of 0.5 in dilute solutions as was to be expected where a standard state of completely dissociated electrolyte was chosen.

(6) A. A. Noyes and K. G. Falk, *J. Am. Chem. Soc.*, **32**, 1011 (1910).

(7) F. H. Verhoek, *ibid.*, **58**, 2577 (1936).

THE RING METHOD OF MEASURING SURFACE TENSION FOR LIQUIDS OF HIGH DENSITY AND LOW SURFACE TENSION[1]

By H. W. Fox and C. H. Chrisman, Jr.

Naval Research Laboratory, Washington, D. C.

Received February 22, 1951

The existing correction tables applicable to the measurement of surface tension by the ring method are not extensive enough to be used with liquids of high density coupled with low surface tension, as for example, the fluorocarbons. The convenience and rapidity of the ring method make it worth while to extend the tables to the region in question. The tables therefore have been extended by fitting a combined hyperbolic and linear equation to the curves derived from existing tables. This equation produces values in agreement with existing tables to better than 0.05 per cent. The extrapolated tables were verified experimentally over their whole range by comparing measurements of the surface tensions of five fluorocarbon liquids made by the differential capillary-rise method (which is independent of corrections) with measurements on the same liquids made by the ring method. The agreement was as good as that associated with the original tables.

Introduction

The method of determining surface tension by measuring the force necessary to detach a ring from a liquid surface has come into widespread use because of its rapidity and convenience. Although this method does not produce results of highest accuracy except with the most tedious painstaking, with reasonable care it is possible to produce results with an error of less than 0.5%.

The ring method was placed on a firm basis in the classical work of Harkins and co-workers.[2,3] These authors measured the surface tensions of liquids by both the capillary rise and ring methods and compared the two values. They prepared a table of correction factors which reconciled the values obtained by the two methods. Freud and Freud[4] analyzed the ring method from the theoretical standpoint, finding excellent agreement between the empirically derived tables and the theory of the ring method. The tables are therefore being widely used and indeed are nearly indispensable if reasonable accuracy is required in using the ring method.

Harkins, *et al.*,[2] found that the correction factor F for the ring method depended on R^3/V and R/r where R is the radius of the ring, r the radius of the wire of the ring and V the maximum volume of liquid lifted above the plane of the liquid surface. Their tables cover the range of R^3/V from 0.30 to 3.50 and of R/r from 30 to 80. For most purposes this range is adequate and permits the choice of a ring whose dimensions are such as to introduce the fewest experimental difficulties. The liquid fluorocarbons and many derivatives only recently come into prominence, have, however, comparatively low surface tensions coupled with high densities. Therefore, when a ring of convenient size (4 to 6 cm. in circumference) is used, one finds that R^3/V is larger than 3.50 and that the proper correction factor lies outside the scope of the tables. Figure 1 shows the limits of the region where rings 6 and 12 cm. in circumference may be used without exceeding the limit of the tables at $R^3/V \gtrsim 3.50$. For $R/r = 30$, combinations of surface tension and density yielding values of R^3/V less than 3.50 lie above the limiting line in each of the two cases represented. For R/r greater than 30 the limiting lines are displaced upward, further restricting the useful areas. It is obvious from Fig. 1 that for successful use of the existing tables for the determination of the surface tension of the fluorocarbons, one must resort to rings at least 12 cm. in circumference. The use of rings of this size introduces serious problems in making and maintaining the rings flat and level.

It is therefore of general interest to extend the Harkins and Jordan tables to regions of $R^3/V > 3.50$ so that the ring method might be used for the fluorocarbons and similar liquids with rings of moderate size.

The present paper describes the extrapolation of the tables to $R^3/V = 7.50$ for R/r equal to 40, 50, 52, 54, 56, 58 and 60. These values of R/r were considered especially useful since there are commercially available rings 6 cm. in diameter with values of R/r between 52 and 56. The procedures outlined below may be used to extend the extrapolations beyond $R^3/V = 7.50$ or to other values of R/r.

Zuidema and Waters[5] analyzed the tabulated data of Harkins and Jordan and presented an equation which described the data closely. They showed that the correction factor F is a parabolic function of $P/(D - d)$ where P is the maximum pull on the ring ($Mg/4\pi R$) and D and d are the densities of the lower and upper phases, respectively, (liquid–air, oil–water, etc). By means of their equation they were able successfully to extrapolate the Harkins and Jordan tables to regions of R^3/V smaller than 0.30; this region is useful in applying the ring method to measurements of interfacial tension where V is likely to be large because of the small differences in density between two liquid phases. When the Zuidema and Waters equation was applied to the raw data for the fluorocarbons however, discrepancies in F were found at $R/r = 54$ which ranged from 4% at $R^3/V = 4.6$ to 7% at $R^3/V = 7.0$. In this region, $P/(D - d)$ ranges from 15 to 10 and the Zuidema and Waters function moves more slowly than required by the experimental data. In fact, the function has a limit of

(1) The opinions or assertions contained in this paper are those of the authors and are not to be construed as official or reflecting the views of the Navy Department.

(2) W. D. Harkins, T. F. Young and L. H. Cheng, *Science*, **64**, 33 (1926).

(3) W. D. Harkins and H. F. Jordan, *J. Am. Chem. Soc.*, **52**, 1751 (1930).

(4) B. B. Freud and H. Z. Freud, *ibid.*, **52**, 1772 (1930).

(5) H. H. Zuidema and G. W. Waters, *Ind. Eng. Chem.*, **13**, 213 (1941).

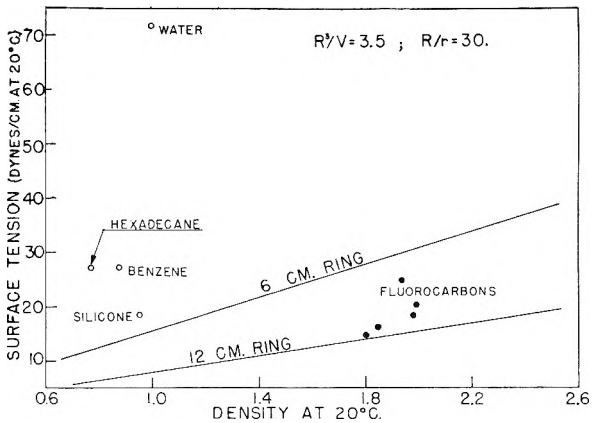

Fig. 1.—Limiting values of surface tension and density for application of the Harkins and Jordan correction tables.

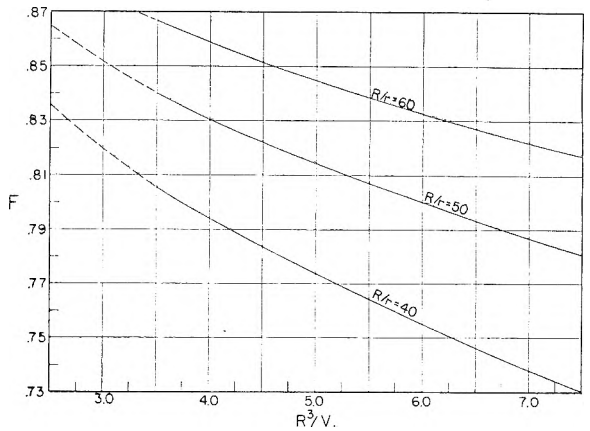

Fig. 2.—Correction factor F as a function of R^3/V. Dashed lines are from the Harkins and Jordan tables.

$F \lesssim 0.84$ at $P/(D - d) \lesssim 0$ whereas experiment shows the need of $F < 0.83$ at $P/(D - d) < 15$.

Extrapolation of the Harkins and Jordan Tables.—The Harkins and Jordan tables were extrapolated by finding equations describing the curves plotted from the tables and extending the curves by means of these equations for $R/r = 40$, 50 and 60 from $R^3/V = 3.5$ to 7.5. Lagrangian interpolation was employed to obtain the curves for $R/r = 52$, 54, 56 and 58. The extrapolated tables were tested experimentally at $R/r = 54.0$ where the interpolation is most distant from the extrapolated curves and the results are described below. Table I shows the extrapolated tables for $R^3/V = 3.5$ to 7.5. The intervals were chosen as 0.25 since the function moves fairly slowly in this region and interpolation is easy. Following Harkins and Jordan, the deciles of R/r are given to four decimal places and the interpolated values to three. A detailed description of the method used in this extrapolation is given in the appendix to this paper. Figure 2 shows the curves for $R/r = 40$, 50 and 60 in the extrapolated region; the dotted lines are in the adjacent region of the Harkins and Jordan tables.

TABLE I

CORRECTION FACTORS (F) FOR THE RING METHOD

R^3/V	$R/r = 40$	50	52	54	56	58	60
3.50	0.8063	0.8407	0.847	0.852	0.858	0.863	0.8672
3.75	.8002	.8357	.842	.848	.853	.858	.8629
4.00	.7945	.8311	.837	.843	.849	.854	.8590
4.25	.7890	.8267	.833	.839	.845	.850	.8553
4.50	.7838	.8225	.829	.835	.841	.847	.8518
4.75	.7787	.8185	.825	.832	.838	.843	.8483
5.00	.7738	.8147	.822	.828	.834	.840	.8451
5.25	.7691	.8109	.818	.825	.831	.837	.8420
5.50	.7645	.8073	.815	.821	.828	.834	.8389
5.75	.7599	.8038	.811	.818	.825	.830	.8359
6.00	.7555	.8003	.808	.815	.821	.827	.8330
6.25	.7511	.7969	.805	.812	.818	.825	.8302
6.50	.7468	.7936	.801	.808	.815	.822	.8274
6.75	.7426	.7903	.798	.806	.813	.819	.8246
7.00	.7384	.7871	.795	.803	.810	.816	.8220
7.25	.7343	.7839	.792	.800	.807	.813	.8194
7.59	.7302	.7807	.789	.797	.804	.811	.8168

Verification of Extrapolation

Experimental.—The surface tensions of a number of liquids were measured at 20.00 ± 0.03° by the differential capillary rise method of Sugden[6] and by the ring method at 20.0 ± 0.1° and the results were compared. The liquids were chosen to give a wide range of values of R^3/V.

Results obtained by us for three pure compounds using the differential capillary rise method were in excellent agreement with the most reliable values given in the literature. The surface tension of water was measured as 72.75 dynes/cm.[7]; benzene, 28.86 dynes/cm.[7]; *n*-hexadecane, 27.60 dynes/cm.[8] The other liquids of this study were carefully tested to make certain that the contact angle with glass was zero since the method depends on this being the case.

The capillary rise cell used in these measurements had large and small capillaries, whose diameters were 0.1 and 0.05 cm., respectively. These dimensions ensured that the rise would be at least 0.3 cm. even for liquids of surface tensions as low as 15 dynes/cm. The rise was measured with a slide micrometer accurate to 0.0001 cm. so that this measurement was good to 0.03% for the smallest rise and proportionately better for liquids of higher surface tension.

The same capillary rise cell was used for all the liquids reported here. Difficulties were encountered in cleaning the cell after measurements on the fluorocarbons. These liquids are insoluble or difficultly soluble in conventional solvents, and they are not destroyed by oxidizing acids. It was necessary to rinse out the cell with CF_3–CCl_3 (Freon 113) which is a good low-boiling solvent for fluorocarbon liquids. This liquid not only effectively dissolved and removed all the fluorocarbon oil left on the walls of the cell but was itself readily removed by blowing clean dry air through the cell. The cell was subsequently boiled in nitric–sulfuric acid (1:2) for 10–15 minutes until it was hydrophilic. The acid was removed by ten rinses with steaming, freshly distilled water and the cell was dried at 110°. With this method of cleaning, no difficulty was encountered in obtaining reproducibility to within 0.02–0.03%. Every surface tension value given here is the average of at least three independent measurements.

To "calibrate" the ring, four liquids were chosen whose F values fell within the scope of the Harkins and Jordan tables. Of five 6-cm. rings obtained from the manufacturer, none was perfect, in that not every portion of the ring lay in the same plane. Moreover, where the rings were welded to the supporting stirrups, more metal had been removed than was actually necessary to make the rings smooth. This had the effect of reducing the diameter of the wire at two points in every ring. Both these effects tend to make the ring break away too early so that the values of the surface tension are invariably low by the same amount percentagewise. For the work reported here, a ring was chosen which had a value of $R/r = 54$ so that the extrapolated tables could be tested at a point where the interpolations were most distant from the deciles.

The diameters of the ring and the wire were measured with a slide micrometer which had been compared with a Bureau of Standards standard length and was accurate to 0.0001 cm. The method of Harkins and Jordan[3] for measuring the diameters was found to be satisfactory. Averages of six

(6) S. Sugden, "The Parachor and Valency," A. A. Knopf, 1930, pp. 215-216.

(7) N. K. Adam, "The Physics and Chemistry of Surfaces," Ed., Oxford Univ. Press, London, 1941, p. 370.

(8) A. I. Vogel, *J. Chem. Soc.*, 133 (1946).

diameters of the ring and twelve diameters of the wire were taken. The ring was found to be out of round by somewhat under 1% but Harkins and Jorkan claim that this is a minor source of error. The circumference of the ring used was found to be 5.990 cm. and R/r was 54.0. The deviation from flatness was measured with a cathetometer and found to be about 0.2 mm. at the worst place. If deviation from flatness has an effect similar to tilting the ring, it is possible to estimate the magnitude of the error which will be produced. The deviation found for the ring is equivalent to an angle of tilt of about 0.5 degree for a ring 6 cm. in circumference. Referring to the Harkins and Jordan[3] graph of the error introduced by tilting the ring, it is clear that the results will be between 0.2 and 0.3% too low. The additional contribution to the error by the excessive removal of metal at the welded joints could be estimated from the calibrating measurements.

Table II shows the discrepancies between the values obtained by the capillary rise method and by the ring method for the four liquids which could be measured with the help of the extant tables. The ring methods gave values about 0.4% low with no apparent systematic differences in the error over the whole range of R^3/V. Since no other errors known to the authors were involved in these measurements, it was assumed that the 0.4% error was due to deviation from flatness of the ring (contributing about half the error) and a too small radius of the wire at the welded joints.

A chainomatic balance especially designed for surface tension measurements was used in this study. Incorporated in it was a platform which could be lowered smoothly and slowly while weight was added by means of a rider and chain. The balance was sensitive to 0.1 mg. and the rider and chain were calibrated with certified weights before use. To obtain good results it was found necessary to insulate the balance from vibration and to fit it with a magnetic damper. The ring was held in a pin chuck fitted with a circular eye which hung from a free swinging hook attached to an agate knife edge. The ring was leveled by bringing a dish of mercury close to it and sighting between the ring and the mercury surface. Very small deviations from the level could be determined in this fashion. This method was found to be easier and more convenient than the method of Harkins and Jordan[3] who used a metal mirror leveled with a spirit level.

The liquid to be measured was held in a thick walled petri dish 10 cm. in diameter. The edge of the dish was finely ground to a good fit with a cover of plate glass. The cover was slotted to permit the wires supporting the ring to pass through. After the ring and cover were in position, the slot was covered except where the wires passed through. This arrangement worked satisfactorily in minimizing evaporation of even the most volatile liquids of this study.

The procedure was as follows: The ring was flamed, leveled as described above, and the zero of the balance determined. A clean petri dish containing the liquid to be measured was placed on the platform and the liquid surface raised to within 2–3 mm. of the ring. The cover was put in place and the slot covered. The balance case was closed and the whole system allowed to come to thermal equilibrium for one hour to ensure that the space above the liquid became saturated with vapor. The liquid was then raised till it touched the ring. Weight was added and the platform simultaneously lowered to keep the balance pointer on zero. The beam arrest was lowered very little so that the pointer could swing only about half a division on either side of zero. This was done to prevent the ring from becoming completely detached at the end-point of the measurement. In this way successive measurements could be made quickly since the position of the platform need only be changed a small amount between measurements. Weight was added and the platform lowered until the pointer could no longer be brought back to zero by lowering the platform. The chain was then backed off 2–3 mg. and the platform raised a little. Then weight was added 0.1 mg. at a time with at least 5 seconds between additions for the non-viscous liquids and 10 seconds for the viscous liquids. The platform was lowered very slowly at the same time always keeping the pointer at zero. When addition of 0.1 mg. made the pointer swing irreversibly to the left, the weight was recorded as the maximum pull on the ring. Successive measurements made in this fashion were invariably within 0.1 mg. of each other. At least four measurements were made in this way at 15-minute intervals. The whole procedure was repeated for each fluid at least twice on different days to ensure that no topical variables were affecting the measurements. The separate measurements on different days always checked within 0.3 mg. The average of the three separate measurements is the value reported in Tables II and III.

Table II

Determination of Ring Correction

		Surface tension (dynes/cm., 20°)				
Compound	R^3/V	Diff. cap. rise	Ring	Difference, %	Ring (cor.)	Difference, %
Water	0.92	72.75	72.57	−0.25	72.85	+0.14
Benzene	1.93	28.86	28.76	− .34	28.87	+ .04
Hexadecane	1.80	27.60	27.44	− .57	27.55	− .18
Hexadecamethylheptasiloxane	3.14	18.61	18.53	− .43	18.60	− .05

Average correction 0.40%.

Table III

Comparison of Surface Tension Measurements by the Differential Capillary Rise and Ring Methods for Liquids of High Density and Low Surface Tension

		Surface tension (dynes/cm., 20°)			
Compound	R_3/V	Diff. cap. rise	Ring	Ring (cor.)	Difference, %
Fluorolube (Hooker)[a]	4.61	25.03	24.85	24.95	−0.32
Fluoro lubricant (du Pont FCD 330)	5.75	20.15	20.06	20.14	− .05
Fluoro kerosene (du Pont FCD 329)	6.16	18.31	18.17	18.24	− .38
Perfluorodimethylcyclohexane	6.65	16.00	15.95	16.01	+ .06
Perfluoromethylcyclohexane	6.97	14.70	14.69	14.75	+ .34

[a] Polymonochlorotrifluoroethane.

Results

Table II shows the differences in the values obtained by the differential capillary rise and ring methods for four liquids when R^3/V falls in the range of the Harkins and Jordan correction tables. There is a systematic error (due to imperfection of the ring) averaging 0.40%. When this correction is applied to the values obtained by the ring method, the percentage difference between the two methods is reduced to less than 0.2%. Harkins and Jordan consider that for values of R/r other than deciles the tables are accurate to 0.4% with a probable error of less than 0.3%.

Table III gives the differences in the values obtained by the two methods for five liquids when R^3/V is larger than 3.50. In this case the raw data for the ring method were corrected with the extrapolated tables shown above. It is evident that when the 0.4% correction determined earlier is applied to the fluorocarbon data, the residual differences are all less than 0.4% over the range of R^3/V from 4.61 to 6.97. It is obvious that as the surface tension decreases, the sensitivity of the balance (0.1 mg.) assumes greater importance percentagewise so that differences of 0.01 dyne/cm. (0.1 mg. $\approx$ *ca.* 0.01 dyne/cm.) are equivalent to 0.05% at surface tensions of 20 dynes/cm. and proportionately more at lower surface tensions.

Conclusions

The tables of corrections for the ring method of determining surface tension of Harkins and Jordan[3] have been extrapolated to $R^3/V = 7.50$ for values of R/r of 40, 50, 52, 54, 56, 58 and 60. The extrapolations were checked experimentally and proved to

have the same order of accuracy as the Harkins and Jordan tables for $R/r = 54.0$. For the other values of R/r tabulated here, the agreement should be at least as good.

These tables may therefore be used with commercially available rings 6 cm. in circumference to measure the surface tensions of liquids of high density and low surface tension by the ring method. For highest accuracy, it is necessary to determine the errors inherent in the ring by calibration with liquids of known surface tensions.

The ring method is therefore now available for measuring surface and interfacial tensions from regions of high interfacial tension and low density by the extrapolation of Zuidema and Waters[5] to regions of low surface tension and high density by the extrapolation presented in this paper.

Appendix

The equations for R/r equal to 40, 50 and 60 were obtained by fitting to the Harkins and Jordan tables[3] equations made up of a hyperbolic component and a straight line component. An exponential component was used tentatively on the table at $R/r = 50$ but was discarded in the final computations since it had no effect on the region of interest. In the example described ($R/r = 50$), R^3/V will be designated as x and F will be designated as y. The data for the curve in question were plotted at intervals of 0.1 x and a hyperbolic component was recognized. The data were divided into two groups of 16 points each and the averages of the x and y values were taken. These averages were substituted in the equation

$$a + bx = x/y \qquad (1)$$

to give

$$a + 1.15b = 1.15/0.92774$$

and

$$a + 2.75b = 2.75/0.85904$$

which when solved gave $a = -0.17040$ and $b = 1.2261$. Substituting these values in equation (I) and equating for y gave

$$y_{\mathrm{I}} = \frac{x}{1.2261\,x - 0.17040} \qquad (2)$$

First approximations for y were computed from equation (2) and residuals formed from the equation

$$y_{\mathrm{I}} - y = \text{residue} \qquad (3)$$

The residues plotted at intervals of 0.1 x showed the presence of an exponential component and a straight line component. Since in the region of interest, the straight line component appeared more prominent, a straight line was written to describe this component. In the portion of the curve which approaches a straight line from $x = 2.4$ to 3.5 the residues at 0.1 x intervals were averaged in two groups and substituted in the equation

$$y = cx + d \qquad (4)$$

giving

$$0.00016667 = 2.65c + d$$

and

$$0.0060833 = 3.25c + d$$

Solving these equations and substituting for c and d gave the equation

$$y = -0.010417x + 0.027771 \qquad (5)$$

By adding equations (2) and (5) the following equation for the second approximation of y is obtained

$$y_{\mathrm{II}} = \frac{x}{1.2261 \times -0.17040} - 0.010417x + 0.027771 \qquad (6)$$

Residues were taken by subtracting the original values of y from values as computed by equation (6). In the region of interest the agreement was within the accuracy requirements, but the exponential component was still evident in the region of lower x values ($R^3/V < 2.4$). Therefore, an equation of the form $y = fe^{gx}$ was written. In writing this equation the values $x = 0.6$ and 2.2 were substituted in the equation in the form

$$\ln y = \ln f + gx$$

to give

$$-2.1804 = \ln f + 0.6g$$
$$-6.3771 = \ln f + 2.2g$$

which when solved gave $f = 0.54521$ and $g = -2.6230$

TABLE IV

CORRECTION FACTOR F FOR THE RING METHOD AT $R/r = 50$

R^3/V	F	
	H & J	Eq. 6
2.4	0.8680	0.8685
2.5	.8651	.8654
2.6	.8624	.8625
2.7	.8598	.8596
2.8	.8570	.8569
2.9	.8545	.8543
3.0	.8521	.8518
3.1	.8494	.8495
3.2	.8472	.8471
3.3	.8449	.8450
3.4	.8424	.8428
3.5	.8404	.8407

The equation

$$y = 0.54521e^{-2.6230x} \qquad (7)$$

was added to equation (6) to give the third approximation as follows

$$y_{\mathrm{III}} = \frac{x}{1.2261x - 0.17040} - 0.010417x + 0.027771 - 0.54521e^{-2.6230x} \qquad (8)$$

Values of F computed from (8) with the exception of $R^3/V = 0.4$ and 0.5 were in error by 0.5% or less throughout, with the error decreasing as R^3/V increases. The error reduces to 0.1% at $R^3/V = 1.5$ and to about 0.05% above $R^3/V = 2.0$. Furthermore, the second approximation (equation (6)) agrees with the Harkins and Jordan tables to better than 0.05% for values of $R^3/V > 2.4$. Since the region of interest is above $R^3/V = 2.4$, the exponential component was neglected in all of the computations involved in making Table I. The data for $R/r = 40$, 50 and 60 were computed from equations of the same form as equation (6) and were tabulated to four decimal places. From these data three-point Lagrangian interpolation was used to compute data to three decimal places for $R/r = 52$, 54, 56 and 58.

Table IV shows the agreement of equation (6) with the Harkins and Jordan tables for $R/r = 50$ and $R^3/V > 2.4$.

BOOK REVIEW

Phase Transformations in Solids. Edited by R. SMOLUCHOWSKI, Chairman, with J. E. MAYER and W. A. WEYL. John Wiley & Sons, Inc., New York, N. Y. x + 660 pp. Price, $9.50.

This monograph contains the papers and some of the discussions from a symposium on the general subject of phase changes which was held in August, 1948. The symposium itself was the outgrowth of an effort initiated by the National Research Council, with the purpose of bringing together a group of specialists to "focus attention on significant basic problems of the solid state and thus lead to a more comprehensive understanding of the field." The task of preparing the papers and discussions for publication has been ably done by the editors noted above.

The seventeen papers fall in three groups, each paper being a complete and independent unit. The first section of the book is devoted to the mathematical theory of phase transitions, including diffusion and crystal growth, with papers by Tisza, J. E. Mayer, Kirkwood, Seitz, Smoluchowski and Buerger. The authors have presented divergent and sometimes conflicting ideas, but the reader, even though he is not working in the field, is sure to receive stimulation from following these efforts to develop a quantitative theory in a science which is so new, and for which modern experimental resources are now furnishing such an abundance of previously unavailable information.

The second section deals with transitions in non-metallic systems. O. K. Rice has a paper on the solid–liquid transition in argon, which represents an attempt to understand the process of melting. M. L. Huggins discusses the factors involved in transitions of the silver halides. Silicates and glasses are treated in three papers by Kracek, Schairer and Weyl, in which the rates and types of transitions are correlated with such things as order-disorder phenomena, the forces between different types of ions, and relative mobilities of different ionic species with respect to the structural network. The section is concluded by a brief paper on the new subject of ferroelectrics by Matthias.

The final section of the book is given over to papers on transitions in metals. C. S. Barrett's paper covers pure metals with particular respect to the theories of transformations normally called martensitic. Much new light in the field is being obtained by study of low-temperature crystallographic changes in lithium. Siegel has a chapter on order–disorder transitions in metal alloys. The paper on precipitation from solid solutions of metals, by A. H. Geisler, is a monograph in itself, consisting of 58 pages, profusely illustrated and having a bibliography of 830 titles. A valuable feature of the bibliography is a separate classification of the references by alloys and by subjects. Menl and Dubé have a chapter on the eutectoid reaction, with special consideration of the factors entering into the mechanism and kinetics of the process. The final chapter by Morris Cohen discusses the martensite transformation and develops the thesis that it is the process of the transformation, rather than the specific product, which is the distinctive feature of the problem.

Throughout the book, there are excellent photographs and diagrams in abundance. In fact, one cannot but be impressed with the wealth of factual detail included. Each chapter has a good bibliography, but there is no index.

The editors point out that the book is designed for specialists: this is quite apparent, especially in the earlier chapters. For workers in the general field of solids, the book will undoubtedly be of inestimable value as a source of ideas and reference to current research. It would be a pity, however, if the book were read only by specialists. Some years ago we rather naively regarded a crystal as an epitome of order, as contrasted with gases and liquids. Recent years have produced the idea of disorder, with its profound significance for the properties and transformations of solids. One now attempts to develop general theories for the solid state by kinetics and thermodynamics based upon statistical considerations. This book reveals how much remains to be done in obtaining a unified and comprehensive grasp of the field. The reader gains the clear impression that he is watching the birth of a new science, with new theoretical approaches and experimental techniques that were not accessible until a decade or so ago. The members of the symposium and the editors are to be congratulated on producing a work that is such a mine of information. It will undoubtedly be a continuing source of stimulation for all who have problems involving the solid state.

DEPARTMENT OF CHEMISTRY
KING COLLEGE
BRISTOL, TENNESSEE

G. H. CARTLEDGE

BOOKS RECEIVED

To December 28, 1951

H. J. DEUEL, JR. "The Lipids." Interscience Publishers, Inc., New York. 1951. 982 pp. $18.50.

ROBERT A. FRIEDEL AND MILTON ORCHIN. "Ultraviolet Spectra of Aromatic Compounds." John Wiley and Sons, Inc., 440 Fourth Avenue, New York 16. 1951. 52 pp. $10.00.

R. N. HASZELDINE AND A. G. SHARPE. "Fluorine and Its Compounds." John Wiley and Sons, Inc., 440 Fourth Avenue, New York 16. 1951. 153 pp. $1.75.

HUGH S. TAYLOR AND SAMUEL GLASSTONE. "A Treatise on Physical Chemistry." D. Van Nostrand Co., Inc., New York. 1951. 701 pp. $12.00.

D. S. VILLARS. "Statistical Design and Analysis of Experiments for Development Research." Wm. C. Brown Co., Dubuque, Iowa. 1951. 455 pp. $6.50.

D. W. WOOLLEY. "A Study of Antimetabolites." John Wiley and Sons, Inc., 440 Fourth Avenue, New York 16. 1952. 269 pp. $5.00.